Application of Calorimetry and Thermal Analysis to determine the liquid range and the environmental toxicity of Ionic Liquids

Memoria presentada por

Juan José Parajó Vieito

para optar al grado de Doctor por la

Universidad de Santiago de Compostela

Santiago de Compostela, Mayo 2016

Universidade de Santiago de Compostela

Departamento de Física Aplicada
Grupo de Propiedades Termofísicas de Fluidos y Biomateriales
Facultade de Física
Campus Vida
15872 Santiago de Compostela

Dra. Josefa Salgado Carballo y **Dra. María Villanueva López**, Profesoras Titulares del Departamento de Física Aplicada de la Universidad de Santiago de Compostela, directoras de esta Tesis Doctoral

INFORMAN:

Que la presente memoria, titulada *Application of Calorimetry and Thermal Analysis to determine the liquid range and the environmental toxicity of Ionic Liquids* fue realizada por el Licenciado en Química con Máster en Energías Renovables y Sostenibilidad Energética, D. Juan José Parajó Vieito bajo nuestra dirección en el Laboratorio de Propiedades Termofísicas de Fluidos y Biomateriales de la USC y constituye su Tesis para optar al grado de Doctor.

Este trabajo está enmarcado en dos proyectos del Plan Nacional de investigación, "Influencia de la Estructura Molecular en las Propiedades Termofísicas y Tribológicas de Líquidos Iónicos en amplios rangos de presión para su uso en Lubricación" (MICINN, CTQ2008-06498-C02-01/PPQ) y "Nuevos lubricantes nanoestructurados basados en líquidos iónicos para energías renovables" (MINECO, CTQ2011-23925), y un proyecto autonómico "Efectos dos líquidos iónicos sobre o solo e as comunidades vexetais. Aplicación a parques eólicos e solares" (EM2013/031). Además parte de este trabajo corresponde a colaboraciones con otros grupos de investigación del Sistema Universitario Gallego que conforman la Red Gallega de Líquidos Iónicos (REGALIs, Xunta de Galicia CN2012/210 y R2014/015).

Así mismo autorizamos la presentación de esta memoria, considerando que reúne los requisitos exigidos en el artículo 34 del reglamento de Estudios de Doctorado.

Y para que así conste, firmamos el presente informe en Santiago de Compostela a 9 de Mayo de 2016.

Dra. Josefa Salgado   Dra. María Villanueva

A Pepi y María

A mi familia

A mis amigos

A Patricia

Agradecimientos

En primer lugar quisiera agradecer a mis directoras de Tesis, la Dra. Josefa Salgado Carballo y la Dra. María Villanueva López por darme la oportunidad de participar en este proyecto, por guiarme a lo largo del mismo y por su paciencia, apoyo y dedicación a lo largo de estos años. Y por supuesto, por los buenos ratos que pasamos.

A la Xunta de Galicia, por la ayuda a través del proyecto LISVAPES (Efectos dos líquidos iónicos sobre o solo e as comunidades vexetais. Aplicación a parques eólicos e solares), EM2013/031. Al Ministerio de Cultura e Innovación por financiar dos de los proyectos en los que se enmarca esta Tesis Doctoral.

Al Dr. Pedro Vázquez Verdes por confiar en mí para la parte experimental en el proyecto LISVAPES.

A Queta, María, Xurxo, José, Luis, Félix, Tamara, Inés, Tere, Fernando, Xavi, Chus, Pablo y a todos los que pasaron (aunque solo fuesen un par de semanas) por el laboratorio, gracias por su compañía, apoyo y alegría en esta etapa. A ti también Pepa, que estuviste ahí hasta la recta final.

A mis padres y abuelos, por su cariño y apoyo, y porque gracias (o pese) a ellos soy como soy. Y sobre todo a ti mamá por enseñarme a afrontar la vida con optimismo.

Al Campo da Angustia C.F., porque tras tantos años, y no pocas derrotas, hice muy buenos amigos y pasé muy buenos momentos.

A mis amigos de toda la vida; Brais, David, José Manuel, Martín y Rubén. Sin olvidarme de ti Pepe, que me hubiese encantado que estuvieses a mi lado en ésta, y otras etapas.

Y por supuesto, estas últimas líneas son para ti, Patricia, porque tú sufriste y disfrutaste conmigo estos años (y los que vendrán), y estuviste siempre cuando te necesité.

A todos ellos, de nuevo, gracias.

Abstract

This PhD Thesis is focused on the applicability of thermal analysis and calorimetry techniques to determine phase transitions, thermal stability and ecotoxicity of ionic liquids (ILs) to be used as lubricants and/or absorbents in heat pumps. The studied compounds are based on different anions (imide, triflate, sulphonate, phosphate) and cations (phosphonium, pyridinium, pyrrolidinium, imidazolium, choline) in order to determine possible dependences of these properties according to a selected ion.

Phase transitions: glass transition (t_g), cold crystallization (t_{cc}), solid-solid transition (t_{ss}) melting (t_m), and freezing (t_f) temperatures were determined through Differential Scanning Calorimetry on the interval temperature of (-75 to 120) ºC. All the selected ILs presented an endothermic peak attributed to melting point, indicating crystalline phase presence for all of them.

Thermal stability was measured by Thermogravimetric Analysis (TGA). Due to the extensive variability on previous bibliographic reports, first of all, a broad study on the experimental conditions dependence has been done, reporting that thermal stability is higher on Nitrogen atmosphere and the associated degradation temperature increase whenever the heating rate decreases. To determine the real thermal stability, dynamic and isothermal methods have been combined, due to the overestimation of dynamic scans on decomposition temperatures. Dynamic scans showed that $[C_4C_1C_1Im][OTf]$ has the highest (436 ºC) and $[C_2C_1Im][C_6SO_4]$ the lowest t_{onset} values for the selected ILs, meanwhile, on lubricant bases, DiPEC7 presents a t_{onset} of 318 ºC and 3 of the lubricant bases show lower t_{onset} values tan ILs. Nevertheless the maximum operation temperature of the selected ILs depends on the exposition time, and it is between 150 ºC and 200 ºC lower than the corresponding onset temperatures. Activation energy was determined by isothermal methods for most selected ILs. In order to validate the obtained these results, kinetic dynamic analysis was also applied to one of the aforementioned ILs ($[C_4C_1C_1Im][NTf_2]$), obtaining very similar values. ILs ageing effect was also analysed with this technique, showing that the successive repetition of heating and cooling cycles, does not affect the thermal stability of the sample, if the temperature limit of these cycles is below the maximum operation temperature previously calculated.

From the results of both techniques, the liquid range of the selected ILs was estimated using as limits of this interval t_m and $t_{onset}/t´_{0.10/10h}$. Liquid range temperature values were determined since 145 ºC for $[C_2py][C_1SO_3]$

to 299 ºC for [C$_4$C$_1$Pyrr][NTf$_2$] for the selected ILs, and 208 ºC for Krytox GPL 105.

With the aim to stablish a protocol of actuation, ecotoxicity of two of the most studied ILs was analysed; microbial activity of soils was studied by isothermal microcalorimetry, *Thermal Activity Monitor (TAM)*, obtaining those doses of 10% of a water solution of these ILs provoked a big stress on microorganisms of the selected soils, followed by their death. These results were also compared with that of seed germination test after adding the same doses of both ILs.

Keywords: Ionic liquids, lubricants, phase transitions, thermal stability, liquid range, temperature operation range, microcalorimetry, TGA, DSC, TAM, green chemistry.

Resumen

Esta Tesis Doctoral se centra en la aplicación de técnicas de análisis térmico y calorimétrico para determinar transiciones de fase, estabilidad térmica y ecotoxicidad de los líquidos iónicos (LIs) para ser propuestos como lubricantes y/o absorbentes en bombas de absorción de calor. Los compuestos estudiados están basados en diferentes aniones (imida, triflato, sulfonato, fosfato) y cationes (fosfonio, piridinio, pirrolinidio, imidazolio y colina) para poder determinar posibles dependencias de estas propiedades según el ión seleccionado.

Mediante Calorimetría Diferencial de Barrido (DSC) se determinaron las transiciones de fase en el intervalo de temperaturas (-75 a 120) ºC transición vítrea (t_g), cristalización fría (t_{cc}), sólido-sólido (t_{ss}), temperaturas de fusión (t_m) y cristalización (t_f), de los diferentes LIs se determinaron Todos los LIs analizados presentaron pico endotérmico atribuido a la fusión, indicando la presencia de fase cristalina en todos los LIs.

La estabilidad térmica se determinó mediante Análisis Termogravimétrico (TGA). Dada la variabilidad de los resultados bibliográficos previos, se ha realizado, en primer lugar, un estudio profundo de la dependencia de las condiciones experimentales, observándose que la estabilidad térmica es mayor en atmósfera de Nitrógeno y que las temperaturas asociadas a la degradación aumentan a medida que disminuye la velocidad de barrido. Para determinar la estabilidad térmica real, se combinaron estudios dinámicos e isotermos, ya que los estudios dinámicos sobreestiman el valor de la temperatura de degradación. Mediante los estudios dinámicos se observó que el $[C_4C_1C_1Im][OTf]$ presenta el mayor valor de la t_{onset} (436 ºC), mientras que el $[C_2C_1Im][C_6SO_4]$ es el valor más bajo de los LIs (251 ºC); para las bases lubricantes, el DiPEC7 presenta un valor de la t_{onset} de 318 ºC y 3 de las bases lubricantes presentan valores menores de la t_{onset} que los LIs. Sin embargo, se observa que las temperaturas máximas de uso dependen del tiempo de exposición, y se ha obtenido que, en general, estas temperaturas límite son entre (150 y 200) ºC menores que las correspondientes t_{onset}. Se determinó la energía de activación mediante métodos isotermos para la mayoría de los LIs seleccionados. Para tratar de validar estos resultados también se aplicaron análisis dinámicos para uno de los LIs estudiados ($[C_4C_1C_1Im][NTf_2]$), encontrándose valores muy similares. Con ésta técnica también se analizó el efecto del envejecimiento en los LIs, observándose que la sucesiva reiteración de ciclos de enfriamiento y calentamiento, no afecta a la

estabilidad térmica de la muestra, si la temperatura límite de estos ciclos está por debajo de la temperatura máxima de operación calculada previamente.

De los resultados de ambas técnicas, se estimó el rango líquido de los LIs seleccionados usando como límites de este intervalo las temperaturas de t_m y $t_{onset}/t'_{0.10/10h}$ respectivamente. Se han determinado valores de rango líquido de temperatura desde 145 ºC para el $[C_2py][C_1SO_3]$ hasta 299 ºC para el $[C_4C_1Pyrr][NTf_2]$ para los LIs, y de 208 ºC para el Krytox GPL 105.

Con el objetivo de introducir protocolos de actuación para determinar los efectos tóxicos de los LIs, se analizó el efecto sobre la actividad microbiana de suelos después de la adición de diferentes dosis de los dos LIs más estudiados en la bibliografía. Para ello se usó un microcalorímetro isotermo ultraestable (TAM), obteniéndose que las dosis del 10% en agua de estos LIs provocan un gran estrés en los microorganismos seguido de la muerte de los mismos, para los suelos seleccionados. Estos resultados se compararon con los obtenidos del test de germinación de semillas después de la adición de las mismas dosis de ambos LIs.

Palabras clave: Líquidos iónicos, lubricantes, transiciones de fase, estabilidad térmica, rango líquido, rango de temperatura de operación, microcalorimetría, TGA, DSC, TAM, química verde.

Resumo

Esta Tese Doutoral centrase na aplicación de técnicas de análise térmico e calorimétrico para determinar transicións de fase, estabilidade térmica e ecotoxicidade dos líquidos iónicos (LIs) para ser propostos como lubricantes e/ou absorbentes en bombas de absorción de calor. Os compostos estudados están baseados en diferentes anións (imida, triflato, sulfonato, fosfato) e catións (fosfonio, piridinio, pirrolinidio, imidazolio, colina) para poder determinar posibles dependencias destas propiedades segundo o ión seleccionado.

Mediante Calorimetría diferencial de Varrido (DSC) determináronse as transición de fase no intervalo de temperaturas (-75 a 120) ºC, transición vítrea (t_g), cristalización fría (t_{cc}), sólido-sólido (t_{ss}), temperaturas de fusión (t_m) e conxelación (t_f). Todos os LIs analizados presentaron pico endotérmico atribuído á fusión, indicando a presenza de fase cristalina en todos eles.

A estabilidade térmica foi determinada mediante Análise Termogravimétrico (TGA). Dada a variabilidade dos resultados bibliográficos previos, realizouse, en primeiro lugar, un estudo profundo da dependencia das condicións experimentais, observándose que a estabilidade térmica é maior en atmosfera de Nitróxeno e que as temperaturas asociadas á degradación aumentan a medida que diminúe a velocidade de varrido. Para determinar a estabilidade térmica real, combináronse estudos dinámicos e isotermos, posto que os estudos dinámicos sobreestiman o valor da temperatura de degradación. Mediante os estudos dinámicos observouse que o [C$_4$C$_1$C$_1$Im][OTf] presenta o maior valor da t_{onset} (436 ºC), namentres [C$_2$C$_1$Im][C$_6$SO$_4$] é o que presenta o valor máis baixo dos LIs (251 ºC); nas bases lubricantes, o DiPEC7 mostra un valor da t_{onset} de 318 ºC e 3 das bases lubricantes presentan valores menores da t_{onset} que os LIs. Con todo, observouse que a temperatura máxima de operación dos LIs depende dos tempos aos que estes estean expostos, e así obtívose que, en xeral, as temperaturas límite son entre (150 e 200) ºC menores que as determinadas t$_{onset}$. Determinouse a enerxía de activación mediante métodos isotermos para a maioría dos LIs seleccionados. Para tratar de validar estes resultados,tamén se aplicaron análises dinámicos para un dos LIs estudados ([C$_4$C$_1$C$_1$Im][NTf$_2$]), atopando valores moi similares. Con esta técnica tamén se analizou o efecto del envellecemento nos LIs, observándose que a sucesiva reiteración de ciclos de arrefriado e quecemento non afecta a estabilidade térmica da mostra, se a temperatura

límite destes ciclos está por debaixo da temperatura máxima de operación calculada previamente.

Dos resultados de ambas técnicas, estimouse o rango líquido dos LIs seleccionados tomando como límite do intervalo as temperaturas t_m e $t_{onset}/t´_{0.10/10h}$. Determináronse valores do rango líquido de temperatura dende 145 ºC para o $[C_2py][C_1SO_3]$ ata 299 ºC para o $[C_4C_1Pyrr][NTf_2]$nos LIs, e de 208 ºC para o Krytox GPL 105, cando determinamos o rango líquido co valor de $t´_{0.10/10h}$.

Co obxectivo de establecer futuros protocolos de actuación, analizouse a variación da actividade microbiana do solo despois da adición de diferentes doses dos dous LIs máis estudados na bibliografía. Para isto usouse un microcalorímetro isotermo ultraestable (TAM), obténdose que as doses do 10% en auga de ámbolos dous LIs provocan un gran estres nos microorganismos seguido da morte dos mesmos, para os solos seleccionados. Finalmente, comparáronse estes resultados cos obtidos dos test de xerminación de sementes despois da adición das mesmas doses dos mesmos LIs.

Palabras clave: Líquidos iónicos, lubricantes, transicións de fase, estabilidade térmica, rango líquido, rango de temperatura de operación, microcalorimetría, TGA, DSC, TAM, química verde.

Index

1.Introduction

1.1. Context

It is well known the need of green solvents on industry to avoid problems as toxicity, flammability and high volatility which allows the release of hazardous substances to the environment. This current situation of the world economy requires the search for alternative energies to conventional fuels, optimization of current energy technologies minimizing the environmental impact, and the search for new and clean working fluids in order to decrease the energy consumption without destroying the developmental needs of different countries [1].

Lubricants are substances capable of reducing friction, heat, and wear when they are introduced as films between solid surfaces. Use of lubricants allows more work to be done for the same amount of energy input, lowering the temperatures of the materials in contact, and greatly extending the lifespan of the moving equipment. Lubrication must have special attention in most of technologies. Some estimations emphasize that bearing failures can cause the 40% of a hydropower plant's operating losses, indicating that the current technology is inadequate for the markets demands [2]. European Union, and governments of the various states in particular, are promoting research in replacing mineral oil by biodegradable bases, such as polyalkylene, ester, vegetable type and Ionic Liquids (ILs), since the currently used compounds are highly polluting; besides this characteristic this new solvents also might have better lubricating properties. Thus, one of the current challenges is the development of new lubricants with a high technical performance and more environmentally friendly. There are several different types of lubricants available for commercial use, each suited to particular applications and circumstances. Today, practically all types of lubricants contain at least one additive. Depending on the application, additives may be mixed with the refined oil to lend it the desired physical properties. For example, the percentage of additives for steam turbines or compressors varies between 0.5% and 5%, whereas for hydraulic systems the percentage of additives is between 2%

and 10% [3]. Several ILs have been evaluated as lubricants and lubricant additives with promising results in recent years [4].

Other important technology to mention is the absorption heat pumps, that are a great opportunity to reduce energy consumption of heating and refrigeration systems, since this technology allows either recovering residual heat or using renewable energies (as solar, bio-hydrogen...) to produce profitable thermal energy. Subsequently, the use of additional electric power is almost negligible. Therefore this is a technology of high added value in regions where the electrical network is not developed, besides its high ecological benefits. Nevertheless, conventional working pairs present several drawbacks which have limited the potential of absorption heat pumps [5]. Some of these problems are corrosion and crystallization in the case of $H_2O/LiBr$, high working pressures, low relative volatility and NH_3 toxicity for NH_3/H_2O. Thus, improvements of absorption heat pumps by developing new working pairs (refrigerant/absorbent) have drawn attention of companies and researchers. Seeking new working pairs involving ILs as absorbents occupy a principal role in these investigations [6].

1.2. Ionic liquids

ILs are a class of molten salts that are liquid below 100 °C. A subclass, denoted room-temperature ionic liquids (RTILs), is even liquid below ambient temperature. The first room temperature ionic liquid which turned up in literature was ethylammonium nitrate, in 1914 by Sugden & Wilkins [7]. Although there have been some experiments considering industrial applications of ILs, they were negated for many decades.

Halide based salts are the most widely studied class of room temperature ionic liquids. Moreover, these salts are precursors for several air and water stable RTILs; *e.g.* numerous di-alkylimidazolium based ionic liquids (C_nMImPF_6, C_nMImBF_4, $C_nMImNTf_2$, etc.) are synthesized from dialkylimidazolium chlorides. The mixture of di-alkylimidazolium chloride ($[R_1R_2Im]Cl$) and $AlCl_3$,

which are termed as chloroaluminate ionic liquids, have been extensively studied for metal/alloy deposition and transition metal catalysis.[8]

ILs possess several properties which make them so interesting; namely, non-volatility, non-flammability, high thermal stability, high polarity, large electrochemical window, high thermal conductivity and one of the most important, their "tunability", *i.e.* it is possible to obtain a wide variety of ILs by the combination of different ions. It was estimated that the possible number of ILs from the combinations of known anion and cation is higher than 10^{12}. Therefore, ILs have been recognized as "designer-solvents." [9]. These salts have bulky, organic cations, *e.g.* alkylated imidazole, pyrrole or pyridine derivatives or quaternized alkyl amines and alkyl phosphines. Common anions are, *e.g.* halides, alkyl sulphates, fluorinated hydrocarbons, carboxylic acids or amino acids [10,11]. The physical and chemical properties of ILs are customizable by the choice of different cation-anion combinations, and by the length of the alkyl chain of the cation. Due to the outstanding and versatile properties of ILs, various applications in chemistry, engineering to materials and pharmaceutical science have been developed in the recent years. The employment of ILs has turned out to be an option to intensify processes, in order to overcome disadvantages of conventional approaches and to reduce energy and material consumption.

The increasing interest on Ionic Liquids in the lasts decades, has coincided with the beginning of the Green Chemistry [12]. Figure 1.1 shows this rising about publications on this topic.
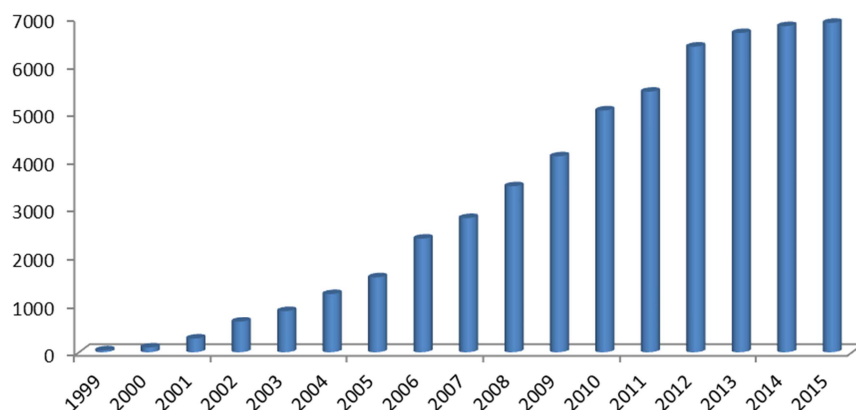
Figure 1.1. Scientific publications about ILs (*data extracted from Scifinder, keyword: "Ionic liquids"*).

Notwithstanding the amazing number of possible ILs and publications, only a small number have been studied. The most frequent cations used in lubrication works are imidazolium, pyridinium, fosfonium and ammonium together with the anions tetrafluoroborate, hexafluorophosphate, phosphate and bis(trifluoromethylsulfonyl)imide (Fig. 1.2). For absorption heat pumps, the most used are also imidazolium and ammonium, mainly with triflate anion [6].
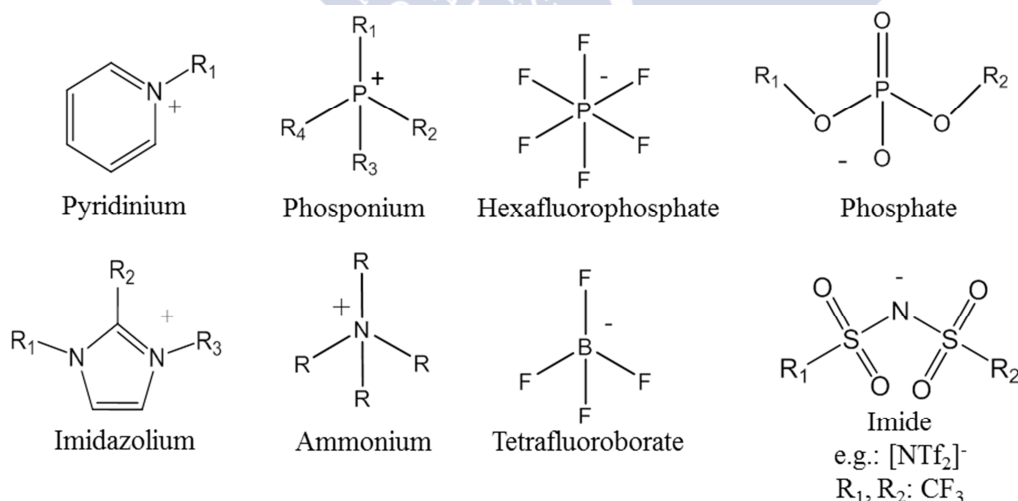
Figure 1.2. Some of the most frequent anions and cations used in lubrication works.

Before considering a new fluid/substance for incorporation into a specific industrial application, a fundamental understanding must be established for the

6

chemical and physical properties of this fluid. For academic research, physic-chemical properties are also indispensable to validate the theoretical models or to select proper ILs [13].

1.2.1. Applicability

Beside the above mentioned applications, lubrication and absorbent for absorption heat pumps [4,6,14,15], ILs can have multiple applicability, in the last years many studies have determined some of these properties for these compounds, *i.e.*, as electrolytes on batteries [16], as safe electrolyte components for Li-metal and Li-ion batteries [17], keep the stability of proteins in an aqueous solution at high temperatures [18], as stationary phases for gas chromatography [19], effect of IL dispersion on Li^+ ion glasses and glass-ceramics [20], media for liquid-liquid extraction [21], as mobile phase additives in high-performance liquid chromatography [22], potential application in the extraction and separation of nonferrous metal [23], as electrolytes [24], as solvents for a wide range of synthetic procedures [10] etc. To decide which IL is the most suitable for a defined application, previous characterization must be performed. The knowledge of structure influence on the thermophysical properties is essential to choose the right combination (anion, cation, functional groups, etc.) of the adequate ILs to the specific application.

1.2.2. Thermophysical properties

Some of the more important thermophysical properties are presented on this section:

➢ Density

Typical densities of ILs range from 0.96 to 1.65 g/cm^3 at 293 K, and decrease with temperature. Values are, in general, larger than most of the current molecular liquids.

This property seems to be strongly dependent on the anion. Some authors have found the following density sequence [25,26]:

$[FAP]^- > [NTf_2]^- > [OTf]^- > [B(CN)_4]^-$.
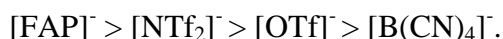
Fernández and Gaciño [27] obtained the following trend for some cations with common anion $[NTf_2]^-$: imidazolium > pyridinium > pyrrolidinium. Density of ILs decreases when the number of the alkyl chains increases.

➢ Viscosity

This property varies widely depending on the type of cation and anion, ranging from 6 to 7600 mPa at 20 ºC and atmospheric pressure. This property depends strongly on the molecular structure and it is highly dependent on the interactions between the ions: electrostatic, van der Waals interactions, and hydrogen bonding [28].

It seems that the viscosity of ILs is more dependent on the anion structure than on the cation. The most known anions follow the trend:

$[FAP]^- < [OTf]^- < [BF_4]^- < [C_2SO_4]^- < C_1SO_4^- < [C_6SO_4]^- < [PF_6]^- < [CH_3COO]^- < [Cl]^- < [Br]^-$.
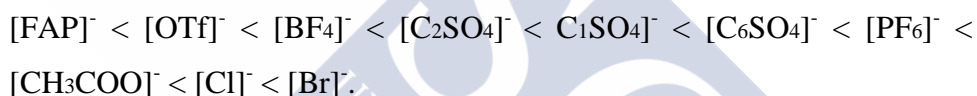
➢ Electrical conductivity

Because ILs are entirely composed by ions, a high electrical conductivity should be expected. However, their values at 25 ºC, ranged from 0.0017 S/m for $[C_8C_4C_4C_4N][OTf]$ to 11.874 S/m for $[C_1C_1Im][Cl]$, which are quite low in comparison with conventional aqueous electrolyte solutions used in electrochemical applications (40-75 S/m). These low conductivity values can be attributed to the available charge carriers, because of ion paring and/or ion aggregation as well as the reduced mobility resulting from the large ion size. Their "tunability" offers the possibility of designing a liquid with a specific conductivity value. [27]

➢ Surface tension

Surface tension is an important property in the study of physics and chemistry at free surfaces because of its influence on transfer rates of

vapour absorption at the vapour- liquid interfaces. For this reason, the relationships between the chemical structure and the surface tension are essential in many engineering fields, such as chemical process and reactor, flow and transport in porous media, materials selection, biomedical and biochemical fields, electronic and electrical engineering, as well as in environmental science and biology. [27]

In general, the liquid/air surface tension values of ILs are higher than those of conventional solvents (hexane 18 mN/m at 298 K) and organic compounds, but not as high as water (71.97 mN/m at 298 K). [27]

➢ Solubility

Ionic liquids can act as both, hydrogen bond acceptors (anion) and donors (cation); for this reason they can interact with substances with both accepting and donating sites. Ionic liquids can be divided into two groups (water-miscible and water immiscible) according to their water solubility. Some water-immiscible ionic liquids are 1-butyl-3-methylimidazolium hexafluorophosphate and 1-decyl-3-methylimidazolium bis(trifluoromethylsulfonyl) imide. Examples of water miscible ionic liquids include [1-Butyl-3-methylimidazolium tetrafluoroborate. Miscibility of ionic liquids in water is mainly dependent on the anion present, although it is also dependent on the structure of the cation.[29]

The low solubility of ILs with base oils is an important issue for their application as additives. In general, the ILs miscibility increases with the polarity of the base stock. [4]

➢ Chemical Stability

Composition of the anion as well as the strength of the anion–cation bond of ionic liquids are crucial factors influencing on their chemical stability [30].

➤ Electrochemical window

The electrochemical potential window, which depends on the oxidative and reductive stabilities of the selected solvent, is a key criterion for electrochemical studies. In case of ILs, the potential window is primarily dependent on the resistance of the cation to reduction and the resistance of the anion to oxidation. ILs generally have a potential window of more than 2.0 V. However, impurities in the ILs have a deep impact on the anodic or cathodic potential limits and the corresponding electrochemical potential window.[31]

➤ Thermal stability

Thermal stability gives information about the higher temperature that a material can support without losing its properties, *i.e.,* about the stable temperature limit. [8]. The knowledge of this temperature is necessary to determine the upper limit of the liquid range temperature, which can be defined as the interval between melting or glass transition and degradation temperatures. The most common criterion employed to characterize the thermal stability of a substance is through the onset temperature (t_{onset}), which is usually measured through dynamic scans under a controlled atmosphere in thermogravimetric analysis. However, some controversial exists about this criterion; this is one of the reasons why in this PhD Thesis the selection of an alternative method to characterize the thermal stability of ILs was proposed

➤ Green chemistry/aspects

Green chemistry is defined as the design of chemical products and processes which reduce or eliminate the use and generation of hazardous substances [32,33]. All the aforementioned properties of ionic liquids make them interesting as potentially 'green' solvents with little associated hazard [34]. For this reason, hazard assessment of ILs became an important

area of research; studies of toxicity, ecotoxicity and biodegradation of ionic liquids have been widely reported [33-37]. So far, toxicity of ILs has been evaluated through different models, *i.e.*, involving microorganisms [38-40] as well as terrestrial invertebrates such as earthworms, [41] aquatic species, including the zebrafish (*Danio rerio*) [42] as well as water fleas (*Daphnia magna*) [43,44] and algae [37]. The toxicity of ionic liquids towards terrestrial plants has also been investigated and more recent studies have even screened human cells [45].

Many classes of ionic liquid are water soluble, although this property is not so noticeable for those containing lipophilic anions, such as bis(trifluoromethyl)- sulfonyl amide [NTf$_2$], or hexafluorophosphate [PF$_6$] anions. Even though ionic liquids may help reduce the risk of air pollution, their water solubility could cause severe contamination when they are released to aquatic environments because of their potential toxicity and inaccessible biodegradability [46]. As a result, this problem can also affect to the soil health in case of leaching contaminated water.

Despite the big database of ILs properties now available, there are some aspects as the long-term thermal degradation; the liquid range temperature and the toxicity that are still open questions. Thereby, this PhD Thesis tries to complete the analysis of these properties for a selection of ILs that could be proposed as lubricants or lubricant additives and absorbents in absorption heat pumps.

1.3. Thermal analysis

The term thermal analysis (TA) implies a broad quantity of analytical experimental techniques such as differential scanning calorimetry (DSC), differential thermal analysis (DTA), thermogravimetric analysis (TGA), thermomechanical analysis (TMA), dynamic mechanical analysis (DMA) and thermal activity monitor (TAM) [47]. Table 1.1 shows each of these techniques and

their related properties. In this work, DSC and TGA techniques will be used to characterize some compounds.

Table 1.1. TA techniques and related properties.

TA method	Property
DSC	Enthalpy
TGA	Mass
DTA	Difference temperature
TMA	Deformation
DMA	Deformation
TAM	Heat flow

Advantages of TA techniques above other analytical methods can be summarized as:

- The sample can be studied over a wide range according to different temperature programs
- Almost any physical state (solid, liquid and gel) can be analyzed
- A small quantity of sample (0.1 μg – 1 g) is needed
- Sample atmosphere can be standardized
- Time required to analysis takes from several minutes to several hours

DSC is one of the most known TA techniques, and is very useful for studying endothermic and/or exothermic phenomena (transitions, chemical reactions, adsorptions…) occurring on samples. [48]

Thermogravimetric analysis (TGA) is the TA technique which examines the mass change of a sample as a function of temperature (dynamic scan) or as a function of time (isothermal scan). Some thermal events present a change in the sample mass as desorption, absorption, sublimation, vaporization, decomposition,

oxidation and reduction, as it can be seen in Figure 1.3. and can be observed with this technique.
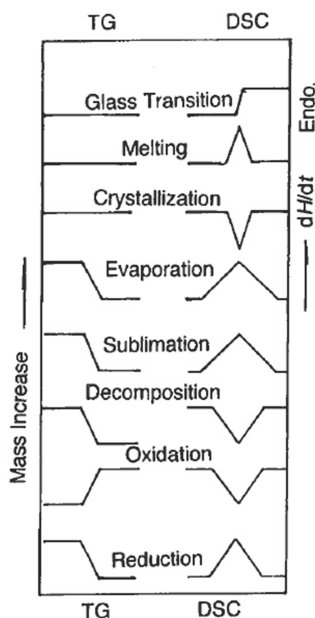
Figure 1.3. Schematic comparison of TG and DSC curves against temperature for a variety of physic-chemical processes [47].

Isothermal microcalorimetry is an extremely general technique which measures the heat production rate that accompanies nearly all physical, chemical and biological process. The role of this technique has been increased during last years in the microbiological field due to its simplicity, versatility and analysis speed. [49]

Applications of DSC, TGA and TAM analysis

DSC technique has a broad range of applications. This technique can provide the measurements of many different phase transition temperatures such as: melting (t_m), freezing (t_f), glass transition (t_g), cold-crystallization (t_{c-c}) and solid-solid (t_{s-s}) temperatures. DSC can be used to estimate the enthalpy of a transition, ΔH. The purity of a sample can be estimated by DSC. Temperature associated with crystal to crystal transitions on polymorphism are measured using DSC.

TGA technique can determine the onset (t_{onset}) and endset (t_{endset}) temperature, moreover the temperature of different peaks on DTG curves (t_{1st}, t_{2nd} …).[50-52]

The following scheme summarize some calorimetry and thermal analysis applications, reported in the literature

Technique	Application
DSC	Determination of proportions of water fractions present in different substances [47]
	Measurements of the enthalpies of crystal-structure transformations [53]
	To perform heat capacity (C_p) measurements of a sample [54]
	Evaluation of catalyst activities [55]
	Estimation of concentration of several clays and minerals [56]
	Characterization of oil shales [57] and petroleum [55]
	Determination of the composition of different pharmaceutical compounds [58]
TGA	Determination of the reaction rate kinetics [59-61]
	Energetic characterization of forest biomass [62]
	Study of coals, oil shales and oil sands on fuels [63]
	Determination of some inorganic materials presence [64,65]
	Determination of reaction sequences on thermal decomposition of substances [66-69]
	Unusual weight loss observed in samples at elevated temperatures [70].
	Identification of different pharmaceuticals compounds [71,72]
	Determination of composition on pure pharmaceuticals [58]
	Characterization of additive content on polymeric materials [73]
	Predicting tool on disease detection [74].
TAM	Detection of heavy metals on microorganisms [75]
	Interesting tool for looking at kinetics of all types of reactions and processes [49]
	Biological applications in food science and technology (milk fermentation, cell death from blanching, microbiological spoilage prevention, thermal treatment or shelf life) [49]
	On pharmaceutical industry; as a rapid, practical and predictive excipient compatibility screening [76] or quantification of small degrees of disorder in lactose [77]
	Drug efficacy on life sciences [78]

1.4.Framework

This PhD Thesis was carried out within the framework of three funded national research projects. This PhD Thesis was developed on the Laboratory of Thermophysical Properties of Fluids and Biomaterials (PTFB).

The first project was LUBIONIC (molecular structure influence on thermophysical and tribological properties of ionic liquids in broad pressure ranges for their use in lubrication), CTQ2008-0698-C02-01, Ministerio de Ciencia e Innovación. This project was carried out in collaboration with the companies Merck KGaA (the company that provided all the ILs samples), Verkol Lubricantes, Repsol, Gamesa and Croda. The aims of this project were to analyse the thermophysical and tribological properties of ILs, according to their molecular structure, in a broad range of temperature and pressure for their use in lubrication. ILs samples were tested as pure lubricants and lubricant additives of conventional base oils in applications under regime of lubrication. The following properties have been analysed: thermal stability, heat capacity, density and viscosity, tribological properties and miscibility of ILs with biodegradable lubricants [25,26,51,79-90].

The second project was RENELUBIL (New nanostructured lubricants on ionic liquids for renewable energies), CTQ2011-2395, Ministerio de Ciencia e Innovación. The objective of this project was to obtain new nanostructured lubricants based on ILs for their use in renewable energies, mainly as gear lubricants. This project started from the need of developing new "green" oils for wind turbines and gear based on biodegradable oils, such as polyalkylene glycols and esters, and ILs. ILs were selected taking into account their potential affinity with base lubricants, their potential toxicity and biodegradability. To analyse the suitability of ILs as lubricants, several properties were analysed: thermal stability, melting and glass transition, viscosity and density at different pressures and the miscibility of ILs in the lubricants. The results allow evaluating if the new

15

lubricants are more effective than the reference oils whether in boundary and lubrication regimes. [4,15,25,50,51,79,80,83-93]

The third project was LISVAPES (Efectos dos líquidos iónicos sobre o solo e as comunidades vexetais. Aplicación a parques eólicos e solares), EM2013/031, Xunta de Galicia. The objective of this Project was the evaluation of toxicity of ILs on different soil and seed samples. First of all it was analysed the thermophysical properties of a large number of ILs [15,50]. Afterwards, addition of different doses of ILs concentration (pure and degraded samples) and common salts to two kind of different soils, and evaluation of germination response after the addition of these ILs doses.

In addition, the Galician network REGALIS R2014/015 (Xunta de Galicia, Spain), composed of 13 researchers groups of the three Galician universities have collaborated to explore the potential of the ILs in the context of fundamental and applied chemistry, materials science and engineering.

1.5. Objectives

The main aim of this PhD Thesis is to perform an experimental study of ILs in order to propose them as possible "green" substitutes on lubrication or additives, through study of several relevant thermophysical properties.

Specific objectives of this PhD Thesis are:

- To determine the different state transitions experienced by the IL during heating and cooling cycles
- To seek for DSC experimental data of some of the selected ILs and the lubricant bases
- To determine the influence of experimental conditions, atmosphere, initial mass, heating rate and water content on the results of degradation temperature.
- To analyse the effect of aging on the t_{onset}

- To analyse the Maximum Operation Temperature (MOT) of the selected ILs and lubricant bases.

- To determine the activation energy of the selected ILs and lubricant bases through isothermal studies.

- To compare activation energy values obtained through isothermal and through dynamic studies of some of the ILs.

- To discern about evaporation or degradation on the mass loss processes occurred during TGA experiments.

- To determine the lower and upper limits of the liquid range of the selected ILs and lubricant bases, with the help of DSC and TGA, respectively.

- To analyse the effect of the addition of different dose on the microbial activity in two different soils and on the germination of seed of different species of pine and eucalyptus.

1.6. References

(1)   Nieto de Castro, C. A.; Lourenço, M. J. V.; Ribeiro, A. P. C.; Langa, E.; Vieira, S. I. C.; Goodrich, P.; Hardacre, C.: Thermal Properties of Ionic Liquids and IoNanofluids of Imidazolium and Pyrrolidinium Liquids. *J. Chem. Eng. Data* **2010**, *55*, 653-661.

(2)   Simmons, G. F.; Cerda Varela, A.; Santos, I. F.; Glavatskih, S.: Dynamic characteristics of polymer faced tilting pad journal bearings. *Tribol. Int.* **2014**, *74*, 20-27.

(3)   research, t. m.

(4)   Otero, I.; López, E. R.; Reichelt, M.; Villanueva, M.; Salgado, J.; Fernández, J.: Ionic Liquids Based on Phosphonium Cations As Neat Lubricants or Lubricant Additives for a Steel/Steel Contact. *ACS App. Mat. Interf.* **2014**, *6*, 13115-13128.

(5)   Seiler, M.; Kühn, A.; Ziegler, F.; Wang, X.: Sustainable Cooling Strategies Using New Chemical System Solutions. *Ind. Eng. Chem. Res.* **2013**, *52*, 16519-16546.

(6)   Lorenzo, M.; Vilas, M.; Verdia, P.; Villanueva, M.; Salgado, J.; Tojo, E.: Long-term thermal stabilities of ammonium ionic liquids designed as potential absorbents of ammonia. *RSC Advances* **2015**, *5*, 41278-41284.

(7)   Sugden, S.; Wilkins, H.: CLXVII.-The parachor and chemical constitution. Part XII. Fused metals and salts. *J. Chem. Soc.* **1929**, 1291-1298.

(8)   Kamavaram, V.; Reddy, R. G.: Thermal stabilities of di-alkylimidazolium chloride ionic liquids. *Int. J. Therm. Sci.* **2008**, *47*, 773-777.

(9)   Zhang, S.; Sun, N.; He, X.; Lu, X.; Zhang, X.: Physical Properties of Ionic Liquids: Database and Evaluation. *J. Phys. Chem. Ref. Data* **2006**, *35*, 1475-1517.

(10)   Welton, T.: Room-temperature ionic liquids. Solvents for synthesis and catalysis. *Chem. rev.* **1999**, *99*, 2071-2084.

(11)   Keil, P.; Kick, M.; König, A.: Long-Term Stability, Regeneration and Recycling of Imidazolium-based Ionic Liquids. *Chem. Ing. Tech.* **2012**, *84*, 859-866.

(12)   Welton, T.: Ionic liquids in Green Chemistry. *Green Chem.* **2011**, *13*, 225-225.

(13)   Huddleston, J. G.; Visser, A. E.; Reichert, W. M.; Willauer, H. D.; Broker, G. A.; Rogers, R. D.: Characterization and comparison of hydrophilic and hydrophobic room temperature ionic liquids incorporating the imidazolium cation. *Green Chem.* **2001**, *3*, 156-164.

(14)   Predel, T.; Pohrer, B.; Schlücker, E.: Ionic Liquids as Alternative Lubricants for Special Applications. *Chem. Eng. Technol.* **2010**, *33*, 132-136.

(15)   Villanueva, M.; Parajó, J. J.; Sánchez, P. B.; García, J.; Salgado, J.: Liquid range temperature of ionic liquids as potential working fluids for absorption heat pumps. *J. Chem. Thermodyn.* **2015**, *91*, 127-135.

(16)   Puga, A. V.: *Líquidos iónicos como electrolitos estables para baterías de litio y otros dispositivos de almacenamiento de energía*; Real Sociedad Española de Química, 2012.

(17)   Navarra, M. A.: Ionic liquids as safe electrolyte components for Li-metal and Li-ion batteries. *MRS Bulletin* **2013**, *38*, 548-553.

(18)   Noritomi, H.: *Increase in Thermal Stability of Proteins by Aprotic Ionic Liquids*, 2013.

(19)   Poole, C. F.; Poole, S. K.: Ionic liquid stationary phases for gas chromatography. *J. Sep. Sci.* **2011**, *34*, 888-900.

(20)   Rathore, M.; Dalvi, A.; Kumar, A.; Ślubowska, W.; Nowinski, J. L.: Ionic liquid dispersed Li+ ion oxide glasses and glass-ceramics: Assessment of electrical transport and thermal stability. *Solid State Ionics* **2015**, *282*, 76-81.

(21)   Huddleston, J. G.; Willauer, H. D.; Swatloski, R. P.; Visser, A. E.; Rogers, R. D.: Room temperature ionic liquids as novel media for 'clean' liquid-liquid extraction. *Chem. Commun.* **1998**, 1765-1766.

(22)   Martín-Calero, A.; Pino, V.; Ayala, J. H.; González, V.; Afonso, A. M.: Ionic liquids as mobile phase additives in high-performance liquid chromatography with electrochemical detection: Application to the determination of heterocyclic aromatic amines in meat-based infant foods. *Talanta* **2009**, *79*, 590-597.

(23)   Tian, G.-c.; Li, J.; Hua, Y.-x.: Application of ionic liquids in hydrometallurgy of nonferrous metals. *T. Nonferr. Met. Soc.* **2010**, *20*, 513-520.

(24)   Usui, H.; Shimizu, M.; Sakaguchi, H.: Applicability of ionic liquid electrolytes to LaSi2/Si composite thick-film anodes in Li-ion battery. *J. Power Sources* **2013**, *235*, 29-35.

(25)   Regueira, T.; Lugo, L.; Fernández, J.: Influence of the pressure, temperature, cation and anion on the volumetric properties of ionic liquids: New experimental values for two salts. *J. Chem. Thermodyn.* **2013**, *58*, 440-448.

(26)   Gacino, F. M.; Regueira, T.; Lugo, L.; Comunas, M. J. P.; Fernandez, J.: Influence of Molecular Structure on Densities and Viscosities of Several Ionic Liquids. *J. Chem. Eng. Data* **2011**, *56*, 4984-4999.

(27)   Fernández, J.; Gaciño, F. M.: Properties and green aspects of ionic liquids: Physical Properties of pure liquids Ionic liquids. In *Ionic liquids in Separation Technology*; Elsevier, Ed., 2014; pp 3-12.

(28)   Pensado, A. S.; Comunas, M. J. P.; Fernandez, J.: The pressure-viscosity coefficient of several ionic liquids. *Tribol Lett* **2008**, *31*, 107-118.

(29)   Gilmore, B. F.: *Antimicrobial Ionic Liquids, Ionic Liquids: Applications and Perspectives*; InTech, 2011.

(30)   García-Suárez, E. J.; Menéndez-Vázquez, C.; García, A. B.: Chemical stability of choline-based ionic liquids supported on carbon materials. *J. Mol. Liq.* **2012**, *169*, 37-42.

(31)   Liu, H.; Liu, Y.; Li, J.: Ionic liquids in surface electrochemistry. *Phys. Chem. Chem. Phys.* **2010**, *12*, 1685-1697.

(32)   Anastas, P. T.; Warner, J. C.: *Green chemistry: theory and practice*; Oxford university press, 2000.

(33)   Seddon, K. R.: Ionic Liquids for Clean Technology. *J. Chem. Technol. Biotechnol.* **1997**, *68*, 351-356.

(34)   Coleman, D.; Gathergood, N.: Biodegradation studies of ionic liquids. *Chem. Soc. Rev.* **2010**, *39*, 600-637.

(35)   Amde, M.; Liu, J.-F.; Pang, L.: Environmental Application, Fate, Effects, and Concerns of Ionic Liquids: A Review. *Environ. Sci. Technol.* **2015**, *49*, 12611-12627.

(36)   Jordan, A.; Gathergood, N.: Biodegradation of ionic liquids - a critical review. *Chem. Soc. Rev.* **2015**, *44*, 8200-8237.

(37)   Matzke, M.; Stolte, S.; Thiele, K.; Juffernholz, T.; Arning, J.; Ranke, J.; Welz-Biermann, U.; Jastorff, B.: The influence of anion species on the toxicity of 1-alkyl-3-methylimidazolium ionic liquids observed in an (eco)toxicological test battery. *Green Chem.* **2007**, *9*, 1198-1207.

(38)   Matsumoto, M.; Mochiduki, K.; Fukunishi, K.; Kondo, K.: Extraction of organic acids using imidazolium-based ionic liquids and their toxicity to Lactobacillus rhamnosus. *Sep. Purif. Technol.* **2004**, *40*, 97-101.

(39)   Matsumoto, M.; Mochiduki, K.; Kondo, K.: Toxicity of ionic liquids and organic solvents to lactic acid-producing bacteria. *J. Biosci. Bioeng.* **2004**, *98*, 344-347.

(40)   Pernak, J.; Goc, I.; Mirska, I.: Anti-microbial activities of protic ionic liquids with lactate anion. *Green Chem.* **2004**, *6*, 323-329.

(41)   Swatloski, R. P.; Holbrey, J. D.; Memon, S. B.; Caldwell, G. A.; Caldwell, K. A.; Rogers, R. D.: Using Caenorhabditis elegans to probe toxicity of 1-alkyl-3-methylimidazolium chloride based ionic liquids. *Chem. Commun.* **2004**, 668-669.

(42)   Pretti, C.; Chiappe, C.; Pieraccini, D.; Gregori, M.; Abramo, F.; Monni, G.; Intorre, L.: Acute toxicity of ionic liquids to the zebrafish (Danio rerio). *Green Chem.* **2006**, *8*, 238-240.

(43)   Garcia, M. T.; Gathergood, N.; Scammells, P. J.: Biodegradable ionic liquids Part II. Effect of the anion and toxicology. *Green Chem.* **2005**, *7*, 9-14.

(44)   Wells, A. S.; Coombe, V. T.: On the Freshwater Ecotoxicity and Biodegradation Properties of Some Common Ionic Liquids. *Org. Process Res. Dev.* **2006**, *10*, 794-798.

(45)   Matzke, M.; Stolte, S.; Arning, J.; Uebers, U.; Filser, J.: Imidazolium based ionic liquids in soils: effects of the side chain length on wheat (Triticum aestivum) and cress (Lepidium sativum) as affected by different clays and organic matter. *Green Chem.* **2008**, *10*, 584-591.

(46)   Zhao, Y.; Zhao, J.; Huang, Y.; Zhou, Q.; Zhang, X.; Zhang, S.: Toxicity of ionic liquids: Database and prediction via quantitative structure–activity relationship method. *J. Hazard. Mater.* **2014**, *278*, 320-329.

(47)   Hatakeyama, T.; Quinn, F. X.: *Thermal analysis. Fundamentals and applications to polymer science*; John Wiley and Son, 1997.

(48)   Sorai, M.: *Comprehensive Handbook of Calorimetry and Thermal Analysis*; John Wiley & Sons, 2004.

(49)   Wadsö, L.; Gómez Galindo, F.: Isothermal calorimetry for biological applications in food science and technology. *Food Control* **2009**, *20*, 956-961.

(50)   Salgado, J.; Parajó, J. J.; Fernández, J.; Villanueva, M.: Long-term thermal stability of some 1-butyl-1-methylpyrrolidinium ionic liquids. *J. Chem. Thermodyn.* **2014**, *74*, 51-57.

(51)   Salgado, J.; Villanueva, M.; Parajó, J. J.; Fernández, J.: Long-term thermal stability of five imidazolium ionic liquids. *J. Chem. Thermodyn.* **2013**, *65*, 184-190.

(52)   Villanueva, M.; Coronas, A.; García, J.; Salgado, J.: Thermal Stability of Ionic Liquids for Their Application as New Absorbents. *Ind. Eng. Chem. Res.* **2013**, *52*, 15718-15727.

(53)   Rajeshwar, K.; Verneker, V. R. P.; Dubow, J.: A Differential Scanning Calorimetry study of the MClO4 (M = Na, K, Rb, Cs, and NH4) system: Heats of crystal-structure transformations and other thermochemical data. *Combust. Flame* **1980**, *37*, 251-260.

(54)   Berlin, E.; Kliman, P. G.; Pallansch, M. J.: Effect of sorbed water on the heat capacity of crystalline proteins. *Thermochim. Acta* **1972**, *4*, 11-16.

(55)   Wendlandt, W. W.: *Thermal analysis*; Wiley, 1986.

(56)   Ramachandran, V. S.; Polomark, G. M.: Application of DSC-DTA technique for estimating various constituents in white coat plasters. *Thermochim. Acta* **1978**, *25*, 161-169.

(57)   Jones, D. B.; Rajeshwar, K.; DuBow, J. B.: Specific Heats of Colorado Oil Shales. A Differential Scanning Calorimetry Study. *Ind. Eng. Chem. Prod. R.D.* **1980**, *19*, 125-128.

(58)   Radecki, A.; Wesołowski, M.: Studies on use of differential thermal and thermogravimetric techniques for checking compositions of some drug formulations. *J. therm. anal.* **1979**, *17*, 73-80.

(59)   Doyle, C. D.: Series Approximations to the Equation of Thermogravimetric Data. *Nature* **1965**, *207*, 290-291.

(60)   Friedman, H. L.: Kinetics of thermal degradation of char-forming plastics from thermogravimetry. Application to a phenolic plastic. *J. Pol. Sci. Part C: Pol. Symp.* **1964**, *6*, 183-195.

(61)   Wang, Z.; Fang, W.; Li, L.; Li, Y.; Yu, X.; Gu, Q.; Zhou, F.: Effects of an ionic liquid as an additive on the thermal denaturation/degradation of lysozyme crystals. *Asia-Pac. J. Chem. Eng.* **2015**, *10*, 163-169.

(62)   Villanueva, M.; Proupín, J.; Rodríguez-Añón, J.; Fraga-Grueiro, L.; Salgado, J.; Barros, N.: Energetic characterization of forest biomass by calorimetry and thermal analysis. *J. Therm. Anal. Calorim.* **2011**, *104*, 61-67.

(63)   Rajeshwar, K.: Thermal analysis of coals, oil shales and oil sands. *Thermochim. Acta* **1983**, *63*, 97-112.

(64)   Erdey, L.; Liptay, G.; Svehla, G.; Paulik, F.: Indirect derivatographic determination of calcium, strontium and barium ions in the presence of one another. *Talanta* **1962**, *9*, 489-493.

(65)   Biffen, F. M.: Determination of Free Lime and Carbonate in Calcium Sillicate Hydrates by Thermobalance. *Anal. Chem.* **1956**, *28*, 1133-1136.

(66)   Mahieu, B.; Apers, D. J.; Capron, P. C.: Thermal decomposition of ammonium dichromate. *J. Inorg. Nuc. Chem.* **1971**, *33*, 2857-2866.

(67)   Judd, M. D.; Plunkett, B. A.; Pope, M. I.: The thermal decomposition of calcium, sodium, silver and copper(II) acetates. *J. therm. anal.* **1974**, *6*, 555-563.

(68)   Judd, M. D.; Plunkett, B. A.; Pope, M. I.: The structures and thermal decomposition of cupric mono, di and trichloracetates. *J. therm. anal.* **1976**, *9*, 83-92.

(69)   Paulik, J.; Paulik, F.; Czárán, E.: The thermal decomposition of platinum tetrammine chloride. *Anal. Chim. Acta* **1978**, *101*, 409-412.

(70)   Clark, R. P.; Gallagher, P. K.; Dillard, B. M.: Thermoanalytical investigation of calcium chromate. *Thermochim. Acta* **1979**, *33*, 141-155.

(71)   Wendlandt, W. W.: The thermal analysis of some non-prescription antacids. *Thermochim. Acta* **1974**, *10*, 93-99.

(72)   Wendlandt, W. W.; Collins, L. W.: The identification of non-prescription internal analgesics by thermal analysis. *Anal. Chim. Acta* **1974**, *71*, 411-417.

(73)   Cassel, R. B.; Gray, A. P.: Microprocessor-controlled thermogravimetric separations. *Thermochim. Acta* **1980**, *36*, 265-277.

(74)   Risoluti R.; Gullifa G.; Materazzi S.; Sorrentino F.; P., C.: Early detection of ß-thalassemia: coupled tga/chemometrics as a powerful predicting tool. In *Mediterranean Conference on Calorimetry and Thermal Analysis (MEDICTA)*: Girona, 2015.

(75)   Chen, H.-Y.; Yao, J.; Zhou, Y.; Chen, H.-L.; Wang, F.; Gai, N.; Zhuang, R.-S.; Ceccanti, B.; Maskow, T.; Zaray, G.: Investigation of the toxic effect of cadmium on Candida humicola and Bacillus subtilis using a microcalorimetric method. *J. Hazard. Mat.* **2008**, *159*, 465-470.

(76)   Schmitt, E. A.; Peck, K.; Sun, Y.; Geoffroy, J.-M.: Rapid, practical and predictive excipient compatibility screening using isothermal microcalorimetry. *Thermochimica Acta* **2001**, *380*, 175-184.

(77)   Hogan, S. E.; Buckton, G.: The quantification of small degrees of disorder in lactose using solution calorimetry. *Int. J. Pharm.* **2000**, *207*, 57-64.

(78)   Bermudez, J.; Bäckman, P.; Schön, A.: Microcalorimetric evaluation of the effects of methotrexate and 6-thioguanine on sensitive T-lymphoma cells and on a methotrexate-resistant subline. *Cell Biophys.*, *20*, 111-123.

(79)   Regueira, T.; Lugo, L.; Fernández, J.: Compressibilities and Viscosities of Reference, Vegetable, and Synthetic Gear Lubricants. *Ind. Eng. Chem. Res.* **2014**, *53*, 4499-4510.

(80)   Otero, I.; López, E. R.; Reichelt, M.; Fernández, J.: Friction and anti-wear properties of two tris(pentafluoroethyl)trifluorophosphate ionic liquids as neat lubricants. *Tribol. Int.* **2014**, *70*, 104-111.

(81)   Paredes, X.; Fandiño, O.; Pensado, A. S.; Comuñas, M. J. P.; Fernández, J.: Experimental density and viscosity measurements of di(2ethylhexyl)sebacate at high pressure. *J. Chem. Thermodyn.* **2012**, *44*, 38-43.

(82)   López, E. R.; Pensado, A. S.; Comuñas, M. J. P.; Pádua, A. A. H.; Fernández, J.; Harris, K. R.: Density scaling of the transport properties of molecular and ionic liquids. *J. Chem. Phys.* **2011**, *134*, 144507.

(83)   Regueira, T.; Lugo, L.; Fernández, J.: High pressure volumetric properties of 1-ethyl-3-methylimidazolium ethylsulfate and 1-(2-methoxyethyl)-1-methyl-pyrrolidinium bis(trifluoromethylsulfonyl)imide. *J. Chem. Thermodyn.* **2012**, *48*, 213-220.

(84)   López, E. R.; Pensado, A. S.; Fernández, J.; Harris, K. R.: On the density scaling of pVT data and transport properties for molecular and ionic liquids. *J. Chem. Phys.* **2012**, *136*, 214502.

(85)   Paredes, X.; Fernandez, J.; Padua, A. A. H.; Malfreyt, P.; Malberg, F.; Kirchner, B.; Pensado, A. S.: Using molecular simulation to understand the structure of [C2C1im]+-alkylsulfate ionic liquids: bulk and liquid-vapor interfaces. *J. Phys. Chem. B.* **2012**, *116*, 14159-70.

(86)   Gaciño, F. M.; Paredes, X.; Comuñas, M. J. P.; Fernández, J.: Effect of the pressure on the viscosities of ionic liquids: Experimental values for 1-ethyl-3-methylimidazolium ethylsulfate and two bis(trifluoromethyl-sulfonyl)imide salts. *J. Chem. Thermodyn.* **2012**, *54*, 302-309.

(87)   Gaciño, F. M.; Paredes, X.; Comuñas, M. J. P.; Fernández, J.: Pressure dependence on the viscosities of 1-butyl-2,3-dimethylimidazolium bis(trifluoromethylsulfonyl)imide and two tris(pentafluoroethyl)trifluorophosphate based ionic liquids: New measurements and modelling. *J. Chem. Thermodyn.* **2013**, *62*, 162-169.

(88)   Comuñas, M. J. P.; Paredes, X.; Gaciño, F. M.; Fernández, J.; Bazile, J. P.; Boned, C.; Daridon, J. L.; Galliero, G.; Pauly, J.; Harris, K. R.; Assael, M. J.; Mylona, S. K.: Reference Correlation of the Viscosity of Squalane from 273 to 373 K at 0.1 MPa. *J. Phys. Chem. Ref. Data* **2013**, *42*, 033101.

(89)   Paredes, X.; Fernández, J.; Pádua, A. A. H.; Malfreyt, P.; Malberg, F.; Kirchner, B.; Pensado, A. S.: Bulk and Liquid–Vapor Interface of Pyrrolidinium-Based Ionic Liquids: A Molecular Simulation Study. *J. Phys. Chem. B.* **2014**, *118*, 731-742.

(90)   Gaciño, F. M.; Regueira, T.; Comuñas, M. J. P.; Lugo, L.; Fernández, J.: Density and isothermal compressibility for two trialkylimidazolium-based ionic liquids at temperatures from (278 to 398) K and up to 120 MPa. *J. Chem. Thermodyn.* **2015**, *81*, 124-130.

(91)   Carvalho, P. J.; Regueira, T.; Fernández, J.; Lugo, L.; Safarov, J.; Hassel, E.; Coutinho, J. A. P.: High pressure density and solubility for the CO2 + 1-ethyl-3-methylimidazolium ethylsulfate system. *J. Supercrit. Fluid* **2014**, *88*, 46-55.

(92)   Mylona, S. K.; Assael, M. J.; Comuñas, M. J. P.; Paredes, X.; Gaciño, F. M.; Fernández, J.; Bazile, J. P.; Boned, C.; Daridon, J. L.; Galliero, G.; Pauly, J.; Harris, K. R.: Reference Correlations for the Density and Viscosity of Squalane from 273 to 473 K at Pressures to 200 MPa. *J. Phys. Chem. Ref. Data* **2014**, *43*, 013104.

(93)   Comuñas, M. J. P.; Paredes, X.; Gaciño, F. M.; Fernández, J.; Bazile, J.-P.; Boned, C.; Daridon, J.-L.; Galliero, G.; Pauly, J.; Harris, K. R.: Viscosity measurements for squalane at high pressures to 350 MPa from T = (293.15 to 363.15) K. *J. Chem. Thermodyn.* **2014**, *69*, 201-208.

2. Materials and experimental methods

2.1. Context

In this chapter, basic information about the studied fluids and the description of the three different calorimetric techniques used for the characterization of these fluids are presented: *Differential Scanning Calorimetry* was used to determine the lowest limit of the liquids range for the selected ILs and fluids, whereas the highest limit was obtained using *Thermogravimetry*. Combination of both techniques, *Simultaneous DSC/TGA,* was also used to complete the information previously obtained from isolated techniques. The final part of this chapter describes the *Isothermal Microcalorimetry* technique used to perform a preliminary study of toxicity of ILs through the changes on the metabolic respiration of microbial populations of two different soils after the addition of different doses of two ILs.

2.2. Materials

Twenty-one ionic liquids and five lubricant bases have been selected for this study. Abbreviations, CAS numbers, chemical structures and mass fraction purities for these materials are shown in Table 2.1.

The motivations to select these ILs were the following:

- ILs 1 to 13 were studied in the framework of the projects LUBIONIC (2009-2011) and RENELUBIL (2012-2015) where properties of ILs were determined to propose new lubricants for renewable energy sources. Solvent Innovation (currently integrated in Merck KGaA) was an adviser of these projects. A number of ILs was selected taking into account three conditions for these fluids: a) being liquids at room temperature, b) to have high hydrophobicity, and c) to have good potentiality to be used as lubricants. After this selection, ILs were synthetized and kindly donated by this company.

- ILs 14 to 19 were studied in the framework of LISVAPES project and collaborations with the Applied Physics group of University of Vigo under the Galician Network of Ionic Liquids (REGALIs) with the aim to propose

new absorbents for absorption heat pumps. All these ILs were selected by their low viscosity and high water solubility and were purchased to IoLiTec.

- ILs 20 and 21 were in the framework of LISVAPES project to study the toxic effects on soils and seeds germination. These ILs presented high thermal stability and they are good candidates to be used in high temperature applications and were purchased to Fluka and Aldrich, respectively.

- For comparison, lubricants 22 to 24 were used. PAG2 and DiPEC7 (donated by Croda-Uniqema), polyalkylene glycol and dipentaerythritol ester respectively, are commonly used on refrigeration equipment working with CO_2 as a refrigerant. Krytox oils (by Brugarolas) are fluorinated synthetic oils, no flammable and no reactant. They have a wide operation range, even under extreme conditions.

Table 2.1. Ionic liquids and lubricants used in this work
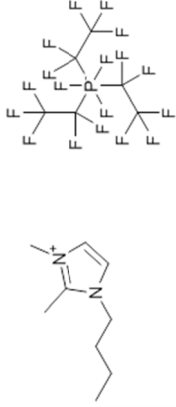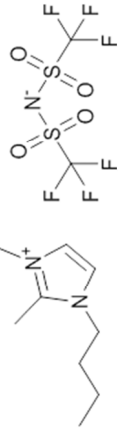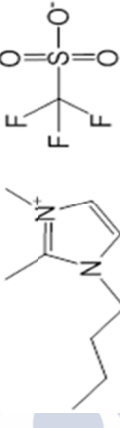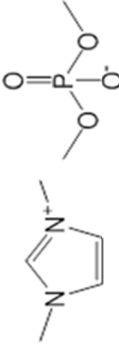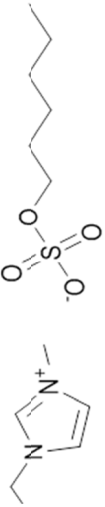
	Name	Abbreviation CAS number	Chemical structure	Mass fraction purity
1	1-butyl-2,3-dimethyl imidazolium tris(pentafluoroethyl) trifluorophosphate	$[C_4C_1Im][(C_2F_5)_3PF_3]$ 1350559-92-0		$\geq 98\%$
2	1-butyl-2,3-dimetilimidazolium bis(trifluoromethyllsulfonyl) imide	$[C_4C_1C_1Im][NTf_2]$ 350493-08-2		$\geq 99\%$
3	1-butyl-2,3-dimethylimidazolium trifluoromethanesulfonate	$[C_4C_1C_1Im][OTf]$ 765910-73-4		$\geq 98\%$
4	1,3-Dimethylimidazolium dimethylphosphate	$[C_1C_1Im][C_1C_1PO_4]$ 654058-04-5		$\geq 99.3\%$
5	1-ethyl-3-methylimidazolium n-hexylsulfate	$[C_2C_1Im][C_6SO_4]$ 942916-86-1		$\geq 98.4\%$

Table 2.1: Ionic liquids and lubricants used in this work (continue)

#	Name	Abbreviation CAS number	Chemical structure	Mass fraction purity
6	1-butyl-1-methylpyrrolidinium tris(pentafluoroethyl) trifluorophosphate	$[C_4C_1Pyrr][(C_2F_5)_3PF_3]$ 851856-47-8		$\geq 99\%$
7	1-butyl-1-methylpyrrolidinium bis(trifluoromethylsulfonyl) imide	$[C_4C_1Pyrr][NTf_2]$ 223437-11-4		$\geq 99.9\%$
8	1-butyl-1-methylpyrrolidinium trifluoromethanesulfonate	$[C_4C_1Pyrr][OTf]$ 367522-96-1		$\geq 98\%$
9	1-butyl-1-methylpyrrolidinium tetracyanoborate	$[C_4C_1Pyrr][B(CN)_4]$ 1266721-18-9		$> 99\%$
10	1-butyl-1-methylpyrrolidinium tris(nonafluorobutyl) trifluorophosphate	$[C_4C_1Pyrr][(C_4F_9)_3PF_3]$ 851856-47-8		$\geq 98\%$

Table 2.1: Ionic liquids and lubricants used in this work (continue)
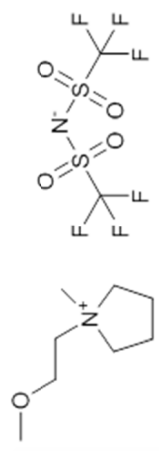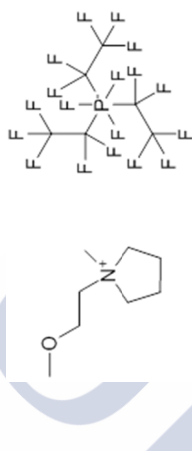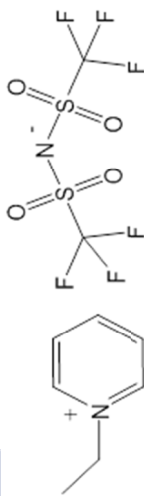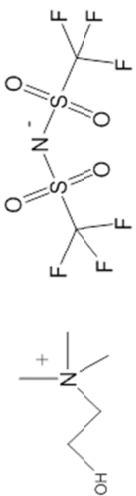
	Name	Abbreviation CAS number	Chemical structure	Mass fraction
11	1-(2-Methoxyethyl)-1-methyl-pyrrolidinium bis(trifluoromethylsulfonyl)imide	$[C_1OC_2C_1Pyrr][NTf_2]$ 757240-24-7		> 99.3%
12	1-(2-Methoxyethyl)-1-methyl-pyrrolidinium tris(pentafluoroethyl)trifluorophosphate	$[C_1OC_2C_1Pyrr][(C_2F_5)_3PF_3]$ 1195983-48-2		> 98%
13	Trihexyl(tetradecyl)phosphonium tris(pentafluoroethyl)trifluorophosphate	$[P_{6,6,6,14}][(C_2F_5)_3PF_3]$ 883860-35-3		> 99%
14	1-ethylpyridinium bis(trifluoromethylsulfonyl)imide	$[C_2Py][NTf_2]$ 712354-97-7		> 99%
15	choline bis(trifluoromethylsulfonyl)imide	$[Chol][NTf_2]$ 827027-25-8		> 99%

Table 2.1: Ionic liquids and lubricants used in this work (continue)

	Name	Abbreviation CAS number	Chemical structure	Mass fraction purity
16	1-ethyl-2-methylimidazolium bis(perfluoroethylsulfonyl)imide	[C$_2$C$_1$1m][BETI] 216299-76-2		> 99%
17	1-ethyl-2-methylimidazolium triflate	[C$_2$C$_1$1m][OTf] 145022-44-2		> 99%
18	1-ethylpyridinium methanesulfonate	[C$_2$Py][C$_1$SO$_3$] 681481-41-4		> 95%
19	1-ethylpyridinium triflate	[C$_2$Py][OTf] 3878-80-6		> 99%
20	1-butyl-3-methylimidazolium tetrafluoroborate	[C$_4$C$_1$1m][BF$_4$] 174501-65-6		> 99.3%
21	1-propyl-3-methylimidazolium bis(trifluoromethylsulfonyl)imide	[C$_3$C$_1$1m][NTf$_2$] 216299-72-8		> 99%

Table 2.1: Ionic liquids and lubricants used in this work (continue)

Name	Abbreviation CAS number	Chemical structure	Mass fraction purity
22 Dipentaerythritol hexaheptanoate	DiPEC7 76939-66-7		> 95%
23 double end-capped poly(propylene glycol)	PAG2 24991-61-5		
24 Perfluoropolyether (n=13) Perfluoropolyether (n=18) Perfluoropolyether (n=30)	Krytox GPL 103 Krytox GPL 104 Krytox GPL 105	where n = 13, 18, 30	> 99.9%

31

2.3. Experimental techniques

2.3.1. Differential Scanning Calorimetry

DSC is a thermal analysis technique that measures the difference in energy provided to a sample and a reference material in function of a controlled temperature. This technique keeps the sample and the reference at the same temperature. A control system (servo system) immediately increases the energy supplied to the sample or the reference, depending on if the process involved during the experiment is endothermic or exothermic. The record of the DSC curve is expressed in terms of heat flow versus temperature or time.

Experiments were performed in a differential scanning calorimeter DSC Q100 TA-Instruments (Figure 2.1), with aluminium pans hermetically sealed and liquid nitrogen as coolant fluid. Temperature and heat calibration of this DSC was performed before to start the experiments. Temperature and enthalpy of melting of indium, determined under the same experimental conditions than the subsequent studies were the parameters used to do it.

As it was pointed out in *Introduction* chapter, the lowest limit of liquid range of an IL was defined by the melting temperature (if the IL presents crystal structure) or glass transition (if only amorphous phase is presented in the IL structure.

Figure 2.1. DSC Q100 TA-Instruments.

Experimental procedure

To determine these transition temperatures, each sample, $(3 - 5)$ mg, was subjected to four ramps, two in cooling and the other two in heating mode, with an isothermal step between them. Thus, the steps were: (a) heating from (25 to 100) °C at 10 °C · min^{-1}, (b) an isothermal step at 100 °C during 10 minutes to remove the volatile impurities and to erase the prior thermal history of the sample, (c) cooling from $(100$ to $- 85)$ °C at 5 °C · min^{-1}, (d) an isothermal step at $- 85$ °C during 5 minutes, (e) heating from (–85 to 50) °C at 10 °C · min^{-1}, and (f) cooling from (50 to -85) °C at 5 °C · min^{-1}. Transition temperatures were determined from the DSC curves during the reheating and recooling, (e) and (f), steps [1].

2.3.2. Thermogravimetry

A thermogravimetric analyser, TGA 7-Perkin Elmer (Figure 2.2), operating in dynamic and isothermal modes under different conditions was used to perform thermogravimetric analysis.
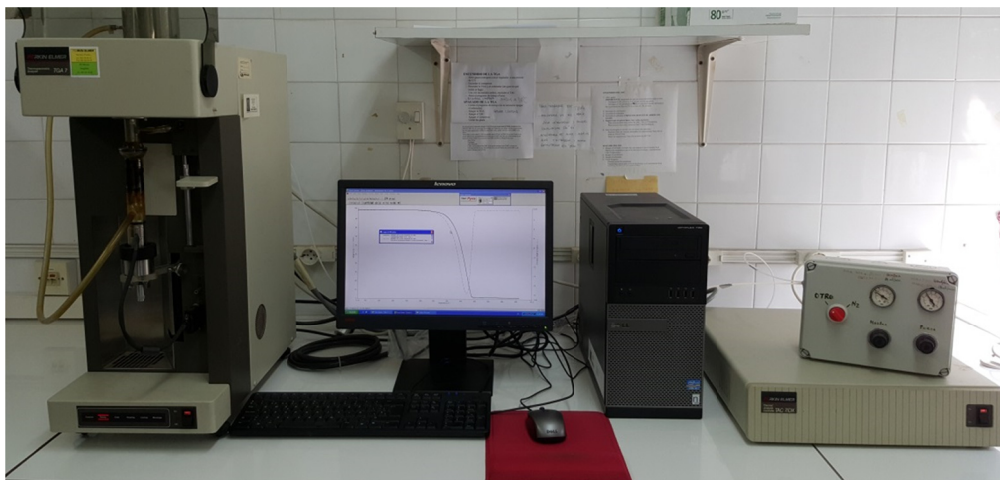
Figure 2.2. TGA 7 Perkin Elmer Analyzer.

Thermogravimetric (TGA) analysis allows us to quantify mass changes of the samples measured as a function of temperature and/or time. The sample atmosphere is carefully controlled by the selection of the purge gas and its flow rate. In most cases, TGA analysis is performed in air atmosphere with a linear ramp temperature. The TGA technique is composed of a thermogravimetric analyzer (Figure 2.3), and a computer. The main parts of the equipment are:

- An electronic ultramicrobalance based on a null balance system, for that it uses a servo-controlled torque motor to compensate mass changes. The electrical power needed to maintain the system in the "null" state is directly proportional to the weight change of the sample. This ultramicrobalance is extremely sensitive and can detect variations of 0.1 μg, with minimum and maximum capacities of less than 1 mg and 1.3 g, respectively. The sample holder is deflected when a sample is placed into it and this deflection is measured by an optical sensor. In order to return the holder to its original position, a supply of electric power is needed, which provides a direct measure of the sample mass.

- A furnace that can work in a wide range of temperatures (from room temperature to 1000 ^{o}C) and with very different heating rates, (from

0.2 to 200) $^{o}C \cdot min^{-1}$, in 0.1 ^{o}C increments. It is a small ceramic oven which is coated with platinum to facilitate the fast heating and cooling processes (up to 200 $^{o}C \cdot min^{-1}$) and to decrease the time between tests. Throughout the entire test, a chromel-alumel thermocouple located at the base of the furnace provides the temperature measurements.
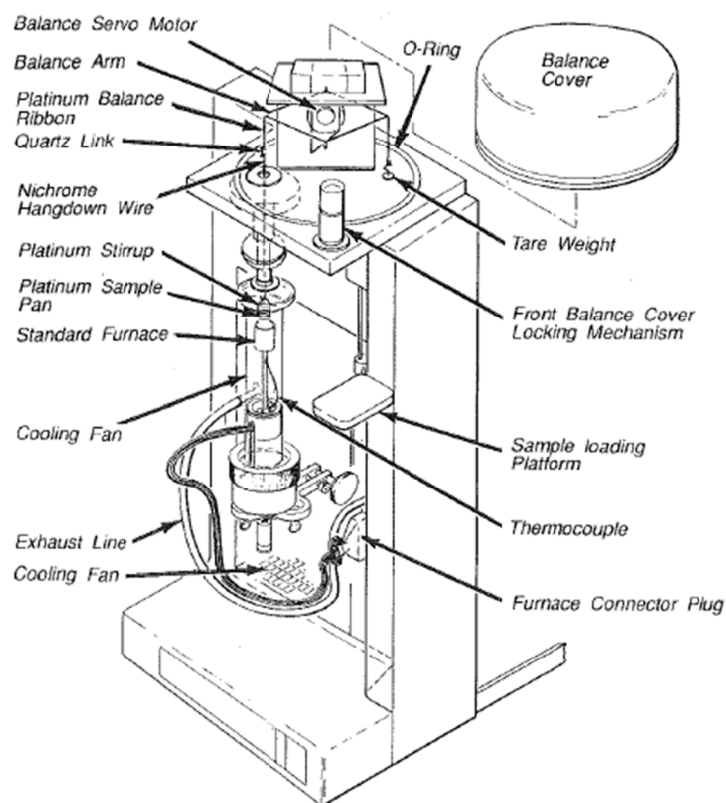
Figure 2.3: TGA 7 furnace and balance assembly components [2]

TGA calibration has been carried out carefully following the Perkin-Elmer instructions of the routine calibration program and with the calibration standards. To perform a complete calibration of the equipment three calibration steps must be executed [2]:

1. Calibration of the furnace: it is automatically done by the software of the apparatus in the selected temperature range.

2. Calibration of the temperature: this routine is performed by measuring the temperatures of the Curie point of various metals and alloys. In this case Alumel, Nickel, Perkalloy and Iron were employed; whose magnetic transition temperatures are (163, 354, 596 and 780) $^{\circ}$C respectively.

3. Weight calibration: a 100 mg standard weight is used for performing this part of the calibration process.

TGA curve analysis

There are many different parameters which affect to the nature and accuracy of the results, mainly due to the dynamic nature of the temperature changes in the sample [3]. Among the factors that should be highlighted are: the heating rate (which has a great influence on the shape of the thermogram, particularly in regard to the determination of the initial, t_i, and final, t_f, temperatures of the mass load process), the furnace atmosphere and sample mass. Thermogravimetric curves have two characteristic temperatures, t_i and t_f. T_i is the starting temperature of the decomposition (or evaporation), i.e., the lowest temperature at which the mass change is detectable, under certain experimental conditions, and t_f is the final temperature, i.e., the lowest temperature at which the mass loss process is over.

Mass loss percentage, M_L, which is defined as positive, is given by the following expression:

$$M_L = \frac{m_i - m_f}{m_i} 100 \tag{2.1}$$

being m_i and m_f the masses corresponding to the temperatures t_i y t_f, respectively. The figures included in this PhD Thesis represent the remaining mass percentage, W, *i.e.* 100-M_L.

In addition to the TGA curve, its derivative (DTG) also provides important information; namely, the rate of mass loss and the temperature corresponding to the maximum decomposition rate. Moreover, through the DTG curve it is easy to distinguish if the process associated with the mass loss is simple or the superposition of several processes. Figure 2.4 shows a TG curve and its corresponding DTG curve associated to a simple process of thermal degradation. The area of the peak (or peaks) curve is proportional to the total mass change related to this step.
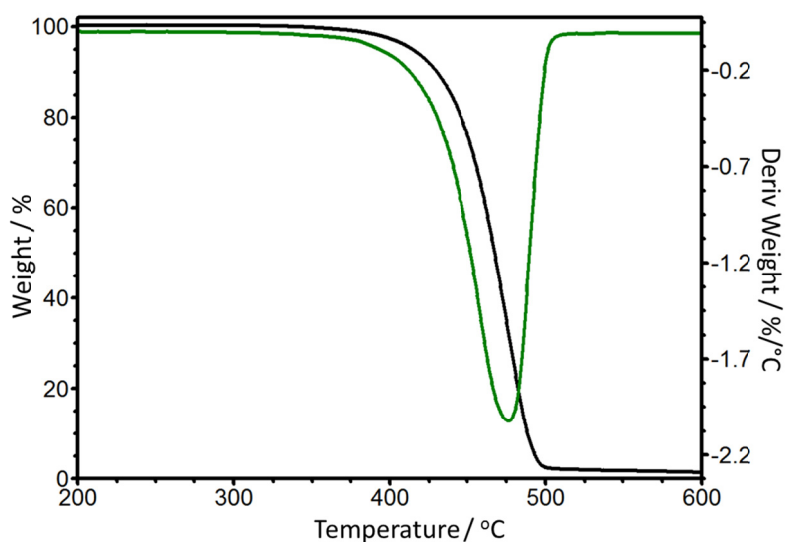
Figure 2.4: TG curve and its corresponding DTG for one of the studied ILs.

DTG (derivative thermogravimetry) is a very important part of this technique, where the inflection point in the mass change step becomes into a minimum in the derivative curve and for an interval of constant mass dm/dT is zero. In some cases overlapping reactions are difficult to resolve. In DTG the mass change with respect to temperature (dm/dT) is plotted against T or t.

Experimental procedure

The experimental procedure of this PhD Thesis has been developed according to similar studies found on the literature [4-13]. With this technique, the thermal stability was studied for several ILs.

Given that experimental conditions can have a vast influence on thermal and calorimetric results, initially, a deep study of the influences of experimental conditions (atmosphere, heating rate, initial mass and water content) for some of the selected ILs has been done. Once these influences have been checked, dynamic scans were performed at the following selected conditions: temperature range (100-800) ºC, heat rate of 10 ºC min^{-1}, sample mass about 5 mg, and air atmosphere with a flow of 20 cm^3 · min^{-1}. Additionally, to complete the kinetic study of the mass loss process, TGA measurements at different heating rates (1, 3, 5, 15 and 20 ºC · min^{-1}) have been done for one of the ILs [C$_4$C$_1$C$_1$Im][NTf$_2$]. From TG/DTG curves, as it can be seen in Figure 2.5, following parameters can be obtained:

- Onset temperature, t_{onset}, as the temperature at which the baseline and the tangent to the mass loss curve at its inflection point (point determined using the minimum of the DTG curve) are cut

- Endset temperature, t_{endset}, as the temperature at which the baseline of total mass loss and the tangent to the mass loss curve at its inflection point are cut

- t_{1st}, temperature where the DTG curve reaches its minimum (that corresponds to the point with the higher mass degradation rate)

- W_{onset}, defined as the percentage of remaining mass at t_{onset}

- $t_{10\%}$, which corresponds to the temperature where the 10% of mass loss is attained.
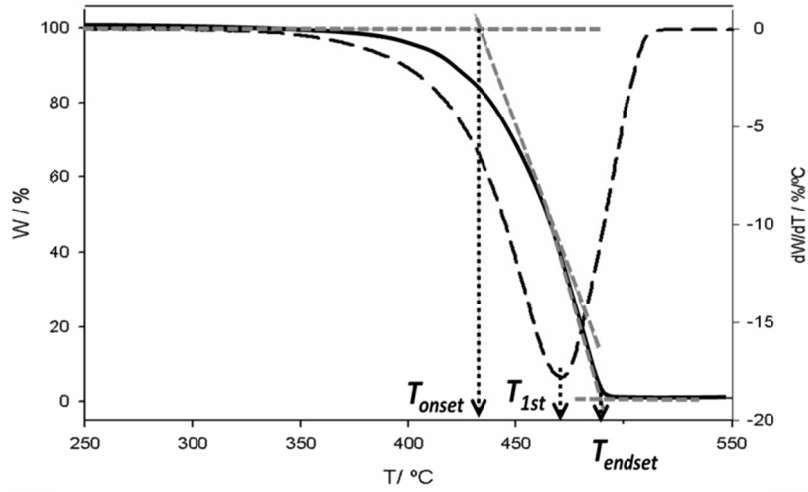
Figure 2.5: Characteristic temperatures obtained from TG (continuous line)/DTG (dashed line) curves for one of the studied ILs.

To complete these studies, isothermal scans at temperatures lower than t_{onset} were performed in order to complete the thermogravimetry results.

2.3.2.1. Kinetic methods

2.3.2.1.1. Kinetic isothermal study

The decomposition kinetics ILs was elucidated through isothermal TGA. A pseudo-zero-order rate expression was used as the decomposition is governed by physical kinetics involving heat and mass transfer [4,6,7,9,10,13-16].

$$\frac{d\alpha}{dt} = k \tag{2.2}$$

where k is the rate constant of pseudo-zero-order, and α is the degree of conversion, that is defined as:

$$\alpha = \frac{m_0 - m}{m_0 - m_\infty} \tag{2.3}$$

where m is the measured experimental mass at temperature T, m_0 the initial mass, and m_∞ the mass at the end of the non-isothermal experiments.

The mass loss rate can be represented in integral form, considering equation (2.2), as:

$$\alpha = kt + C \tag{2.4}$$

where t is time and C is another constant. So, representing for each isothermal scan α versus time, we obtain the rate constant k from a linear fitting of these experimental data.

In case of isothermal studies, the temperature dependence on the rate of loss mass, k, is represented by the Arrhenius equation:

$$k = A \, exp\left(\frac{-E}{RT}\right) \tag{2.5}$$

where E is the activation energy and A is the pre-exponential coefficient.

2.3.2.1.2. Kinetic dynamic study

In order to verify the activation energy of the mass loss process obtained by the kinetic isothermal study, dynamic methods (Kissinger and Friedman) were also employed.

Kinetic information can be extracted from dynamic experiments by various methods. All kinetic methods utilize the basic reaction rate equation that relates the rate of conversion, $d\alpha/dt$, at constant temperature to some function of the conversion, $f(\alpha)$, through a rate constant, k:

$$\frac{d\alpha}{dt} = kf(\alpha) \tag{2.6}$$

where k is the temperature-dependent rate constant, and $f(\alpha)$ depends on the particular decomposition mechanism.

Substituting Arrhenius dependence (equation 2.5) into equation (2.6), one obtains:

$$\frac{d\alpha}{dt} = Af(\alpha)e^{-\frac{E}{RT}} \tag{2.7}$$

If the temperature of the sample is changed by a controlled and constant heating rate, $\beta = dT/dt$, the variation of the degree of conversion can be analysed as a function of temperature, being this temperature dependent on the time of heating.

2.3.2.1.2.1.   Kissinger method

Fox *et al.* [5] suggest Kissinger's method to determine the activation energy of the degradation process of ($[C_4C_1C_1][Cl]$ y $[C_4C_1C_1][BF_4]$) from plots of the logarithms of the heating rate *vs.* the inverse of temperature at the maximum of the reaction rate in constant heating rate experiments.[17-20]

Differentiation of equation (2.7) gives rise to:

$$\frac{d^2\alpha}{dt^2} = \frac{E\beta}{RT^2}\frac{d\alpha}{dt} + Ae^{-\frac{E}{RT}}\frac{df}{d\alpha}\frac{d\alpha}{dt} = \left[-\frac{E\beta}{RT^2} + Ae^{-\frac{E}{RT}}\frac{df}{d\alpha}\right]\frac{d\alpha}{dt} \tag{2.8}$$

Taking into account that at the inflection point of the TGA curve (T_{1st}) the second derivative of is zero, the equation (2.8) takes the form:

$$\frac{E\beta}{RT_{1st}^2} + Ae^{-\frac{E}{RT_m}}\frac{df}{d\alpha}\bigg|_{\alpha_m} = 0 \tag{2.9}$$

where α_m is the conversion corresponding at T_{1st}. Making a reorganization of equation (2.9) and taking logarithms, the following expression can be obtained:

$$ln\frac{\beta}{T_{1st}^2} = ln\left[\frac{AR}{E}\frac{df}{d\alpha}\bigg|_{\alpha_m}\right] - \frac{E}{RT_{1st}} \tag{2.10}$$

It should be pointed out that T_{1st}, the temperature corresponding to the inflection point of the thermodegradation curve, corresponds to the maximum reaction rate.

2.3.2.1.2.2. Friedman method

Isoconversional methods are based on the isoconversion principle which states that the reaction rate is only temperature dependent, for a given constant conversion value [5]. The most commonly isoconversional method used to determine the apparent activation energy is the Friedman method [5,21]. This method considers that the temperature dependence at a given degree of conversion, α. Simple rearrangement of equation (2.7) leads to the following equation [22]:

$$ln\left(\frac{d\alpha}{dt}\right)_\alpha = k_F - \frac{E_\alpha}{RT} \quad ; \text{where } k_F = ln\left(Af(\alpha)\right) \tag{2.11}$$

where k_F is a constant and E_α is the apparent activation energy at degree of conversion, α.

This method can be used to determine the apparent activation energy over the entire conversion range.[23]

2.3.3. Simultaneous DSC/TGA

Additionally a simultaneous DSC/TGA from Mettler Toledo (Fig. 2.6) was used. This device provides trustworthy results using a TGA balance with a complementary DSC heat flow sensor using the same sample for both techniques. It allows users to analyze a wide variety of sample types up to 1600 °C.

DSC/TGA was used to determine the kind of peak detected at onset temperature in order to know the kind of process: evaporation or degradation (endothermic or exothermic, respectively during heating). Experiments were performed under N_2 or air atmosphere, at a heating rate of 5 ^{o}C · min^{-1} in a temperature range between (50 and 420) ^{o}C.
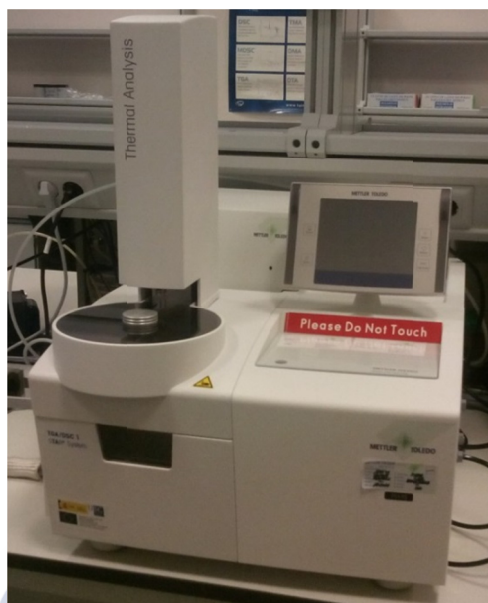
Figure 2.6. DSC/TGA1 Mettler Toledo

2.3.4. Microcalorimetry

An isothermal microcalorimeter 2277 Thermal Activity Monitor (TAM) Thermometric AB (Fig. 2.7) was employed. This is a multi-channel heat conduction microcalorimeter, i.e. the heat produced in the sample is then conducted away through a heat flow sensor, being constant the temperature of the sample [24]. Microcalorimetry is a technique that permits monitoring of the activity of a living process in situ for a prolonged period without disturbing the system [25]. It is an useful tool for evaluating the metabolism of microbial biomass in soils. The short-term effect of the addition of different amounts of ILs under closed, static experimental environment was evaluated with this technique; namely, five different concentrations of aqueous solutions (10%, 1%, 0.1%, 0.01% and 0% (control) in weight in distilled water) of the ILs on microbial activity of these soils was studied by this technique. Measurements were carried out at 22ºC in hermetically sealed 5 ml stainless steel ampoules closed with a Teflon coated septa and an steel cap. All the heat conduction calorimeters need to have a reference to reduce the noise level and taking into account that the measured signal is the difference between the signals from the sample and the reference heat

flow sensors, the disturbances affect similarly sample and reference and then the calorimetric signal is not affected by these disturbances. Soil samples of 1 g size at water-holding capacity, treated with 0.2 ml of a glucose solution in water with a concentration of 6.25 g / l to activate the metabolism of soil microorganisms, were used as control [26]. The heat released by the microorganisms was recorded until the total consumption of glucose (at least three days). Three replicates were performed for each case. Additionally, a comparison between the effects of this IL in the pine soil microbial activity and the corresponding to a well-known salt, sodium chloride (NaCl), in the same conditions, was established.

Figure 2.7. Microcalorimeter 2277 Thermal Activity Monitor (TAM) Thermometric AB.

Electrical calibration of TAM was done before to start the experiments. This process is performed from the calibration unit sending an electrical power through the electrical resistance (50 Ω) located at the base of the ampoule.

The sample and reference ampoules are placed in ampoule holders. The heat flow sensors are positioned between the ampoule holders and the surrounding heat sink.

It should be noticed that isothermal calorimeter used in this PhD Thesis commonly have 1000 times higher specific sensitivity (W/g sample) than DSC instruments running in isothermal mode, mainly because the DSC samples are very much smaller [24]

2.3.4.1.   Soil Sampling preparation

Two Galician Regosol soils located in Borreiros- Viviero (Lugo) (Figure 2.8), one under Pinus pinaster Aiton and other under Eucaliptus globulus Labill, both reforested 20 years ago and traditionally dedicated to pasture and cereal culture, were chosen.

Figure 2.8: Location of sampling zone, in Galicia (NW of Spain) with geographical coordinates O-43º37'51.94'' N-7º37'22.63''. Both soils are separated 100 m approximately, in an average zone of hillside and with a slope of 28.88 % that facilitates dragging in case of important rainfalls.

Six grids of $1m^2$ were selected randomly in a surface of 100 m^2 in every sampling zone. Samples from the surface layer, between (0 and 10) cm, were collected in the selected grids after removal of the litter layers, which consisted mainly of undecomposed leaves. These samples were joined to establish a unique soil sample. Before the analysis, visible plant particles were removed from the soil by hand and sample was sieved at 2 mm. Fraction less than 2 mm was homogenised and used for this study. Samples were kept to 4 ºC in hermetic bags to assure a minimum microbial activity before start the calorimetric experiments and guarantee a suitable reproducibility in calorimetric determinations.

2.3.5. Germination response

Seed germination test of species of *Pinus halepensis*, *Pinus nigra*, *Pinus pinaster*, *Pinus sylvestris* and *Pinus radiata* were carried out. In each, five different concentrations of aqueous solutions (10%, 1%, 0.1%, 0.01% and 0% (control) in weight) of the two of the selected ILs ($[C_4C_1Im][BF_4]$ and $[C_3C_1Im][NTf_2]$) were tested. Five replies with 25 seeds per Petri dish were incubated for every species and treatments. The seeds were incubated in a Phytotron (Climas AGP890) and were maintained for 16 h under light at 24 ºC and in the dark for 8 h at 16 ºC. Germinated seeds were counting every Monday, Wednesday and Friday. Germination had been completed in all the species after 45 days of incubation.

Additionally, results of this study were compared under the same conditions with the corresponding to the addition of a well-known salt, sodium chloride (NaCl), which present adverse effects on germination and plants growth [27-30].

The average germination percentage level and the average T_{50} rate (time that each replicate took to reach 50% of germination) were calculated, and also the temporal distribution of germination. The germination data of each species were analysed using Oneway Analysis of Variance (ANOVA) followed by a Duncan Test using $p < 0.05$ as the significance criteria. Data sets were previously checked for Normality and the germination percentage data were arcsine transformed prior to ANOVA performance. Programme ''PASW Statistics 18'' for Windows was used for statistical calculations.

2.4. References

(1)   Tokuda, H.; Hayamizu, K.; Ishii, K.; Susan, M. A. B. H.; Watanabe, M.: Physicochemical Properties and Structures of Room Temperature Ionic Liquids. 1. Variation of Anionic Species. *J. Phys. Chem. B* **2004**, *108*, 16593-16600.

(2)   Elmer, P.: Users Manual. Series TGA7 Thermal Analysis System. **1993**.

(3)   Hatakeyama, T.; Quinn, F. X.: *Thermal analysis. Fundamentals and applications to polymer science*; John Wiley and Son, 1997.

(4)   Hao, Y.; Peng, J.; Hu, S.; Li, J.; Zhai, M.: Thermal decomposition of allyl-imidazolium-based ionic liquid studied by TGA–MS analysis and DFT calculations. *Thermochim. Acta* **2010**, *501*, 78-83.

(5)   Fox, D. M.; Gilman, J. W.; De, L. H. C.; Trulove, P. C.: TGA decomposition kinetics of 1-butyl-2,3-dimethylimidazolium tetrafluoroborate and the thermal effects of contaminants. *J. Chem. Thermodyn.* **2005**, *37*, 900-905.

(6)   Kamavaram, V.; Reddy, R. G.: Thermal stabilities of di-alkylimidazolium chloride ionic liquids. *Int. J. Therm. Sci.* **2008**, *47*, 773-777.

(7)   Arellano, I. H. J.; Guarino, J. G.; Paredes, F. U.; Arco, S. D.: Thermal stability and moisture uptake of 1-alkyl-3-methylimidazolium bromide. *J. Therm. Anal. Calorim.* **2011**, *103*, 725-730.

(8)   Amarasekara, A. S.; Owereh, O. S.: Thermal properties of sulfonic acid group functionalized Broensted acidic ionic liquids. *J. Therm. Anal. Calorim.* **2011**, *103*, 1027-1030.

(9)   Salgado, J.; Parajó, J. J.; Fernández, J.; Villanueva, M.: Long-term thermal stability of some 1-butyl-1-methylpyrrolidinium ionic liquids. *J. Chem. Thermodyn.* **2014**, *74*, 51-57.

(10)   Salgado, J.; Villanueva, M.; Parajó, J. J.; Fernández, J.: Long-term thermal stability of five imidazolium ionic liquids. *J. Chem. Thermodyn.* **2013**, *65*, 184-190.

(11)   Schmidt, C.; Glueck, T.; Schmidt-Naake, G.: Modification of Nafion membranes by impregnation with ionic liquids. *Chem. Eng. Technol.* **2008**, *31*, 13-22.

(12)   Villanueva, M.; Coronas, A.; García, J.; Salgado, J.: Thermal Stability of Ionic Liquids for Their Application as New Absorbents. *Ind. Eng. Chem. Res.* **2013**, *52*, 15718-15727.

(13)   Villanueva, M.; Parajó, J. J.; Sánchez, P. B.; García, J.; Salgado, J.: Liquid range temperature of ionic liquids as potential working fluids for absorption heat pumps. *J. Chem. Thermodyn.* **2015**, *91*, 127-135.

(14)   Kosmulski, M.; Gustafsson, J.; Rosenholm, J. B.: Thermal stability of low temperature ionic liquids revisited. *Thermochim. Acta* **2004**, *412*, 47-53.

(15)   Valkenburg, M. E. V.; Vaughn, R. L.; Williams, M.; Wilkes, J. S.: Thermochemistry of ionic liquid heat-transfer fluids. *Thermochim. Acta* **2005**, *425*, 181-188.

(16)   Baranyai, K. J.; Deacon, G. B.; MacFarlane, D. R.; Pringle, J. M.; Scott, J. L.: Thermal Degradation of Ionic Liquids at Elevated Temperatures. *Aust. J. Chem.* **2004**, *57*, 145-147.

(17)   R, G.; Friedrich A Fau - Taubert, A.; A, T.: - Tuning the phase behavior of ionic liquids in organically functionalized silica ionogels. *Dalton Trans* **2010**, *14*, 603-11.

(18)   Pas, S. J.; Dargusch, M. S.; MacFarlane, D. R.: Crystallisation kinetics of some archetypal ionic liquids: isothermal and non-isothermal determination of the Avrami exponent. *Phys. Chem. Chem. Phys.* **2011**, *13*, 12033-12040.

(19)   Muhammad, N.; Gao, Y.; Khan, M.; Khan, Z.; Rahim, A.; Iqbal, F.; khan, A.; Iqbal, J.: Effect of ionic liquid on thermo-physical properties of bamboo biomass. *Wood Sci. Technol.* **2015**, *49*, 897-913.

(20)   Wang, Z.; Fang, W.; Li, L.; Li, Y.; Yu, X.; Gu, Q.; Zhou, F.: Effects of an ionic liquid as an additive on the thermal denaturation/degradation of lysozyme crystals. *Asia-Pac. J. Chem. Eng.* **2015**, *10*, 163-169.

(21)   Friedman, H. L.: Kinetics of thermal degradation of char-forming plastics from thermogravimetry. Application to a phenolic plastic. *J. Pol. Sci. Part C: Pol. Symp.* **1964**, *6*, 183-195.

(22)   Vyazovkin, S.; Sbirrazzuoli, N.: Isoconversional kinetic analysis of thermally stimulated processes in polymers. *Macromol. Rapid Comm.* **2006**, *27*, 1515-1532.

(23)   Sewry, J. D.; Brown, M. E.: "Model-free" kinetic analysis? *Thermochim. Acta* **2002**, *390*, 217-225.

(24)   Wadsö, L.; Gómez Galindo, F.: Isothermal calorimetry for biological applications in food science and technology. *Food Control* **2009**, *20*, 956-961.

(25)   Núñez-Regueira, L.; Rodríguez-Añón, J. A.; Proupín-Castiñeiras, J.; Núñez-Fernández, O.; Villanueva-López, M.: Erratum to "Microcalorimetric study of changes in the microbial activity in a humic Cambisol after reforestation with eucalyptus in Galicia (NW Spain)" [Soil Biology & Biochemistry 38(1) (2006) 115–124]. *Soil Biol. Biochem.* **2006**, *38*, 850.

(26)   Barja, I.; Núñez, L.: Microcalorimetric measurements of the influence of glucose concentration on microbial activity in soils. *Soil Biol. Biochem.* **1999**, *31*, 441-447.

(27)   Yetişir, H.; Uygur, V.: Plant growth and mineral element content of different gourd species and watermelon under salinity stress. *Turk. J. Agric. For.* **2009**, *33*, 65-77.

(28)   Duan, D.-Y.; Li, W.-Q.; Liu, X.-J.; Ouyang, H.; An, P.: Seed germination and seedling growth of Suaeda salsa under salt stress. In *Annales Botanici Fennici*; Helsinki: Societas Biologica Fennica Vanamo, 1964-, 2007; Vol. 44; pp 161-169.

(29)   Wei, Y.; Xu, X.; Tao, H.; Wang, P.: Growth performance and physiological response in the halophyte Lycium barbarum grown at salt-affected soil. *Ann. Appl. Biol.* **2006**, *149*, 263-269.

(30)   Demiral, M. A.: Comparative response of two olive (Olea europaea L.) cultivars to salinity. *Turk. J. Agric. For.* **2005**, *29*, 267-274.

3. Results and discussion

In order to know the liquid range of some of the ILs, thermal analysis techniques, as it was exposed in previous chapters, were used. The lowest temperature limit is defined by glass transition or melting temperature, depending on the crystallinity degree and/or thermal history of the sample. These transitions, together with cold crystallization, solid-solid transitions, etc. are detectable by Differential Scanning Calorimetry (DSC). Afterwards Thermogravimetry (TGA) was used to characterize the "upper limit temperature operation" of each IL. Additionally the influence of experimental conditions was previously studied with the aim to find the better requirements to experimental procedures.

Finally, preliminary analysis of the eco-toxicity of some ILs using microcalorimetric and germination response studies were also developed in this thesis.

Results are broadly explained and discussed in this chapter; some of the results have been published in the following papers:

1. J. Salgado; M. Villanueva; J.J. Parajó; J. Fernández; Long-term thermal stability of five imidazolium ionic liquids. *J. Chem. Thermodyn.* **2013**, 65, 184-190.

2. J. Salgado; J.J. Parajó; J. Fernández; M. Villanueva; Long-term thermal stability of some 1-butyl-1-methylpyrrolidinium. *J. Chem. Thermodyn.* **2014**, 74, 51-57.

3. M. Villanueva; J.J. Parajó; P.B. Sánchez; J. García, J.; Liquid range temperature of ionic liquids as potential working fluids for absorption heat pumps. *J. Chem. Thermodyn.* **2015**, 91, 127-135.

4. J. J. Parajó; M. Villanueva; I. Otero; J. Fernández; J. Salgado; Long-term thermal stability of some ionic liquids and other five synthetic lubricant bases. on final writing phase. *It will be sent for publication to J. Chem. Thermodyn.* **2016**.

5. J. Salgado; J. J. Parajó; T. Teijeira; J. Proupín; M. Villanueva; J. A. Rodríguez-Añón; P. V. Verdes; O. Reyes; Addition effects of two imidazolium based ionic liquids on seed germination and on soil microbial activity. on final writing phase. *It will be sent for publication in J. Hazard. Mater*. **2016**.

3.1. DSC (*Temperature transitions*)

Figure 3.1 shows the second ramps of heating and cooling of DSC curves of some of the selected ILs: $[C_2Py][NTf_2]$, $[Chol][NTf_2]$, $[C_2Py][OTf]$, $[C_2C_1Im][OTf]$, $[C_2Py][C_1SO_3]$, $[C_2C_1Im][BETI]$, $[C_4C_1C_1Im][(C_2F_5)_3PF_3]$, $[C_4C_1Pyrr][(C_2F_5)_3PF_3]$, $[C_4C_1Pyrr][(C_4F_9)_3PF_3]$, $[C_2C_1Im][C_6SO_4]$, $[C_1OC_2C_1Pyrr][(C_2F_5)_3PF_3]$ and $[P_{6,6,6,14}][(C_2F_5)_3PF_3]$, following the methodology previously detailed in *Materials and experimental methods*, the first heating and cooling ramps were not considered, because they are strongly dependent with the thermal story of the sample.
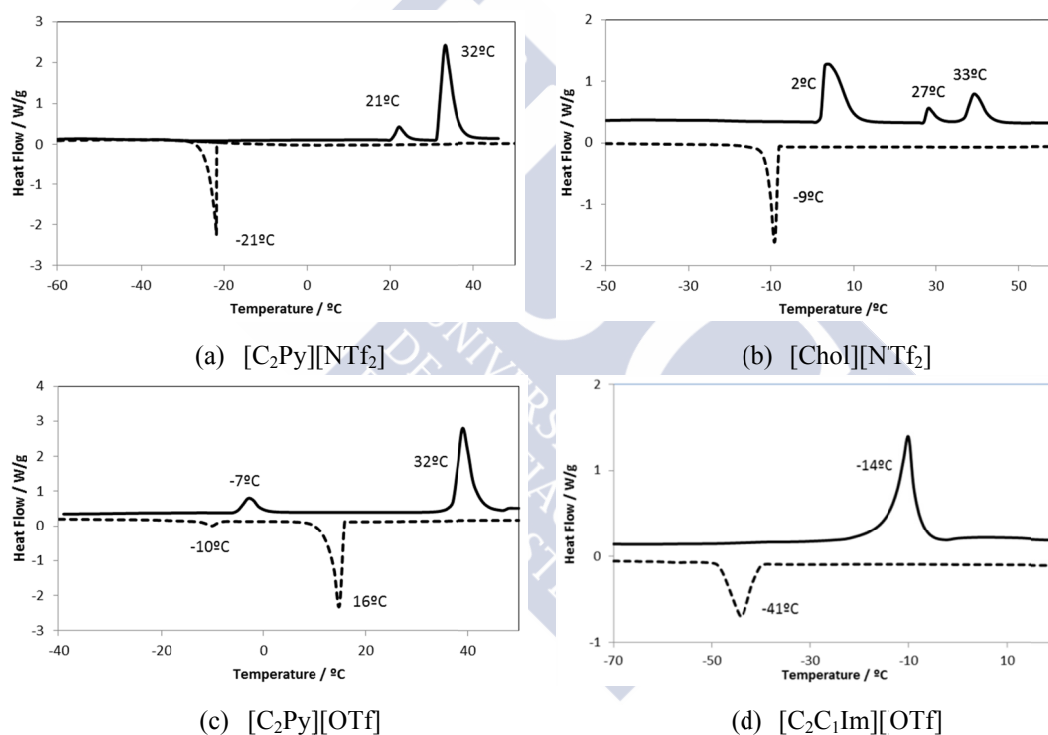
(a) $[C_2Py][NTf_2]$

(b) $[Chol][NTf_2]$

(c) $[C_2Py][OTf]$

(d) $[C_2C_1Im][OTf]$

Figure 3.1. DSC curves (Exo down) on cooling (dashed line) and heating (solid line) scanning for the selected ILs.

(e) [C$_2$Py][C$_1$SO$_3$]

(f) [C$_2$C$_1$Im][BETI]

(g) [C$_4$C$_1$C$_1$Im][(C$_2$F$_5$)$_3$PF$_3$]

(h) [C$_4$C$_1$Pyrr][(C$_2$F$_5$)$_3$PF$_3$]

(i) [C$_4$C$_1$Pyrr][(C$_4$F$_9$)$_3$PF$_3$]

(j) [C$_2$C$_1$Im][C$_6$SO$_4$]

(k) [C$_1$OC$_2$C$_1$Pyrr][(C$_2$F$_5$)$_3$PF$_3$]

(l) [P$_{6,6,6,14}$][(C$_2$F$_5$)$_3$PF$_3$]
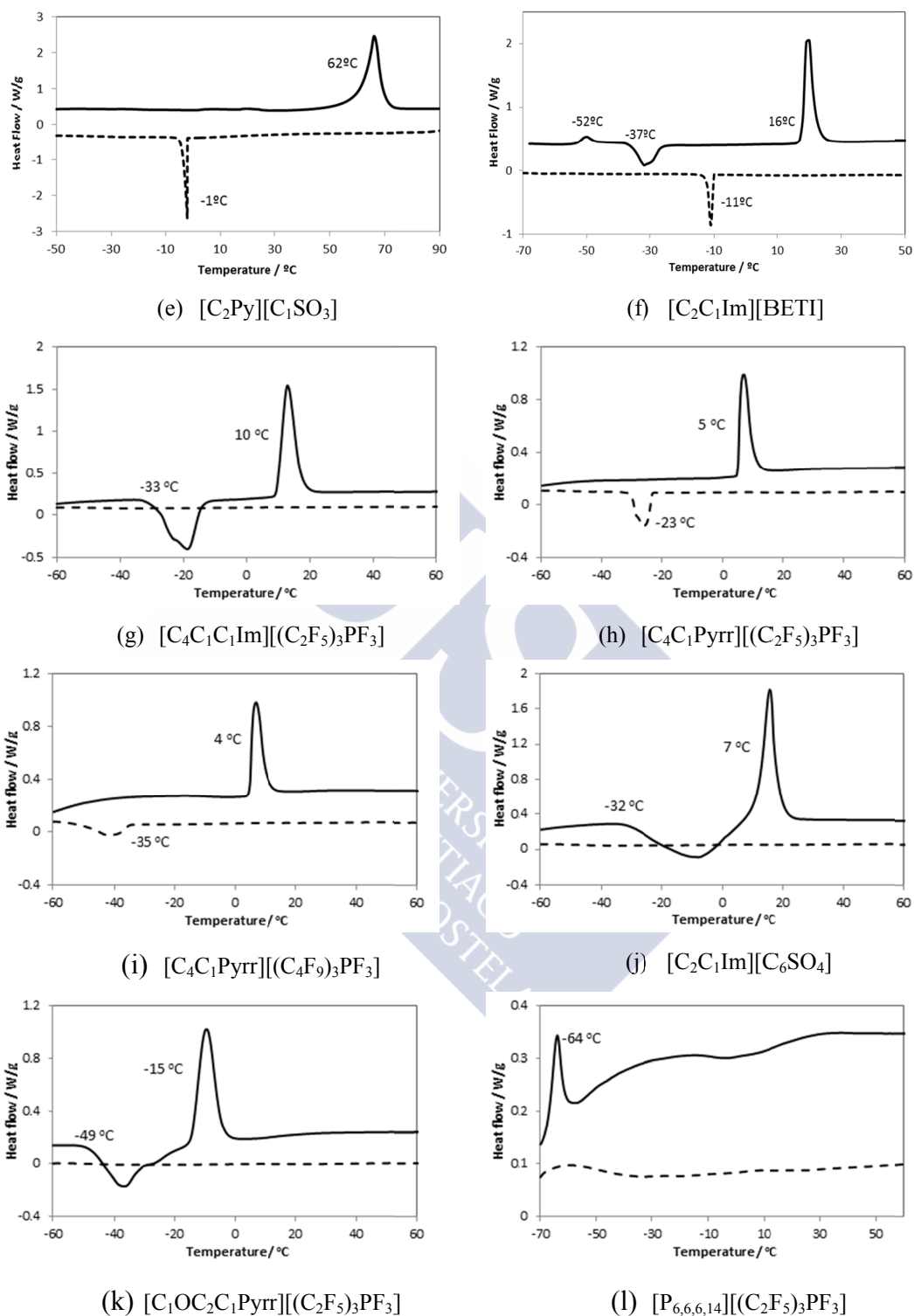
Figure 3.1. DSC curves (Exo down) on cooling (dashed line) and heating (solid line) scanning for the selected ILs (continue).

All the ILs show melting peak and most of them, also, freezing peak. This means that these ILs are very good crystal-formers, although the DSC curves profiles show important differences associated to different thermal behaviours. Table 3.1 summarizes state transition temperatures, such as melting, freezing, cold crystallization and glass temperatures determined from these curves. Up to our knowledge, scarce data of the thermal behaviour of these ILs in heating and/or cooling ramps can be found in literature. Values of transition temperatures found in literature for these ILs are also presented in Table 3.1.

Important agreements between ours and other author results have been observed, thus for [C$_2$C$_1$Im][BETI], Ngo *et al.* [1] obtained freezing temperature (-12 ºC) similar than our result (Fig. 3.1.f), but values for melting point (-1 ºC) differ considerably than ours, probably due to different experimental conditions and different thermal history, but, on the contrary, our results are in good concordance with that of Shirota *et al.* [2] for the melting point. [C$_2$C$_1$Im][BETI] presents a glass transition (-52 ºC) with enthalpic recovery. To distinguish it from a solid-solid transition we have zoomed in the DSC scan and checked that it corresponds to a "stair step" which is the common appearance for a glass transition [3]. Afterwards, [C$_2$C$_1$Im][BETI] shows a subcooling phenomenon, characterised by an incomplete crystallization on cooling ramp, then a part of this IL pass from a glassy to a subcooled state, suffering a cold crystallization followed by the melting transition. This cold crystallization phenomenon is usually observed in the thermal behaviour of many ILs. Agreeing with these results, Calvar *et al.* [4] and Fredlake *et al.* [5] found that some imidazolium based ILs presented similar behaviour, nevertheless it cannot be observed in pyridinium based ILs.

Table 3.1. Freezing (t_f), melting (t_m), glass transition (t_g), cold crystallization (t_{cc}) and solid-solid transition (t_{ss}) temperatures measured in our laboratory and literature reported for all selected ILs.

Compound	t_m / (°C)	t_g / (°C)	t_f / (°C)	Other / (°C)
$[C_4C_1C_1Im][OTf]$	2 [6]			
$[C_4C_1C_1Im][NTf_2]$	-13 [7], -2 [8]	≥20 [9]		
$[C_4C_1Pyrr][NTf_2]$	-8 [10], -19 [11], -18 [12], -22 [13], -15 [14], -13 [15], -18 [16]	-87 [12], -88 [13], -89 [11], -87 [17], -83 [14], -81 [15]	-39 [10], -54 [11]	-24 [16], -30 [11] (t_{ss})
$[C_1OC_2C_1Pyrr][NTf_2]$		-91 [11], -95 [18]		
$[C_4C_1Pyrr][OTf]$	3 [6,10]		-2 [10]	
$[C_4C_1Im][BF_4]$	-71 [19,20], -81 [20-23]	-85 [5,24], -87 [25], -80 [26]		
$[C_4C_1Pyrr][B(CN)_4]$	19 [27]			
$[C_3C_1Im][NTf_2]$		-87 [28], -88 [29], -89 [30]		
$[C_2Py][OTf]$	32/-7		16 /-10	
$[C_2Py][C_1SO_3]$	62		-1	
$[Chol][NTf_2]$	27/33, 27 [31], 30 [32]		-9	2, -1 [31] (t_{ss})
$[C_2C_1Im][BETI]$	16, -1 [1], 15 [2]	-52	-11, -12 [1]	-37 (t_{cc})
$[C_2Py][NTf_2]$	32, 31 [33]	-38 [33]	-22	21, 20 [33] (t_{ss})
$[C_2C_1Im][OTf]$	14, -11 [34], -9 [35]		-4, -9 [34]	
$[P_{6,6,6,14}][(C_2F_5)_3PF_3]$	-64, -65 [36]			
$[C_4C_1C_1Im][(C_2F_5)_3PF_3]$	5			-23 (t_{cc})
$[C_4C_1Pyrr][(C_2F_5)_3PF_3]$	7, 2 [10], 4 [37,38]		-26, -9 [10], -27 [37]	-40 [37] (t_{cc})
$[C_1OC_2C_1Pyrr][(C_2F_5)_3PF_3]$	-15			-49 (t_{cc})
$[C_4C_1Pyrr][(C_4F_9)_3PF_3]$	4	-62	-35	
$[C_1C_1Im][C_1C_1PO_4]$	< -65 [39]	-64 [40]		
$[C_2C_1Im][C_6SO_4]$	7			-32 (t_{cc})

Expanded uncertainties are U(t) = ±2 °C (0.95 level of confidence).

[Chol][NTf$_2$] showed a very different profile on heating ramp than the rest of ILs (Fig. 3.1.b). This profile is characterized by three endothermic peaks at (2, 27 and 33) ºC. The first is attributed to a solid-solid transition and the last to a melting process. The origin of the peak at 27 ºC, which is not completely resolved with the last peak, could be associated either to solid-solid or to melting transition. Taking into account that the temperatures of second and third peaks (27 ºC and 33 ºC) do no change when the heating rate increases at 10 ºC · min^{-1} (results are not shown), it could be possible that the melting process of this IL takes place in two different phases at 27 ºC and 33 ºC. Similar behaviour and temperatures were also found by Yoshizawa-Fujita *et al.* [31] for this IL, being this shape usual in DSC of polymers with high molecular weight [41,42]. Additionally, Nockeman *et al.* [32], indicates that the melting temperature for [Chol][NTf$_2$] is 30 ºC although these authors do not show the DSC curves of this IL, being this value in relative good concordance with our results.

On the other hand, [C$_2$Py][NTf$_2$] crystallizes, at -21 ºC, on cooling, but does not form a glass in the temperature range studied (Fig. 3.1.a). A solid–solid transition at 21 ºC and the melting point at 32 ºC are detected in heating ramp, agreeing in both cases with the results of Liu *et al.* [33]. This behaviour, not unusual in ILs, is also observed by Machanová *et al.* [43] and Stefan *et al.* [44] for ammonium and pyrrolidinium based IL, with the [NTf$_2$]$^-$ anion, observing in the last case, even two solid-solid transitions before the melting.

Wachter *et al.* [34] and Bonhôte *et al.* [35] observed melting and freezing temperature transitions of [C$_2$C$_1$Im][OTf] very different to ours (Fig. 3.1.d). This fact can be explained taking into account the difference in heating rate; these authors have chosen a very small rate of 0.5 ºC · min^{-1}.

[C$_4$C$_1$Pyrr][(C$_2$F$_5$)$_3$PF$_3$] shows an exothermic peak on cooling ramp at -26 ºC and an endothermic peak in heating at 7 ºC (Fig. 3.1.h); similar results have been found by other authors [37,38]. Fletcher *et al.* [37] reported a cold crystallization temperature at -40 ºC, probably due to the use of a cooling rate twice than ours,

and possibly the sample has not enough time to crystalize in the cooling ramp, appearing the cold crystallization in the heating one. Similarly than in the previous IL and due to the different experimental conditions, Wachter *et al.* [10] indicated at (2 and -9) ºC melting and freezing transitions, respectively, very different to ours.

$[P_{6,6,6,14}][(C_2F_5)_3PF_3]$ shows an endothermic peak in heating at -64 ºC (Fig. 3.1.l), very similar value than Otero *et al* [36], -65 ºC; the cooling ramp did not register any transition over the limited temperature range of the used equipment.

For the rest of the selected ILs, no references have been found, thus, $[C_2Py][OTf]$ shows two exothermic peaks on cooling and two endothermic peaks on heating (Fig. 3.1.c) ramps. Other authors as Calvar *et al.* [4] have observed similar behaviour in some pyridinium and imidazolium based ILs with the same anion, $[OTf]^-$, suggesting a polymorphic-like behaviour, which leads to the formation of crystals with different structures stated. Nevertheless, a deeper study is necessary to complement and to confirm this result. $[C_4C_1C_1Im][(C_2F_5)_3PF_3]$ (Fig. 3.1.g), $[C_2C_1Im][C_6SO_4]$ (Fig. 3.1.j) and $[C_1OC_2C_1Pyrr][(C_2F_5)_3PF_3]$ (Fig. 3.1.k) show an exothermic peak (corresponding to a t_{cc}) and an endothermic one (corresponding to a t_m) in heating (Fig. 3.1) and it cannot be detected any peak on cooling ramp over the temperature range of the equipment. $[C_2Py][C_1SO_3]$ (Fig. 3.1.e) and $[C_4C_1Pyrr][(C_4F_9)_3PF_3]$ (Fig. 3.1.i) present exothermic peak (corresponding to a t_f) on cooling ramp and an endothermic one (corresponding to a t_m) on the heating ramp.

From results of Table 3.1, the sequence obtained for melting temperature of selected ILs was:

$[C_2Py][C_1SO_3]$ > $[C_2Py][OTf]$ ≈ $[C_2Py][NTf_2]]$ ≈ $[Chol][NTf_2]$ > $[C_4C_1Pyrr][B(CN)_4$ > $[C_2C_1Im][BETI]$ ≈ $[C_2C_1Im][C_6SO_4]$ > $[C_2C_1Im][OTf]$ > $[C_4C_1C_1Im][(C_2F_5)_3PF_3]$ > $[C_4C_1Pyrr][(C_2F_5)_3PF_3]$ ≥ $[C_4C_1Pyrr][(C_4F_9)_3PF_3]$ ≥ $[C_4C_1Pyrr][OTf]$ ≥ $[C_4C_1C_1Im][OTf]$ > $[C_4C_1C_1Im][NTf_2]$ > $[C_4C_1Pyrr][NTf_2]$ ≈

$[C_1OC_2C_1Pyrr][(C_2F_5)_3PF_3]$ > $[P_{6,6,6,14}][(C_2F_5)_3PF_3]$ > $[C_1C_1Im][C_1C_1PO_4]$ > $[C_4C_1Im][BF_4]$
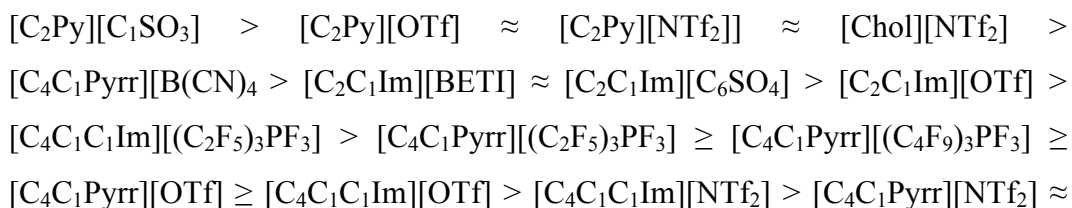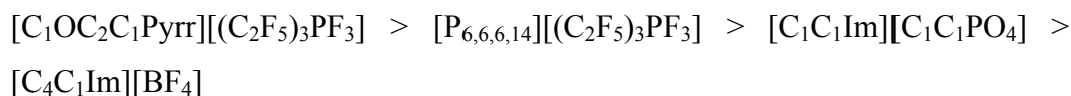
Although a clear trend could not be established, results seems to show that the imidazolium cations presented the lowest values of melting points and pyridinium the highest, for the same anion, as it can be seen more clearly in Figure 3.2. Similar trend cannot be observed related to the anion influence.
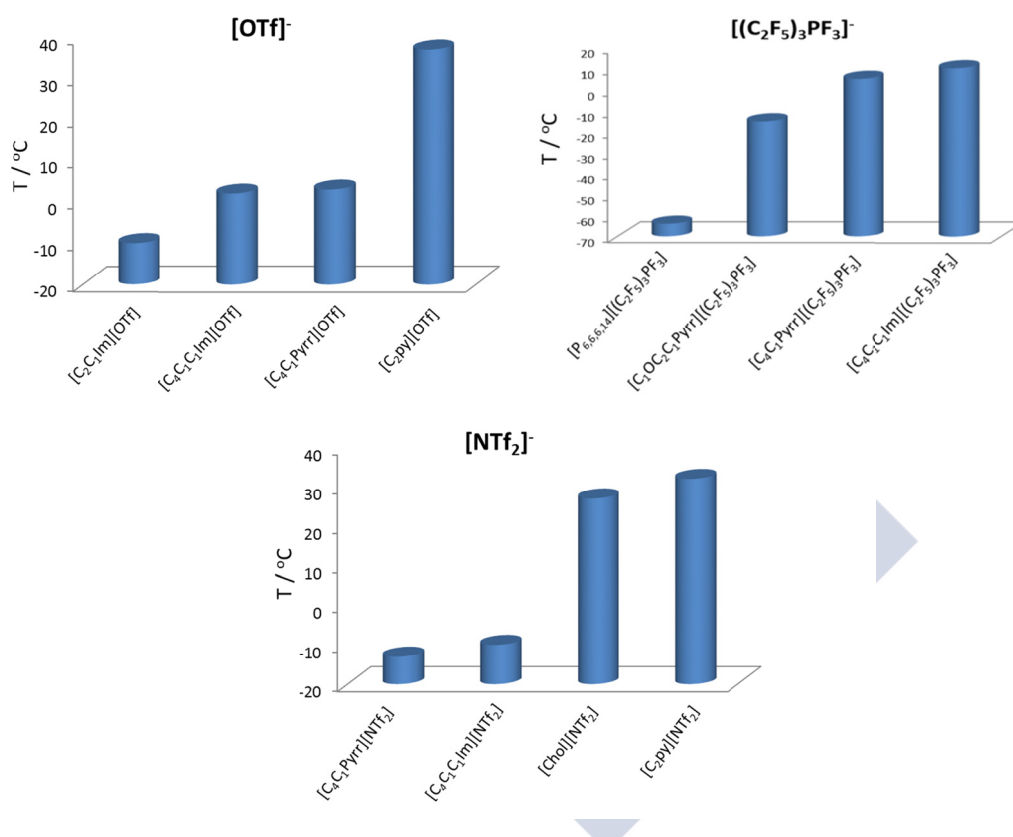
Figure 3.2. Melting temperatures for the ILs with the $[OTf]^-$, $[(C_2F_5)_3PF_3]^-$ and $[NTf_2]^-$ anions.

Similarly and with regard to freezing temperatures the sequence was a little bit different:
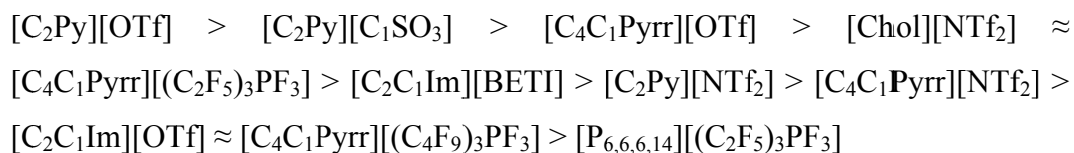
$[C_2Py][OTf]$ > $[C_2Py][C_1SO_3]$ > $[C_4C_1Pyrr][OTf]$ > $[Chol][NTf_2]$ ≈ $[C_4C_1Pyrr][(C_2F_5)_3PF_3]$ > $[C_2C_1Im][BETI]$ > $[C_2Py][NTf_2]$ > $[C_4C_1Pyrr][NTf_2]$ > $[C_2C_1Im][OTf]$ ≈ $[C_4C_1Pyrr][(C_4F_9)_3PF_3]$ > $[P_{6,6,6,14}][(C_2F_5)_3PF_3]$

A trend with anion or cation cannot be established for freezing temperatures. Although it is important to remark that, in both sequences, the two first ILs remain the same.

Substantial supercooling is observed for some of the ILs, with freezing point significantly lower than melting point, being the differences t_m-t_f around (20 to 30) ºC, except for $[C_2Py][NTf_2]$, $[C_2C_1Im][OTf]$, $[C_4C_1Pyrr][(C_4F_9)_3PF_3]$ and $[C_2Py][C_1SO_3]$ which is higher than 50 ºC, indicating a very slow crystallization rate. This fact is a very important and positive feature for the application of ionic liquids as absorbents in absorption heat pumps and avoid problem of crystallization commonly observed in the current working pairs, as it previously was pointed out (*Introduction* chapter).

3.2. Thermogravimetric results

Although it is well known that the experimental conditions, such as heating rate, sample pan materials, sample weight and atmosphere can influence on the thermal analysis results, scarce bibliographic data show numerical values about this influence on ILs or even the published values present some incoherence. For example: Ngo *et al.*[1] have found differences higher than 100 ºC between the onset temperatures (t_{onset}) of $[C_2C_1Im][PF_6]$ measured in aluminum (375 ºC) and alumina (481 ºC) pans, whereas only a difference of 2 ºC was found for $[C_2C_1Im][NTf_2]$ under the same conditions. On the other hand, for this last IL, Ngo *et al.*[1] obtained a value of 453 ºC at 20 ºC · min^{-1} whereas Noda *et al.*[45] have found a value of 417 ºC when using a heating rate of 10 ºC min^{-1}, both in Nitrogen atmosphere, *i.e.* an increase in more than 30 ºC was found in the onset temperature when using different heating rates. Fox *et al.*[46] found an increase of 100 ºC in the onset temperature of $[C_4C_1Im][BF_4]$ when the heating rate increases from (10 to 20) ºC · min^{-1}. Similar results have been reported by other authors like Awad *et al.*[47], Kosmulski *et al.*[48], Hao *et al.*[49] and Amarasekara and Owereh[50].

Then, the first proposal of this work is the study of the influence of these experimental conditions on TGA curves and onset temperatures of some ILs.

3.2.1. Influence of experimental conditions

In this section, the influence of the analysis conditions, namely atmosphere, heating rate, sample mass or water content, in dynamic scans will be checked.

3.2.1.1. Atmosphere influence

With the aim to define the most advisable analysis conditions of ILs for lubrication applications, five ILs, $[C_4C_1C_1Im][NTf_2]$, $[C_4C_1C_1Im][(C_2F_5)_3PF_3]$, $[C_4C_1Pyrr][OTf]$, $[C_1OC_2C_1Pyrr][NTf_2]$ and $[P_{6,6,6,14}][(C_2F_5)_3PF_3]$, were analyzed in a dynamic mode from (100 to 800) ºC at 10 ºC · min^{-1} in both, air and Nitrogen atmospheres. Figure 3.3 shows the comparison of TG and DTG curves in both atmospheres for $[C_1OC_2C_1Pyrr][NTf_2]$. Results of t_{onset}, t_{endset}, $t_{10\%}$, t_{peak}, and W_{onset} obtained from the TG and DTG curves, for every atmosphere, are presented in Table 3.2. These results show that the studied ILs are slightly more stable in Nitrogen atmosphere. Small differences in t_{onset}, until 19 ºC, for N_2 and air atmospheres can be observed. Nevertheless, for each IL similar values of W_{onset} were obtained in air and N_2 indicating that mass loss at onset temperature seems to be not atmosphere dependent. Villanueva *et al.* [51] studied the differences between these atmospheres on the IL $[C_2C_1Im][NTf_2]$ finding a similar behavior, differences in t_{onset} of 25 ºC at 10 ºC · min^{-1}. Ghaemy *et al.* [52], studied the thermal stability of poly(etherimidazoleimide) (PEII)s under these two atmospheres, obtaining values 30 ºC higher in N_2 than air atmosphere on the $t_{10\%}$. Heym *et al.* [53] studied the thermal stability under He and N_2 of $[C_4C_1Im][NTf_2]$ at 0.5 ºC · min^{-1} concluding that this IL shows higher thermal stability under N_2 atmosphere. Nevertheless, Hao *et al.* [49], studied the thermal stability under Air and N_2 of Allyl-methylimidazolium Chloride ($[AC_1Im][Cl]$) at 10 ºC · min^{-1} finding differences of 1 ºC. And Huddleston *et al.* [54] concluded, after analysis of the data published by

Bonhôte *et al.* [35], that TGA experiments of several imidazolium ILs performed under N_2 and air atmosphere produce the same results. Nevertheless, this observation must be treated with caution, due to the fact that, although it is true that there are many similarities, the results obtained with both atmospheres are not specified in detail on the original work.
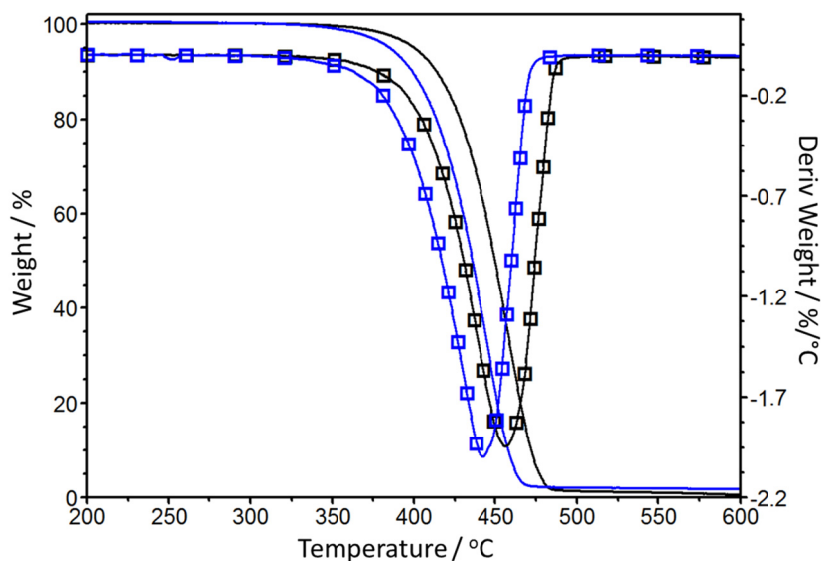
Figure 3.3. Comparison of TG and DTG (□) curves under N_2 (black) and air (blue) for $[C_1OC_2C_1Pyrr][NTf_2]$.

Table 3.2. Thermal results from the dynamic scans in N_2 and air atmospheres.

IL	Atmosphere	t_{onset} (ºC)	t_{endset} (ºC)	$t_{10\%}$ (ºC)	W_{onset} (%)	t_{1st} (ºC)	t_{2nd} (ºC)
$[C_4C_1C_1Im][(C_2F_5)_3PF_3]$	Air	363	437	364	88	395	413
	N_2	376	460	379	91	402	442
$[C_4C_1C_1Im][NTf_2]$	Air	424	488	407	79	470	476
	N_2	436	487	408	75	478	---
$[C_4C_1Pyrr][OTf]$	Air	399	436	382	88	414	---
	N_2	416	447	404	80	438	---
$[C_1OC_2C_1Pyrr][NTf_2]$	Air	411	460	399	82	443	---
	N_2	424	475	414	83	457	---
$[P_{6,6,6,14}][(C_2F_5)_3PF_3]$	Air	363	451	356	88	396	445
	N_2	382	477	382	90	407	467

Expanded standard uncertainties are U(t) = 5 ºC and U(W) = 2% (0.95 level of confidence).

Literature about the degradation of these ILs on N_2 atmosphere is scarce and in most cases comparisons are difficult due to the influence of the other experimental conditions on the results. Thus, Fox *et al.* [55] and Bazito *et al.* [7] have found similar t_{onset} values for $[C_4C_1C_1Im][NTf_2]$, (435 and 430) ºC respectively, and Jin *et al.* [56] similar $t_{10\%}$ values, 414 ºC, for the same IL. However, Fox *et al.* [57] and Sun *et al.* [58], have found t_{onset} values higher than ours, (459 and 450) ºC respectively, but operational conditions are not completely clear.

Since the purpose of the study is the characterization of the ILs and lubricants bases thermal stability, in order to estimate the maximum temperature of operation as lubricants, and taking into account the above results, further analysis were performed only in air atmosphere for being this one the more restrictive.

3.2.1.2. Initial mass influence

A comparison of TG curves for $[C_4C_1C_1Im][NTf_2]$ with different sample masses and identical heating rate, 10 ºC · min^{-1}, obtained in air atmosphere is presented in Figure 3.4.
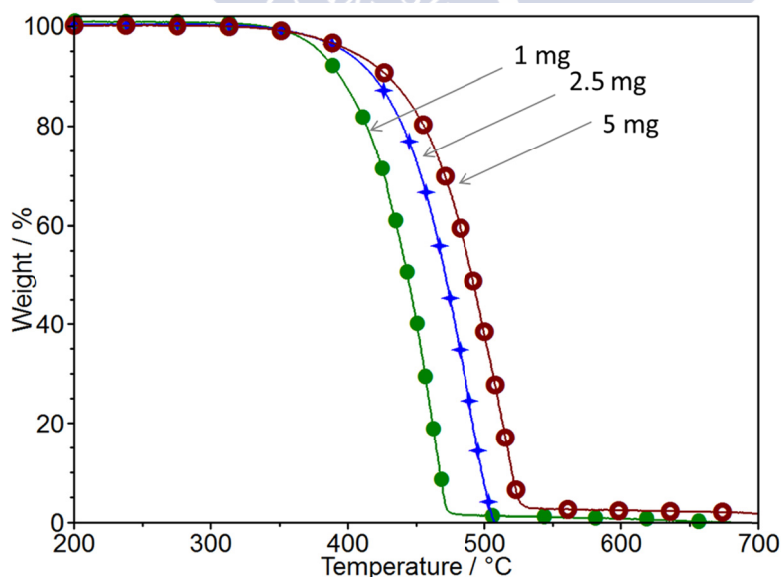
Figure 3.4. TG curves of $[C_4C_1C_1Im][NTf_2]$ obtained at 20 °C · min^{-1} in air atmosphere with different sample masses.

As it can be seen, the process of degradation shifts to higher temperatures with increasing mass, as is reported by other authors [48,51,59]. Onset temperatures for the different initial mass are 417, 438 and 456 ºC for 1, 2.5 and 5 mg, respectively.

3.2.1.3.   Heating rate influence

Several authors have reported that heating rate have a strong influence on the dynamic scans [51,55,60,61]. TG and DTG curves of $[C_4C_1C_1Im][NTf_2]$ obtained at different heating rates, 1, 3, 5, 10, 15 and 20 ºC · min^{-1} in air atmosphere and similar mass (2.5 ± 0.3) mg, are presented in Figure 3.5.

Table 3.3 shows t_{onset}, t_{endset}, $t_{10\%}$, t_{1st}, and W_{onset} values obtained at the different heating rates. Degradation process takes place at temperatures higher than 350 ºC in all cases. Onset temperatures can range to 73 ºC according to the heating rate. ΔT between onset and endset temperatures grows as the heating rate increases. According to Hatakeyama and Quinn [62], the reason for this behaviour is that at low heating rates the sample temperature is more uniform and diffusion of product gases can occur within the sample, lowing the decomposition temperature.
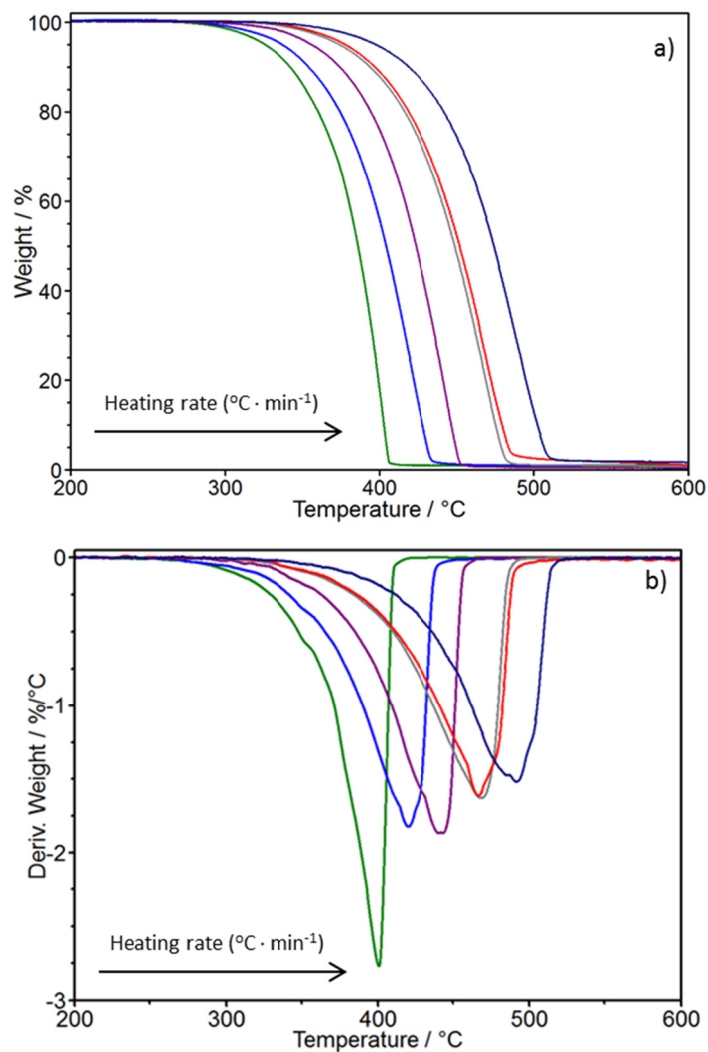
Figure 3.5. Heating rate influence on TG (a) and DTG (b) curves of $[C_4C_1C_1Im][NTf_2]$ at 1 ºC · min^{-1} (green), 3 ºC · min^{-1} (blue), 5 ºC · min^{-1} (purple), 10 ºC · min^{-1} (grey), 15 ºC · min^{-1} (red), 20 ºC · min^{-1} (navy blue) in air atmosphere.

Table 3.3. Thermal results from the dynamic scans in air atmosphere at different heating rates.

Heating rate (°C · min⁻¹)	t_{onset} (°C)	t_{endset} (°C)	$t_{10\%}$ (°C)	W_{onset} (°C)	t_{1st} (°C)
1	369	406	342	73	401
3	376	433	354	79	420
5	398	452	374	78	441
10	419	480	393	78	465
15	422	484	397	78	468
20	442	507	419	80	492

Expanded standard uncertainties are U(t) = 5 °C and U(W) = 2% (0.95 level of confidence).

3.2.1.4. Water content influence

Water quantities could be considered important [54], but the samples of ILs were employed in this work without purification because in many potential industrial applications as lubricants, contact with air cannot be avoided. With the aim to determine the water influence on thermal stability of ILs, we have performed some TGA experiences of ILs purified and saturated of water.

Three samples of the selected ILs ([C$_1$OC$_2$C$_1$Pyrr][NTf$_2$], [C$_1$OC$_2$C$_1$Pyrr][(C$_2$F$_5$)$_3$PF$_3$] and [P$_{6,6,6,14}$][(C$_2$F$_5$)$_3$PF$_3$]) were stored in an open bottle for a week in order to reach the water saturation level content. These samples are referred in this work as "water-saturated". The increased water content was measured by weighting the samples every 24 hours, with a precision of ± 0.00001 g.

A Karl-Fischer coulometric titrator (Metler Toledo DL32) was used in order to measure water content in the samples of ILs (Fig. 2.9). This titrator can determine water contents in the range from 1 ppm to 1% and it is based on the standard reaction equation for the Karl-Fischer reaction [63].

Water contents of the pure and water-saturated samples are shown in Table 3.4. As it can be seen, [C$_1$OC$_2$C$_1$Pyrr][NTf$_2$] has a high capacity for absorbing water, reaching a water content value that is around twenty times that of the pure sample. For the ILs with anion [(C$_2$F$_5$)$_3$PF$_3$]⁻, the water saturation content is quite lower; although in case of [P$_{6,6,6,14}$]⁺ cation the water content in supply conditions was the highest, the water content on the saturation level was the lowest.

In Figure 3.6, comparisons of the TG and DTG curves obtained for $[C_1OC_2C_1Pyrr][NTf_2]$ and $[C_1OC_2C_1Pyrr][(C_2F_5)_3PF_3]$ saturated and under supply conditions are presented. As it can be observed on Figure 3.6 and on Table 3.4, ILs do not show appreciable differences in the thermal stability after the water saturation. No significant differences in DTG curves of saturated and as supplied samples are also observed.

Table 3.4. Water contents and degradation onset temperatures for the ILs corresponding to water saturation content and to supply conditions measured under atmospheric pressure, (992 ± 5) hPa, and relative humidity of 80 %.

IL	Water content (ppm)		t_{onset} (°C)	
	As supplied	saturated	As supplied	saturated
$[C_1OC_2C_1Pyrr][NTf_2]$	174	3700	411	406
$[C_1OC_2C_1Pyrr][(C_2F_5)_3PF_3]$	139	1028	352	349
$[P_{6,6,6,14}][(C_2F_5)_3PF_3]$	193	264	363	356

Expanded standard uncertainties are U(t) = 5 °C and U(W) = 2% with 0.95 level of confidence.

Huddleston *et al.* [54] have found, in general, that drying improves the thermal stability of ILs, but in the studies here presented no significant differences were observed between the stability for pure and water saturated ILs. Valkenburg *et al.* [64] studied the effect of water on the thermal stability of the ILs $[C_2C_1Im][BF_4]$, $[C_4C_1Im][BF_4]$ and $[C_1C_1C_3Im][NTf_2]$ and they did not found significant changes on the onset temperatures.

a) $[C_1OC_2C_1Pyrr][NTf_2]$

b) $[C_1OC_2C_1Pyrr][(C_2F_5)_3PF_3]$
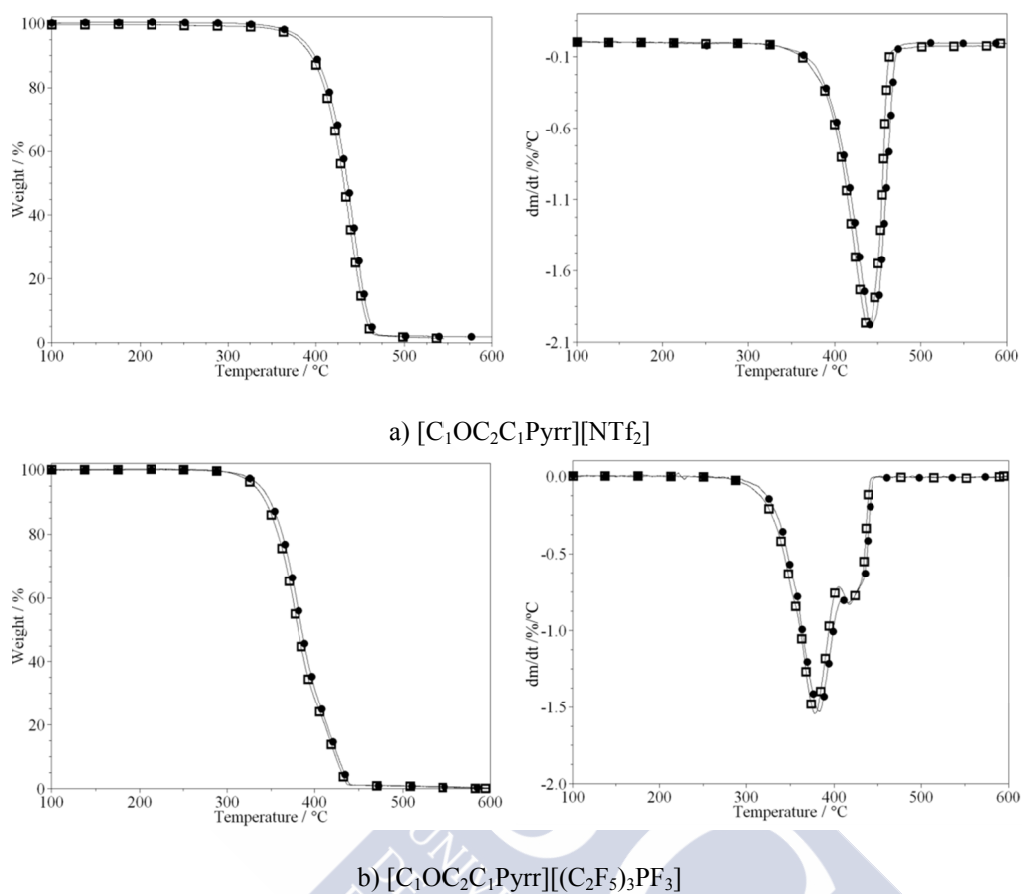
Figure 3.6. Comparison of TG and DTG curves, under water saturation content (□) and under supply conditions (●).

3.2.2. Dynamic study

Taking into account those previous results, the experimental conditions were careful chosen, then all the experiments were performed with similar initial mass sample, air atmosphere, which is the most restrictive, and 10 ºC · min^{-1} were selected, which is the most used in bibliographic references. TG and DTG curves corresponding to the dynamic scans of the 26 studied compounds, in these conditions, are presented on Figure 3.7. From all the curves, t_{onset} and t_{endset}, the temperature peaks on DTG curves (t_{1st} and t_{2nd}), the remaining mass at t_{onset} (W_{onset}), and the temperature at different degradation levels, were determined folllowing the methodology exposed in the previous chapter, *Materials and experimental methods*. All these data are presented in Table 3.5.
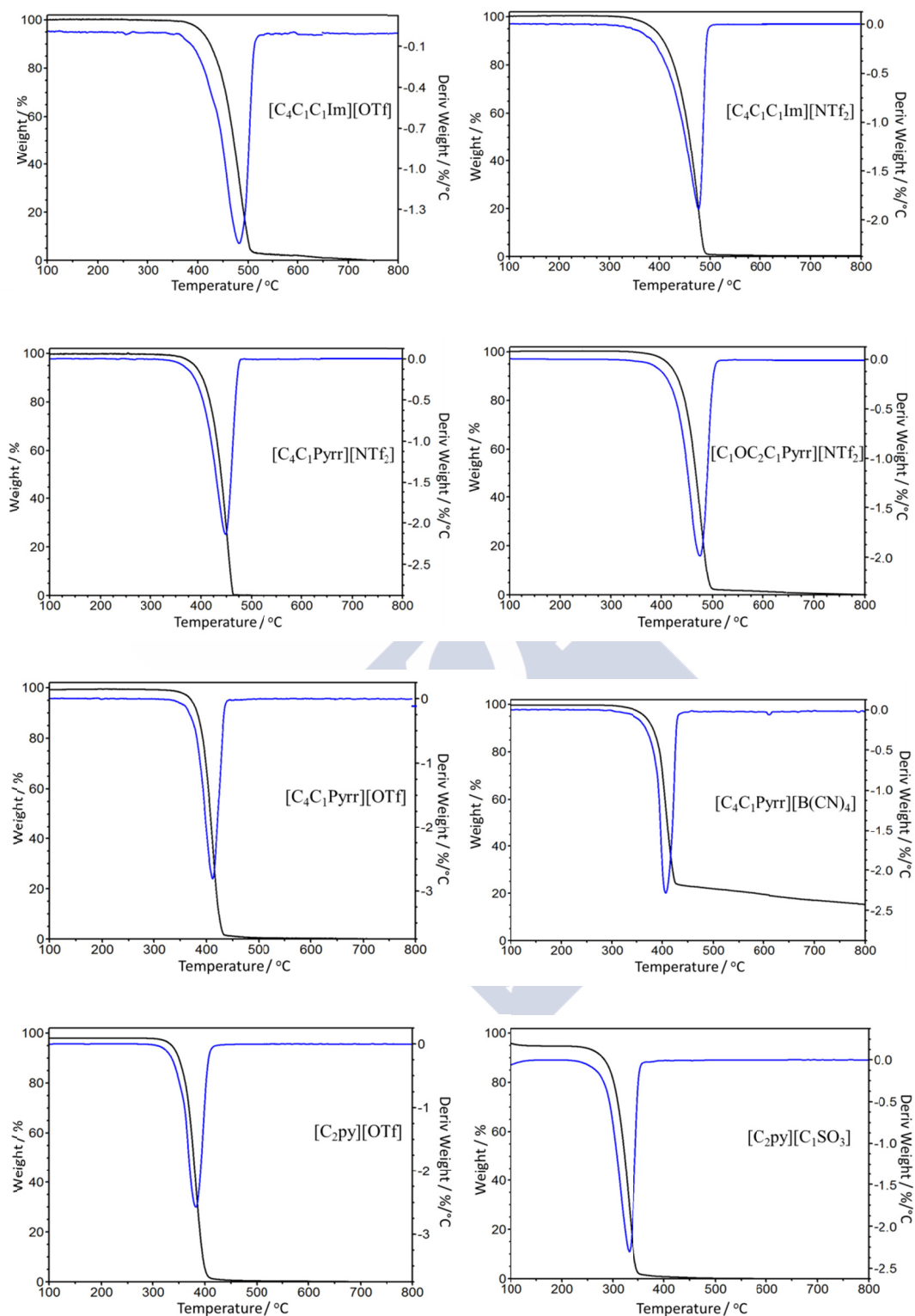
Figure 3.7. TG (black) and DTG (blue) curves for all the studied compounds.
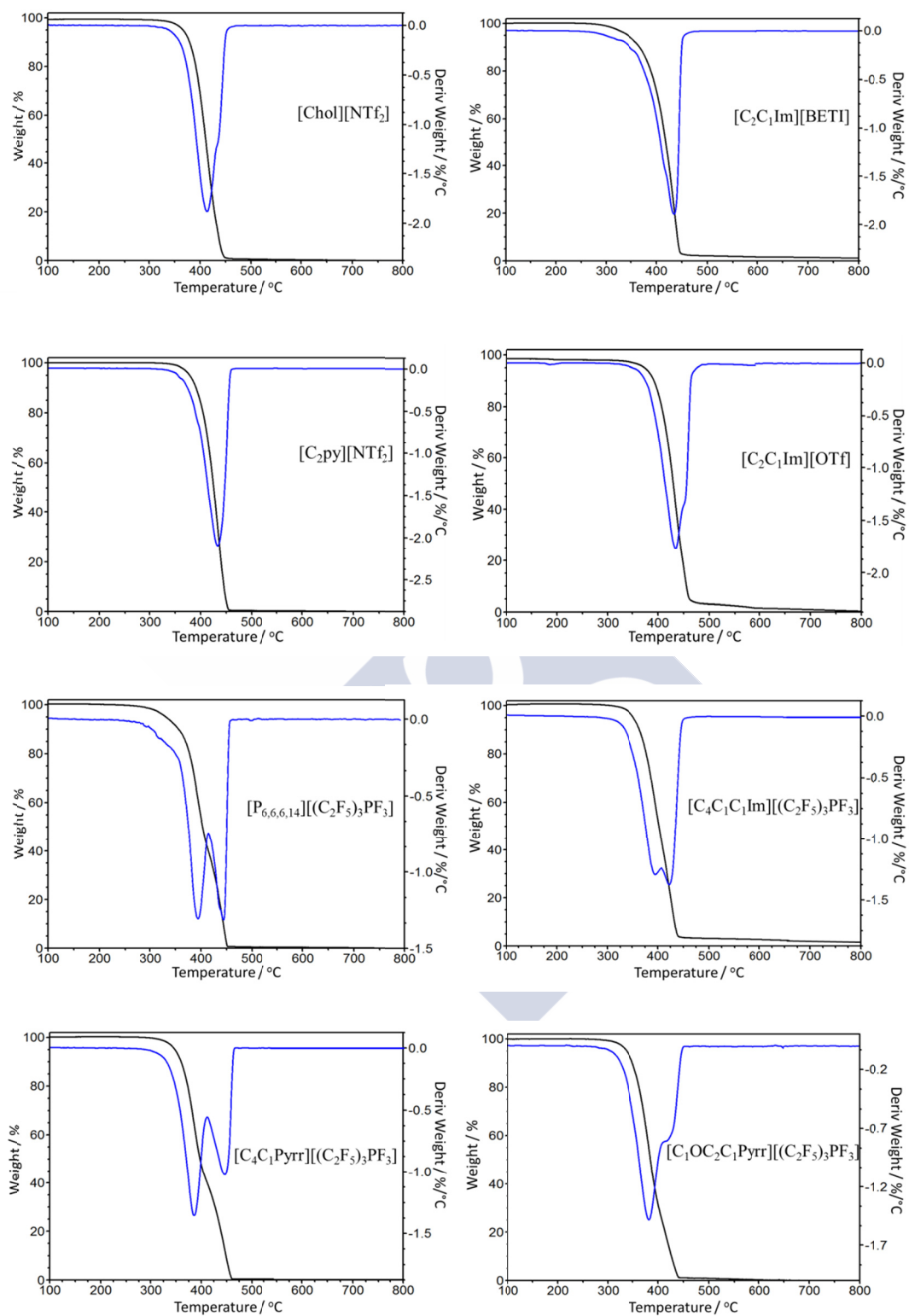
Figure 3.7. TG (black) and DTG (blue) curves for all the studied compounds (continue).
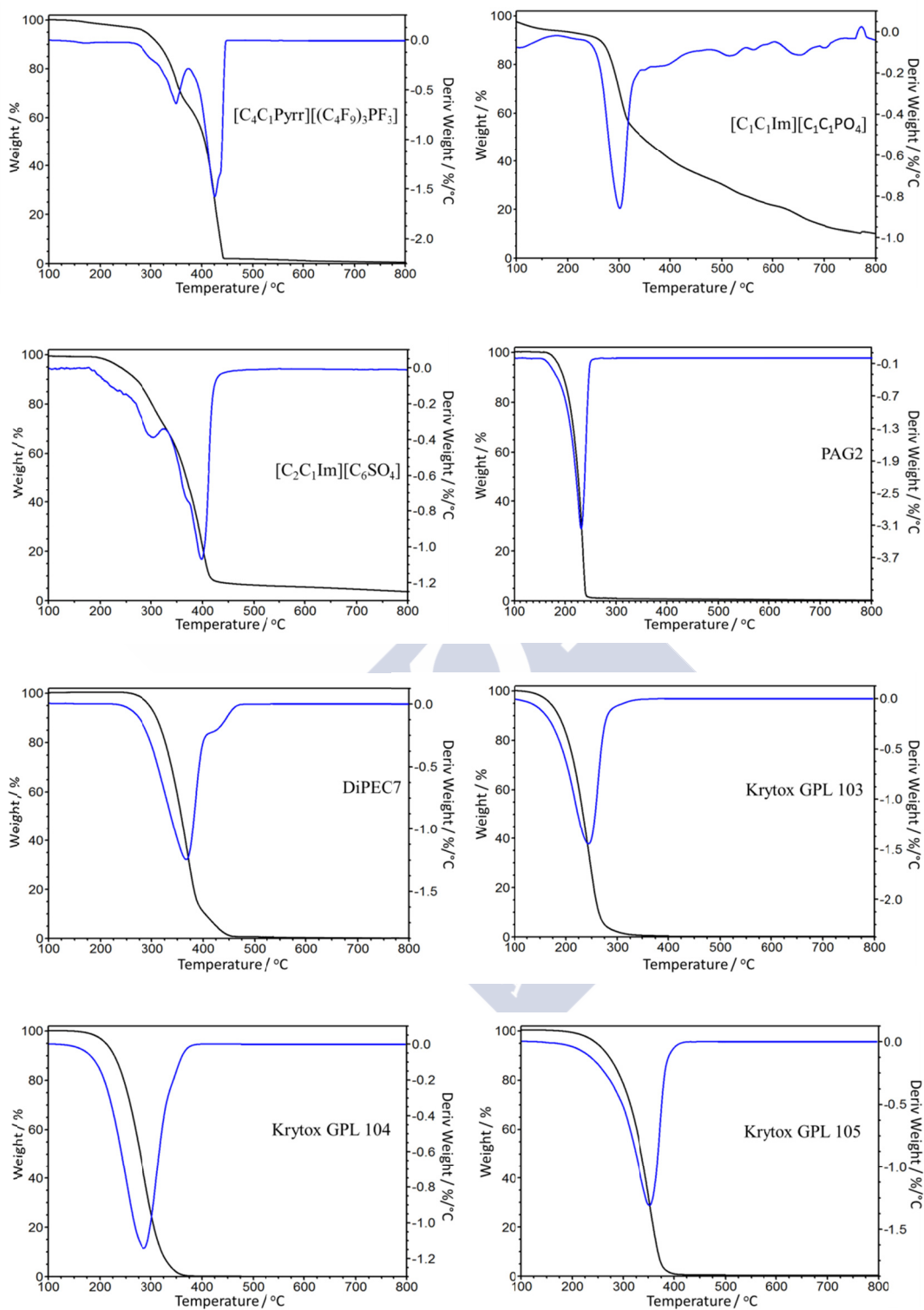
Figure 3.7. TG (black) and DTG (blue) curves for all the studied compounds (continue).
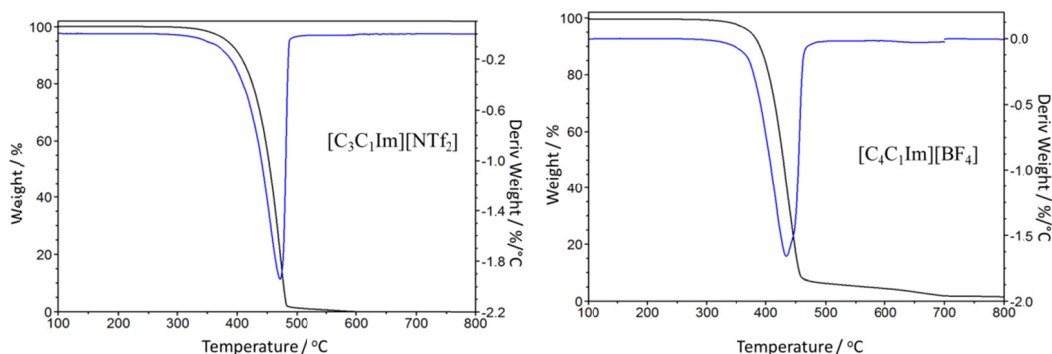
Figure 3.7. TG (black) and DTG (blue) curves for all the studied compounds (continue).

According to the results shown in Table 3.5, thermal stability of the majority of analysed ILs (17 over 21) is better than that corresponding to the selected bases. The most thermally stable base was DiPEC7, followed by Krytox GPL 105, Krytox GPL 104, PAG2 and Krytox GPL 103. Only two of the selected bases have a better stability than some of the analysed ILs.

A very interesting feature can be seen when comparing the t_{onset} of $[C_4C_1Pyrr][(C_2F_5)_3PF_3]$, $[C_1OC_2C_1Pyrr][(C_2F_5)_3PF_3]$, $[C_4C_1Pyrr][NTf_2]$ and $[C_1OC_2C_1Pyrr][NTf_2]$; a slightly decrease of only 6 ºC on this characteristic temperature is detected when replacing $[C_4C_1Pyrr]^+$ by $[C_1OC_2C_1Pyrr]^+$. This fact completely agrees with obtained results for Zhou *et al.* [11]; these authors have found that replacing the butyl group in the cation with a methoxyethyl group tends to decrease the thermal stability for ILs with the anions $[C_nF_{2n+1}BF_3]^-$ (for n=0 to 4) and $[NTf_2]^-$.

Table 3.5. Characteristic thermogravimetric parameters for all the studied compounds

Compound	t_{onset} (ºC)	t_{endset} (ºC)	$t_{10\%}$ (ºC)	W_{onset} (%)	t_{1st} (ºC)	t_{2nd} (ºC)
$[C_4C_1C_1Im][OTf]$	436	502	424	84	479	---
$[C_3C_1Im][NTf_2]$	430	481	404	77	472	
$[C_4C_1C_1Im][NTf_2]$	424	476	407	79	470	476
$[C_4C_1Pyrr][NTf_2]$	417	461	402	81	452	---
$[C_1OC_2C_1Pyrr][NTf_2]$	411	460	399	82	443	---
$[Chol][NTf_2]$	410	460	401	85	442	---
$[C_2py][NTf_2]$	409	471	397	83	450	---
$[C_2C_1Im][OTf]$	404	458	388	87	436	---
$[C_4C_1Im][BF_4]$	400	455	390	84	435	
$[C_4C_1Pyrr][OTf]$	399	436	382	88	414	---
$[C_4C_1Pyrr][B(CN)_4]$	387	421	381	86	407	---
$[C_2py][OTf]$	371	416	365	86	399	---
$[C_2C_1Im][BETI]$	368	425	354	85	407	---
$[P_{6,6,6,14}][(C_2F_5)_3PF_3]$	363	451	356	88	396	445
$[C_4C_1C_1Im][(C_2F_5)_3PF_3]$	363	437	364	88	395	413
$[C_4C_1Pyrr][(C_2F_5)_3PF_3]$	358	458	360	90	381	441
$[C_1OC_2C_1Pyrr][(C_2F_5)_3PF_3]$	352	419	349	88	384	417
DiPEC7	318	445	307	86	370	420
$[C_4C_1Pyrr][(C_4F_9)_3PF_3]$	315	440	316	90	350	426
$[C_2py][C_1SO_3]$	315	353	298	85	339	---
Krytox GPL 105	298	373	270	79	352	---
$[C_1C_1Im][C_1C_1PO_4]$	274	326	262	87	303	---
$[C_2C_1Im][C_6SO_4]$	251	413	269	94	398	---
Krytox GPL 104	235	321	228	87	288	---
PAG2	212	240	197	76	234	---
Krytox GPL 103	200	267	186	83	244	---

Expanded standard uncertainties are U(t) = 5 ºC and U(W) = 2% (0.95 level of confidence).

Figure 3.8 represents, for comparison, a selection of the different kind of anions and the most stable lubricant. It can be seen that exists a wide variety of thermal behaviours; namely, different curve shapes, diversity of "size" thermal degradation interval, different location of the main thermal degradation step.
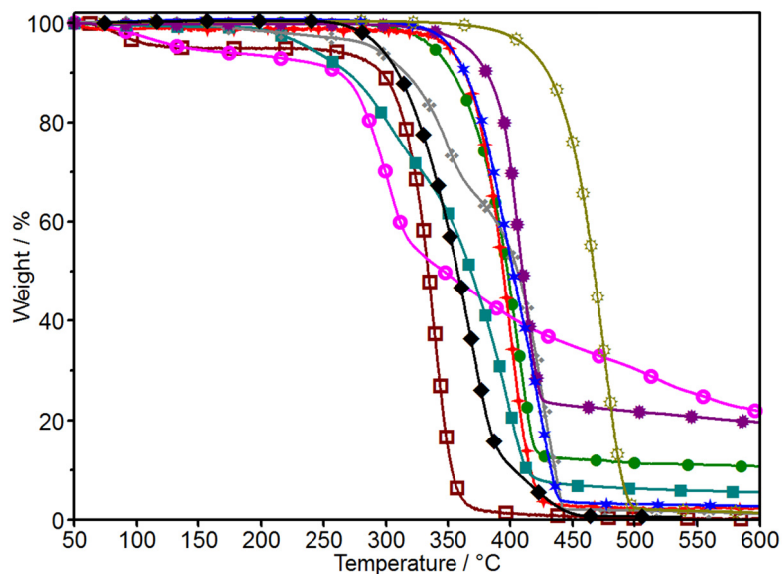
Figure 3.8. TG curves for ILs with the different anions and one lubricant base: (●)[C$_2$C$_1$Im][BETI], (✦)[C$_2$Py][OTf], (□)[C$_2$Py][C$_1$SO$_3$], (○)[C$_1$C$_1$Im][C$_1$C$_1$PO$_4$], (■)[C$_2$C$_1$Im][C$_6$SO$_4$], (✻)[C$_4$C$_1$Pyrr][B(CN)$_4$], (❖)[C$_4$C$_1$Pyrr][(C$_4$F$_9$)$_3$PF$_3$], (✿)[C$_1$OC$_2$C$_1$Pyrr][NTf$_2$], (◆)DiPEC7, (★)[C$_4$C$_1$C$_1$Im][(C$_2$F$_5$)$_3$PF$_3$].

In order to better visualize the anion influence on the thermal stability, Figures 3.9 and 3.10 have been presented. These figures represent thermogravimetric results for different anions with the same cation family (imidazolium and pyrrolidinium, respectively), agreeing with other authors results: thermal stability of ILs is intensely anion dependent [36,48,50,55,65-68].
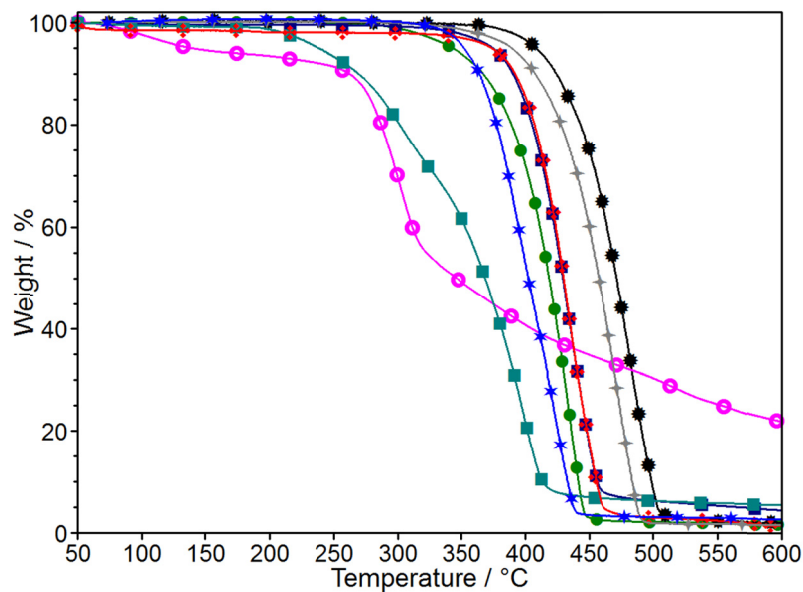
Figure 3.9. TG curves for imidazolium cation: ($\circ$)[C$_1$C$_1$Im][C$_1$C$_1$PO$_4$], ($\blacksquare$)[C$_4$C$_1$Im][BF$_4$], ($\blacksquare$)[C$_2$C$_1$Im][C$_6$SO$_4$], ($\ast$)[C$_4$C$_1$C$_1$Im][OTf], ($\star$)[C$_4$C$_1$C$_1$Im][(C$_2$F$_5$)$_3$PF$_3$], ($\diamond$)[C$_2$C$_1$Im][OTf], ($\bullet$)[C$_2$C$_1$Im][BETI], ($+$)[C$_4$C$_1$C$_1$Im][NTf$_2$].
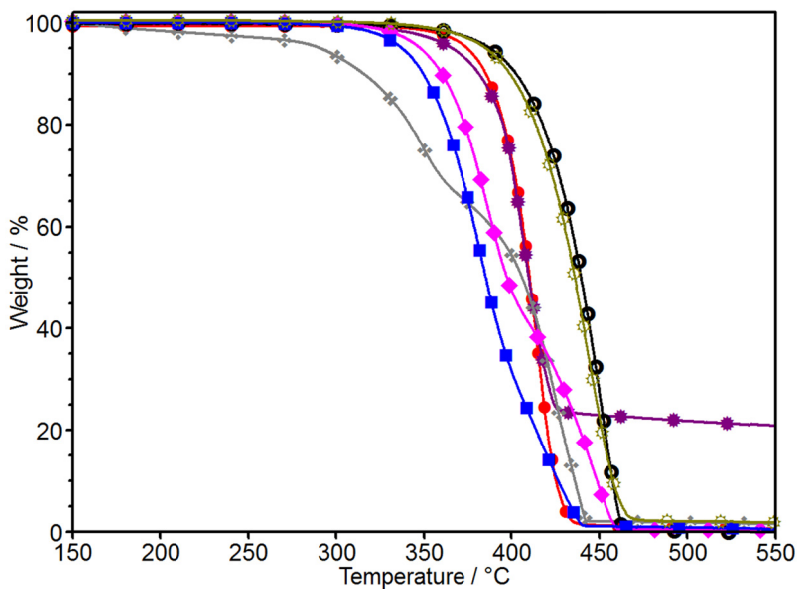
Figure 3.10. TG curves for pyrrolidinium cation: ($\bullet$)[C$_4$C$_1$Pyrr][OTf], ($\times$)[C$_4$C$_1$Pyrr][(C$_4$F$_9$)$_3$PF$_3$], ($\ast$)[C$_4$C$_1$Pyrr][B(CN)$_4$], ($\circ$)[C$_4$C$_1$Pyrr][NTf$_2$], ($\blacklozenge$)[C$_4$C$_1$Pyrr][(C$_2$F$_5$)$_3$PF$_3$], ($\circ$)[C$_1$OC$_2$C$_1$Pyrr][NTf$_2$], ($\blacksquare$)[C$_1$OC$_2$C$_1$Pyrr][(C$_2$F$_5$)$_3$PF$_3$].

Cation influence on thermal stability of the ILs is much lower than the anion, as other authors have reported [48]. For example, in case of $[NTf_2]^-$, similar values of onset temperatures have been measured, ranging between (424 and 409) ºC, being this range (363 and 352) ºC in case of $[(C_2F_5)_3PF_3]$. Nevertheless, different behaviour is observed for $[OTf]^-$, which shows differences between onset values as high as 65 ºC. According to Table 3.5 it is possible to establish different sequences of thermal stability:

- ✓ Cation: $[Imidazolium]^+ > [Pyrrolidinium]^+ > [Pyridinium]^+ > [Choline]^+$

- ✓ Anion: $[NTf_2]^- \geq [OTf]^- \geq [BF_4]^- > [B(CN)_4]^- > [BETI]^- > [(C_2F_5)_3PF_3]^- > [(C_4F_9)_3PF_3]^- > [C_1SO_3]^- > [C_1C_1PO_4]^- > [C_6SO_4]^-$

Figure 3.11 represents a comparison of the TG curves for a selection of ILs and the five selected lubricants. It can be seen that the thermal stabilities of the ILs and the lubricant bases are very different.
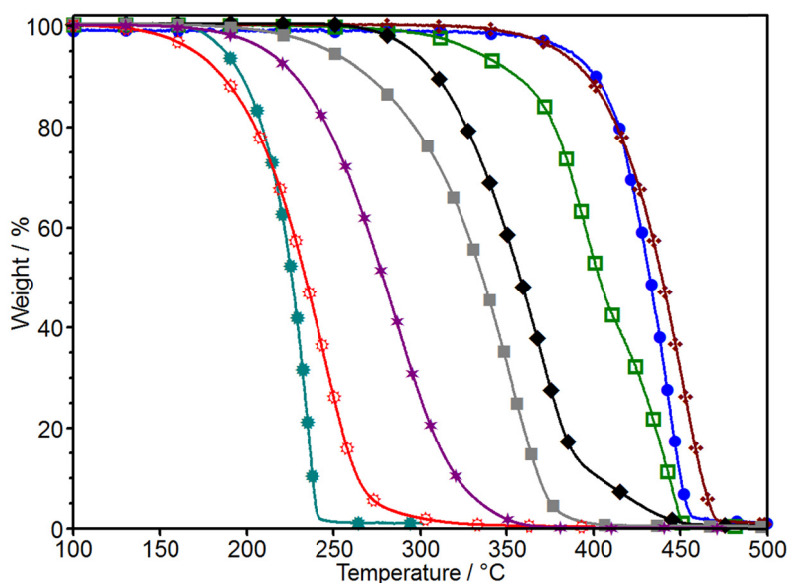
Figure 3.11. TG curves for lubricant bases and some ILs: (●)[Chol][NTf₂], (✤)[C₂Py][NTf₂], (□)[P₆,₆,₆,₁₄][(C₂F₅)₃PF₃], (◆)DiPEC7, (■)Krytox GPL 105, (○)Krytox GPL 104, (✶)Krytox GPL 103, (✹)PAG2.

As it can be seen in Figure 3.12, $[NTf_2]^-$, $[BF_4]^-$, $[OTf]^-$, $[C_1SO_3]^-$, $[B(CN)_4]^-$ (Fig.3.12a) and $[BETI]^-$ (Fig. 3.12b) anions show a well-defined peak, which means a one-step mass loss; however $[C_1C_1PO_4]^-$ (Fig. 3.12a), $[(C_2F_5)_3PF_3]^-$, $[C_6SO_4]^-$ and $[(C_4F_9)_3PF_3]^-$ (Fig. 3.12b) show overlapped peaks that are related with a mass loss in various steps. For $[C_1C_1Im][C_1C_1PO_4]$ and $[C_4C_1Pyrr][B(CN)_4]$ a broader temperature interval should be necessary to complete the mass loss process. As it can be observed in Figure 3.12c, lubricant bases, in general, show the mass loss peak at lower temperatures than ILs. DiPEC7 shows better results than Krytox GPL and PAG2; Krytox GPL bases show an increment on their characteristic temperatures with the molecular weight. Krytox GPL show a single peak on DTG curves while DiPEC7 seems to present two, which means different degradation processes.
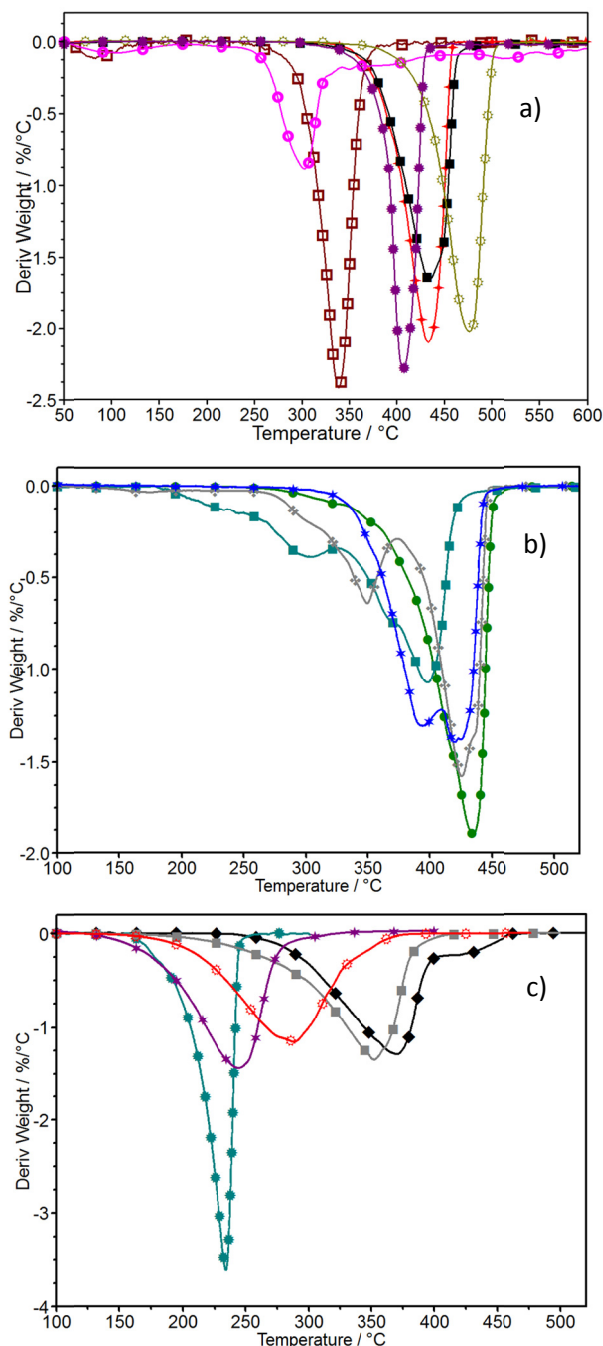
Figure 3.12. DTG curves for lubricant bases and different anion types ILs: (✦)[C$_2$Py][OTf], (✿)[C$_1$OC$_2$C$_1$Pyrr][NTf$_2$], (■)[C$_4$C$_1$Im][BF$_4$], (□)[C$_2$Py][C$_1$SO$_3$], (◯)[C$_1$C$_1$Im][C$_1$C$_1$PO$_4$], (✹)[C$_4$C$_1$Pyrr][B(CN)$_4$], (■)[C$_2$C$_1$Im][C$_6$SO$_4$], (●)[C$_2$C$_1$Im][BETI], (❖)[C$_4$C$_1$Pyrr][(C$_4$F$_9$)$_3$PF$_3$], (✶)[C$_4$C$_1$C$_1$Im][(C$_2$F$_5$)$_3$PF$_3$], (◆)DiPEC7, (■)Krytox GPL 105, (✿)Krytox GPL 104, (✳)Krytox GPL 103, (✹)PAG2.

Figures 3.13 and 3.14 show the t_{onset} and t_{endset} comparison for the 21 ILs and the 5 lubricant bases. It can be clearly seen that the most part of ILs have higher thermal stability than the selected lubricant bases, and ILs with $[BF_4]^-$, $[NTf_2]^-$ and $[OTf]^-$ anions were the most stable meanwhile $[C_1C_1PO_4]^-$ and $[C_6SO_4]^-$ were the least stable; besides all the ILs presented better thermal stability than three of the selected lubricant bases (Krytox GPL 104, PAG2 and Krytox GPL 103), as it was previously mentioned.

With regard to degradation temperature interval that can be defined as the range of temperature in which thermal decomposition of the sample occurs, different behaviours between ILs have also been observed. Thus, for ILs with $[NTf_2]^-$, $[OTf]^-$ and $[BF_4]^-$ anions, $\varDelta t$ (t_{enset}-t_{onset}) takes similar value, around 50 ºC. This means that once initiated the IL decomposition, in approximately 5 minutes, at the selected heating rate (10 ºC · min^{-1}), the sample has almost completely disappeared. In contrast, it was found that the phosphate and sulphate anions are associated with lower thermal stability, especially in cases of ILs $[C_2C_1Im][C_6SO_4]$ and $[C_1C_1Im][C_1C_1PO_4]$, which initiate degradation at temperatures below 275 ºC and have a wider degradation temperature interval (Fig. 3.7). For example, in case of $[C_2C_1Im][C_6SO_4]$ values of $\varDelta t$ higher than 160 ºC were observed.
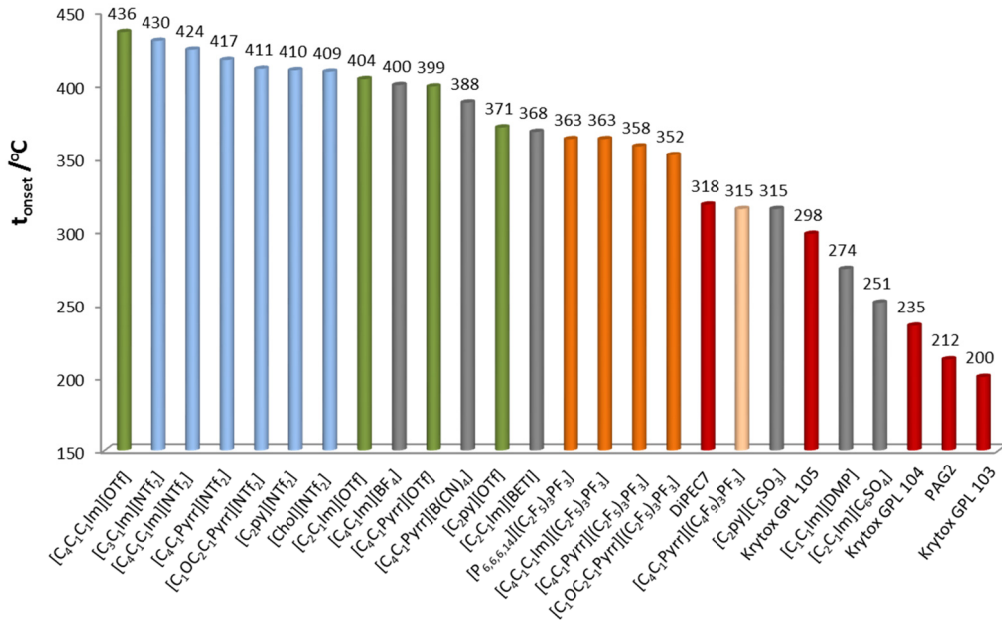
Figure 3.13. t_{onset} comparison for all the selected ILs and lubricant bases. Different colours identify different anions families (green: [OTf]⁻, blue: [NTf₂]⁻, orange: [(C₂F₅)₃PF₃]⁻, light orange: [(C₄F₉)₃PF₃]⁻), red colour: base lubricants and grey for the rest of anions: [BF₄]⁻, [B(CN₄)]⁻, [BETI]⁻ , [MeSO₃]⁻, [DMP]⁻ and [C₆SO₄]⁻.
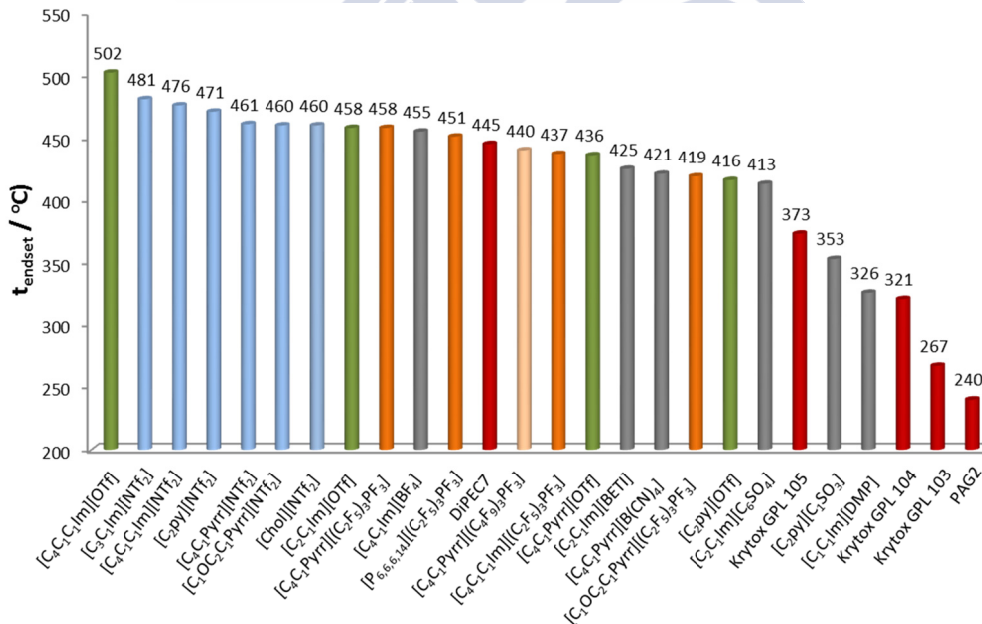
Figure 3.14. t_{endset} comparison for all the selected ILs and lubricant bases. Different colours identify different anions families (green: [OTf]⁻, blue: [NTf₂]⁻, orange: [(C₂F₅)₃PF₃]⁻, light orange: [(C₄F₉)₃PF₃]⁻), red colour: base lubricants and grey for the rest of anions: [BF₄]⁻, [B(CN₄)]⁻, [BETI]⁻ , [C₁SO₃]⁻, [DMP]⁻ and [C₆SO₄]⁻.

82

Literature about the degradation of these ILs and lubricants is scarce, and in most cases comparisons are difficult due to the influence of experimental conditions on results, as it has been pointed out, as well as to the different criteria followed by different authors.

Thus, Bittner *et al.* [65] used temperature of maximal decomposition rate (*i.e.* t_{1st} in this work) and they found similar results than those here obtained for $[C_2Py][NTf_2]$.

Heym *et al.* [53], with the scope of studying deeply the thermal stability, used the temperature to reach a mass loss of 1% during TGA experiments at different heating rates obtaining 348 °C for $[C_2C_1Im][OTf]$, being in concordance with ours data ($t_{10\%}$=388 °C).

$[C_1OC_2C_1Pyrr][NTf_2]$ presents a t_{onset} of 411°C and $t_{10\%}$ of 399°C, which are consistent with results of Fox *et al.* [57] who have reported for t_{onset} at two different heating rates of (10 and 20) °C · min^{-1}, (436 and 450) °C respectively, under N_2 atmosphere, and those of Reiter *et al.* [69] who obtained an onset temperature at a heating rate of 5 °C · min^{-1} of (345 and 306) °C under N_2 and O_2 atmospheres respectively for this IL.

Holopainen *et al.*[38] have found that decomposition temperature of $[C_4C_1Pyrr][(C_2F_5)_3PF_3]$ is higher than 300 °C, which agrees quite well with the results obtained in this thesis.

Important disagreement can be found in literature with regard to the thermal stability of $[C_4C_1Pyrr][NTf_2]$, thus Biso *et al.* [70] have reported 410 °C as the temperature at which thermal decomposition takes place with a 5% weight loss ($t_{5\%}$) of in N_2 atmosphere and 20 °C · min^{-1}, being this value quite similar to the $t_{10\%}$ presented in Table 3.5, 402 °C. Similarly, Chancelier *et al.* [71] reported for an onset temperature of 423 °C and 451°C, measured by TGA in argon flow atmosphere and DSC in Nitrogen atmosphere, respectively, using in both cases a heating rate of 5 °C · min^{-1}, being both values in relatively good agreement with

our result. Nevertheless, Shamsipur *et al.* [72], using TGA and DSC techniques, in similar conditions to this work, obtained the lowest value of bibliography (346ºC).

Fox *et al.* [57], have reported t_{onset} of $[C_4C_1C_1Im][NTf_2]$ at two different heating rate of (10 and 20) ºC · min^{-1}, (459 and 464) ºC respectively, on N_2 atmosphere, also coherent with the result here obtained, 417ºC, taking into account the experimental conditions.

Decomposition temperature (t_d) of $[C_2C_1Im][BETI]$ was previously calculated by Ngo *et al.*[1], obtaining different values using either aluminium (423 ºC) or alumina (462 ºC) sample pan, both of them higher than the data obtained in this work (368 ºC), but these researchers using N_2 atmosphere and a heating rate of 20 ºC · min^{-1}, tending both factor to increase stability, as it was pointed out in the previous section 3.2.1

In spite of the different experimental conditions, N_2 atmosphere and 5 ºC · min^{-1}, Królikowska [27] has reported a t_d for $[C_4C_1Pyrr][B(CN)_4]$ of 383 ºC, being similar that the value here presented. Likewise, Vitz *et al.* [73], have reported a t_d under N_2 atmosphere and 20 ºC · min^{-1}, only, 6 ºC lower than us for $[C_1C_1Im][C_1C_1PO_4]$. Zhou *et al.* [11] have found an t_d value (5 and 6) ºC higher than ours, for $[C_1OC_2C_1Pyrr][NTf_2]$ and $[C_4C_1Pyrr][NTf_2]$ respectively, with the same heating rate and N_2 gas.

On the other hand, Meindersma *et al.* [74] obtained a similar TG and DTG pattern for the $[C_4C_1Pyrr][B(CN)_4]$, although they reported a t_{onset} lower than that obtained in this work, but this can be explained taking into account that these authors calculated this temperature differently than us, thus they used the temperature at which the $dW/dt \neq 0$ [75].

Noack *et al.* [8] have found $t_{10\%}$ values for $[C_4C_1C_1Im][NTf_2]$ of 359 ºC (almost 50 ºC lower than our value). In this case, these authors used the same heating rate than us, nevertheless the rest of operational conditions are not well

indicated; and then, all those differences can be probably due to different analytical conditions.

There is not good concordance between decomposition temperature value reported in bibliography for [C$_4$C$_1$Im][BF$_4$]. Huddlestone *et al.* [54] have found similar values than ours, 403 ºC, Fredlacke *et al.* [5] and Holbrey and Seddon [76] have found decomposition temperatures at (361 and 360) ºC, respectively and Erdmenger *et al.* [26] have reported a decomposition temperature of 380 ºC. These differences can be explained taking into account that the tetra-fluoroborate-based ILs can easily hydrolyze and the hydrolysis extent, and as a consequence the water content, is markedly dependent on the temperature [77,78].

Additionally, in a review, Maton *et al.* [79] collected the onset temperatures of 60 imidazolium base ILs with different anions, among those are [NTf$_2$]$^-$ and [OTf]$^-$. These results show that for ILs with the same cation, those with the [NTf$_2$]$^-$ anion present higher values of t_{onset} than the ILs with [OTf]$^-$ anion, except for the ILs with the cation [C$_2$C$_1$Im]$^+$. Moreover, Fredlake *et al.* [5] also studied the thermal stability of several imidazolium based ILs, reporting the onset and start temperatures, t_{onset} and t_{start} respectively, being the last one the temperature at which the decomposition begins. The values of t_{start} are determined as the temperature at which the baseline and the TG curve separate from each other. These last authors found that the t_{onset} of [C$_4$C$_1$Im][NTf$_2$] is higher than that of [C$_4$C$_1$Im][OTf], whereas the t_{start} displayed the opposite behaviour. All these facts reveals that both anions, [NTf$_2$]$^-$ and [OTf]$^-$, present similar results in thermal stability studies and then the cation effect is more appreciable than in other combinations.

According to the remaining mass at t_{onset} (W_{onset}), measured values range between 7% for [C$_2$C$_1$Im][C$_6$SO$_4$] and 23% for [C$_2$C$_1$Im][NTf$_2$] and [C$_2$C$_1$Im][BETI], being remarkable that higher levels of this parameter correspond to those with the lower Δt (t_{enset}-t_{onset}) interval and vice versa. From the obtained results, it can be concluded that in general, values for W_{onset} are too high to can

85

consider t_{onset} as the maximum operation temperature. This feature, and the fact that variations on the experimental conditions can lead important changes in results, would involve that this dynamic analysis can be used just at comparative level, *i.e.*, to determine thermal stability sequence for a given set of ILs. To know the maximum operation temperature it is necessary to perform isothermal scans [1,48,51,55,61,68,79-81].

3.2.2.1.   Heating-cooling cycles. ILs ageing

Regarding to absorption heat pumps application, ILs behaviour after long periods of time, *i.e.* the ageing of the ILs after consecutive absorption-desorption cycles, remains as an open question. Up to our knowledge, very few experiments have been done to study ageing effect on ILs [57].

So, in this section this question is outlined using thermal techniques. Heating-cooling cycles were chosen to adapt the experimental procedure to absorption heat pump application. The experimental procedure consists in essays of 8 successive cycles "heating up to 175 ºC - cooling up to 50 ºC" under air atmosphere.

Figure 3.15 shows the second (the first one was not considered because a little percentage of impurities, specially water, released to rise 100 ºC) and the last heating TG curve for $[C_2C_1Im][OTf]$ and $[C_2Py][C_1SO_3]$. No significant degradation related to successive heating-cooling cycles was found.
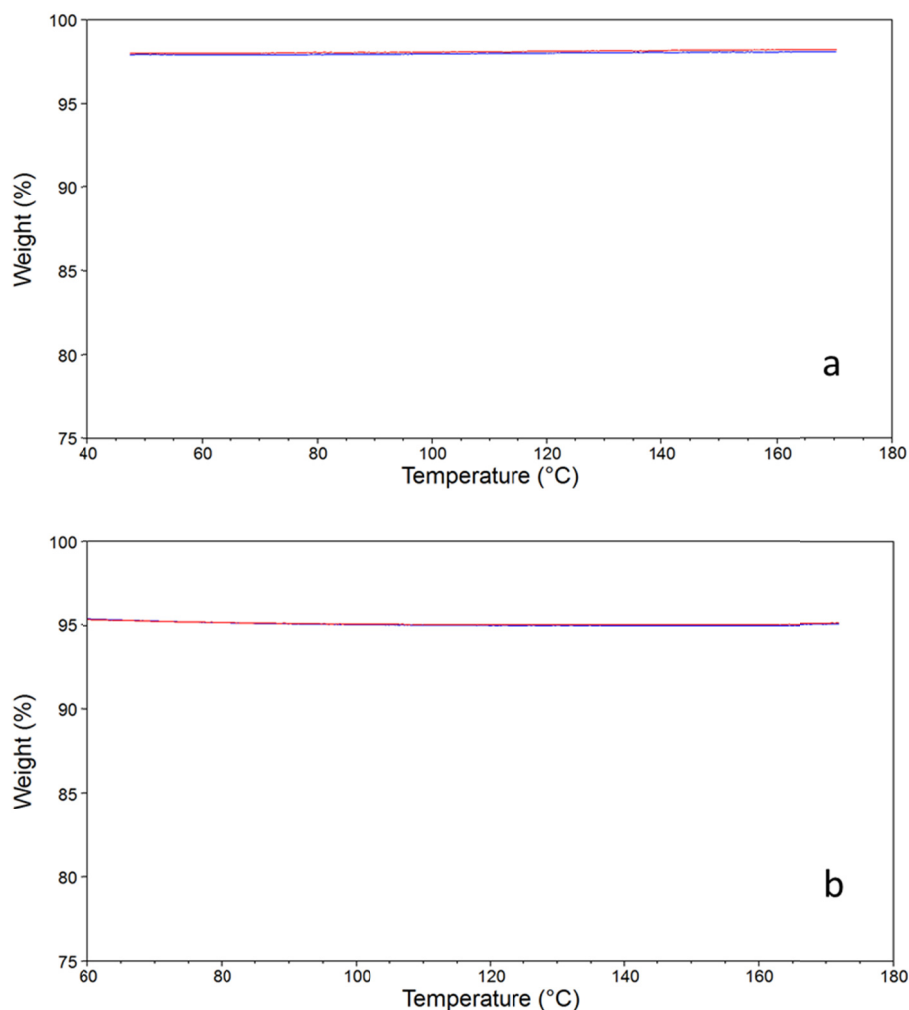
Figure 3.15. Comparison between the second and last curves of heating-cooling cycles of (a) [C$_2$C$_1$Im][OTf] and (b) [C$_2$Py][C$_1$SO$_3$] ILs.

After the successive heating-cooling cycles, the same sample of these ILs was subjected to a heating from 50 ºC to 800 ºC at 10 ºC · min^{-1} (figures not shown), *i. e.* the experimental conditions corresponding to dynamic studies, with the aim to determine the changes in characteristic temperatures after the cycles. Table 3.6 reports a comparison of onset temperatures obtained from this dynamic study after the cycles (t'_{onset}) and as supplied (t_{onset}). Results showed there are no significant changes in dynamic curves as a consequence of the ageing.

Even though during this process ILs do not undergo other effects related with physical absorption, chemical interactions or mechanical factors, results seem to indicate that ageing does not affect to thermal stability.

Table 3.6. Onset temperatures (t'_{onset}) of selected ILs obtained from dynamic studies after aging cycles.

IL	t'_{onset} / ºC	t_{onset} / ºC
[Chol][NTf$_2$]	410	410
[C$_2$py][NTf$_2$]	401	409
[C$_2$C$_1$Im][OTf]	405	404
[C$_2$py][OTf]	370	371
[C$_2$C$_1$Im][BETI]	362	368
[C$_2$py][C$_1$SO$_3$]	321	315

Expanded uncertainties are U(t)=±4 ºC (0.95 level of confidence)

3.2.3. Isothermal study

The onset temperature, t_{onset}, can be used as a relative thermal stability parameter, *i.e.*, to determine which IL (or lubricant), in a given set, is the most (or least) stable. But it cannot be employed as an "absolute" parameter of the thermal stability, since, as it can be clearly seen for example in Figure 10, the corresponding mass loss below temperatures than t_{onset} is important. Therefore, a reformulation of the study of the characterization of the "real" mass loss process of ILs is required. To do this, isothermal studies at temperatures below t_{onset} were performed. Isothermal scans have been carried out only in oxidative atmosphere, using the same air flow above mentioned. Temperatures of these essays have been chosen using the following criteria: the highest temperature for isothermal tests was set at least 40 ºC below the t_{onset}, and from that, isothermal tests were performed at temperatures 20 ºC under the previous one, until the temperature for which no degradation over 10% was observed. [46,50,59,82]

Several measures at different temperatures have been performed in the isothermal study, as it has been explained on experimental procedure in *Materials and experimental methods* Chapter. Fifteen ILs and two lubricant bases have been chosen to develop this study.

Figure 3.16 shows the mass loss of the chosen compounds over time during isothermal scans. Comparing, in all of them, the t_{onset} values and the isothermal TGA results corresponding to the first isothermal temperatures, it can be observed that there is appreciable degradation at these "isothermal" temperatures, even though these temperatures are lower than the corresponding onset temperatures calculated from previous studies, which means onset temperature is not a parameter as good as is usually considered to characterize the thermal stability. For example, for the IL $[C_1OC_2C_1Pyrr][(C_2F_5)_3PF_3]$, whose onset temperature was 352 ºC, in an isothermal scan 50 ºC below, over 80% of the initial mass is lost in just 50 minutes.
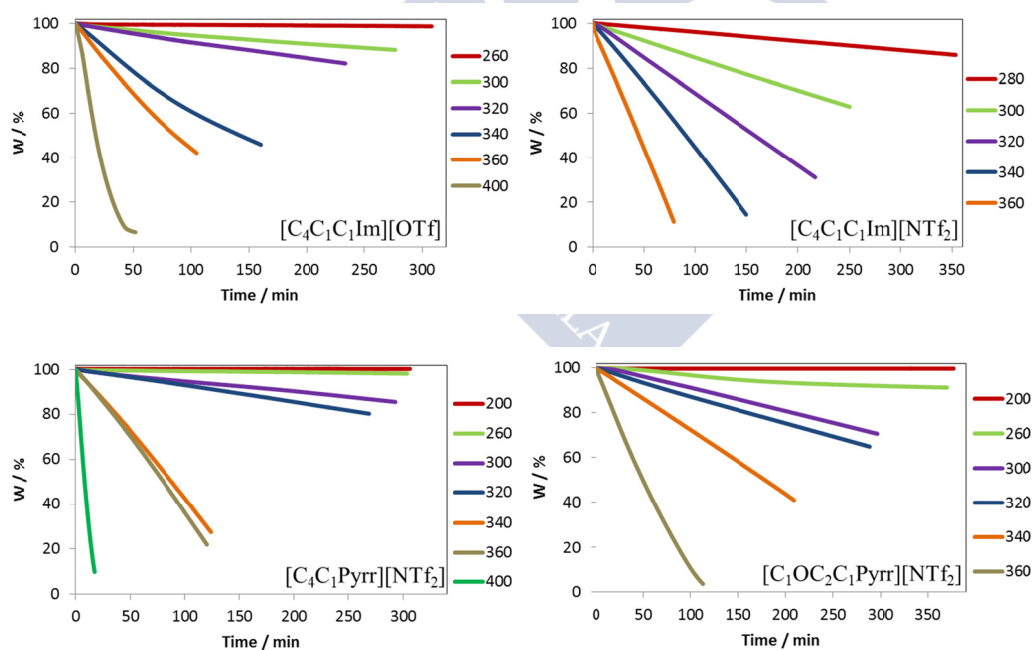
Figure 3.16. Isothermal scans of the selected ILs and lubricants at different Celsius degrees.

89
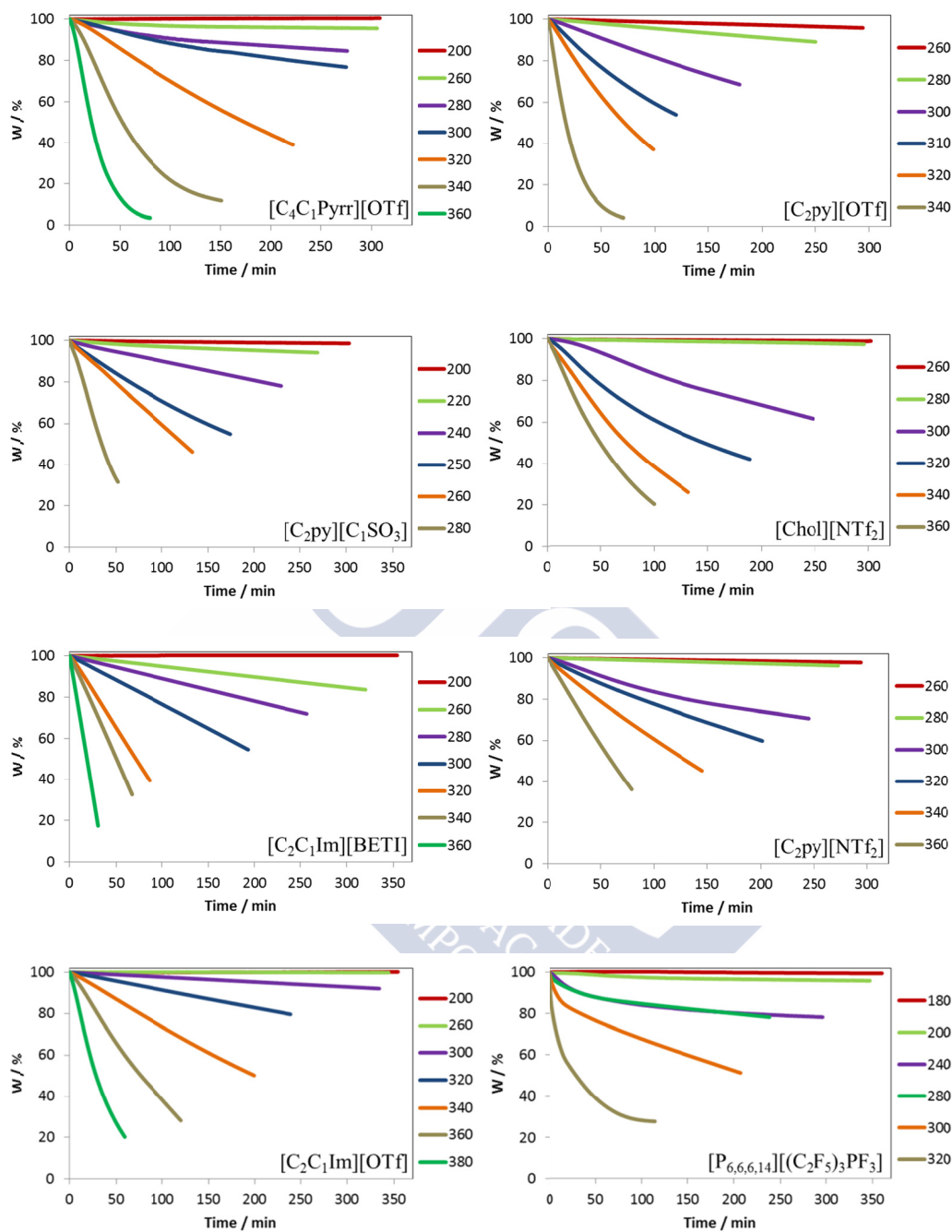
Figure 3.16. Isothermal scans of the selected ILs and lubricants at different Celsius degrees (continue).
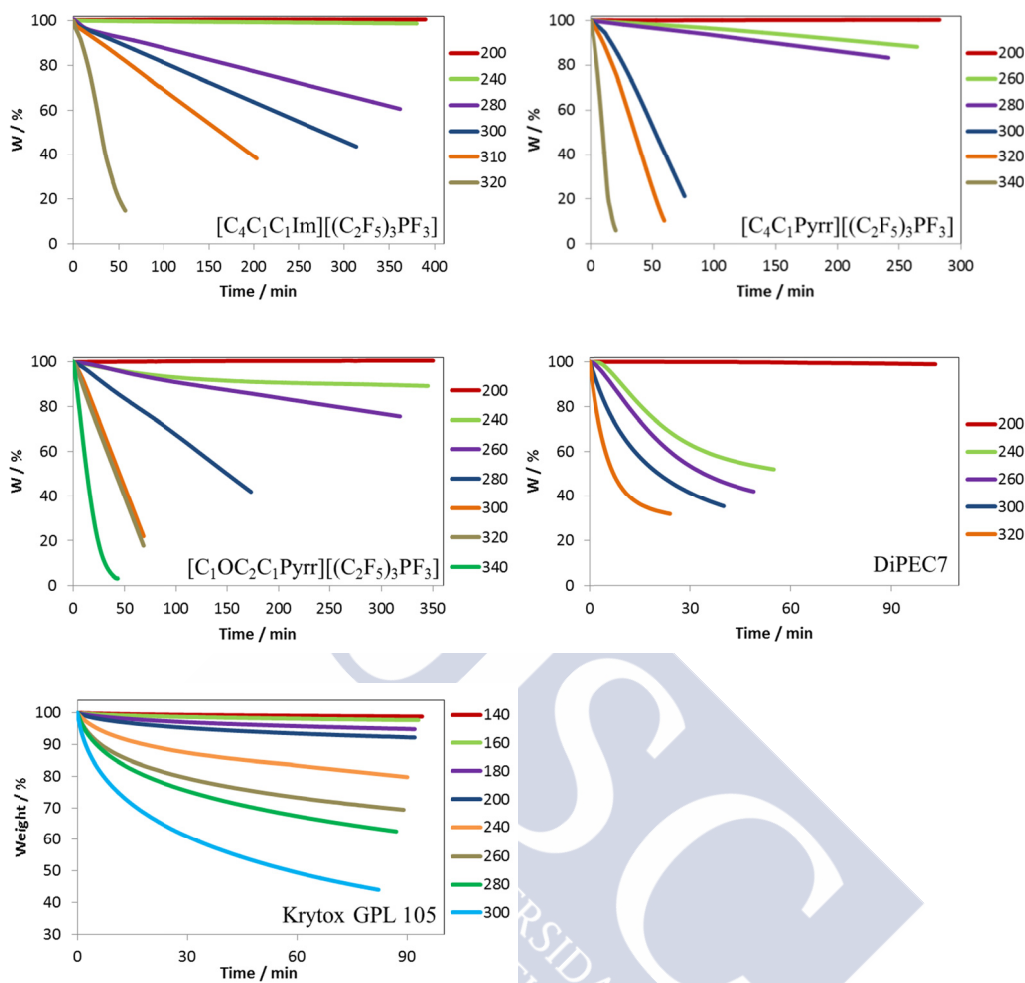
Figure 3.16. Isothermal scans of the selected ILs and lubricants at different Celsius degrees (continue).

By the contrary, a thermal degradation is hardly appreciable in the TGA scans during more than 5 hours at two temperatures, (200 and 260) ºC, for the selected ILs and (140 and 200) ºC for Krytox GPL 105 and DiPEC7 respectively.

Further analysis of isothermal scans, Table 3.7, shows the differences between the different ion types at the same isothermal scan temperature. On isothermal scan at 400 ºC for [C_4C_1Pyrr][NTf_2] we have found that the degradation in air is quicker (IL takes less time to achieve a concrete mass loss), than that obtained by Chancelier *et al.* [71] under argon atmosphere; in our case

91

there is a mass loss of 94% after 19 minutes and Chancelier *et al* [71] reported the same mass loss after 1 hour.

Table 3.7. Mass loss values after 50 minutes on isothermal scans at specified temperature.

IL	T / °C	mass loss / %
[C$_4$C$_1$Pyrr][NTf$_2$]	260	0.5
	300	3
	340	27
[C$_4$C$_1$Pyrr][OTf]	260	2
	300	6
	340	48
[C$_4$C$_1$Pyrr][(C$_2$F$_5$)$_3$PF$_3$]	260	2
	300	47
	340	97
[C$_1$OC$_2$C$_1$Pyrr][NTf$_2$]	260	1
	300	4
	340	14
[C$_1$OC$_2$C$_1$Pyrr][(C$_2$F$_5$)$_3$PF$_3$]	260	5
	300	46
	340	98
[C$_4$C$_1$Pyrr][NTf$_2$]	260	0.5
	300	9
	340	11
[C$_4$C$_1$Pyrr][OTf]	260	1
	300	9
	340	90
[C$_4$C$_1$Pyrr][C$_1$SO$_3$]	260	20
[C$_4$C$_1$C$_1$Im][NTf$_2$]	300	8
	340	26
[C$_4$C$_1$C$_1$Im][OTf]	300	3
	340	23
[C$_2$C$_1$Im][BETI]	300	12
	340	50
[C$_2$C$_1$Im][OTf]	300	1
	340	13
[C$_4$C$_1$C$_1$Im][(C$_2$F$_5$)$_3$PF$_3$]	300	10
[Ph$_3$t][(C$_2$F$_5$)$_3$PF$_3$]	300	23
Krytox GPL 104	260	25
	300	47
DiPEC7	260	59
	300	70

Figure 3.17, shows the isothermal TGA curves at 300 ºC for 5 ILs and 2 lubricant bases. From this figure, it can be concluded that the imidazolium are slightly more stable than the pyrrolidinium ILs; thermal stability for the ILs with the anions [NTf$_2$]⁻ and [OTf]⁻ is similar, and the ILs with [(C$_2$F$_5$)$_3$PF$_3$]⁻ are the less stable; lubricant bases have similar behaviour at the beginning of the process being Krytox GPL 105 slightly higher than DiPEC7 as time passes. Therefore, to estimate the maximum operation temperature of each of the compounds, an analysis of isothermal behaviour at temperatures below than t_{onset} is necessary
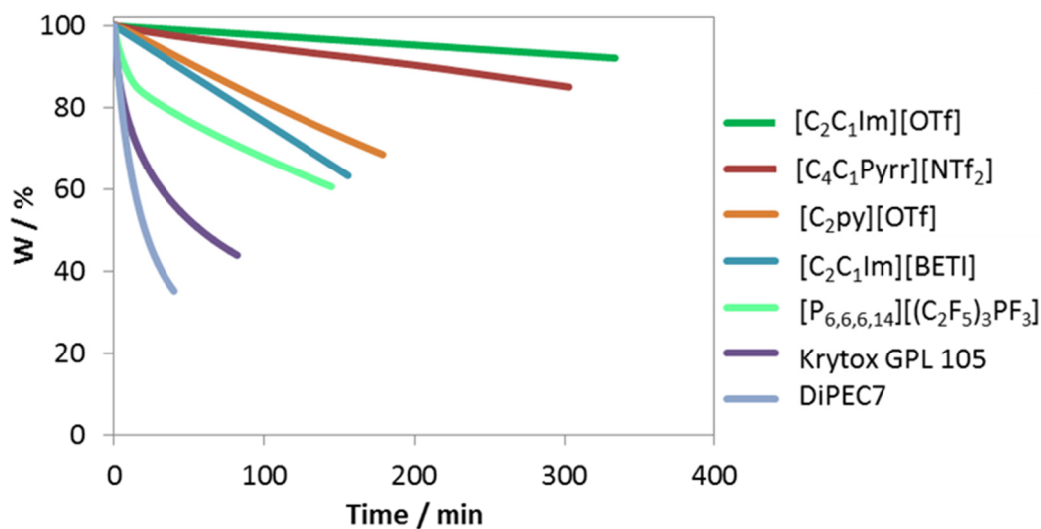
Figure 3.17. Comparison of the TGA isothermal scans at 300 ºC for some of the selected compounds.

According to Figure 3.17, a sequence of thermal stability for these compounds would be:

[C$_2$C$_1$Im][OTf] > [C$_4$C$_1$Pyrr][NTf$_2$] > [C$_2$py][OTf] > [C$_2$C$_1$Im][BETI] > [P$_{6,6,6,14}$][(C$_2$F$_5$)$_3$PF$_3$] > Krytox GPL 105 > DiPEC7
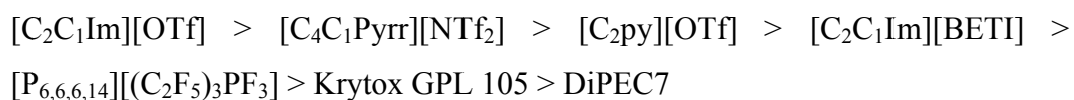
Although this sequence is not exactly the same as that obtained from the dynamic study, the small discrepancies point out that ILs with anions [NTf$_2$]⁻ and [OTf]⁻ present similar thermal stability and the lubricant bases are the less stable compounds here studied.

93

3.2.3.1. Maximum operation temperature

Up to now, does not exist a clear criterion on the degradation level allowed in the different applications, finding in literature a wide range, from 1 % in one year [61], 1 % in 10 h [75] or 10 % in 10 h [60]. In this works, three thermal degradation levels (1 %, 5 % and 10 % at different temperatures) were selected in order to obtain information about how much time an IL takes to degrade at different operation temperatures.

From isothermal scans, times that each ionic liquid takes to lose the 1%, 5% and 10% percentages of initial mass ($t'_{1\%}$, $t'_{5\%}$ and $t'_{10\%}$, respectively) were determined. Figure 3.18 shows $t'_{1\%}$, $t'_{5\%}$ and $t'_{10\%}$ values against temperature for some of the studied compounds. As it can be also seen from this figure, good correlations of the experimental data with a decreasing exponential function (equation (3.1)) were obtained:

$$t' = Ae^{-Bt} \tag{3.1}$$

being *t'* the time in minutes, *t* the temperature in ºC, and, A and B correlation coefficients. Table 3.8 shows the values of the A and B parameters. From these fits the maximum time at which an IL could be used in reliable conditions can be estimated, taking into account that, depending on intended application, different appropriate degrees of degradation and time periods should be chosen.

Table 3.8. Parameters A and B for the equation (3.1) for the selected compounds.

IL	1% weight loss		5% weight loss		10% weight loss	
	B (min)	C (°C^{-1})	B (min)	C (°C^{-1})	B (min)	C (°C^{-1})
[C$_4$C$_1$Pyrr][NTf$_2$]			$3.194 \cdot 10^8$	-0.0489	$8.501 \cdot 10^8$	-0.0510
[C$_4$C$_1$Pyrr][OTf]	$1.449 \cdot 10^7$	-0.0389	$4.315 \cdot 10^{10}$	-0.0639	$1.737 \cdot 10^{11}$	-0.0660
[C$_4$C$_1$Pyrr][FAP]	$1.168 \cdot 10^8$	-0.0582	$6.099 \cdot 10^8$	-0.0576	$8.787 \cdot 10^9$	-0.0583
[C$_4$C$_1$C$_1$Im][NTf$_2$]	$1.149 \cdot 10^8$	-0.0533	$4.744 \cdot 10^8$	-0.0529	$6.394 \cdot 10^8$	-0.0546
[C$_4$C$_1$C$_1$Im][OTf]	$8.281 \cdot 10^6$	-0.0427	$1.615 \cdot 10^8$	-0.0464	$4.784 \cdot 10^8$	-0.0475
[C$_4$C$_1$C$_1$Im][FAP]	$2.878 \cdot 10^{10}$	-0.0779	$6.354 \cdot 10^9$	-0.0658	$8.685 \cdot 10^9$	-0.0639
[C$_2$C$_1$Im][BETI]	$4.393 \cdot 10^5$	-0.0384	$2.236 \cdot 10^6$	-0.0386	$4.605 \cdot 10^6$	-0.0380
[C$_2$C$_1$Im][OTf]	$1.216 \cdot 10^8$	-0.0498	$6.899 \cdot 10^8$	-0.0505	$2.248 \cdot 10^9$	-0.0521
[C$_2$py][C$_1$SO$_3$]	$1.665 \cdot 10^8$	-0.0705	$3.713 \cdot 10^8$	-0.0665	$1.908 \cdot 10^8$	-0.0611
[C$_2$py][NTf$_2$]	$2.283 \cdot 10^7$	-0.0483	$2.019 \cdot 10^8$	-0.0494	$3.977 \cdot 10^8$	-0.0493
[C$_2$py][OTf]	$5.897 \cdot 10^8$	-0.0610	$8.540 \cdot 10^9$	-0.0652	$2.812 \cdot 10^{10}$	-0.0671
[Chol][NTf$_2$]	$4.997 \cdot 10^8$	-0.0567	$4.997 \cdot 10^8$	-0.0564	$3.424 \cdot 10^9$	-0.0564
[C$_1$OC$_2$C$_1$Pyrr][NTf$_2$]	$1.057 \cdot 10^6$	-0.0372	$6.748 \cdot 10^5$	-0.0315	$3.698 \cdot 10^6$	-0.0346
[C$_1$OC$_2$C$_1$Pyrr][(C$_2$F$_5$)$_3$PF$_3$]	$1.127 \cdot 10^5$	-0.0366	$5.632 \cdot 10^5$	-0.0371	$9.855 \cdot 10^6$	-0.0443
[P$_{6,6,6,14}$][(C$_2$F$_5$)$_3$PF$_3$]	$3.144 \cdot 10^6$	-0.0544	$4.584 \cdot 10^7$	-0.0573	$9.669 \cdot 10^7$	-0.0564
DiPEC7	$3.004 \cdot 10^5$	-0.0467	$3.767 \cdot 10^4$	-0.0353	$2.112 \cdot 10^4$	-0.0313
Krytox GPL 105	$5.099 \cdot 10^3$	-0.0355	$2.896 \cdot 10^5$	-0.0429	$8.810 \cdot 10^5$	-0.0425

95
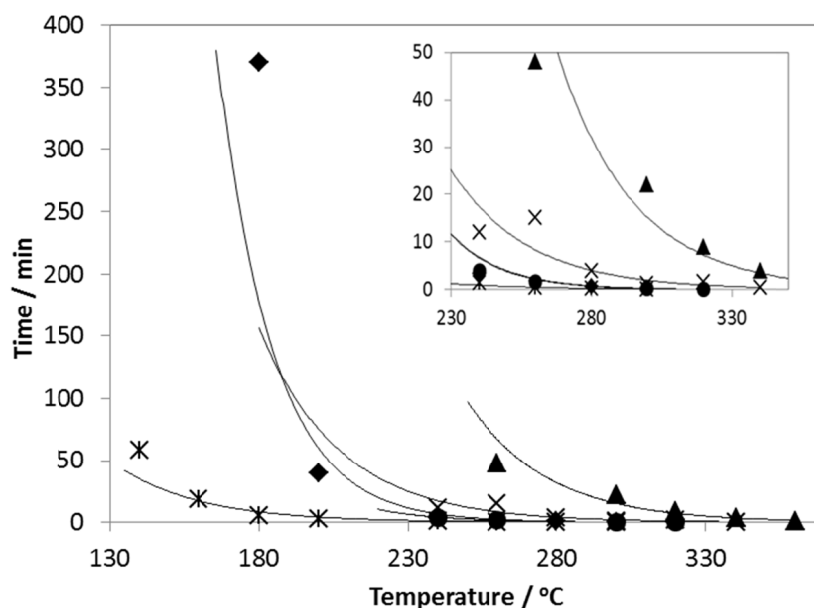
Figure 3.18. Mass loss of 1 % for: $[C_1OC_2C_1Pyrr][NTf_2]$ (▲), $[C_1OC_2C_1Pyrr][(C_2F_5)_3PF_3]$ (✕), $[P_{6,6,6,14}][(C_2F_5)_3PF_3]$ (◆), Krytox GPL 105 (✱), DiPEC7 (●).

Wooster *et al.* [75] suggested that the temperature at which 1% degradation occurs in 10 hours ($T_{0.01/10h}$) is a good indicator of thermal stability and they established a method to estimate it from dynamic scans using the equation:

$$T_{0.01/10h} = 0.82 \ T_{(dw/dT \neq 0)} \tag{3.2}$$

being $T_{(dW/dT \neq 0)}$ the lowest temperature (in Kelvin) at which the first derivative of the weight loss versus T curve is non-zero. The $T_{(dW/dT \neq 0)}$ value provides an estimation of the lowest T at which volatile products are evolved, under the conditions of the experiment. Following this methodology, the estimation of maximum temperature operation was done for all the ILs subjected to isothermal analysis in this work (indicated as $t_{0.01/10h}$, in Table 3.9). Additionally, for comparison, the temperatures associated to the loss of 1 %, 5 % and 10 % in 10 h estimated from the parameters corresponding to equation (3.1) for every degradation level were also presented in Table 3.9.

Table 3.9. Estimated temperatures (in ºC) corresponding to the loss of 1 % during 10 h ($t_{0.01/10h}$) according to Wooster *et al.* [75], and to the loss of 1 %, 5 % and 10 % in 10 h ($t'_{0.01/10h}$, $t'_{0.05/10h}$ and $t'_{0.10/10h}$) obtained from isothermal scans.

IL	$t_{0.01/10h}$	$t'_{0.01/10h}$	$t'_{0.05/10h}$	$t'_{0.10/10h}$
	Dynamic study		*Isothermal study*	
$[C_4C_1Pyrr][NTf_2]$	261	---	268	284
$[C_4C_1Pyrr][OTf]$	266	249	282	296
$[C_4C_1Pyrr][(C_2F_5)_3PF_3]$	242	207	237	247
$[C_4C_1C_1Im][NTf_2]$	252	231	257	266
$[C_4C_1C_1Im][OTf]$	274	225	276	284
$[C_4C_1C_1Im][(C_2F_5)_3PF_3]$	231	224	244	258
$[C_2C_1Im][BETI]$	213	172	213	235
$[C_2C_1Im][OTf]$	258	245	276	291
$[C_2py][C_1SO_3]$	183	178	201	207
$[C_2py][NTf_2]$	250	218	258	272
$[C_2py][OTf]$	243	226	253	263
$[Chol][NTf_2]$	253	240	265	276
$[C_1OC_2C_1Pyrr][NTf_2]$	258	201	223	252
$[C_1OC_2C_1Pyrr][(C_2F_5)_3PF_3]$	180	143	184	219
$[P_{6,6,6,14}][(C_2F_5)_3PF_3]$	196	157	196	213
DiPEC7	195	112	117	121
Krytox GPL 105	125	60	144	172

As it can be observed in Table 3.9, the values obtained for $t_{0.01/10h}$, , calculated from the dynamic scans and using equation (3.2), are significantly lower than the onset temperatures and these values are higher, in all the cases, than the corresponding to $t'_{0.01/10h}$ obtained from isothermal scans. Better agreement was obtained between the predicted $t_{0.01/10h}$ values using Wooster *et*

97

al.[75] relation and the $t'_{0.05/10h}$ values obtained from isothermal scans and equation (3.1), in most cases.

This fact indicates that, in spite of Wooster *et al.* [75] presents a very good and rapid method to determine the long term stability from the dynamic scans, these results should be taken with caution if it will be used in an industrial application that needs small loss of weight. In this situation a deeper study using isothermal experiments is needed.

3.2.4. Activation energy

3.2.4.1. Kinetic isothermal analysis

Figure 3.19 shows fittings corresponding to the linear dependence of the rate constant with temperature, calculated from isothermal experiments for some Ils and lubricant bases by the method of Arrhenius. From these fittings, values of activation energies for the mass loss process have been calculated.
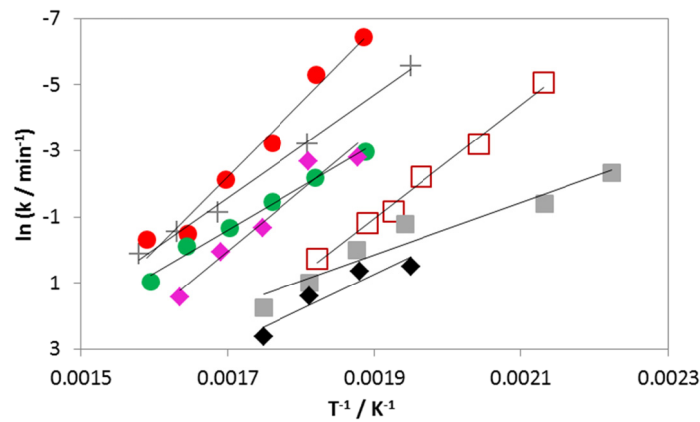
Figure 3.19. Arrhenius method plot for some of the selected ILs: (●) $[C_2C_1Im][BETI]$, (□) $[C_2Py][C_1SO_3]$, (◆) DiPEC7, (+) $[C_4C_1C_1Im][NTf_2]$, (●) $[C_4C_1Pyrr][OTf]$, (◆) $[C_4C_1Pyrr][(C_2F_5)_3PF_3]$, (■) Krytox GPL 105.

Table 3.10. Pre-exponential coefficients, *A*, and activation energies, *E*, for the selected ILs obtained from the Arrhenius equation (2.5).

IL	E / kJ $\cdot$ mol^{-1}	A / min^{-1}
[C$_4$C$_1$Pyrr][NTf$_2$]	147	1.56 10^{12}
[C$_4$C$_1$Pyrr][OTf]	187	3.78 10^{7}
[C$_4$C$_1$Pyrr][(C$_2$F$_5$)$_3$PF$_3$]	153	1.05 10^{16}
[C$_4$C$_1$C$_1$Im][NTf$_2$]	129	1.29 10^{10}
[C$_4$C$_1$C$_1$Im][OTf]	148	1.10 10^{12}
[C$_4$C$_1$C$_1$Im][(C$_2$F$_5$)$_3$PF$_3$]	139	9.36 10^{11}
[C$_2$C$_1$Im][BETI]	109	2.42 10^{9}
[C$_2$C$_1$Im][OTf]	161	1.58 10^{13}
[C$_2$py][C$_1$SO$_3$]	142	4.91 10^{13}
[C$_2$py][NTf$_2$]	143	9.37 10^{11}
[C$_2$py][OTf]	185	2.08 10^{16}
[Chol][NTf$_2$]	169	2.43 10^{14}
[C$_1$OC$_2$C$_1$Pyrr][NTf$_2$]	113	2.41 10^{10}
[C$_1$OC$_2$C$_1$Pyrr][(C$_2$F$_5$)$_3$PF$_3$]	102	5.85 10^{8}
[P$_{6,6,6,14}$][(C$_2$F$_5$)$_3$PF$_3$]	104	1.10 10^{10}
DiPEC7	88	1.14 10^{9}
Krytox GPL 105	65	3.58 10^{6}

As Table 3.10 shows, activation energy values of ILs range between (102 and 187) kJ $\cdot$ mol^{-1} for [C$_1$OC$_2$C$_1$Pyrr][(C$_2$F$_5$)$_3$PF$_3$] and [C$_4$C$_1$Pyrr][OTf], respectively. Base lubricants presented the lowest values of this parameter. Although, according to our data, it can be concluded there is no relation among t_{onset} and *E* values for selected fluids, the highest values of *E* correspond to ILs with anion [OTf]$^-$, with t_{onset} higher than 370 ºC, and in the same way, base lubricants, with the lowest t_{onset}, present the lowest values of activation energy. Up to know, no references with values of this parameter for these ILs have been found, although these values are in concordance with those reported in the literature for other ILs [49,56,59,64]. The activation energy of the imidazolium ILs is lower than the pyrrolidinium ILs with the same anion. Besides, the sequence

99

observed is the same: $[NTf_2]^-$ < $[(C_2F_5)_3PF_3]^-$ < $[OTf]^-$ for both imidazolium and pyrrolidinium ILs.

In the next section, the activation energy obtained from isothermal studies will be compared with that obtained from the application of two kinetic dynamic methods for the $[C_4C_1C_1Im][NTf_2]$ IL.

3.2.4.2.   Kinetic dynamic analysis

Plots obtained from the application of the Kissinger´s method for $[C_4C_1C_1Im][NTf_2]$ can be seen in Figure 3.20. Assuming the validity of equation (2.10), activation energy values have been obtained and presented in Table 3.11.
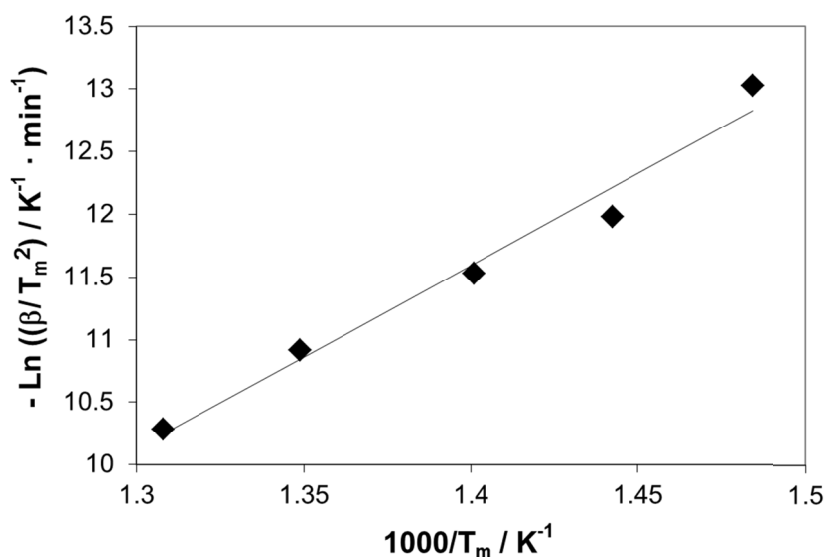
Figure 3.20. Kissinger's method plot for $[C_4C_1C_1Im][NTf_2]$ (◆).

Data obtained from the application of the selected isoconversional method to dynamic studies of thermal degradation/evaporation of $[C_4C_1C_1Im][NTf_2]$ can be seen in Figure 3.21. This study was performed for ten alpha values between (10 and 70) %. To obtain the degradation activation energy, *ln (dα/dt)* for Friedman method (Fig. 3.21) are plotted against *1000/T*. For each conversion value, the

activation energy has been obtained from the slope of the fitting equation taking into account the equation (2.11).
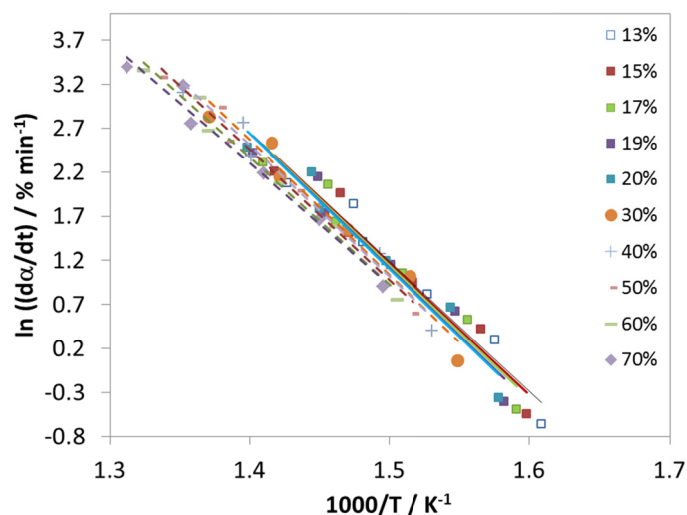
Figure 3.21. Activation Energy plot for $[C_4C_1C_1Im][NTf_2]$ from the Friedman method

Apparent activation energies, E_a, obtained through this method are shown in Table 9. As it can be seen, no significant differences have been found for apparent activation energy for the different conversion degree for a given IL. Vyazovkin *et al.* [83] have found that if E_a is roughly constant over the entire conversion range and if no shoulders are observed in the reaction rate curve, it is clearly that the process is dominated by a single-step model. Then, we could say that the process occurred in the ILs here studied can be described by a single-step model, Table 3.11.

Table 3.11. Apparent activation energies, E_α, for $[C_4C_1C_1Im][NTf_2]$ obtained for each conversion value by applying Friedman method

Conversion (%)	E_α (kJ · mol^{-1})
13	123
15	124
17	126
19	127
20	128
30	127
40	124
50	122
60	119
70	115
Average	**124 ± 4**

The activation energies obtained for $[C_4C_1C_1Im][NTf_2]$ through the three different methods are shown in Table 3.13.

Table 3.12. Activation energies, E, for $[C_4C_1C_1Im][NTf_2]$ from the different models for dynamic and isothermal methods.

E / kJ · mol^{-1}	Dynamic		Isothermal
	Friedman	Kissinger	
$[C_4C_1C_1Im][NTf_2]$	124 ± 4	127 ± 11	129 ± 5

As it can be seen, the activation energy values calculated from these different methods are quite similar. Up to now, no references with values of this parameter for this IL have been found by other authors. Taking into account that Friedman method obtains the energy value considering the shape of the TG curve (different conversion values) and Kissinger method only uses a point of the TG curve but both give similar energy values, it could be proposed that, unless for the

IL analysed, there is an unique process during the experiment or, in case of being more than one, there is a predominant process, which selects the final energy value. Moreover, the coincidence of isothermal results with dynamic ones, gives an optional and faster way to determine the degradation activation energy; however, isothermal studies will be always necessary to know with more accuracy the stability of an IL.

3.3. Liquid range

As it was described on the *Introduction* chapter, one of the objectives of this PhD Thesis is try to determine the lower and upper limits of the liquid range of the selected ILs and lubricant bases, with the help of DSC and TGA.

According to DSC studies, the lower limit is given by t_m, and the upper limit can be measured by thermogravimetric analysis, which can provide several characteristic temperatures depending on the kind of experiment (t_{onset} , $t'_{0.01/10h}$. $t'_{0.05/10h}$ and $t'_{0.10/10h}$, from sections 3.2.2 and 3.2.3.1, respectively). Thus, in a first approximation, it could be calculated a liquid range temperature using dynamic experiments for all the compounds, i.e., with t_{onset} and t_m, as is shown in Table 3.13.

Table 3.13. Liquid range temperature (t_{onset} - t_m) for the studied compounds

Compound	t_{onset} (^oC)	t_m (^oC)	Liquid range temperature
[C$_4$C$_1$C$_1$Im][OTf]	436	2	434
[C$_4$C$_1$C$_1$Im][NTf$_2$]	424	-2	426
[C$_4$C$_1$Pyrr][NTf$_2$]	417	-15	432
[Chol][NTf$_2$]	410	30	380
[C$_2$py][NTf$_2$]	409	31	378
[C$_2$C$_1$Im][OTf]	404	14	390
[C$_4$C$_1$Pyrr][OTf]	399	3	396
[C$_4$C$_1$Pyrr][B(CN)$_4$]	387	19	368
[C$_4$C$_1$Im][BF$_4$]	373	-81	454
[C$_2$py][OTf]	371	32	339
[C$_2$C$_1$Im][BETI]	368	15	353
[P$_{6,6,6,14}$][(C$_2$F$_5$)$_3$PF$_3$]	363	-64	427
[C$_4$C$_1$C$_1$Im][(C$_2$F$_5$)$_3$PF$_3$]	363	5	358
[C$_4$C$_1$Pyrr][(C$_2$F$_5$)$_3$PF$_3$]	358	7	351
[C$_1$OC$_2$C$_1$Pyrr][(C$_2$F$_5$)$_3$PF$_3$]	352	-15	367
[C$_4$C$_1$Pyrr][(C$_4$F$_9$)$_3$PF$_3$]	315	4	311
[C$_2$py][C$_1$SO$_3$]	315	62	253
[C$_1$C$_1$Im][C$_1$C$_1$PO$_4$]	274	-65	339
[C$_2$C$_1$Im][C$_6$SO$_4$]	251	7	244
[C$_1$OC$_2$C$_1$Pyrr][NTf$_2$]	411	---	
Krytox GPL 105	298	-36 [84]	334
Krytox GPL 104	235	-51 [84]	286
Krytox GPL 103	200	-60 [84]	260

But as it was exposed above, the t_{onset} overrates decomposition temperature; the liquid range temperature was then corrected using $t'_{0.10/10h}$ and t_m values, as it is shown in Table 3.14.

Table 3.14. Liquid range temperature ($t'_{0.10/10h}$ - t_m) for the studied compounds

Compound	$t'_{0.10/10h}$ (ºC)	t_m (ºC)	Liquid range temperature
[C$_4$C$_1$C$_1$Im][OTf]	284	2	282
[C$_4$C$_1$C$_1$Im][NTf$_2$]	252	-2	254
[C$_4$C$_1$Pyrr][NTf$_2$]	284	-15	299
[Chol][NTf$_2$]	276	30	246
[C$_2$py][NTf$_2$]	250	31	219
[C$_2$C$_1$Im][OTf]	291	14	277
[C$_4$C$_1$Pyrr][OTf]	296	3	293
[C$_2$py][OTf]	263	32	231
[C$_2$C$_1$Im][BETI]	235	15	220
[P$_{6,6,6,14}$][(C$_2$F$_5$)$_3$PF$_3$]	213	-64	277
[C$_4$C$_1$C$_1$Im][(C$_2$F$_5$)$_3$PF$_3$]	258	5	253
[C$_4$C$_1$Pyrr][(C$_2$F$_5$)$_3$PF$_3$]	247	7	240
[C$_1$OC$_2$C$_1$Pyrr][(C$_2$F$_5$)$_3$PF$_3$]	219	-15	234
[C$_2$py][C$_1$SO$_3$]	207	62	145
[C$_1$OC$_2$C$_1$Pyrr][NTf$_2$]	252	---	
Krytox GPL 105	172	-36 [84]	208

Thus, taking into account both of previous data, a comparison of these two different liquid range temperatures is presented in Figure 3. 22. It can be seen an overestimation on liquid range temperature for this ILs of, at least, 103 ºC (for [C$_4$C$_1$Pyrr][OTf]), and in the case of the selected lubricant base 126 ºC, if onset temperature is taken to determine this parameter.
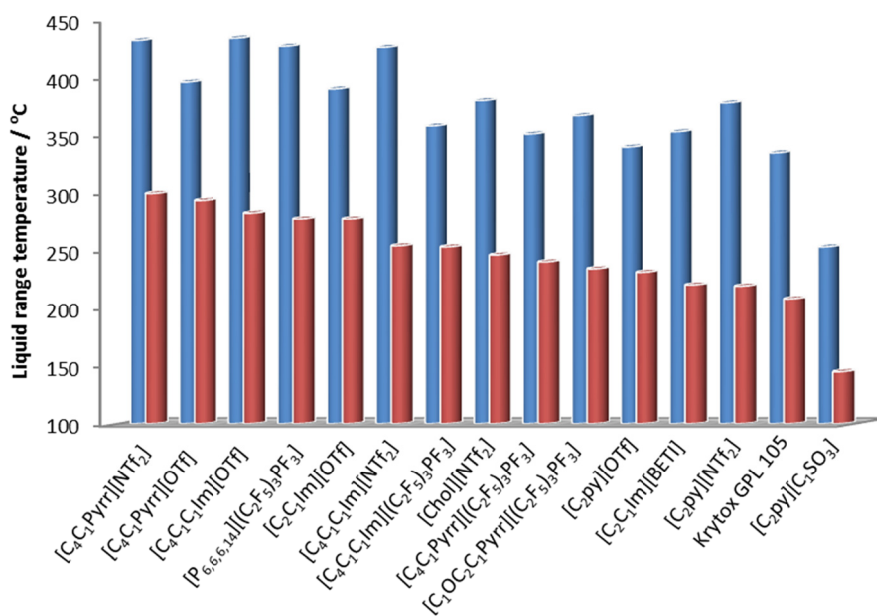
Figure 3.22. Comparison of the two liquid range temperature methods, $t'_{0.10/10h}$ (red) and t_{onset} (blue), for the studied compounds.

3.4. Trying to discern about degradation and evaporation

3.4.1. Visual observation

One of the most discussed questions in conferences, meetings and workshops where the thermal stability was treated is the mechanisms associated to the mass loss. We have tried to make progress on this topic and discern if t degradation or evaporation or both took place in TGA experiences of a IL. For this purpose we have followed the methodology of Götz *et al.* [85] who have suggested that it is possible to do it visually if it is observed colour change. We have done this for three of our ILs and one of the lubricants, Krytox GPL 105, in air atmosphere as it can be seen in Figure 3.23. In general, the evaporation of ILs, both under UHV (Ultra High Vacuum) and atmospheric conditions, is accompanied by the change in colour due to the partial decomposition and/or degradation of residual liquids [38,86].

106

[C$_1$OC$_2$C$_1$Pyrr]
[NTf$_2$]

[P$_{6,6,6,14}$]
[(C$_2$F$_5$)$_3$PF$_3$]

before   after   before   after

[C$_1$OC$_2$C$_1$Pyrr]
[(C$_2$F$_5$)$_3$PF$_3$]

GPL 105

before   after   before   after
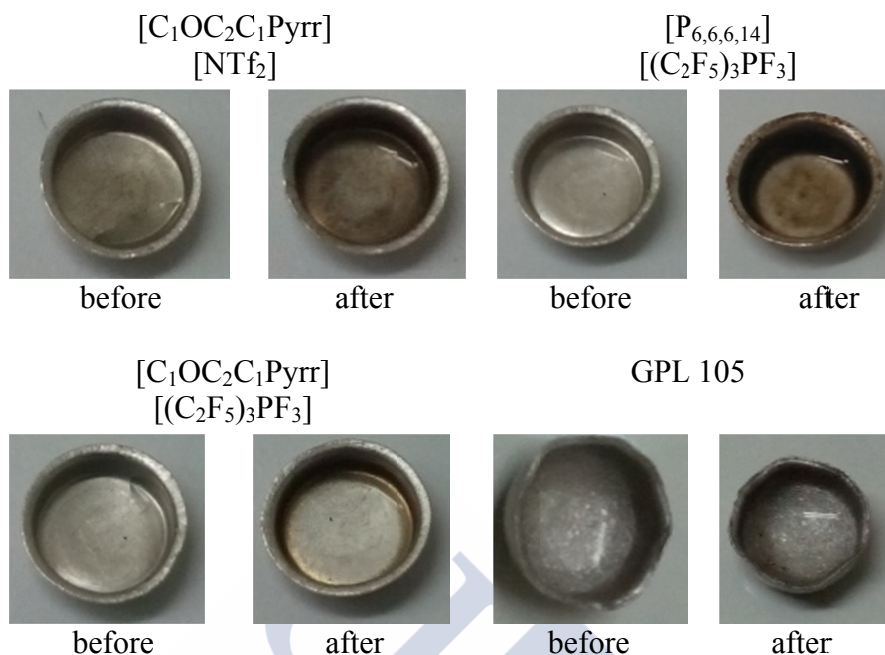
Figure 3.23. Colour change of ILs and GPL 105 lubricant for a mass loss of 10% for different isothermal scans. Isothermal TGA of 360 ºC for [C$_1$OC$_2$C$_1$Pyrr][NTf$_2$], 320 ºC for [P$_{6,6,6,14}$][(C$_2$F$_5$)$_3$PF$_3$], 340 ºC for [C$_1$OC$_2$C$_1$Pyrr][(C$_2$F$_5$)$_3$PF$_3$] and 260 ºC for GPL 105.

After this study, colour changes suggest that the mass loss of the three ILs is probably caused by degradation (alone or accompanied with evaporation), however there is no appreciable colour change for the GPL 105 lubricant, which suggests that the mass loss is possibly produced by evaporation.

Furthermore we have choose one of the selected ILs and tried to see variances between different mass loss percentage, as it is shown in Figure 3.24.
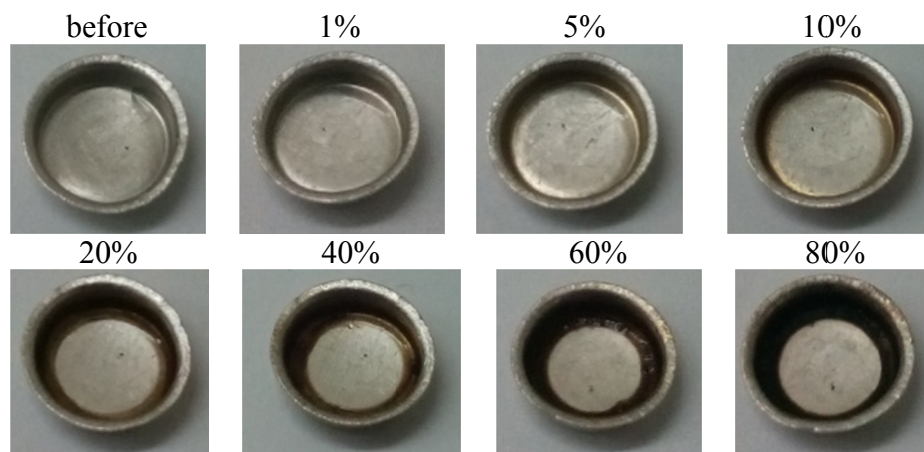
Figure 3.24. Colour change of $[C_1OC_2C_1Pyrr][(C_2F_5)_3PF_3]$ at the same isothermal scan 340 ºC in different mass loss percentages.

As it was expected colour change is bigger when the mass loss is higher. It is possible to determine that, visually, mass loss of ILs is due to decomposition.

3.4.2. DSC/TGA Study

With the objective of discern about the mechanisms (evaporation or decomposition or both) that takes place during the mass loss, besides the visual degradation, some heating rate experiments with DSC/TGA and DSC techniques were carried out for a lubricant base, PAG2, and three ILs, $[C_1OC_2C_1Pyrr][(C_2F_5)_3PF_3]$, $[P_{6,6,6,14}][(C_2F_5)_3PF_3]$ and $[C_3C_1Im][NTf_2]$ with the aim to open new methodologies and possibilities to explore and to nuance this open question. We have tried to determine if mass loss occurred during TGA process is due to decomposition (mainly exothermic reaction) or evaporation (endothermic reaction) using DSC techniques.

Figure 3.25a present the TG signal obtained from simultaneous DSC-TGA of PAG2 in air and Nitrogen atmospheres. These curves presented similar shape although a big shift to higher temperatures (approximately 90 ºC) can be observed when the atmosphere changes from air to Nitrogen. Despite this shift was expected, an increase in 90 ºC is much higher than that reported in section 3.2.1.1.

for different ILs, where differences are around 20 ºC. Figure 3.25b shows the DSC signal of this base lubricant in both atmospheres, when different behaviours can be observed, while a unique big exothermic peak is observed in air atmosphere, compatible with combustion, a small endothermic peak is observed in Nitrogen atmosphere, compatible with evaporation. It is important to indicate that the sensibility of the DSC signal of the simultaneous has not been sufficient to identify this small peak and similar experiences (atmosphere, heating rate and temperature interval) was performed in the DSC used for the analysis of transitions (section 3.1), which is much more sensitive and allows the identification of the weak energetic processes.
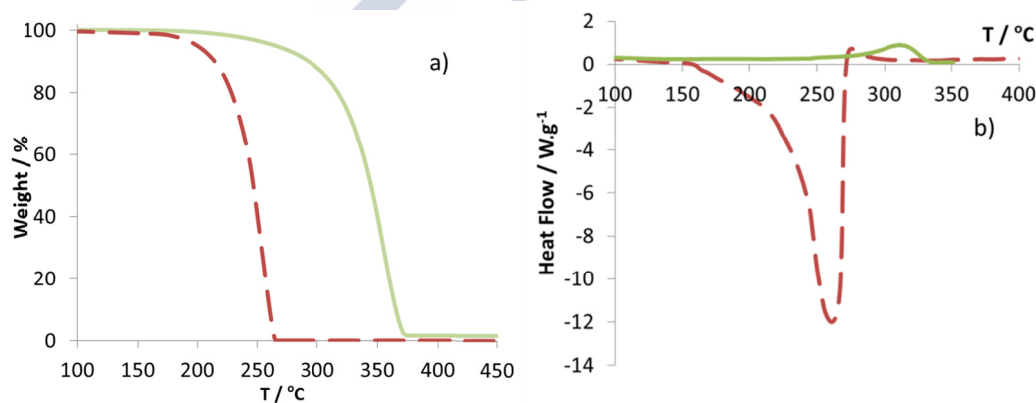
Figure 3.25. (a) TG signal obtained from simultaneous DSC-TGA and (b) DSC curves of PAG2 in air (dashed red line) and Nitrogen (solid green line) atmospheres.

Similar behaviour has been observed in the TG and DSC curves of $[C_3C_1Im][NTf_2]$ as it can be seen in Figures 3.26a and 3.26b. This result agrees with literature, where some authors indicates that ILs with $[NTf_2]^-$ anion are the most volatile ILs in high vacuum or inert atmospheres, although, even these relatively volatile ILs have a vapour pressures that are four orders of magnitude lower compared to high boiling hydrocarbons [53].
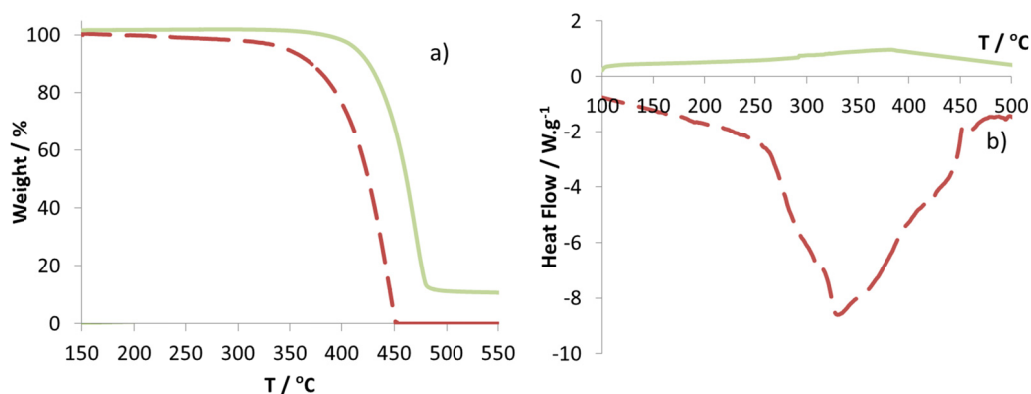
Figure 3.26. (a) TG signal obtained from simultaneous DSC-TGA and (b) DSC curves of $[C_3C_1Im][NTf_2]$ in air (dashed red line) and Nitrogen (solid green line) atmospheres.

Nevertheless for the ILs $[P_{6,6,6,14}][(C_2F_5)_3PF_3]$ and $[C_1OC_2C_1Pyrr][(C_2F_5)_3PF_3]$ important variations has been found in TG and DSC curves as it can be seen in figures 3.27a and 3.27b and 3.28a and 3.28b, respectively. Firstly, some steps can be observed in TG curves, indicating that more than process appeared during the degradation of this IL in Nitrogen and air atmospheres. Every step has a corresponding peak in DSC profiles, but in this case, all the peaks are exothermic, in both atmospheres, although the intensity of the peaks observed in air atmosphere are higher than in Nitrogen atmosphere, this is a big amount of energy has been released in air, also compatible with a combustion. Nevertheless, no evaporation is possible in the studied situation for $[P_{6,6,6,14}][(C_2F_5)_3PF_3]$ and $[C_1OC_2C_1Pyrr][(C_2F_5)_3PF_3]$ neither air nor Nitrogen. These results agree with the previous visual observations for these ILs.
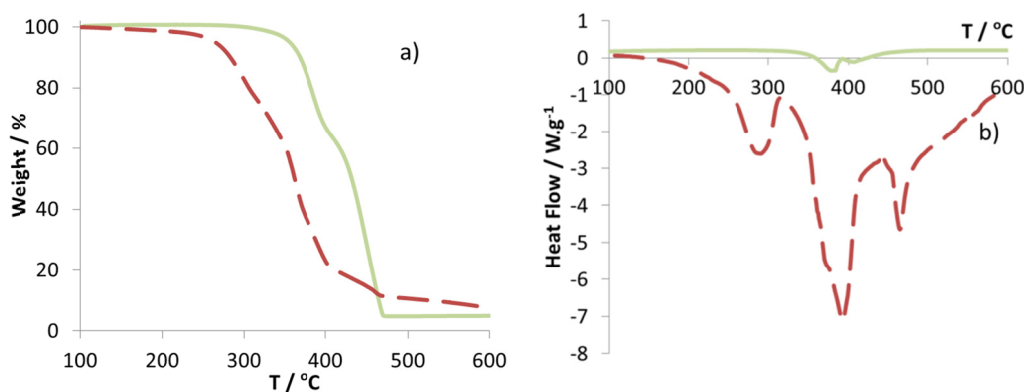
Figure 3.27. (a) TG signal obtained from simultaneous DSC-TGA and (b) DSC curves of $[P_{6,6,6,14}][(C_2F_5)_3PF_3]$ in air (dashed red line) and Nitrogen (solid green line) atmospheres.
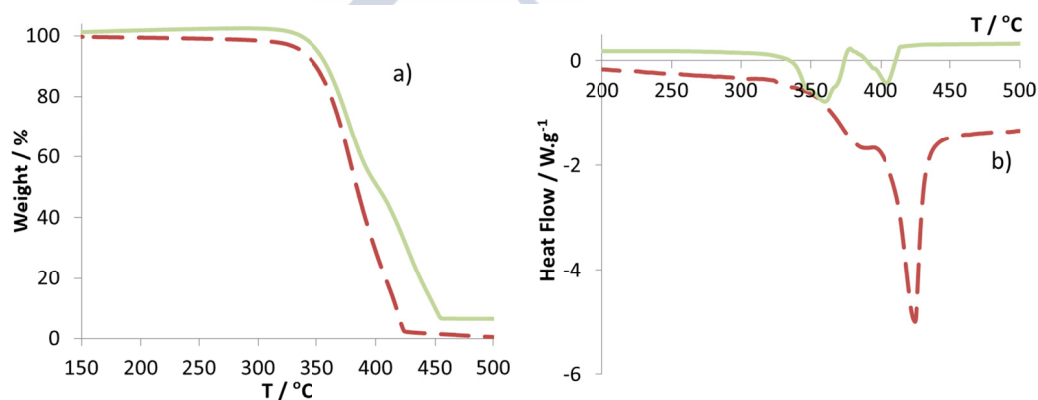
Figure 3.28. (a) TG signal obtained from simultaneous DSC-TGA and (b) DSC curves of $[C_1OC_2C_1Pyrr][(C_2F_5)_3PF_3]$ in air (dashed red line) and Nitrogen (solid green line) atmospheres.

As a result of all these findings, ILs can present different mechanism of degradation in Nitrogen atmosphere, but decomposition is the most probably in oxidative atmosphere, as well as for the base lubricants.

Taking into account that the most suitable IL for an application under no-reactive atmosphere, will be the IL that present evaporation, because the fluid can be recover without any modification, this methodology is very useful.

111

3.5. Ecotoxicity

As it was exposed in previous chapter, the thermal analysis is a powerful technique that allows obtaining information of all the processes that involve a change of energy absorbing or releasing heat. Thus in the last part of this Thesis, we want to introduce a new methodology to detect changes, with the dose of IL, on the heat released by microorganism of soil during the respiration when a substrate is added.

3.5.1. Microcalorimetry

Power-time curves of soils under pine and soil under eucalyptus treated with the different doses of the IL $[C_4C_1Im][BF_4]$ and the corresponding control curve are presented in Figures 3.29 and 3.30 respectively. Similarly, the power-time curves of soils under pinus and soil under eucalyptus treated with the different doses of $[C_3C_1Im][NTf_2]$ are shown in Figures 3.31 and 3.32 respectively.
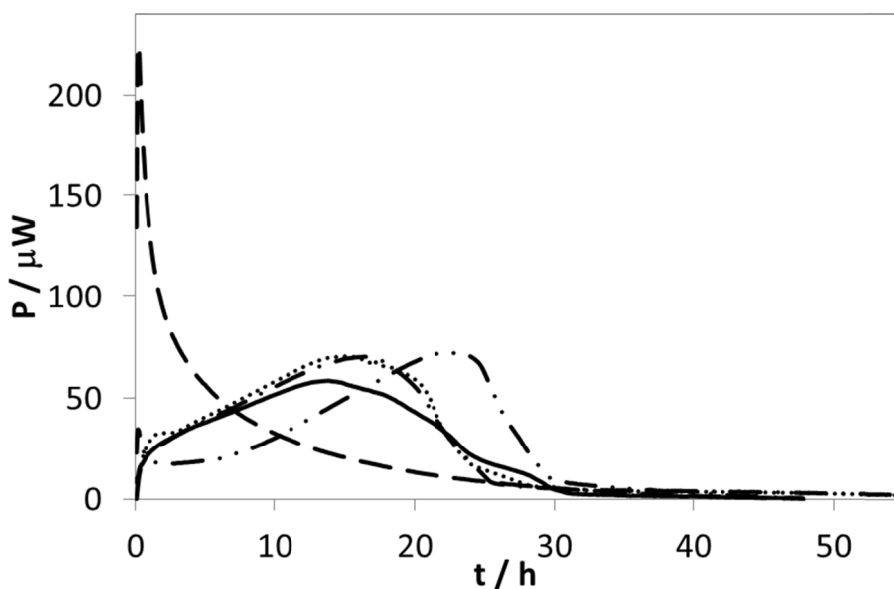
Figure 3.29. Power–time curves of pine soil samples activated with glucose and different treatments of IL $[C_4C_1Im][BF_4]$ (—— Control, − − 10%, − ·· − 1%, − · − 0.1%, ······ 0.01%)
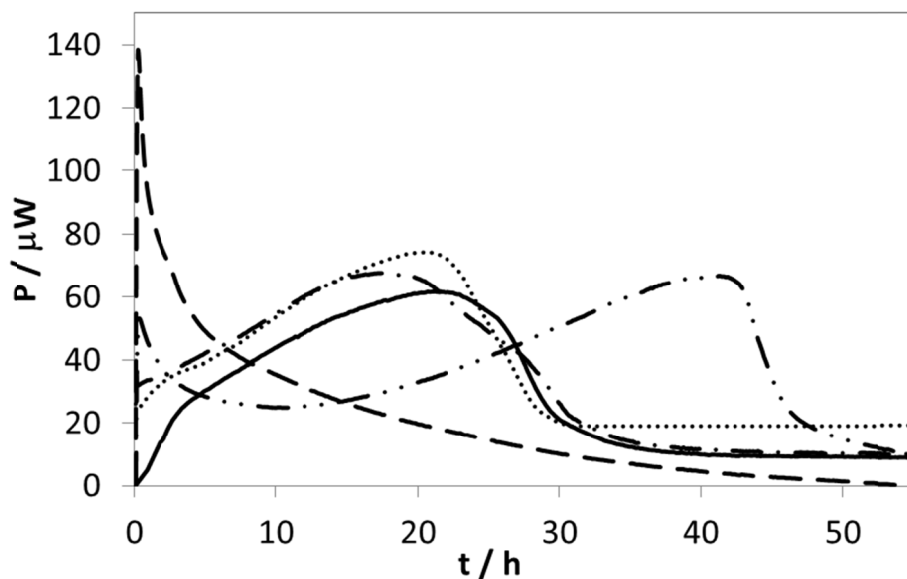
Figure 3.30. Power–time curves of eucalyptus soil samples activated with glucose and different treatments of IL $[C_4C_1Im][BF_4]$ (── Control, ─ ─ 10%, ─·─ 1%, ─·─ 0.1%, ······ 0.01%)
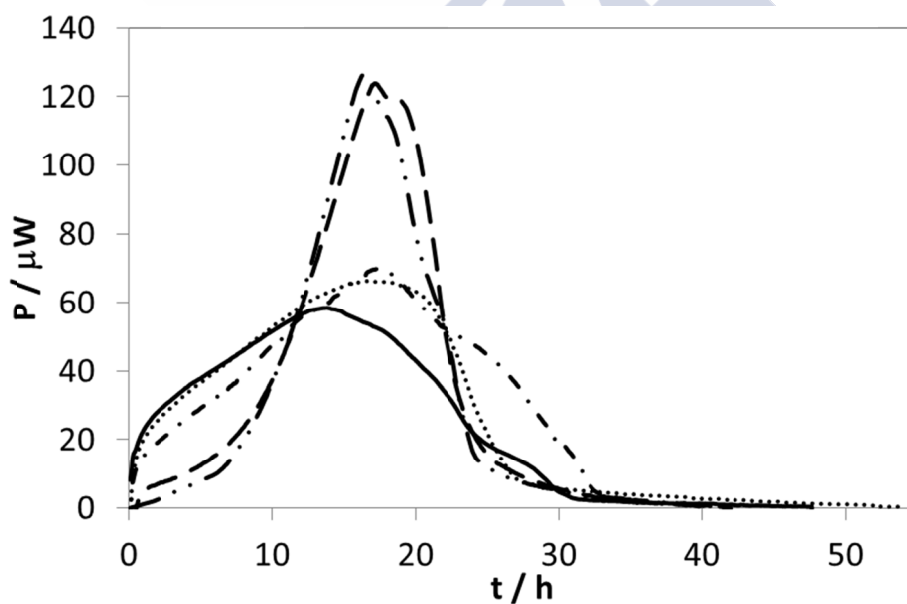
Figure 3.31. Power–time curves of pine soil samples activated with glucose and different treatments of IL $[C_3C_1Im][NTf_2]$ (── Control, ······ 10%, ─·─ 1%, ─ ─ 0.1%, ─··─ 0.01
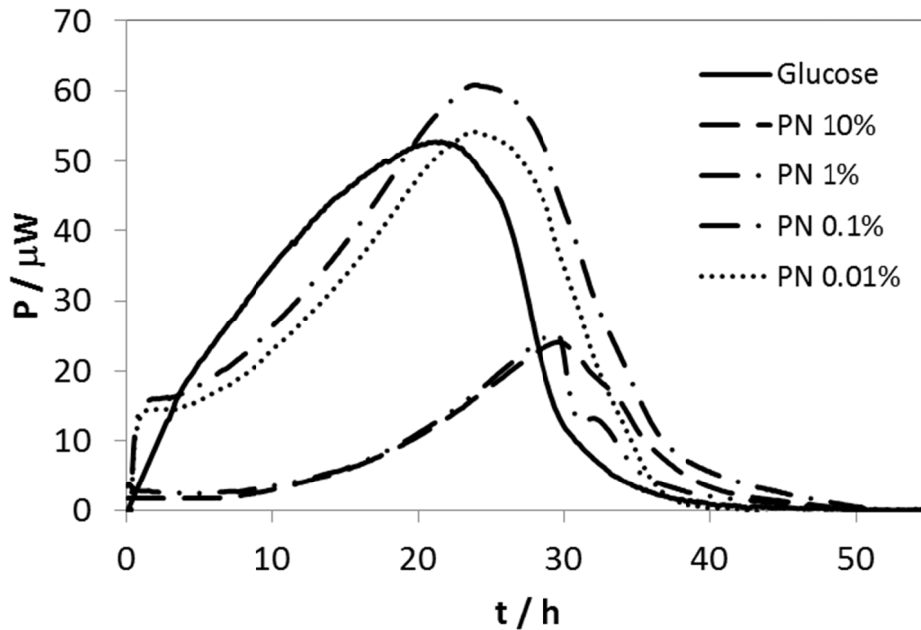
Figure 3.32. Power–time curves of eucalyptus soil samples activated with glucose and different treatments of IL $[C_3C_1Im][NTf_2]$ (—— Control, — — 10%, — ·· — 1%, — · — 0.1%, ······ 0.01%)

Table 3.15 presents values of the heat released by microorganism (Q), thermal power at the maximum of the peak (P_M), delay time of activity (t_D) time for the maximum of thermal power (t_M), time to finish the activity (t_F) and constant of microbial growth rate (**k**) obtained for the soil under pine and after the addition of the four doses of both ILs, as well as the corresponding values to the control samples.

In Figure 3.29 the thermal power (W) curves against time (hours) corresponding to the under *P. pinaster* soil samples to which different doses of $[C_3C_1Im][NTf_2]$ have been added, and that corresponding to the control curve (soil activated glucose), are shown. From the comparison between the curves corresponding to this control and the two highest concentrations (1% and 10%), the peak is narrower and higher, in both cases, with regard to control curve. This behaviour could be explained with the assumption that the high concentrations of the IL have a selective toxic effect, by inhibiting the growth of some type of microorganisms and strengthening the growth of others that can support the

presence of the IL in the soil. Even more, the death of those microorganisms could improve the proliferation of the more resistant giving rise to a higher peak when comparing to the control curve. Nevertheless the differences between the curves of the two lowest doses and the corresponding control are small, only a broader time interval of growth can be observed in samples of soil treated with the IL. It could be even said that the lower doses of IL could strengthen the growth of the microorganisms present in the soil, this fact reflected in a higher peak height and in a broader time interval of growth when compare with control curve. Thus, it can be concluded that the addition of the selected IL in low concentrations does not induce toxic effects on the microbial growth of this soil.

Table 3.15. Characteristic parameters for the soil under eucaliptus obtained by TAM experiences

		Q (J)	P_M (μW)	t_D (min)	t_M (min)	t_F(min)	k (x 10^{-3} min^{-1})
	Control	4.1	60	30	830	2590	1.2
[C$_4$C$_1$lm][BF$_4$]	10%	3.7	225	0	20	900	---
	1%	2.8	62	444	1380	2100	1.9
	0.1%	4.1	67	50	985	2220	1.3
	0.01%	4.3	67	80	975	2290	1.3
[C$_3$C$_1$lm][NTf$_2$]	10%	5.0	124	390	1040	2220	3.0
	1%	4.7	127	360	990	2400	3.6
	0.1%	5.0	70	50	1068	2340	1.6
	0.01%	4.3	63	45	1020	2100	1.3

Maximun Standard error for Q: ±0.4 J, Standard error for k<1%, Standard error for the different times (t_D, t_M and t_F) <10%

Tables 3.15 and 3.16 present values of the heat released by microorganism (Q), thermal power at the maximum of the peak (P_M), delay time of activity (t_D), time for the maximum of thermal power (t_M), time to finish the activity (t_F) and constant of microbial growth rate (k) obtained for the soil under eucalyptus and

pine, respectively, after the addition of the four doses of both ILs, as well as the corresponding values to the control samples.

Table 3.16. Characteristic parameters for the soil under pine obtained by TAM experiences

		Q (J)	P_M (µW)	t_D (min)	t_M (min)	t_F(min)	k (x 10^{-3} min^{-1})
Control		4.0	53	150	1300	3120	1.6
[C$_4$C$_1$Im][BF$_4$]	10%	3.9	138	0	15	1200	---
	1%	6.5	62	900	2460	4000	0.8
	0.1%	5.1	59	0	1045	3600	1.1
	0.01%	3.6	55	20	1250	2100	1.7
[C$_3$C$_1$Im][NTf$_2$]	10%	1.4	24	600	1776	4065	1.8
	1%	1.1	25	600	1764	3180	1.9
	0.1%	5.0	62	90	1425	3420	1.2
	0.01%	6.1	68	90	1505	3600	1.2

Maximun Standard error for Q: ±0.4 J, Standard error for k<1%, Standard error for the different times (t_D, t_M and t_F) <10%

Some small differences can be observed between the power-time curves of the control for soils under pine and under eucalyptus. Soil under pine shows a symmetric exothermic peak from the beginning of the experiment until elapsed 30 hours, with the maximum at 15 hours, whereas the microbial activity of soil under eucalyptus corresponds to an asymmetric peak finished after 35 hours of experience with a maximum at 22 hours after start experiment.

Important differences have been observed between both selected ILs and between the four studied doses. The addition of the highest dose of [C$_4$C$_1$Im][BF$_4$] yields an intense and short peak that finish at approximately 10 hour after start experiment. The dose of 1% of this IL provokes a loss of the symmetry of the peak, no activity is observed during the first eight hours of the experiment, and the maximum of the peak appears at 25 hours approximately (i.e. a shift of 10 hours

116

with regard to control curve). The addition of the two lowest doses does not generate important changes in microbial activity with regard to control.

On the other hand, it is well know that one of the environmental factors that limit the productivity of plants, provoking even the plants death, is the salinity. Then and with the aim to compare the ILs effects, similar experiences have been carried out with NaCl salt for the concentration of 10% in soil under pine (Fig. 3.33). Comparison of power-time curves of similar doses of both selected ILs and salt is presented in figure 9
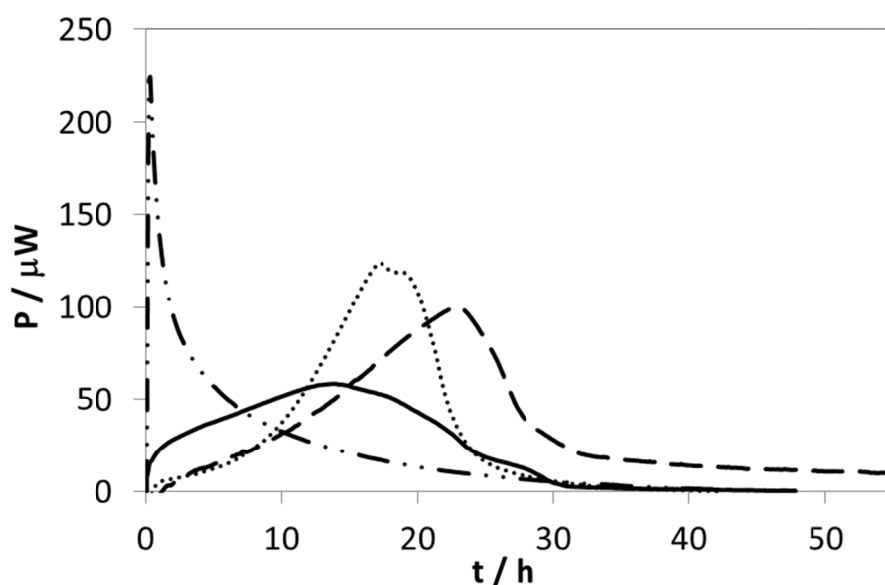
Figure 3.33. Comparison of power–time curves of pinus soil activated with glucose and treated with aqueous solution at 10% of IL and NaCl with the control. (—— Control, ······ [C_3C_1Im][NTf_2], — ·· — [C_4C_1Im][BF_4], — — NaCl).

NaCl addition generates a delay in the microbial activity with regard to control sample, similarly than [C_3C_1Im][NTf_2]. In both cases scarcely heat liberated by the metabolism of the microorganisms is registered during the first 8 hours of experiment, although the delay on the maximum of the peak is higher in the response of the addition of NaCl than in case of [C_3C_1Im][NTf_2]. The most different response corresponds to the addition of [C_4C_1Im][BF_4] characterized by

117

a narrow and high pitch exothermic peak. Integration of these curves provides values of the total heat evolved during the process.

Figure 3.33 shows a comparison between the effects of this IL on the soil microbial activity and the corresponding to a well-known salt, sodium chloride, in the same conditions (10%). From these curves it can be said that, qualitatively, the effects of the IL are similar to that detected with the sodium chloride; a slight retard on the growth of microbial population producing an increase on the peak time and also a higher value of the peak height. A difference between salt and IL curves can be observed at the beginning of the reaction; for ClNa, an immediate and continuous growth is observed whereas for the IL curve a slight retard on the initial growth step was detected.

Studzinska and Buszewski [87] have proved that hazardous effects of imidazolium ILs are closely connected with organic matter content in soil. Soil with more organic carbon was observed to sorb IL cations more extensively than soil with little or no organic matter; hence, the more fertile the soil, the lower probability of hazardous effect of ILs to plants.

Nonetheless the toxicity of ionic liquids is in itself a property which can be tuned and exploited for other beneficial uses, for example in developing novel antimicrobials.

3.5.2. Germination response

To provide more information to compare, the effects of these ILs on seed germination were also determined, being this parameter more sensitive to toxicity than the microbial activity.

Significant differences have been observed for the germination percentages of the control for the selected species and significant differences have also been observed for the values corresponding to applied treatments of both ILs.

With regards the values of percentage of control germination (Fig. 3.34) three groups can be stablished, the first one, with the highest values (62%) corresponding to *P. radiate*, the second one corresponds to *E. globulus* (54%) and *P. nigra* (52%) and the last one formed by *P. pinaster* (33%), *P. sylvestris* (26%) and *P. halepensis* (18%)

The two highest doses of both ILs provokes the total extinguishment of germination for all the species, except for *P. radiate* treated with the dose of 1% of $[C_3C_1Im][NTf_2]$. The dose of 0.1% produces a reduction in this parameter in comparison with the obtained for the lowest dose and control. IL $[C_4C_1Im][BF_4]$ presents stronger effect on germination than $[C_3C_1Im][NTf_2]$ in *P. radiata*, whereas the opposite relation can be observed in *E. globulus*, *P. halepensis* and *P. nigra*. *P. pinaster* and *P. sylvestris* did not shown significant differences between both ILs for all the doses.

Similar results have been found by Wang and co-workers [88] that conducted a study on the effect of 1-butyl-3- methylimidazolium tetrafluoroborate on wheat seedlings. The increase of this IL concentration in soil showed a significant negative effect both on germination and roots and shoot length of the wheat plants. At low concentrations, 1-butyl-3-methylimidazolium tetrafluoroborate did not inhibit, and even promoted wheat seedling growth.
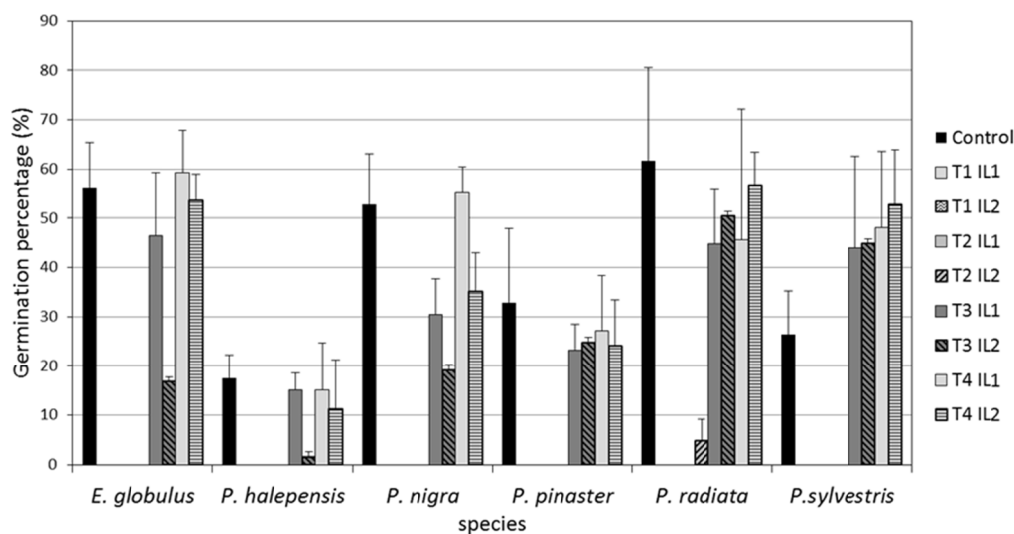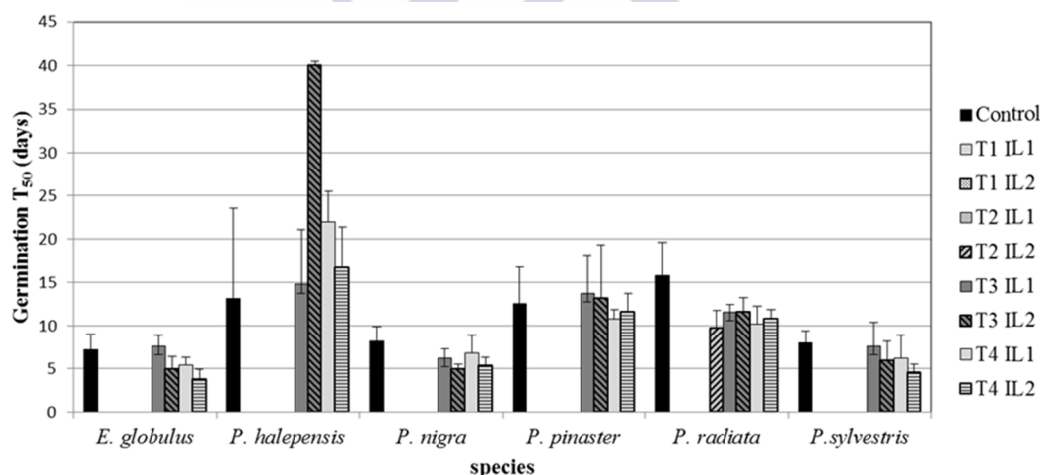
Figure 3.34. Germination percentages and standard deviation reached for every treatment and species. IL1: $[C_4C_1Im][BF_4]$, IL2: $[C_3C_1Im][NTf_2]$, T1: 10%, T2: 1%, T3: 0.1%, T4: 0.01%.

After the ANOVA analysis, there were highly significant differences ($p<0.001$) between both species and treatments, and also within each IL ($p<0.005$) in relation to the treatments. The interaction ionic liquid by specie by treatment was also significant ($p=0.013$) indicating a singular response of every specie to the different treatments and possibly to every ionic liquid. For this reason, ANOVA analyses were performed for every species, obtaining that *P. pinaster*, *P. radiata* and *P. sylvestris* present significant differences between treatments, nevertheless no differences were found between ionic liquids. Duncan test shows that results obtained after the weakest treatment are similar to that of control, besides results corresponding to the two highest doses. However results for 0.1% are statistically different than all the others.

For *E. globulus*, *P. halepensis* and *P. nigra* species, significant interaction between IL and treatment were obtained, thus independent ANOVA analysis for every specie and IL were performed. The lowest dose provokes similar germination percentages to that of the control, except for *P. halepensis* and de *P.*

nigra where the addition of the lowest dose of $[C_3C_1Im][NTf_2]$ reduces the germination with regard to the control. Others treatments significantly reduce it.

Figure 3.35 presents a comparison between the germination percentages of the six selected species after the addition of the doses of 10% and 1% with regard to the corresponding control for both ILs and the salt, sodium chloride. No differences between the germination percentages for the three compounds has been found for the highest dose (10%), nevertheless the effects of the salt seems to be less harmful than the ILs at 1%. All the species presented significant germination values, being the biggest absolute value, the corresponding to *P. radiate* (44.8%) and the lowest to *E. globulus* (3.2%). Nevertheless the percentage of germination with regards of the corresponding control presents different trend: *P. halepensis* > *P. radiata* > *P. nigra* > *P. sylvestris* > *P. pinaster* > *E. globulus*.
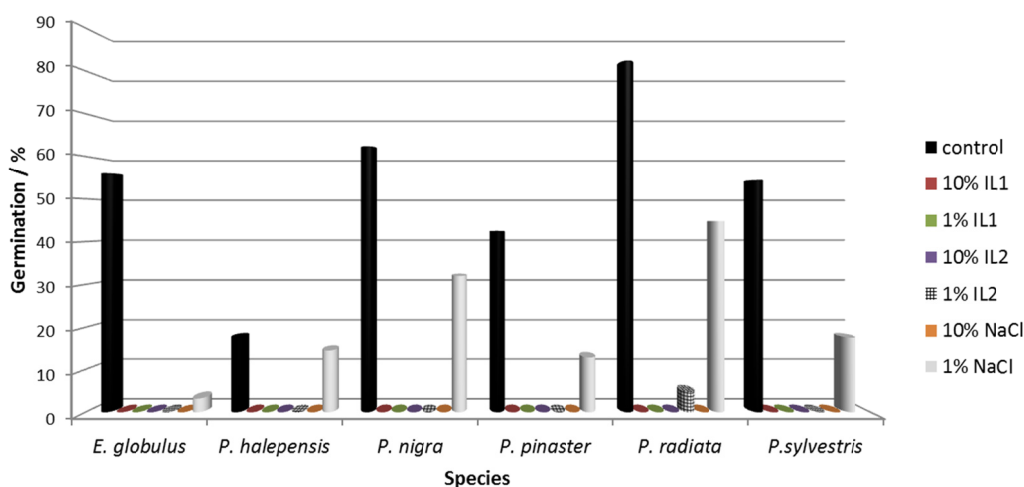
Figure 3.35. Germination percentages for all the selected species after the addition of the two highest doses of both ILs, IL1: $[C_4C_1Im][BF_4]$, IL2: $[C_3C_1Im][NTf_2]$, and the salt NaCl.

Figure 3.36 shows the time that each replicate took to reach 50% of final value of germination percentage (T_{50}) for every specie and treatment. Results present an important dependence with the specie, thus *E. globulus*, *P. nigra* and *P. sylvestris* are that reached before (around 7 days) this value. On the contrary *P. halepensis*,

P. pinaster and *P. radiata* needed more than 13 days to complete the half of the germination. The exaggerated value of T_{50} of *P. halepensis* obtained for the dose of 0.1% of $[C_3C_1Im][NTf_2]$ could be explained taking into account that only two germinations have been observed the 40th day of the experiment.

ANOVA test shows no significant differences in T_{50} between both ILs for all the treatments applied, and highly significant differences ($p<0.001$) have been found between species. Duncan test find three groups for this parameter in function of the speed of germination: the first, the quickest, join *E. globulus*, *P. nigra* and *P. sylvestris*, the second, *P. radiata* and *P. pinaster* and the last, *P. halepensis* (the specie which presents the highest values of T_{50} and with more variation between ILs and treatments).

 Figure 3.36 Germination T50 and and standard deviation reached for every treatment and species. IL1: $[C_4C_1Im][BF_4]$, IL2: $[C_3C_1Im][NTf_2]$, T1: 10%, T2: 1%, T3: 0.1%, T4: 0.01%.

Similarly, the temporary distribution of the germination is different for every species and the ILs addition did not provoke important changes in distribution profiles. Similarly than in the case of T_{50}, *E. globulus*, *P. nigra* and *P. sylvestris* are the species that early begin and finish germination (it start the first day of the experiment, it should be abundant and around the 12th day it has been

122

already completed). Germination of *P. pinaster* and *P. radiata* started the 3th of the experiment and after the 24th day no germinations have been observed. Finally, germination of *P. halepensis*, shifts toward higher values of time, starting germinating on the 5th day and until the 33th day the germination is almost constant and scanty, with the exception of the treatment of 0.1% of $[C_3C_1Im][NTf_2]$ which only two seed (of a total of 125) germinates after 40 days of start experiment.

3.6. References

(1)   Ngo, H. L.; LeCompte, K.; Hargens, L.; McEwen, A. B.: Thermal properties of imidazolium ionic liquids. *Thermochim. Acta* **2000**, *357-358*, 97-102.

(2)   Shirota, H.; Mandai, T.; Fukazawa, H.; Kato, T.: Comparison between Dicationic and Monocationic Ionic Liquids: Liquid Density, Thermal Properties, Surface Tension, and Shear Viscosity. *J. Chem. Eng. Data* **2011**, *56*, 2453-2459.

(3)   Thomas, L. C.: Modulated DSC paper 5: measurement of glass transition and enthalpic recovery.

(4)   Calvar, N.; Gómez, E.; Macedo, E. A.; Domínguez, Á.: Thermal analysis and heat capacities of pyridinium and imidazolium ionic liquids. *Thermochim. Acta* **2013**, *565*, 178-182.

(5)   Fredlake, C. P.; Crosthwaite, J. M.; Hert, D. G.; Aki, S. N. V. K.; Brennecke, J. F.: Thermophysical Properties of Imidazolium-Based Ionic Liquids. *J. Chem. Eng. Data* **2004**, *49*, 954-964.

(6)   Hayyan, M.; Mjalli, F. S.; AlNashef, I. M.; Hashim, M. A.: Stability and kinetics of generated superoxide ion in trifluoromethanesulfonate anion-based ionic liquids. *Int. J. Electrochem. Sci.* **2012**, *7*, 9658-9667.

(7)   Bazito, F. F. C.; Kawano, Y.; Torresi, R. M.: Synthesis and characterization of two ionic liquids with emphasis on their chemical stability towards metallic lithium. *Electrochim. Acta* **2007**, *52*, 6427-6437.

(8)   Noack, K.; Schulz, P. S.; Paape, N.; Kiefer, J.; Wasserscheid, P.; Leipertz, A.: The role of the C2 position in interionic interactions of imidazolium based ionic liquids: a vibrational and NMR spectroscopic study. *Phys. Chem. Chem. Phys.* **2010**, *12*, 14153-14161.

(9)   Buffeteau, T.; Grondin, J.; Danten, Y.; Lassègues, J.-C.: Imidazolium-Based Ionic Liquids: Quantitative Aspects in the Far-Infrared Region. *J. Phys. Chem. B* **2010**, *114*, 7587-7592.

(10)   Wachter, P.; Schreiner, C.; Schweiger, H.-G.; Gores, H. J.: Determination of phase transition points of ionic liquids by combination of thermal analysis and conductivity measurements at very low heating and cooling rates. *J. Chem. Thermodyn.* **2010**, *42*, 900-903.

(11)   Zhou, Z. B.; Matsumoto, H.; Tatsumi, K.: Cyclic quaternary ammonium ionic liquids with perfluoroalkyltrifluoroborates: Synthesis, characterization, and properties. *Chem. Eur. J.* **2006**, *12*, 2196-2212.

(12)   MacFarlane, D. R.; Meakin, P.; Sun, J.; Amini, N.; Forsyth, M.: Pyrrolidinium Imides: A New Family of Molten Salts and Conductive Plastic Crystal Phases. *J. Phys. Chem. B* **1999**, *103*, 4164-4170.

(13)   Sun, J.; MacFarlane, D. R.; Forsyth, M.: A new family of ionic liquids based on the 1-alkyl-2-methyl pyrrolinium cation. *Electrochim. Acta* **2003**, *48*, 1707-1711.

(14)   Tokuda, H.; Hayamizu, K.; Ishii, K.; Susan, M. A. B. H.; Watanabe, M.: Physicochemical Properties and Structures of Room Temperature Ionic Liquids. 1. Variation of Anionic Species. *J. Phys. Chem. B* **2004**, *108*, 16593-16600.

(15)   Martinelli, A.; Matic, A.; Jacobsson, P.; Börjesson, L.; Fernicola, A.; Scrosati, B.: Phase Behavior and Ionic Conductivity in Lithium Bis(trifluoromethanesulfonyl)imide-Doped Ionic Liquids of the Pyrrolidinium Cation and Bis(trifluoromethanesulfonyl)imide Anion. *J. Phys. Chem. B* **2009**, *113*, 11247-11251.

(16)   Henderson, W. A.; Passerini, S.: Phase Behavior of Ionic Liquid−LiX Mixtures: Pyrrolidinium Cations and TFSI- Anions. *Chem. Mater.* **2004**, *16*, 2881-2885.

(17)   Dean, P. M.; Pringle, J. M.; Forsyth, C. M.; Scott, J. L.; MacFarlane, D. R.: Interactions in bisamide ionic liquids-insights from a Hirshfeld surface analysis of their crystalline states. *New J. Chem.* **2008**, *32*, 2121-2126.

(18)   Yuyama, K.; Masuda, G.; Yoshida, H.; Sato, T.: Ionic liquids containing the tetrafluoroborate anion have the best performance and stability for electric double layer capacitor applications. *J. Power Sources* **2006**, *162*, 1401-1408.

(19)   Spinks, G. M.; Lee, C. K.; Wallace, G. G.; Kim, S. I.; Kim, S. J.: Swelling Behavior of Chitosan Hydrogels in Ionic Liquid−Water Binary Systems. *Langmuir* **2006**, *22*, 9375-9379.

(20)   Chen, H.-L.; Wei, G.-T.: The Use Ionic Liquid as the Eluent Additive for HPLC Separation of Ionic Dyes. *J. Chin. Chem. Soc-TAIP* **2010**, *57*, 836-843.

(21)   Mwongela, S. M.; Siminialayi, N.; Fletcher, K. A.; Warner, I. M.: A comparison of ionic liquids to molecular organic solvents as additives for chiral separations in micellar electrokinetic chromatography. *J. Sep. Sci.* **2007**, *30*, 1334-1342.

(22)   Liu, F.-h.; Jiang, Y.: Room temperature ionic liquid as matrix medium for the determination of residual solvents in pharmaceuticals by static headspace gas chromatography. *J. Chromatograph. A* **2007**, *1167*, 116-119.

(23)   Kim, Y. H.; Cheruvally, G.; Choi, J. W.; Ahn, J. H.; Kim, K. W.; Ahn, H. J.; Choi, D. S.; Song, C. E.: Electrochemical Properties of PEO-Based Polymer Electrolytes Blended with Different Room Temperature Ionic Liquids. *Macromol. Sy.* **2007**, *249-250*, 183-189.

(24)   Jin, H.; O'Hare, B.; Dong, J.; Arzhantsev, S.; Baker, G. A.; Wishart, J. F.; Benesi, A. J.; Maroncelli, M.: Physical Properties of Ionic Liquids Consisting of the 1-Butyl-3-Methylimidazolium Cation with Various Anions and the Bis(trifluoromethylsulfonyl)imide Anion with Various Cations. *The Journal of Physical Chemistry B* **2008**, *112*, 81-92.

(25)   Shamim, N.; McKenna, G. B.: Glass Dynamics and Anomalous Aging in a Family of Ionic Liquids above the Glass Transition Temperature. *The Journal of Physical Chemistry B* **2010**, *114*, 15742-15752.

(26)   Erdmenger, T.; Vitz, J.; Wiesbrock, F.; Schubert, U. S.: Influence of different branched alkyl side chains on the properties of imidazolium-based ionic liquids. *J. Mater. Chem.* **2008**, *18*, 5267-5273.

(27)   Królikowska, M.: (Solid + liquid) and (liquid + liquid) phase equilibria of (IL + water) binary systems. The influence of the ionic liquid structure on mutual solubility. *Fluid Phase Equilibr.* **2014**, *361*, 273-281.

(28)   Bulut, S.; Eiden, P.; Beichel, W.; Slattery, J. M.; Beyersdorff, T. F.; Schubert, T. J. S.; Krossing, I.: Temperature Dependence of the Viscosity and Conductivity of Mildly Functionalized and Non-Functionalized [Tf2N]− Ionic Liquids. *Chem. Phys. Chem.* **2011**, *12*, 2296-2310.

(29)   Gómez, E.; Calvar, N.; Domínguez, Á.; A. Macedo, E.: Thermal Analysis and Heat Capacities of 1-Alkyl-3-methylimidazolium Ionic Liquids with NTf2−, TFO−, and DCA− Anions. *Ind. Eng. Chem. Res.* **2013**, *52*, 2103-2110.

(30)   Zheng, W.; Mohammed, A.; Hines, L. G.; Xiao, D.; Martinez, O. J.; Bartsch, R. A.; Simon, S. L.; Russina, O.; Triolo, A.; Quitevis, E. L.: Effect of Cation Symmetry on the Morphology and Physicochemical Properties of Imidazolium Ionic Liquids. *J. Phys. Chem. B* **2011**, *115*, 6572-6584.

(31)   Yoshizawa-Fujita, M.; Kousa, Y.; Kidena, K.; Ohira, A.; Takeoka, Y.; Rikukawa, M.: Proton transport properties in an ionic liquid having a hydroxyl group. *Phys. Chem. Chem. Phys.* **2011**, *13*, 13427-13432.

(32)   Nockemann, P.; Binnemans, K.; Thijs, B.; Parac-Vogt, T. N.; Merz, K.; Mudring, A.-V.; Menon, P. C.; Rajesh, R. N.; Cordoyiannis, G.; Thoen, J.; Leys, J.; Glorieux, C.: Temperature-Driven Mixing-Demixing Behavior of Binary Mixtures of the Ionic Liquid Choline Bis(trifluoromethylsulfonyl)imide and Water. *J. Phys. Chem. B* **2009**, *113*, 1429-1437.

(33)   Liu, Q.-S.; Yang, M.; Yan, P.-F.; Liu, X.-M.; Tan, Z.-C.; Welz-Biermann, U.: Density and Surface Tension of Ionic Liquids [Cnpy][NTf2] (n = 2, 4, 5). *J. Chem. Eng. Data* **2010**, *55*, 4928-4930.

(34)   Wachter, P.; Schweiger, H.-G.; Wudy, F.; Gores, H. J.: Efficient determination of crystallisation and melting points at low cooling and heating rates with novel computer controlled equipment. *J. Chem. Thermodyn.* **2008**, *40*, 1542-1547.

(35)   Bonhôte, P.; Dias, A.-P.; Papageorgiou, N.; Kalyanasundaram, K.; Grätzel, M.: Hydrophobic, Highly Conductive Ambient-Temperature Molten Salts. *Inorg. Chem.* **1996**, *35*, 1168-1178.

(36)   Otero, I.; López, E. R.; Reichelt, M.; Villanueva, M.; Salgado, J.; Fernández, J.: Ionic Liquids Based on Phosphonium Cations As Neat Lubricants or Lubricant Additives for a Steel/Steel Contact. *ACS App. Mat. Interf.* **2014**, *6*, 13115-13128.

(37)   Fletcher, S. I.; Sillars, F. B.; Hudson, N. E.; Hall, P. J.: Physical Properties of Selected Ionic Liquids for Use as Electrolytes and Other Industrial Applications. *J. Chem. Eng. Data* **2009**, *55*, 778-782.

(38)   Holopainen, S.; Nousiainen, M.; Puton, J.; Sillanpää, M.; Bardi, U.; Tolstogouzov, A.: Evaporation of ionic liquids at atmospheric pressure: Study by ion mobility spectrometry. *Talanta* **2011**, *83*, 907-915.

(39)   Mazza, M.; Catana, D.-A.; Vaca-Garcia, C.; Cecutti, C.: Influence of water on the dissolution of cellulose in selected ionic liquids. *Cellulose* **2009**, *16*, 207-215.

(40)   Strehmel, V.; Laschewsky, A.; Wetzel, H.; Görnitz, E.: Free radical polymerization of n-butyl methacrylate in ionic liquids. *Macromolecules* **2006**, *39*, 923-930.

(41)   Hay, J. N.: *Thermal Analysis Techniques and Applications,* ; S.B. Warrington: Cambridge, 1992.

(42)   Anouti, M.; Timperman, L.: A pyrrolidinium nitrate protic ionic liquid-based electrolyte for very low-temperature electrical double-layer capacitors. *Phys. Chem. Chem. Phys.* **2013**, *15*, 6539-6548.

(43)   Machanová, K.; Wagner, Z.; Andresová, A.; Rotrekl, J.; Boisset, A.; Jacquemin, J.; Bendová, M.: Thermal Properties of Alkyl-triethylammonium bis\{(trifluoromethyl)sulfonyl\}imide Ionic Liquids. *J. Sol. Chem.* **2015**, *44*, 790-810.

(44)   Stefan, C.; Lemordant, D.; Biensan, P.; Siret, C.; Claude-Montigny, B.: Thermal stability and crystallization of N-alkyl-N-alkyl′-pyrrolidinium imides. *J. Therm. Anal. Calorim.* **2010**, *102*, 685-693.

(45)   Noda, A.; Hayamizu, K.; Watanabe, M.: Pulsed-Gradient Spin-Echo 1H and 19F NMR Ionic Diffusion Coefficient, Viscosity, and Ionic Conductivity of Non-Chloroaluminate Room-Temperature Ionic Liquids. *J. Phys. Chem. B* **2001**, *105*, 4603-4610.

(46)   Fox, D. M.; Gilman, J. W.; De, L. H. C.; Trulove, P. C.: TGA decomposition kinetics of 1-butyl-2,3-dimethylimidazolium tetrafluoroborate and the thermal effects of contaminants. *J. Chem. Thermodyn.* **2005**, *37*, 900-905.

(47)   Awad, W. H.; Gilman, J. W.; Nyden, M.; Harris Jr, R. H.; Sutto, T. E.; Callahan, J.; Trulove, P. C.; DeLong, H. C.; Fox, D. M.: Thermal degradation studies of alkyl-imidazolium salts and their application in nanocomposites. *Thermochim. Acta* **2004**, *409*, 3-11.

(48)   Kosmulski, M.; Gustafsson, J.; Rosenholm, J. B.: Thermal stability of low temperature ionic liquids revisited. *Thermochim. Acta* **2004**, *412*, 47-53.

(49)   Hao, Y.; Peng, J.; Hu, S.; Li, J.; Zhai, M.: Thermal decomposition of allyl-imidazolium-based ionic liquid studied by TGA–MS analysis and DFT calculations. *Thermochim. Acta* **2010**, *501*, 78-83.

(50)   Amarasekara, A. S.; Owereh, O. S.: Thermal properties of sulfonic acid group functionalized Broensted acidic ionic liquids. *J. Therm. Anal. Calorim.* **2011**, *103*, 1027-1030.

(51)   Villanueva, M.; Coronas, A.; García, J.; Salgado, J.: Thermal Stability of Ionic Liquids for Their Application as New Absorbents. *Ind. Eng. Chem. Res.* **2013**, *52*, 15718-15727.

(52)   Ghaemy, M.; Hassanzadeh, M.; Taghavi, M.; Amini Nasab, S. M.: Synthesis and characterization of trifluoromethylated poly(ether–imidazole–imide)s based on unsymmetrical diamine bearing carbazole and imidazole chromophores in ionic liquids: Study of electrochemical properties by using nanocomposite electrode. *J. Fluorine Chem.* **2012**, *142*, 29-40.

(53)   Heym, F.; Etzold, B. J. M.; Kern, C.; Jess, A.: Analysis of evaporation and thermal decomposition of ionic liquids by thermogravimetrical analysis at ambient pressure and high vacuum. *Green Chem.* **2011**, *13*, 1453-1466.

(54)   Huddleston, J. G.; Visser, A. E.; Reichert, W. M.; Willauer, H. D.; Broker, G. A.; Rogers, R. D.: Characterization and comparison of hydrophilic and hydrophobic room temperature ionic liquids incorporating the imidazolium cation. *Green Chem.* **2001**, *3*, 156-164.

(55)   Fox, D. M.; Awad, W. H.; Gilman, J. W.; Maupin, P. H.; De Long, H. C.; Trulove, P. C.: Flammability, thermal stability, and phase change characteristics of several trialkylimidazolium salts. *Green Chem.* **2003**, *5*, 724-727.

(56)   Jin, Y.; Fang, S.; Chai, M.; Yang, L.; Hirano, S.-i.: Ether-Functionalized Trialkylimidazolium Ionic Liquids: Synthesis, Characterization, and Properties. *Ind. Eng. Chem. Res.* **2012**, *51*, 11011-11020.

(57)   Fox, E. B.; Smith, L. T.; Williamson, T. K.; Kendrick, S. E.: Aging Effects on the Properties of Imidazolium-, Quaternary Ammonium-, Pyridinium-, and Pyrrolidinium-Based Ionic Liquids Used in Fuel and Energy Production. *Energ. Fuel.* **2013**, *27*, 6355-6361.

(58)   Sun, X.-G.; Liao, C.; Shao, N.; Bell, J. R.; Guo, B.; Luo, H.; Jiang, D.-e.; Dai, S.: Bicyclic imidazolium ionic liquids as potential electrolytes for rechargeable lithium ion batteries. *J. Power Sources* **2013**, *237*, 5-12.

(59)   Kamavaram, V.; Reddy, R. G.: Thermal stabilities of di-alkylimidazolium chloride ionic liquids. *Int. J. Therm. Sci.* **2008**, *47*, 773-777.

(60)   Liang, R.; Yang, M.; Xuan, X.: Thermal stability and thermal decomposition kinetics of 1-butyl-3-methylimidazolium dicyanamide. *Chin. J. Chem. Eng.* **2010**, *18*, 736-741.

(61)   Seeberger, A.; Andresen, A.-K.; Jess, A.: Prediction of long-term stability of ionic liquids at elevated temperatures by means of non-isothermal thermogravimetrical analysis. *Phys. Chem. Chem. Phys.* **2009**, *11*, 9375-9381.

(62)   Hatakeyama, T.; Quinn, F. X.: *Thermal analysis. Fundamentals and applications to polymer science*; John Wiley and Son, 1997.

(63)   GMbH, M. T.: *Fundamentals of the Coulometric Karl Fischer Titration with selected applications*.

(64)   Valkenburg, M. E. V.; Vaughn, R. L.; Williams, M.; Wilkes, J. S.: Thermochemistry of ionic liquid heat-transfer fluids. *Thermochim. Acta* **2005**, *425*, 181-188.

(65)   Bittner, B.; Wrobel, R. J.; Milchert, E.: Physical properties of pyridinium ionic liquids. *J. Chem. Thermodyn.* **2012**, *55*, 159-165.

(66)   Fernandez, A.; Torrecilla, J. S.; Garcia, J.; Rodriguez, F.: Thermophysical Properties of 1-Ethyl-3-methylimidazolium Ethylsulfate and 1-Butyl-3-methylimidazolium Methylsulfate Ionic Liquids. *J. Chem. Eng. Data* **2007**, *52*, 1979-1983.

(67)   Salminen, J.; Papaiconomou, N.; Kumar, R. A.; Lee, J.-M.; Kerr, J.; Newman, J.; Prausnitz, J. M.: Physicochemical properties and toxicities of hydrophobic piperidinium and pyrrolidinium ionic liquids. *Fluid Phase Equilib.* **2007**, *261*, 421-426.

(68)   Siedlecka, E. M.; Czerwicka, M.; Stolte, S.; Stepnowski, P.: Stability of Ionic Liquids in Application Conditions. *C. Org. Chem.* **2011**, *15*, 1974.

(69)   Reiter, J.; Paillard, E.; Grande, L.; Winter, M.; Passerini, S.: Physicochemical properties of N-methoxyethyl-N-methylpyrrolidinum ionic liquids with perfluorinated anions. *Electrochim. Acta* **2013**, *91*, 101-107.

(70)   Biso, M.; Mastragostino, M.; Montanino, M.; Passerini, S.; Soavi, F.: Electropolymerization of poly(3-methylthiophene) in pyrrolidinium-based ionic liquids for hybrid supercapacitors. *Electrochim. Acta* **2008**, *53*, 7967-7971.

(71)   Chancelier, L.; Diallo, A. O.; Santini, C. C.; Marlair, G.; Gutel, T.; Mailley, S.; Len, C.: Targeting adequate thermal stability and fire safety in selecting ionic liquid-based electrolytes for energy storage. *Phys. Chem. Chem. Phys.* **2014**, *16*, 1967-1976.

(72)   Shamsipur, M.; Beigi, A. A. M.; Teymouri, M.; Pourmortazavi, S. M.; Irandoust, M.: Physical and electrochemical properties of ionic liquids 1-ethyl-3-methylimidazolium tetrafluoroborate, 1-butyl-3-methylimidazolium trifluoromethanesulfonate and 1-butyl-1-methylpyrrolidinium bis(trifluoromethylsulfonyl)imide. *J. Molec. Liq.* **2010**, *157*, 43-50.

(73)   Vitz, J.; Erdmenger, T.; Haensch, C.; Schubert, U. S.: Extended dissolution studies of cellulose in imidazolium based ionic liquids. *Green Chem.* **2009**, *11*, 417-424.

(74)   Meindersma, G. W.; Simons, B. T. J.; de Haan, A. B.: Physical properties of 3-methyl-N-butylpyridinium tetracyanoborate and 1-butyl-1-methylpyrrolidinium tetracyanoborate and ternary LLE data of [3-mebupy]B(CN)4 with an aromatic and an aliphatic hydrocarbon at T = 303.2 K and 328.2 K and p = 0.1 MPa. *J. Chem. Thermodyn.* **2011**, *43*, 1628-1640.

(75)   Wooster, T. J.; Johanson, K. M.; Fraser, K. J.; MacFarlane, D. R.; Scott, J. L.: Thermal degradation of cyano containing ionic liquids. *Green Chem.* **2006**, *8*, 691-696.

(76)   D. Holbrey, J.; R. Seddon, K.: The phase behaviour of 1-alkyl-3-methylimidazolium tetrafluoroborates; ionic liquids and ionic liquid crystals. *J. Chem. Soc.* **1999**, 2133-2140.

(77)   Freire, M. G.; Neves, C. M. S. S.; Marrucho, I. M.; Coutinho, J. A. P.; Fernandes, A. M.: Hydrolysis of Tetrafluoroborate and Hexafluorophosphate

Counter Ions in Imidazolium-Based Ionic Liquids. *The Journal of Physical Chemistry A* **2010**, *114*, 3744-3749.

(78)   Kwon, K.; Park, J.; Lee, C. K.; Kim, H.: Stability of Ni and Ti in Hydrogen Evolution in the Presence of 1-Butyl-3-methylimidazolium Tetrafluoroborate. *Int. J. Electrochem. Sci* **2012**, *7*, 9835-9843.

(79)   Maton, C.; De Vos, N.; Stevens, C. V.: Ionic liquid thermal stabilities: decomposition mechanisms and analysis tools. *Chem. Soc. Rev.* **2013**, *42*, 5963-5977.

(80)   Del Sesto, R. E.; McCleskey, T. M.; Macomber, C.; Ott, K. C.; Koppisch, A. T.; Baker, G. A.; Burrell, A. K.: Limited thermal stability of imidazolium and pyrrolidinium ionic liquids. *Thermochim. Acta* **2009**, *491*, 118-120.

(81)   Uerdingen, M.: Ionic Liquids as Lubricants. Handbook of Green Chemistry. **2010**, 203–219.

(82)   Arellano, I. H. J.; Guarino, J. G.; Paredes, F. U.; Arco, S. D.: Thermal stability and moisture uptake of 1-alkyl-3-methylimidazolium bromide. *J. Therm. Anal. Calorim.* **2011**, *103*, 725-730.

(83)   Vyazovkin, S.; Burnham, A. K.; Criado, J. M.; Pérez-Maqueda, L. A.; Popescu, C.; Sbirrazzuoli, N.: ICTAC Kinetics Committee recommendations for performing kinetic computations on thermal analysis data. *Thermochim. Acta* **2011**, *520*, 1-19.

(84)   Krytox®,   D.   T.   p.   o.: http://www2.dupont.com/Lubricants/en_US/assets/downloads/DuPont_Krytox_Typical_Properties_H-58510-7.pdf. 2013.

(85)   Götz, M.; Reimert, R.; Bajohr, S.; Schnetzer, H.; Wimberg, J.; Schubert, T. J. S.: Long-term thermal stability of selected ionic liquids in nitrogen and hydrogen atmosphere. *Thermochim. Acta* **2015**, *600*, 82-88.

(86)   Gross, J. H.: Molecular Ions of Ionic Liquids in the Gas Phase. *J. Am. Soc. Mass Spectr.* **2008**, *19*, 1347-1352.

(87)   Studzińska, S.; Buszewski, B.: Study of toxicity of imidazolium ionic liquids to watercress (Lepidium sativum L.). *Anal. Bioanal. Chem.* **2008**, *393*, 983-990.

(88)   Wang, L.-S.; Wang, L.; Wang, L.; Wang, G.; Li, Z.-H.; Wang, J.-J.: Effect of 1-butyl-3-methylimidazolium tetrafluoroborate on the wheat (Triticum aestivum L.) seedlings. *Environ. Toxicol.* **2009**, *24*, 296-303.

4.Conclussions

4. Conclusions

This PhD Thesis was carried out under the framework of three research projects, two of them funded by Spanish Science and Innovation Ministry, LUBIONIC and RENELUBIL, focussed on the analysis and development of lubricants based on ILs, and an autonomic project, funded by Xunta de Galicia, motivated by the evaluation of ecotoxicity of ILs on soils and seeds. The main conclusions of this work are the following:

- Phase transitions (melting, freezing, glass, etc.) of twelve ILs were determined using scanning differential calorimetry technique. All these ILs presented melting peaks, indicating that all of them showed a crystalline phase.
- Melting temperature of selected ILs ranged from -81 ℃ (obtained for $[C_4C_1Im][BF_4]$) and 62 ℃ (for $[C_2Py][C_1SO_3]$)
- Substantial supercooling was observed for all the ILs that presented freezing peak, being these temperatures significantly lower than melting point, with t_m-t_f differences around (20 to 30) ℃, except for $[C_2Py][NTf_2]$, $[C_2C_1Im][OTf]$, $[C_4C_1Pyrr][(C_4F_9)_3PF_3]$ and $[C_2Py][C_1SO_3]$ whose values were higher than 50 ℃, indicating a very slow crystallization rate.
- Determination of the thermal stability depends on experimental conditions (atmosphere, mass sample, heating rate and water content). Results of this work show that this property is higher in nitrogen than in air atmosphere, with differences up to 19 ℃ in onset temperatures. Sample mass also affects the results, hence similar mass, with the aim to perform the best comparison, were chosen for all the next experiments. The most affecting parameter studied in this work is the heating rate; differences higher than 75 ℃ in the values of characteristic temperature were measured when the heating rate changed from (1 to 20) ℃ · min^{-1}. Finally, the water content does not affect the thermal stability of the IL analysed; an increase in 20 times the water content does not change the values of characteristic temperatures.

- Anion influence on ILs thermal stability is higher than the cation influence. The most stable anions were $[BF_4]^-$, $[NTf_2]^-$ and $[OTf]^-$ and the less stable was $[C_6SO_4]^-$. With regard to the cations, the trend obtained was $[Imidazolium]^+ >$ $[Pirrolidinium]^+ > [Piridinium]^+ > [Choline]^+$. The most part of ILs have higher thermal stability than the selected lubricant bases.

- No significant changes have been observed neither TGA curves nor onset temperatures after the 8 successive heating-cooling cycles between 50ºC and 175ºC for the ILs $[C_2C_1Im][OTf]$ and $[C_2Py][C_1SO_3]$.

- Isothermal scans at temperatures lower than the corresponding onset temperatures showed important degradation. A thermal degradation is hardly appreciable in the TG scans during more than 5 hours at two temperatures: (200 and 260) ºC for the selected ILs, and (140 and 200) ºC for Krytox GPL 105 and DiPEC7 respectively.

- Maximum Operation Temperature (MOT) was calculated through isothermal scans for the selected ILs and lubricant bases at three different levels of degradation, namely (1, 5 and 10)% of initial mass loss during 10 hours. These values were compared with MOT values obtained by other authors using dynamic scans. These results showed that MOT obtained through a dynamic experiment overrate that obtained by isothermal scans, *i.e.*, MOT value of $[C_4C_1C_1Im][OTf]$ obtained from dynamic scans was 274 ºC, meanwhile the corresponding to isothermal study was 225 ºC (mass loss of 1% during 10 h).

- Activation energy of degradation process was calculated from isothermal studies for 15 ILs using Arrhenius equation. The obtained values range from 187 kJ · mol^{-1} for $[C_4C_1Pyrr][OTf]$ to 102 kJ · mol^{-1} for $[C_1OC_2C_1Pyrr][(C_2F_5)_3PF_3]$.

- Kinetic analysis using two dynamic methods (Kissinger and Friedman) was also performed for IL $[C_4C_1C_1Im][NTf_2]$. Energy values obtained in both cases were similar to that determined in the isothermal study. (127 ± 7 kJ · mol^{-1}).

- The real liquid interval, calculated as the difference between temperature at which the 10% of degradation is reached in 10 hours and melting temperature, ranges from 208 ºC for Krytox GPL 105 and 282 ºC for IL $[C_4C_1C_1Im][OTf]$.

- Visual observation experiments of the remaining degraded sample were done for some ILs and one of the lubricant bases. The main conclusion was, in case of the ILs, that a sample colour change is related to the level of degradation; the colour change was much more intense as higher was the degradation level. In case of the lubricant, there was no appreciable colour change, which suggests that the mass loss was possibly produced by evaporation. For the same purpose DSC-TGA and DSC experiments were carried out under air and nitrogen atmosphere for some of the above ILs and another lubricant base. The results showed similar observations to the visual interpretations. ILs can present different mechanism of degradation in nitrogen atmosphere, but decomposition is the most probably in oxidative atmosphere. Base lubricants also decompose in air atmosphere, but in nitrogen atmosphere the most probable mechanism is evaporation.

- Taking into account that the most suitable IL for an application under no-reactive atmosphere will be the IL that does not present degradation, because the fluid can be recovered without any modification, this methodology is very useful in order to discern which process suffers the sample under heating.

- In order to analyse the environmental toxicity of two selected ILs, $[C_3C_1Im][NTf_2]$, and $[C_4C_1Im][BF_4]$, the effect of the addition of different doses (0.01% to 10 %) on the microbial activity in two different soils was performed using isothermal microcalorimetry, observing different effect depending on the IL and on the doses considered. In case of $[C_3C_1Im][NTf_2]$, the addition of this IL in low concentrations does not induce toxic effects on the microbial growth of the selected soils. In case of the $[C_4C_1Im][BF_4]$ the behaviour was different; the addition of the highest doses (10%) yields an intense and short peak at the beginning of the experiment, the dose of 1% provokes a shift of 10 hours with regard to control curve, the addition of the

two lowest doses does not generate important changes in microbial activity with regard to control.

- Toxic effects on microbial population of these ILs were compared with that of NaCl observing similar behaviours for $[C_3C_1Im][NTf_2]$ and NaCl. Nevertheless, the effects of $[C_4C_1Im][BF_4]$ are harmful that the salt.

- Toxic effect on germination response on seeds of different species of pine and eucalyptus has also been performed for the same ILs than microbial growth study. Significant differences have been observed on germination percentages among the control and ILs treatments for the selected species. The two highest doses of both ILs provokes the total inhibition of germination for almost all the species (except for *P. radiate* treated with the dose of 1% of $[C_3C_1Im][NTf_2]$). The dose of 0.1% produces a reduction in this parameter in comparison with the obtained for the lowest dose and control. $[C_4C_1Im][BF_4]$ IL presents stronger effect on germination than $[C_3C_1Im][NTf_2]$ in *P. radiata*, whereas no significant differences between both ILs for all the doses can be observed for *E. globulus*, *P. halepensis* and *P. nigra*. *P. pinaster* and *P. sylvestris*.

5.Appendix

Table Index

Figure Index

142

Resumen

En las últimas décadas, el interés por la conservación del medioambiente, y en concreto el crecimiento de los problemas de contaminación y degradación del medio, ha originado la necesidad y por ende la inquietud de encontrar nuevos fluidos para su uso como disolventes, lubricantes y fluidos de trabajo más respetuosos con el medioambiente, tratando de evitar los problemas de toxicidad, inflamabilidad y en algunos casos, alta volatilidad de los compuestos actuales. Además, la situación actual de la economía mundial requiere la búsqueda de energías alternativas frente a las fuentes convencionales y la optimización de las tecnologías actuales para obtener un mayor rendimiento intentando minimizar al máximo su impacto medioambiental.

Los Líquidos Iónicos (LIs) son compuestos que se encuentran en estado líquido a inferiores a 100 ºC. En 1914, se describió el primer Líquido Iónico, el $[C_2NH_3][NO_3]$, pero no fue hasta la década de los 70 cuando se sintetizó el primero. Varios autores trataron de desarrollar un electrolito para construir baterías más eficaces que pudieran emplearse en la construcción de ojivas nucleares y sondas espaciales. Las sales fundidas que emplearon eran líquidas a temperaturas que dañaban el material que se encontraba alrededor. Por este motivo, una pequeña comunidad de investigadores comenzó a buscar sales que permanecieran en estado líquido a temperaturas más bajas.

Durante el último decenio los LIs han suscitado un gran interés tanto en el mundo académico como entre los más diversos sectores tecnológicos e industriales, debido a la infinidad de aplicaciones en la que pueden ser usados. Estos compuestos poseen características físico-químicas muy atractivas, tales como alta estabilidad térmica y química, baja presión de vapor, alta densidad, baja viscosidad, amplio potencial electroquímico… Debido a estas propiedades pueden ser usados en diversas aplicaciones industriales; ingeniería de materiales, en el sector energético (como por ejemplo electrolitos para células solares, pilas de combustible, fluidos de transferencia de calor, lubricantes o aditivos de

147

lubricantes), en la industria farmacéutica y como alternativa "verde" para evitar/reducir la producción de sustancias peligrosas para el medioambiente. La enorme cantidad de aniones y cationes que podrían combinarse para formar un LI, y el hecho de que la elección de los iones (la longitud de la cadena alquílica, el grupo funcional presente en el compuesto; éter, hidroxilo, ciano…, la presencia de grupos aromáticos) determina las propiedades físico-químicas del compuesto final, justifican la potencialidad de estos compuestos. Los cationes más habituales son los imidazolios, piridinios y tetraalquilfosfonios, pirrolidinios, y entre los aniones más comunes suelen estar los halogenuros, sulfatos, triflatos e imidas.

Los líquidos iónicos suelen denominarse "fluidos verdes" debido a que no son volátiles, en consecuencia, al utilizarse para sustituir a los solventes orgánicos tradicionales, de elevada volatilidad y por tanto peligrosos contaminantes atmosféricos, ha hecho que, de manera casi generalizada, se les considere inocuos para el medio ambiente, habiendo sido incluso calificados como no tóxicos, aunque en realidad su (eco)toxicidad nunca ha sido estudiada en profundidad, y cada vez está siendo más cuestionada. Por otro lado, hay que tener en cuenta que el problema de la contaminación no se reduce a la atmósfera, ya que los LIs solubles en agua pueden llegar fácilmente, a través de las aguas residuales, a los cursos de agua superficiales, a las aguas subterráneas y a los ambientes acuáticos en general. Hasta ahora la toxicidad de los LIs se ha investigado casi exclusivamente in vitro, habiéndose evaluado mediante ensayos con algunas enzimas, diferentes tipos de células y algunos organismos tales como la lombriz de tierra, el pez cebra (*Danio rerio Hamiltomn-Buchanan*), la dafnia (*Daphnia magna Straus*) o ensayos de inhibición del crecimiento de algas. En estos estudios se ha puesto de manifiesto que la toxicidad de los LIs puede variar mucho entre organismos y depende de la estructura del LI. De todas formas, hay que destacar que, hasta la fecha, en los estudios realizados hay un olvido generalizado de los ecosistemas terrestres, ya que hasta el momento los trabajos en los que se investiga el efecto tóxico de los LIs tanto para el suelo como para la vegetación

son verdaderamente escasos. Este olvido resulta sorprendente si se tiene en cuenta que una vez el uso industrial de los LIs sea habitual, es más que probable que se produzcan derrames accidentales de los líquidos, bien sea de aquellos almacenados o bien durante las operaciones de transporte y manipulación de los mismos. Obviamente, como consecuencia de dichos derrames los LIs llegarán en primer lugar al suelo, lo que hace necesario investigar su posible toxicidad para éste.

Antes de considerar un nuevo fluido/sustancia para una aplicación industrial específica, es necesario un amplio conocimiento de sus propiedades físicas y químicas. Algunas de las propiedades termofísicas más estudiadas son: la densidad (cantidad de masa en un determinado volumen de una sustancia), la viscosidad (resistencia interna al flujo de un fluido), la conductividad eléctrica (capacidad de un material o sustancia para conducir corriente eléctrica), la tensión superficial (cantidad de energía necesaria para aumentar la superficie de un fluido por unidad de área), la solubilidad (capacidad de una sustancia o un cuerpo para disolverse al mezclarse con un líquido), la estabilidad química (estabilidad termodinámica de un sistema químico), la ventana electroquímica (rango de voltaje eléctrico dentro del cual la sustancia no se oxida ni se reduce), la estabilidad térmica (estabilidad de una sustancia cuando es sometida a altas temperaturas), y la química "verde" (o química sostenible, que consiste en una filosofía química dirigida hacia el diseño de productos y procesos químicos que implique la reducción o eliminación de productos químicos).

El trabajo desarrollado en esta Tesis, está enfocado al estudio de líquidos iónicos para su posible uso como lubricantes o como absorbentes en bombas de calor y se ha llevado a cabo en el Laboratorio de Propiedades Termofísicas de Fluidos y Biomateriales de la Facultad de Física de la Universidad de Santiago de Compostela. Este trabajo está marcado en 2 proyectos del Plan Nacional de investigación, "Influencia de la Estructura Molecular en las Propiedades Termofísicas y Tribológicas de Líquidos Iónicos en amplios rangos de presión

para su uso en Lubricación" (LUBIONIC) y "Nuevos lubricantes nanoestructurados basados en líquidos iónicos para energías renovables" (RENELUBIL), y un proyecto autonómico "Efectos dos líquidos iónicos sobre o solo e as comunidades vexetais. Aplicación a parques eólicos e solares" (LISVASPES). Además parte de este trabajo corresponde a colaboraciones con otros grupos de investigación del Sistema Universitario Gallego que conforman la Red Gallega de Líquidos Iónicos (REGALIs), financiada por la Xunta de Galicia desde el año 2012. Parte de los resultados de los estudios se han publicado en tres trabajos en la revista Journal Chemical Thermodynamics, y el resto se publicarán en dos artículos más, uno más se enviará a esta misma revista y otro al Journal of Hazardous Materials.

Los sistemas de refrigeración por absorción, comúnmente conocidos como bombas de calor, son dispositivos que funcionan cíclicamente y usan un par de trabajo, refrigerante-absorbente. Hasta hace relativamente poco se utilizaban como refrigerantes los compuestos clorofluorocarbonados (CFCs), pero cuando estos compuestos llegan al nivel estratosférico pierden su estabilidad química y reaccionan eficazmente con el ozono, consumiéndolo y contribuyendo a la destrucción de la capa de ozono y al calentamiento global del planeta, como es bien sabido. Por ello, fueron progresivamente sustituidos por los pares $H_2O/LiBr$ y NH_3/H_2O. Sin embargo, estos pares de trabajo presentan también problemas importantes, como la corrosión, la cristalización y la disminución de la solubilidad de los fluidos a bajas temperaturas. La búsqueda de nuevos tipos de fluidos de trabajo que permita una mejora en la eficiencia energética ha situado a las mezclas de líquidos iónicos (absorbente) con NH_3, CO_2, alcohol o H_2O (refrigerantes) como una alternativa a las mezclas anteriores. Y en este ámbito es también crucial conocer el intervalo de temperaturas de rango líquido para elegir aquellos que eviten los problemas de los actuales pares de trabajo.

Por otro lado, entre las propiedades fundamentales que permitirían establecer que un LI es un buen candidato para ser usado como lubricante, están la

densidad y viscosidad a distintas temperaturas y presiones, además de los coeficientes de fricción y desgaste entre los materiales en los que vaya a ser aplicado este lubricante. Un lubricante eficiente debe mantener sus propiedades en todo el rango de temperaturas en el que puede ser usado, sin que se detecten problemas de cristalización a temperaturas bajas ni de degradación a temperaturas altas. Algunas de estas propiedades, como densidad, viscosidad, coeficiente de fricción y desgaste ya han sido ampliamente estudiadas en otras Tesis Doctorales recientes del grupo de investigación. Esta Tesis completa la base de datos con el cálculo del intervalo de temperaturas de uso de una amplia colección de LIs. El trabajo aquí presentado se centra en la aplicabilidad de técnicas de calorimetría y análisis térmico en el estudio de los LIs para su potencial uso en las dos aplicaciones ya indicadas. La versatilidad de estas técnicas permitirá analizar aspectos tan diferentes como las temperaturas de fusión y cristalización, los mecanismos de degradación y la toxicidad medioambiental de los LIs.

En los últimos años el análisis térmico, como única técnica o combinada con otras, ha ganado aceptación en el estudio de las propiedades de la materia orgánica del suelo, sus fracciones o el efecto que produce en él una perturbación como pueden ser un incendio o el cambio de uso. Por otro lado, la microcalorimetría isoterma ultraestable (TAM), permite la determinación del calor asociado a la actividad metabólica de los microorganismos del suelo después de la adición de un nutriente (glucosa, por ejemplo). Usando esta técnica, otro de los temas abordados en el presente trabajo es la toxicidad de los LIs en el suelo. Los resultados se compararán con la inhibición sufrida en la germinación de semillas de especies autóctonas como consecuencia de la adición de los mismos líquidos iónicos.

Para el desarrollo de la parte experimental, la compañía Merck ha donado algunos de los LIs estudiados. Los LIs citados son los siguientes: $[C_4C_1C_1Im][(C_2F_5)_3PF_3]$, $[C_4C_1C_1Im][NTf_2]$, $[C_4C_1C_1Im][OTf]$, $[C_1C_1Im][C_1C_1PO_4]$, $[C_2C_1Im][C_6SO_4]$, $[C_4C_1Pyrr][(C_2F_5)_3PF_3]$,

[C$_4$C$_1$Pyrr][NTf$_2$], [C$_4$C$_1$Pyrr][OTf], [C$_4$C$_1$Pyrr][B(CN)$_4$], [C$_4$C$_1$Pyrr][(C$_4$F$_9$)$_3$PF$_3$], [C$_1$OC$_2$C$_1$Pyrr][NTf$_2$], [C$_1$OC$_2$C$_1$Pyrr][(C$_2$F$_5$)$_3$PF$_3$] y [P$_{6,6,6,14}$][(C$_2$F$_5$)$_3$PF$_3$]. Por otra parte, los líquidos iónicos [C$_2$Py][NTf$_2$], [Chol][NTf$_2$], [C$_2$C$_1$Im][BETI], [C$_2$C$_1$Im][OTf], [C$_2$Py][C$_1$SO$_3$] y [C$_2$Py][OTf] han sido suministrados por la compañía IoLiTec, y los LIs [C$_4$C$_1$Im][BF$_4$] y [C$_3$C$_1$Im][NTf$_2$] fueron adquiridos a Fluka y Sigma Aldrich, respectivamente. Para comparar propiedades se estudiaron cinco lubricantes comerciales, PAG2 y DiPEC7 fueron donados por Croda-Uniquema, y tres Krytox GPL por Brugarolas. A la hora de seleccionar estos 21 LIs, se han elegido éstos por tener una estructura similar a otros LIs que, en base a datos presentes en la bibliografía, cumplían una serie de características interesantes, como ser líquidos a temperatura ambiente, presentar una alta hidrofobicidad y, en general, una buena potencialidad para su uso como lubricantes.

Para la caracterización termofísica se realizaron ensayos calorimétricos y de análisis térmico usando dos conocidas técnicas experimentales, la calorimetría diferencial de barrido (DSC) y la termogravimetría (TGA). La calorimetría diferencial de barrido (Differential Scanning Calorimetry, DSC) es una de las técnicas calorimétricas más utilizadas y permite detectar fenómenos endotérmicos y exotérmicos (transiciones de fase, adsorciones, reacciones químicas…) en la muestra cuando se realiza un calentamiento o enfriamiento controlado de la misma. Con esta técnica se han determinado las temperaturas de transición del estado sólido al líquido (fusión y transición vítrea, principalmente).

El estudio por DSC se ha realizado sobre muestras de (3 – 5) mg, que fueron sometidas a cuatro rampas de temperatura, dos de enfriamiento y otras dos de calentamiento, entre (100 y – 85) ºC. Las primeras rampas de enfriamiento y de calentamiento no se han tenido en cuenta para las determinaciones, sólo para eliminar el efecto de la historia térmica. De las segundas rampas de enfriamiento y calentamiento se han determinado transiciones de fase para los siguientes LIs: [C$_2$Py][NTf$_2$], [Chol][NTf$_2$], [C$_2$Py][OTf], [C$_2$C$_1$Im][OTf], [C$_2$Py][C$_1$SO$_3$],

[C$_2$C$_1$Im][BETI], [C$_4$C$_1$C$_1$Im][(C$_2$F$_5$)$_3$PF$_3$], [C$_4$C$_1$Pyrr][(C$_2$F$_5$)$_3$PF$_3$], [C$_4$C$_1$Pyrr][(C$_4$F$_9$)$_3$PF$_3$], [C$_2$C$_1$Im][C$_6$SO$_4$], [C$_1$OC$_2$C$_1$Pyrr][(C$_2$F$_5$)$_3$PF$_3$] y [P$_{6,6,6,14}$][(C$_2$F$_5$)$_3$PF$_3$], y se ha recurrido a bibliografía para completar los datos de los restantes líquidos iónicos. Se ha obtenido una gran correlación entre los resultados de esta Tesis y los datos presentados por otros autores. Todos los líquidos estudiados presentaron picos de fusión y cristalización, aunque no se ha obtenido una tendencia clara para los valores de las temperaturas de transición de fase; en el caso particular de la temperatura de fusión, se podría, sin embargo, concluir que los cationes imidazolio muestran valores más bajos y los piridinio los más altos, para el mismo anión.

Las medidas de estabilidad térmica se han llevado a cabo mediante una balanza termogravimétrica, que registra el cambio de masa de una muestra como función de la temperatura (estudio dinámico) o del tiempo (estudio isotermo). Esta técnica permite realizar experimentos en un amplio rango de temperaturas (desde ambiente hasta 850 ºC).

En primer lugar, ante la falta de unanimidad de estudios previos a la hora de seleccionar unas condiciones experimentales óptimas y dada la influencia que éstas ejercen sobre los resultados, se ha realizado un análisis de la dependencia de las mismas sobre las temperaturas características de la degradación; así se ha visto el efecto de la atmósfera (aire o nitrógeno), la masa inicial, la velocidad de calentamiento y el contenido en agua en algunas de las muestras. A partir de las conclusiones obtenidas, se han establecido las siguientes condiciones experimentales para los posteriores análisis dinámicos: atmósfera de aire, masa inicial de (4 – 6) mg y velocidad de calentamiento de 10 ºC · min^{-1}. Dichos estudios dinámicos han sido hechos sobre los 26 compuestos seleccionados (21 LIs y 5 lubricantes). A partir de los resultados obtenidos, se concluye que hay una mayor influencia del anión que del catión sobre las temperaturas características de la estabilidad de los líquidos iónicos, pudiendo establecerse la siguiente secuencia, para un catión común dado: [NTf$_2$]$^-$ ≥ [OTf]$^-$ > [B(CN)$_4$]$^-$ > [BETI]$^-$ >

$[(C_2F_5)_3PF_3]^-$ > $[(C_4F_9)_3PF_3]^-$ > $[C_1SO_3]^-$ > $[C_1C_1PO_4]^-$ > $[C_6SO_4]^-$. En general los líquidos iónicos presentaron mejor estabilidad, en resultados dinámicos, que los lubricantes. Una vez obtenida la temperatura onset (t_{onset}), y utilizando la temperatura de fusión calculada mediante el DSC, se ha determinado el rango líquido para los compuestos analizados, obteniéndose un valor máximo de 434 ºC correspondiente al LI $[C_4C_1C_1Im][OTf]$ y un valor mínimo 244 ºC en el caso del $[C_2C_1Im][C_6SO_4]$, mientras que para los lubricantes, estos rangos han sido prácticamente en todos los casos inferiores que los de los LIs, siendo (334 y 260) ºC los valores extremos asociados al Krytox GPL 105 y al Krytox GPL 103, respectivamente. Mediante esta técnica también se han hecho estudios sobre el envejecimiento de los LIs cuando éstos son sometidos a reiterados ciclos de calor. El principal resultado de este estudio ha sido que no hay diferencias significativas en cuanto a la estabilidad térmica de esos LIs antes y después de ser sometidos a dichos ciclos.

Se comprobó que los estudios dinámicos de estabilidad sobreestiman la temperatura de uso de los fluidos, ya que se observa degradación completa de todos ellos a temperaturas ligeramente inferiores a la temperatura onset. Por ello, para conocer la estabilidad térmica a largo plazo, se realizaron estudios termogravimétricos isotermos, que se han llevado a cabo únicamente en atmósfera oxidativa (aire); las temperaturas de estos ensayos han sido elegidas a partir de la temperatura onset determinada en el ensayo dinámico, usando el criterio siguiente: la temperatura más alta para los ensayos isotermos se fijó al menos 40 ºC por debajo de la temperatura onset y, a partir de ésa, se fueron realizando ensayos isotérmicos a temperaturas 20 ºC por debajo de la anterior. Este análisis se ha hecho sobre 15 líquidos iónicos: $[C_4C_1C_1Im][(C_2F_5)_3PF_3]$, $[C_4C_1C_1Im][NTf_2]$, $[C_4C_1C_1Im][OTf]$, $[C_4C_1Pyrr][(C_2F_5)_3PF_3]$, $[C_4C_1Pyrr][NTf_2]$, $[C_4C_1Pyrr][OTf]$, $[C_1OC_2C_1Pyrr][NTf_2]$, $[C_1OC_2C_1Pyrr][(C_2F_5)_3PF_3]$, $[P_{6,6,6,14}][(C_2F_5)_3PF_3]$, $[C_2Py][NTf_2]$, $[Chol][NTf_2]$, $[C_2C_1Im][BETI]$, $[C_2C_1Im][OTf]$, $[C_2Py][C_1SO_3]$ y $[C_2Py][OTf]$, y dos bases lubricantes DiPEC7 y

Krytox GPL 105. Los resultados obtenidos ratificaron la observación previa; por ejemplo, en el caso del [C$_4$C$_1$C$_1$Im][OTf], que tiene una temperatura onset de 436 ºC y, sin embargo, en los estudios isotermos, a 400 ºC, en sólo 50 minutos de experimento pierde cerca de un 90% de su masa inicial. Así, gracias a estos estudios isotermos, se ha podido determinar un valor más adecuado para la temperatura máxima de operación de cada LI y compararla con la obtenida por otros métodos encontrados en la bibliografía.

También se han realizado estudios sobre la cinética del proceso que tiene lugar durante la pérdida de masa en un ensayo termogravimétrico, empleando los datos de los ensayos isotermos de los LIs anteriormente mencionados. Se han obtenido valores para las energías de activación que oscilaron entre los 187 kJ · mol^{-1} para el [C$_4$C$_1$Pyrr][OTf] y los 102 kJ · mol^{-1} para el [C$_1$OC$_2$C$_1$Pyrr][(C$_2$F$_5$)$_3$PF$_3$]. Adicionalmente, se han hecho estudios dinámicos para el [C$_4$C$_1$C$_1$Im][NTf$_2$] empleando dos métodos cinéticos diferentes (Kissinger y Friedman), con el fin de realizar una comparación entre los resultados obtenidos con ambos métodos y con el estudio isotermo. Los valores de las energías de activación determinadas aplicando estos tres métodos fueron similares (127±7 kJ · mol^{-1})

Como ya se ha indicado, uno de los principales objetivos de esta Tesis Doctoral es establecer el rango líquido de temperatura de los compuestos seleccionados. Dicho intervalo de temperatura puede ser definido como la diferencia entre la temperatura de fusión y la de degradación. Dada la ambigüedad a la hora de definir de manera adecuada la temperatura máxima de estabilidad, la estimación previa del rango líquido de temperatura considerando como temperatura de degradación la *t$_{onset}$* se ha corregido con la temperatura a la que se pierde un 10% de LI en 10 horas (*t´$_{0.10/10h}$*), determinada mediante el estudio isotermo, y que es uno de los parámetros más usados en la bibliografía para definir la estabilidad térmica a largo plazo de los LIs. Los nuevos valores de rango líquido de temperatura obtenidos de esta forma oscilaron, en el caso de los LIs

estudiados, entre los 145 ºC para el [C$_2$py][C$_1$SO$_3$] y los 299 ºC para el [C$_4$C$_1$Pyrr][NTf$_2$], siendo de 208 ºC para el Krytox GPL 105.

Complementariamente, se ha intentado discernir si durante la pérdida de masa registrada en los ensayos termogravimétricos, se producía evaporación o descomposición o ambas. Para ello se han llevado a cabo dos estudios: Comparación visual y análisis simultáneo DSC-TGA. En primer lugar se realizó una comparación del aspecto de muestras de 3 LIs y una base lubricante antes y después de degradar; y a continuación una nueva comparación de muestras de un LI sometido a una temperatura de calentamiento constante y distintos tiempo de exposición. Se analizó cualitativamente si las muestras presentaban cambios de color, se carbonizaban o simplemente se evaporaban. Mediante este método se pudo concluir que, en atmósfera de aire, predomina la degradación frente a la evaporación, para los 3 LIs seleccionados para este estudio.

Por otro lado se compararon los picos DSC (endotérmicos y/o exotérmicos) asociados a la degradación (medida en TGA). Ambas señales fueron obtenidas simultáneamente, con DSC-TGA Mettler Toledo. Se concluyó que en atmósfera de aire se producía predominantemente descomposición, mientras que en Nitrógeno la pérdida de masa puede estar relacionada con procesos de evaporación, sobre todo en el caso de los LIs con anión [NTf$_2$]$^-$, resultados totalmente concordantes con la bibliografía.

Finalmente, se estudió el efecto tóxico de dos de los LIs seleccionados, sobre la actividad microbiana de dos suelos y sobre germinación de semillas de especies autóctonas. Concretamente, se ha analizado la toxicidad de diferentes dosis (10, 1, 0.1 y 0.01%) de los LIs [C$_4$C$_1$Im][BF$_4$] y [C$_3$C$_1$Im][NTf$_2$] sobre una muestra de 1 g de un suelo extraído bajo cultivos de pino y eucalipto por comparación con un control (0% de LI), mediante el registro del flujo de calor en un microcalorímetro isotermo (TAM). Se han observado fenómenos muy variados e interesantes; desde la muerte de los microorganismos presentes por un gran estrés en el caso de la dosis del 10% de [C$_4$C$_1$Im][BF$_4$], así como un ligero retardo

en la actividad microbiana para el 1% de este mismo LI, hasta un incremento de la actividad microbiana para las dosis más bajas de $[C_3C_1Im][NTf_2]$. Se compararon los resultados obtenidos para los LIs con los correspondientes a los de una sal de uso común (NaCl al 10%), observándose que los comportamientos son similares para el caso de la sal y del $[C_3C_1Im][NTf_2]$, aunque en el caso del NaCl se produce un ligero retardo en la actividad microbiana en comparación con la curva registrada para ese LI.

Con respecto a la germinación, se observó una total inhibición para las dos dosis más altas de ambos LIs (10 y1)% de todas las especies estudiadas: *Pinus radiata*, *Eucalyptus globulus*, *P. nigra*, *P. pinaster*, *P. sylvestris* y *P. halepensis.*

Publications of the PhD student Juan José Parajó Vieito:

1. J. Salgado; M. Villanueva; J.J. Parajó; J. Fernández; Long-term thermal stability of five imidazolium ionic liquids. *J. Chem. Thermodyn.* **2013**, 65, 184-190.

2. J. Salgado; J.J. Parajó; J. Fernández; M. Villanueva; Long-term thermal stability of some 1-butyl-1-methylpyrrolidinium. *J. Chem. Thermodyn.* **2014**, 74, 51-57.

3. M. Villanueva; J.J. Parajó; P.B. Sánchez; J. García, J.; Liquid range temperature of ionic liquids as potential working fluids for absorption heat pumps. *J. Chem. Thermodyn.* **2015**, 91, 127-135.

Long-term thermal stability of five imidazolium ionic liquids

CrossMark

Josefa Salgado *, María Villanueva, Juan J. Parajó, Josefa Fernández

Laboratorio de Propiedades Termofísicas and Grupo TERBIPROMAT, Departamento de Física Aplicada, Facultade de Física, Universidad de Santiago de Compostela, 15782 Santiago de Compostela, Spain

ABSTRACT

Thermal stability is an essential property to select the most suitable compounds for applications as high-temperature lubricants, thermal fluids and solvents for high-temperature organic reactions. Thermal stability of five imidazolium ionic liquids (ILs) was determined using a thermogravimetrical analyzer (TG). The ILs were 1-butyl-2,3-dimethylimidazolium tris(pentafluoroethyl) trifluorophosphate, 1-butyl-2,3-dimethylimidazolium bis(trifluoromethylsulfonyl) imide, 1-butyl-2,3-dimethylimidazolium trifluoro-methanesulfonate, 1-ethyl-3-methylimidazolium ethylsulfate and 1,3-dimethylimidazolium dimethyl-phosphate. Onset temperatures were determined from dynamic experiments for the five ILs at scanning rate of $10\,°C \cdot min^{-1}$ under air atmosphere. Additionally, dynamic scans were carried out with nitrogen gas for two 1-butyl-2,3-dimethylimidazolium ILs, finding that onset temperatures are $14\,°C$ higher than those obtained with air gas flow. The three 1-butyl-2,3-dimethylimidazolium ILs present the highest onset temperatures under air atmosphere. For these last ILs, isothermal scans at lower temperatures than the onset temperature, were performed in air gas flow, finding that the most stable is 1-butyl-2,3-dimethylimidazolium trifluoromethanesulfonate. Finally, for these ILs, lifetimes were also determined for several temperatures.

© 2013 Elsevier Ltd. All rights reserved.

1. Introduction

Increasing interest is well known in the use of ionic liquids (ILs) in the energy sector, specifically in the area of renewable energy, as electrolytes for solar cells, fuel cells, heat transfer fluids, lubricants or lubricant additives of wind turbines [1].

We must mention that during the 1980s there were very few patents for this class of salts; however, only in 2012 more than 3200 were registered. In 1914, Walden [2] described the first ionic liquid, the ethyl ammonium nitrate but it was not until the 1970s when the first ionic liquid was synthesized. Wilkes *et al.* [3] and his collaborators tried to develop an electrolyte to build more efficient batteries that could be used in the construction of nuclear warheads and space probes. The molten salts used were liquid at temperatures damaging the surrounding material. So, a small community of investigators began looking for salts that remain liquid at lower temperatures [3].

In a recent review, Bermúdez *et al.* [4] concluded that ILs are a family of new high performance lubricants which may find commercial and technological applications where other lubricants are not suitable or fail to prevent friction, wear and surface damage of materials, but some additional efforts are necessary for commercial implementation.

The development of ILs for several of these applications requires the knowledge of their thermophysical properties. Taking into account that in these and other potential uses as thermal fluids or solvents, ILs can be subjected to high temperatures and long-time exposures, their thermal stability is an essential property when selecting the most suitable ones. Thermal stability of ILs is affected by many parameters, *e.g.*, the cation and anion type, structural modifications of the cation (alkyl chain length, different functionalities in the alkyl chain) and impurities (water, chlorides, etc.) [5]. As is well known, the anion is the most relevant moiety in the IL thermal stability. In a recent review, Siedlecka *et al.* [6] concluded that imidazolium ILs are more stable than pyridinium, phosphonium, ammonium, pyrrolidinium and pyperidinium ILs.

To date, onset decomposition temperature (t_{onset}) of several ILs has been determined using the scanning thermogravimetric analysis (TGA) method. Nevertheless, in recent years, the definitions of stability and of the maximum operation temperature for ionic liquids (ILs) remain an open question [4,6–8]. Thus, in the previous decade, but also among several authors nowadays, the thermal stabilities of ILs were evaluated primarily using thermogravimetric (TG) analysis at a single linear heating rate in inert atmosphere. Most of the TG studies were performed with a heating rate of $10\,°C \cdot min^{-1}$, but some authors even use higher values as $15\,°C \cdot min^{-1}$ [9], $20\,°C \cdot min^{-1}$ [10–12] and others use lower rates such as $5\,°C \cdot min^{-1}$ [13]. Due to the scanning nature of the experiment, the decomposition temperatures obtained from these

* Corresponding author. Tel.: +34 881814110; fax: +34 881814112.
 E-mail address: j.salgado.carballo@usc.es (J. Salgado).

experiments, often overestimated the long term thermal stabilities of the ILs. This fact indicates that the degradation of the ionic liquid starts at lower temperatures than the onset values, as numerous authors have pointed out during the last decade [5,7,8]. Nevertheless, this parameter can be used as a relative parameter of thermal stability, but never as the top limit of temperature in a particular application. Hence, fast TG analysis scans under a protective atmosphere do not imply long-term thermal stability below these temperatures. Meine et al. [14] found that the ILs 1-ethyl-3-methylimidazolium chloride, $[C_2C_1Im][Cl]$, and 1-butyl-3-methylimidazolium chloride, $[C_4C_1Im][Cl]$, presented degradation at 120 °C, although onset temperatures were 278 °C and 291 °C, respectively. Nowadays it is known that the maximum operation temperature of the ILs is much lower than the decomposition temperatures [5,7,15]. Isothermal studies have shown that the ILs exhibit appreciable decomposition at temperatures significantly lower than those indicated by the peak or onset decomposition temperatures determined from scanning TG experiments [5,15–17].

With the aim of characterizing the anion effect, in this work the thermal stability of five ILs was analysed. These liquids were three 1-butyl-2,3-dimethylimidazolium tris(pentafluoroethyl) trifluorophosphate ($[C_4C_1C_1Im]^+$) ILs based in the anions trifluoromethyllsulfonyl imide ($[NTf_2]^-$), tris(pentafluoroethyl) trifluorophosphate ($[FAP]^-$), and trifluoromethanesulfonate ($[OTf]^-$) as well as 1-ethyl-3-methylimidazolium hexylsulfate $[C_2C_1Im][C_6SO_4]$, and 1-ethyl-3-methylimidazolium dimethylphosphate $[C_1C_1Im][DMP]$. Dynamic TG studies on trialkylimidazolium ILs are very scarce; only few studies [5,11,18–21] have been published for $[C_4C_1C_1Im][NTf_2]$. Thus, Fox et al. [5] studied the useful range of temperature in the liquid phase of several ionic liquids, among them five trialkylimidazolium ILs with different hydrocarbon chains and anions. In their work, a dynamic thermogravimetric study of the IL $[C_4C_1C_1Im][NTf_2]$ was performed under N_2 atmosphere, obtaining a decomposition temperature at 5% mass fraction loss, around 435 °C. We are not aware about other TG isothermal or dynamical analysis of the ILs studied in this work that were chosen in a research project aiming to study their potential use as lubricants and hydraulic fluids. In addition, we should point out that alkyl sulfate-based ILs with an imidazolium-type cation can be
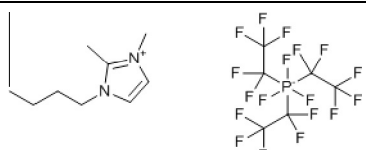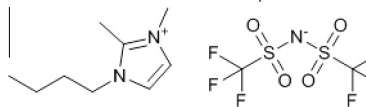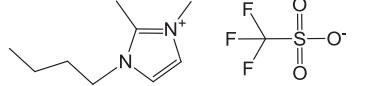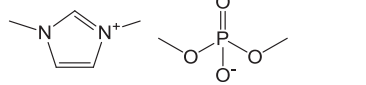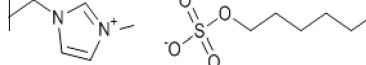
considered as some of the most promising ILs for application in industrial processes because they can be easily synthesized in an atom-efficient and halide-free way, at a reasonable cost. Promising results were found for oil refining [22] and on reducing lignin molar mass [23] among other [24] applications. Imidazolium ILs with $[DMP]^-$ anion have also been proposed to break up lignin and cellulose [25], for extractive desulfurization [26] of gasoline and in absorption refrigeration [27]. Viscosities and densities over a broad range of temperature were recently reported for $[C_4C_1Im][NTf_2]$, $[C_4C_1C_1Im][FAP]$ and $[C_2C_1Im][C_6SO_4]$ [28]. The viscosity-pressure coefficients were also recently measured for $[C_4C_1C_1Im][NTf_2]$ and $[C_4C_1C_1Im][FAP]$ [29].

2. Experimental

The chemical structure, molecular formula, CAS number, provenance and purity of the five ionic liquids are listed in table 1. These liquids were kindly provided by Merck KGaA. The specified mole fraction purity of the samples is higher than 0.98. By chromatography of ionic exchange, HPLC or electrophoresis it has been found that the mole fraction purity of the five ILs is higher than 0.98.

A thermogravimetric analyser (TGA 7- Perkin Elmer), operating in dynamic and isothermal modes under dry nitrogen and dry air atmospheres, was used to perform thermogravimetric analysis. Liquid samples of (3–5) mg were placed in an open platinum pan. Dynamic experiments were performed at temperatures from (100 to 800) °C, with a heating rate of 10 °C · min^{-1} and a purge gas flow of 20 cm^3 · min^{-1}. Using the thermal analysis software, the onset temperature was calculated by the intersection of the straight baseline along the temperature axis from a low temperature region where there is no weight loss, and a straight line created through the inflection point (previously determined as the minimum in the derivative of the mass loss curve, DTG) of the mass versus temperature data. From these curves, the temperature at the 10% of mass loss, $t_{10\%}$, mass loss at onset temperature, W_{onset}, as well as the temperature of the minimum of the DTG peaks, t_{1st} and t_{2nd}, were determined. Each analysis was repeated three times, the standard deviation average values being lower than 2% in all the cases.

TABLE 1
Provenance and purity of the ionic liquids used in this work.[a]

Name	Chemical formula CAS number	Chemical structure	Mole fraction purity
1-Butyl-2,3-dimethylimidazolium tris(pentafluoroethyl) trifluorophosphate	$[C_4C_1C_1Im][FAP]$ Not available		>0.98
1-Butyl-2,3-dimethylimidazolium bis(trifluoromethylsulfonyl) imide	$[C_4C_1C_1Im][NTf_2]$ 350493-08-2		>0.999
1-Butyl-2,3-dimethylimidazolium trifluoromethanesulfonate	$[C_4C_1C_1Im][OTf]$ 765910-73-4		>0.98
1,3-Dimethylimidazolium dimethylphosphate	$[C_1C_1Im][DMP]$ 654058-04-5		0.993
1-Ethyl-3-methylimidazolium hexylsulfate	$[C_2C_1Im][C_6SO_4]$ 942916-86-1		>0.999

[a] All ILs were supplied by Merck.

On the other hand, isothermal TG analysis under air atmosphere was used to determine the long-term thermal stability of ILs. Air atmosphere was chosen because is more realistic to predict the long term stabilities in real applications as lubrication systems or thermal fluids. The highest temperature selected for isothermal scans was approximately 40 °C lower than the onset temperature and a 20 °C decreasing step was used for the selection of the other temperatures in almost all of the cases.

3. Results and discussion

3.1. Atmosphere influence

It is well known that the experimental conditions, such as heating rate, sample pan materials, sample weight and atmosphere can influence on the thermal analysis results. Thus, Ngo et al. [19] found differences higher than 100 °C between the onset temperatures of $[C_2C_1Im][PF_6]$ measured in aluminium (375 °C) and alumina (481 °C) pans, whereas only a difference of 2 °C was found for $[C_2C_1Im][NTf_2]$ under the same conditions. On the other hand, for this last IL, Ngo et al. [19] obtained a value of 453 °C at 20 °C · min⁻¹ whereas Noda et al. [20] found a value of 417 °C when using a heating rate of 10 °C · min⁻¹, both in nitrogen atmosphere, i.e., an increase in more than 30 °C was found in the onset temperature when using different heating rates. Fox et al. [30] found an increase of 100 °C in the onset temperature of $[C_4C_1im][BF_4]$ when the heating rate increases from 10 °C · min⁻¹ to 20 °C · min⁻¹. Similar results have been reported by other authors like Awad et al. [31], Kosmulski et al. [17], Hao et al. [32] and Amarasekara and Owereh [10].

With the aim to define the most advisable analysis conditions of ILs for lubrication applications, two ILs, $[C_4C_1Im][NTf_2]$ and $[C_4C_1Im][FAP]$, were analysed in a dynamic mode from 75 °C to 800 °C at 10 °C · min⁻¹ in both, air and nitrogen atmospheres. Figure 1 shows the comparison of TG and DTG curves in both atmospheres for $[C_4C_1Im][NTf_2]$. Table 2 shows t_{onset}, $t_{10\%}$, t_{peak}, and W_{onset} values obtained in air and in nitrogen atmospheres and corresponding data reported by other authors. In the literature there are few studies corresponding to these ILs. These results show that the ILs studied are slightly more stable in the nitrogen atmosphere. Small differences in t_{onset}, up to 14 °C, for N_2 and air atmospheres can be observed. Nevertheless, the mass loss at onset temperature seems to be not dependent on the atmosphere; for each IL similar values of W_{onset} were obtained in air and N_2.

Since the objective of the study is the characterization of the thermal stability of ILs, in order to estimate the maximum temperature of operation as lubricants, and taking into account the above

FIGURE 1. Comparison of TG (solid) and DTG (dashed) curves under N_2 (□) and air (○) for $[C_4C_1Im][FAP]$.

TABLE 2
Thermal results from the dynamic scans in N_2 and in the air atmosphere.

IL	Atmosphere	t_{onset}/°C	$t_{10\%}$/°C	W_{onset}/%	t_{1st}/°C	t_{2nd}/°C
$[C_4C_1Im][FAP]$	N_2	376	379	91	402	442
	Air	363	364	88	395	413
$[C_4C_1Im][NTf_2]$	N_2	436	408			
		435 [5]	414 [18]	75	478	
		430 [11]				
	Air	424	407	79	470	476
$[C_4C_1Im][OTf]$	Air	436	424	84,1	479	
$[C_2C_1Im][C_6SO_4]$	Air	251	269	93.8	398	
$[C_1C_1Im][DMP]$	Air	274	262	87.2	303	
	N_2	268 [33]				

Standard uncertainties are $u(t)$ = 2% and $u(W)$ = 2%.

results, further analyses were performed only in air atmosphere for being this one the more restrictive.

3.2. Dynamic study

Figure 2 shows the TG and DTG curves, obtained under air atmosphere for the five ILs. The most stable ILs, which are those containing the cation $[C_4C_1C_1Im]^+$, showed greater mass losses (a sharp decay is observed in their DTG curves, although they are more stable because thermal degradation starts at higher temperatures). $[C_4C_1C_1Im][FAP]$ shows two resolved peaks, whereas the degradation of $[C_4C_1C_1Im][NTf_2]$ and $[C_4C_1C_1Im][OTf]$ exhibits only one step. This fact suggests that the $[FAP]^-$ ILs could have different mechanism of decomposition. $[C_1C_1Im][DMP]$ and $[C_2C_1Im][C_6SO_4]$ need a broader temperature interval to complete the thermal degradation and they also presented two resolved peaks in DTG curves. Table 2 shows that the values obtained in this work for $[C_4C_1C_1Im][NTf_2]$ in N_2 agree very well with the onset temperatures determined by Fox et al. [5] and Bazito et al. [11]. Additionally, our datum of the $t_{10\%}$, 408 °C is slightly lower than the value reported by Jin et al. [18]. Vitz et al. [33] obtained a similar value to ours for the $[C_1C_1Im][DMP]$ (sample purity of 80%) at 20 °C · min⁻¹ under N_2 atmosphere.

As mentioned above, the most used parameter to identify the thermal stability is the onset temperature, which ranges for the five ILs studied ILs from 251 °C to 436 °C, being the lowest value for $[C_2C_1Im][C_6SO_4]$ and the highest for $[C_4C_1C_1Im][OTf]$. Taking into account the values of the onset temperature showed in table 2, thermal stability in air of the liquids decreases with the following trend: $[C_4C_1C_1Im][OTf]$ > $[C_4C_1C_1Im][NTf_2]$ > $[C_4C_1C_1Im][FAP]$ > $[C_1C_1Im][DMP]$ > $[C_2C_1Im][C_6SO_4]$. We should remark that the difference of the onset temperatures of the two first ILs is only 12 °C. It is well known that the thermal stability of the ILs is strongly anion dependent [1,5,6,10,21,34,35]. Previous works [21,34,35] suggest that the $[NTf_2]^-$ anion confers the highest thermal stability to the ILs, but some $[OTf]^-$ ILs have excellent values of this property. Thus, Nakata et al. [36] found that the $[C_2C_1Imin][OTf]$ is the most stable of five dialkylimidazolium ILs with $[I]^-$, $[BF_4]^-$, $[SCN]^-$, $[C_2SO_4]^-$ and $[OTf]^-$ anions. Bittner et al. [9] have recently investigated several pyridinium ILs finding for 1-butyl-3-methylpyridinium ILs the sequence $[BF_4]^-$ > $[NTf_2]^-$ > $[FAP]^-$ > $[OTf]^-$. Tokuda et al. [37] have found that the onset temperature 1-butyl-3-methylimidazolium IL with $[OTf]^-$ anion is 14 °C lower than those of the corresponding IL with $[NTf_2]^-$ anion. These different trends could be explained taking into account the influence of the cation.

3.3. Isothermal study

To make a more realistic description of the thermal stability of the ILs, the three ILs studied in this work with the highest onset
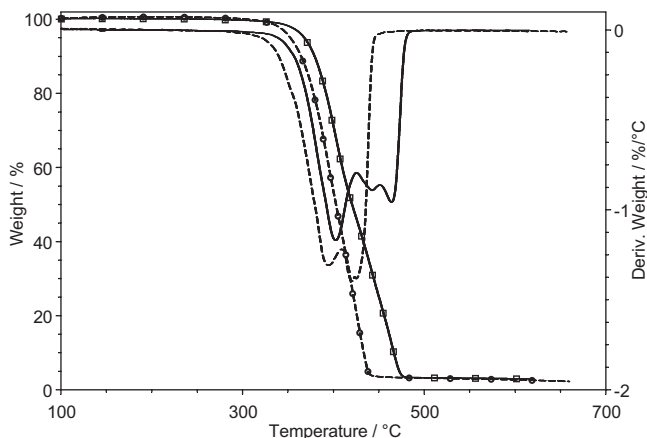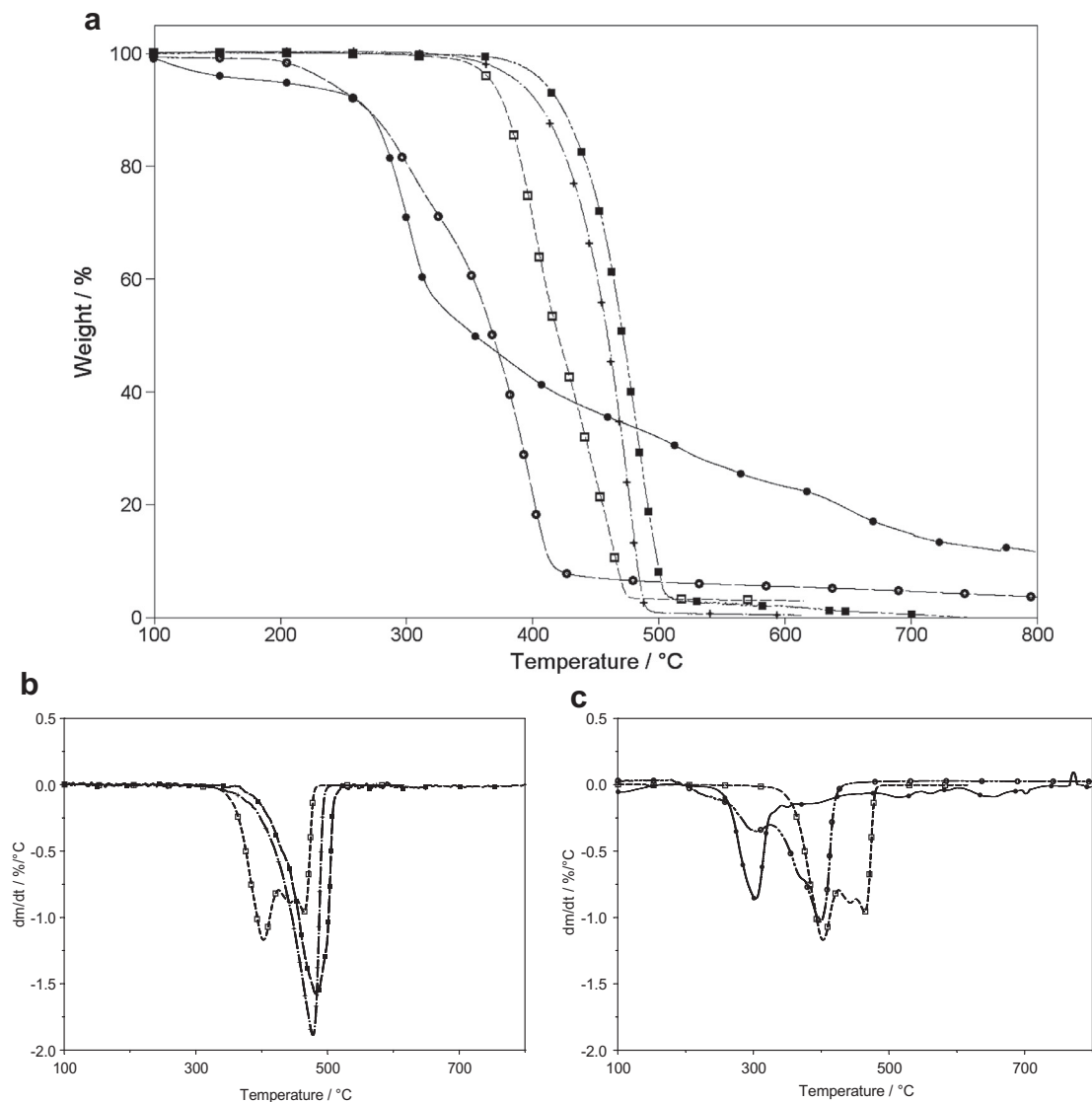
FIGURE 2. TG (a) and DTG (b,c) curves for the five ILs: (●) [C$_1$C$_1$Im][DMP], (○) [C$_2$C$_1$Im][C$_6$SO$_4$], (□) [C$_4$C$_1$C$_1$Im][FAP], (+) [C$_4$C$_1$C$_1$Im][NTf$_2$], (■) [C$_4$C$_1$C$_1$Im][OTf].

temperatures, [C$_4$C$_1$C$_1$Im][OTf], [C$_4$C$_1$C$_1$Im][NTf$_2$] and [C$_4$C$_1$C$_1$-Im][FAP], were subjected to several isothermal experiments at different temperatures, as it was already indicated.

Figure 3 shows the TG curves of these three ILs, as a function of time for different exposition temperatures. The main observation is, as it was expected, a fast degradation at temperatures close to t_{onset}. Hardly appreciable thermal degradation is observed in the ILs exposed more than 5 h at temperatures 200 °C lower than their t_{onset} values.

To compare the thermal stability, figure 4 shows the TG curves of the three ILs selected at 300 °C. From this figure, it can be concluded that the thermal stability decreases with the following sequence: [C$_4$C$_1$C$_1$Im][OTf] > [C$_4$C$_1$C$_1$Im][NTf$_2$] > [C$_4$C$_1$C$_1$Im][FAP]. This trend is the same as that of the onset temperatures.

3.4. Kinetics of isothermal decomposition

As can be seen in figure 3, the mass losses against time for the three ILs present practically linear dependences during the first part of the degradation, i.e., the degradation rate is constant at a given temperature. Because of the decomposition rate of ionic liquids depends in general on the mass and heat transfer and no on chemical reactions, the kinetics of decomposition can be represented as a pseudo-zero-order expression [15,17,32,38].

$$d\alpha/dt' = k, \tag{1}$$

where k is the rate constant of pseudo-zero-order, and α is the degree of conversion, which can be defined as a function of W_t, mass of the sample at time t', and of W_i, the initial mass, by the following expression:

$$\alpha = \frac{(W_i - W_t)}{W_i}. \tag{2}$$

The degradation rate can be represented in integral form, considering equation (1), as:

$$\alpha = kt' + C, \tag{3}$$

where t' is time and C is another constant. So, representing for each isothermal scan α versus time, we obtain the rate constant k from a linear fitting of these experimental data.

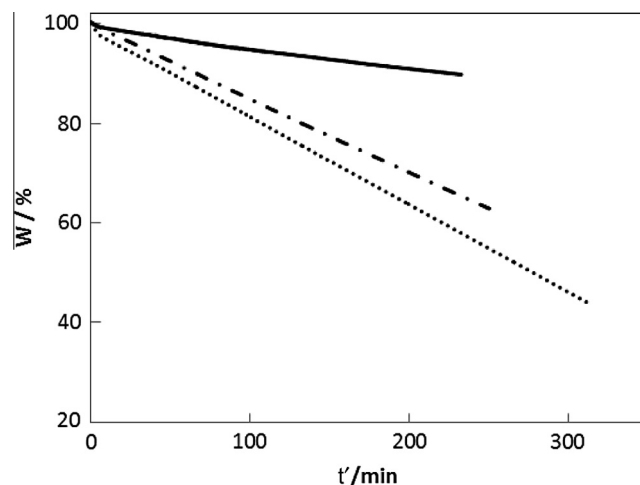The temperature dependence on k, is represented by the Arrhenius equation:
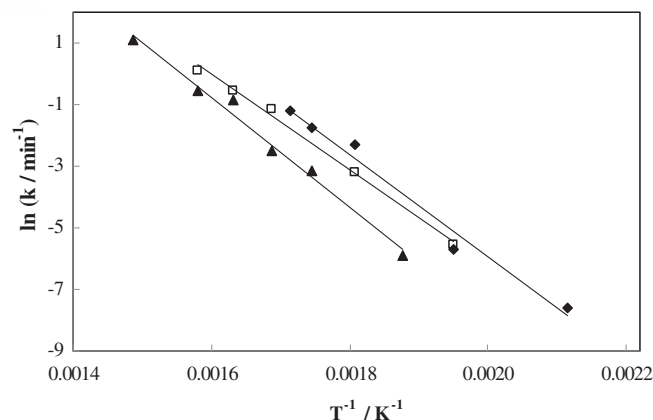
$$k = A \exp\left(\frac{-E_a}{RT}\right), \tag{4}$$

FIGURE 4. Isothermal scans at 300 °C for the three selected ILs: (---) [C$_4$C$_1$C$_1$-Im][FAP], (–·–·–) [C$_4$C$_1$C$_1$Im][NTf$_2$], (---) (—) [C$_4$C$_1$C$_1$Im][OTf].

FIGURE 5. Arrhenius plots for the three ILs: [C$_4$C$_1$C$_1$Im][FAP] (♦), [C$_4$C$_1$C$_1$Im][NTf$_2$] (□), [C$_4$C$_1$C$_1$Im][OTf] (▲).

Hao *et al.* [32] for 1-allyl-3-methylimidazolium chloride and by Kamavaran *et al.* [15] for [C$_1$C$_4$Im][Cl] and [C$_1$C$_6$Im][Cl].

3.5. Lifetime

Up to now, a clear criterion does not exist on the degradation level allowed in the different applications, finding in literature a wide range, from 1% in one year [7] to 10% in 10 h [39]. In this work we have analysed two degradation levels, 5% and 10%, at different temperatures in order to give information about how much time the ILs takes to degrade and the maximum operation temperature.

From isothermal scans, the time that each ionic liquid takes to decompose 5% and 10% percentage of mass ($t'_{5\%}$ and $t'_{10\%}$) were determined and presented in table 4. Figure 6 shows $t'_{5\%}$ and $t'_{10\%}$ against temperature. A decreasing exponential function fits quite well the experimental values as it also represented in this figure. From these equations the maximum time at which an IL could be used in good conditions can be estimated. Using the criterion of Liang *et al.* [39], 10% loss in 10h, the maximum temperatures of operation were obtained from the above equations, being 258 °C, 266 °C and 284 °C for [C$_4$C$_1$C$_1$Im][OTf], [C$_4$C$_1$C$_1$Im][NTf$_2$] and [C$_4$C$_1$-C$_1$Im][FAP], respectively. Taking into account that in all of these calculations an important loss of accuracy can appear, 10% approx-

FIGURE 3. Isothermal scans of each IL: (a) [C$_4$C$_1$C$_1$Im][FAP], (b) [C$_4$C$_1$C$_1$Im][NTf$_2$], (c) [C$_4$C$_1$C$_1$Im][OTF].

where E_a is the activation energy and A is the pre-exponential coefficient. Thus, from a linear fit of ln k versus $1/T$ (figure 5), the activation energy can be obtained. The activation energies and pre-exponential coefficients obtained for the three ILs are shown in table 3.

Up to now, no references with values of this parameter for these ILs have been found. Somewhat lower E_a values were obtained by

TABLE 3

Pre-exponential coefficients and activation energies of the studied ILs obtained from Arrhenius equation (4).

| IL	$E_a/(kJ \cdot mol^{-1})$	A/min^{-1}
$[C_4C_1Im][FAP]$	139	0.979
$[C_4C_1Im][NTf_2]$	129	0.995
$[C_4C_1Im][OTf]$	148	0.987

TABLE 4

Thermal degradation times (in min) for degrees of decomposition of 5% and 10% determined/calculated from the isothermal scans to the three selected ILs.

Ionic liquid	$t/°C$	$t'_{5\%}/min$	$t'_{10\%}/min$
$[C_4C_1Im][FAP]$	200	10760^a	20760^a
	240	1507^a	3022^a
	280	25.6	78.5
	300	20.6	50.4
	310	12.5	30.3
	320	4.2	9.2
$[C_4C_1Im][NTf_2]$	240	2409^a	4681^a
	280	130.9	254^a
	300	33.1	65.9
	320	19.1	34.4
	340	10.3	19.9
	360	3.2	8
$[C_4C_1Im][OTf]$	260	1674^a	3460
	300	94.6	226^a
	320	56.1	123.1
	340	12.3	23.6
	360	7.9	15.3
	400	2.4	4.6

^{a} Extrapolated values.
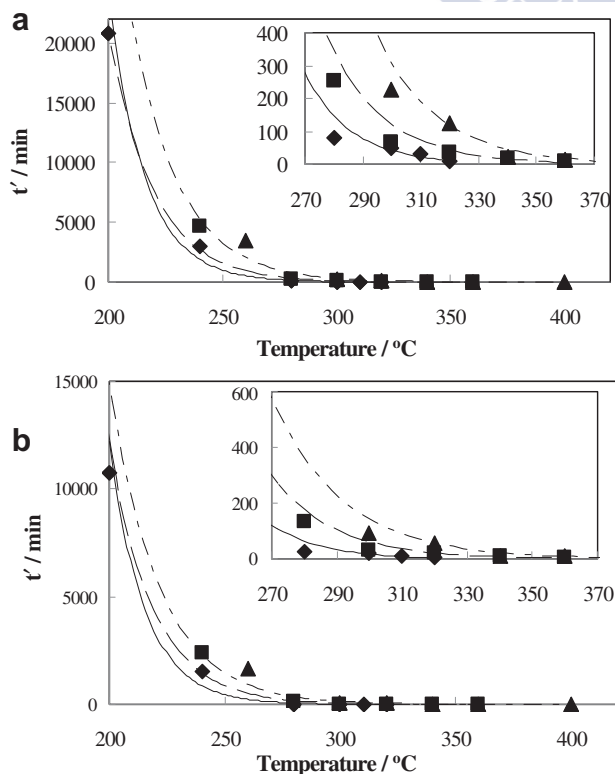
FIGURE 6. Correlation of experimental values of degradation times for the three ILs against temperature for 10% (a) and 5% (b) of degradation: $[C_4C_1Im][FAP]$ (♦), $[C_4C_1Im][NTf_2]$ (□), $[C_4C_1Im][OTf]$ (▲).

imately, temperatures of 250 °C should not be overcome in any case to asses this criterion.

4. Conclusions

Onset temperatures for five ILs have been determined by dynamic thermogravimetric analysis, under N_2 and air atmospheres. According to the results, $[C_4C_1Im][OTf]$ is the most stable and $[C_2C_1Im][C_6SO_4]$ the least stable. Owing to the fact that air atmosphere is more restrictive than N_2 (differences of 10 °C in t_{onset} were obtained), the isothermal study was performed in air. According to isothermal scans, thermal stability for the five ILs decreases with the following sequence: $[C_4C_1Im][OTf] > [C_4C_1Im][NTf_2] > [C_4C_1Im][FAP] > [C_1C_1Im][DMP] > [C_2C_1Im][C_6SO_4]$. Activation energies of the studied ILs, obtained from the Arrhenius equation, have values between (129 and 148) $kJ \cdot mol^{-1}$. An equation has been determined to estimate the useful time for the three ILs studied.

Finally, it is interesting to emphasize the high reliability of the information provided by isothermal studies; as an example, the IL $[C_4C_1im][NTf_2]$, whose t_{onset} is 424 °C, shows a degradation higher than 80% after being 100 min at 360 °C. Using the criterion of 10% loss in 10 h for the present isothermal studies, the maximum temperature of operation for this IL should not exceed 250 °C.

References

[1] A. Fernandez, J.S. Torrecilla, J. Garcia, F. Rodriguez, J. Chem. Eng. Data 52 (2007) 1979–1983.
[2] P. Walden, Bull. Acad. Imper. Sci. St. Petersburg 8 (1914) 405–422.
[3] J.S. Wilkes, J.A. Levisky, R.A. Wilson, C.L. Hussey, Inorg. Chem. 21 (1982) 1263–1264.
[4] M.D. Bermúdez, A.-E. Jiménez, J. Sanes, F.-J. Carrión, Molecules 14 (2009) 2888–2908.
[5] D.M. Fox, W.H. Awad, J.W. Gilman, P.H. Maupin, H.C. De Long, P.C. Trulove, Green Chem. 5 (2003) 724–727.
[6] E.M. Siedlecka, M. Czerwicka, S. Stolte, P. Stepnowski, C. Org, Chem. 15 (2011) 1974.
[7] A. Seeberger, A.-K. Andresen, A. Jess, Phys. Chem. Chem. Phys. 11 (2009) 9375–9381.
[8] M. Uerdingen, in: P. Wasserscheid, A. Stark (Eds.), Green Solvents, Wiley-VCH Verlag GmbH&Co, KGaA, Weinheim, 2010, pp. 203–219.
[9] B. Bittner, R.J. Wrobel, E. Milchert, J. Chem. Thermodyn. 55 (2012) 159–165.
[10] A.S. Amarasekara, O.S. Owereh, J. Therm. Anal. Cal. 103 (2011) 1027–1030.
[11] F.F.C. Bazito, Y. Kawano, R.M. Torresi, Electrochim. Acta 52 (2007) 6427–6437.
[12] C. Schmidt, T. Glueck, G. Schmidt-Naake, Chem. Eng. Technol. 31 (2008) 13–22.
[13] U. Domanska, Thermochim. Acta 448 (2006) 19–30.
[14] N. Meine, F. Benedito, R. Rinaldi, Green Chem. 12 (2010) 1711–1714.
[15] V. Kamavaram, R.G. Reddy, Int. J. Therm. Sci. 47 (2008) 773–777.
[16] A.F. Ferreira, P.N. Simões, A.G.M. Ferreira, J. Chem. Thermodyn. 45 (2012) 16–27.
[17] M. Kosmulski, J. Gustafsson, J.B. Rosenholm, Thermochim. Acta 412 (2004) 47–53.
[18] Y. Jin, S. Fang, M. Chai, L. Yang, S.-i. Hirano, Ind. Eng. Chem. Res. 51 (2012) 11011-11020.
[19] H.L. Ngo, K. LeCompte, L. Hargens, A.B. McEwen, Thermochim. Acta 357–358 (2000) 97–102.
[20] A. Noda, K. Hayamizu, M. Watanabe, J. Phys. Chem. B 105 (2001) 4603–4610.
[21] H. Shirota, T. Mandai, H. Fukazawa, T. Kato, J. Chem. Eng. Data 56 (2011) 2453–2459.
[22] C.D. Wilfred, C.F. Kiat, Z. Man, M.A. Bustam, M.I.M. Mutalib, C.Z. Phak, Fuel Process. Technol. 93 (2012) 85–89.
[23] A. George, K. Tran, T.J. Morgan, P.I. Benke, C. Berrueco, E. Lorente, B.C. Wu, J.D. Keasling, B.A. Simmons, B.M. Holmes, Green Chem. 13 (2011) 3375–3385.
[24] X. Paredes, J. Fernandez, A.A.H. Padua, P. Malfreyt, F. Malberg, B. Kirchner, A.S. Pensado, J. Phys. Chem. B 116 (2012) 14159–14170.
[25] B.D. Rabideau, A. Agarwal, A.E. Ismail, J. Phys. Chem. B 117 (2013) 3469–3479.

[26] Y. Nie, C. Li, A. Sun, H. Meng, Z. Wang, Energy Fuels 20 (2006) 2083–2087.
[27] W. Chen, S. Liang, Y. Guo, K. Cheng, X. Gui, D. Tang, J. Therm. Sci. 21 (2012) 557–563.
[28] F.M. Gaciño, T. Regueira, L. Lugo, M.J.P. Comuñas, J. Fernandez, J. Chem. Eng. Data 56 (2011) 4984–4999.
[29] F.M. Gaciño, X. Paredes, M.J.P. Comuñas, J. Fernández, J. Chem. Thermodyn. 54 (2012) 302–309.
[30] D.M. Fox, J.W. Gilman, L.H.C. De, P.C. Trulove, J. Chem. Thermodyn. 37 (2005) 900–905.
[31] W.H. Awad, J.W. Gilman, M. Nyden, R.H. Harris Jr, T.E. Sutto, J. Callahan, P.C. Trulove, H.C. DeLong, D.M. Fox, Thermochim. Acta 409 (2004) 3–11.
[32] Y. Hao, J. Peng, S. Hu, J. Li, M. Zhai, Thermochim. Acta 501 (2010) 78–83.
[33] J. Vitz, T. Erdmenger, C. Haensch, U.S. Schubert, Green Chem. 11 (2009) 417–424.
[34] R.G. Reddy, Z. Zhang, M.F. Arenas, D.M. Blake, High Temp. Mater. Processes 22 (2003) 87–94.
[35] J. Salminen, N. Papaiconomou, R.A. Kumar, J.-M. Lee, J. Kerr, J. Newman, J.M. Prausnitz, Fluid Phase Equilib. 261 (2007) 421–426.
[36] Y. Nakata, K. Kohara, K. Matsumoto, R. Hagiwara, J. Chem. Eng. Data 56 (2011) 1840–1846.
[37] H. Tokuda, K. Hayamizu, K. Ishii, M.A.B.H. Susan, M. Watanabe, J. Phys. Chem. B 108 (2004) 16593–16600.
[38] M.E.V. Valkenburg, R.L. Vaughn, M. Williams, J.S. Wilkes, Thermochim. Acta 425 (2005) 181–188.
[39] R. Liang, M. Yang, X. Xuan, Chin. J. Chem. Eng. 18 (2010) 736–741.

JCT 13-270

Long-term thermal stability of some 1-butyl-1-methylpyrrolidinium ionic liquids

CrossMark

Josefa Salgado, Juan J. Parajó, Josefa Fernández, María Villanueva *

Group of Thermophysical Properties of Fluids and Biomaterials, Departamento de Física Aplicada, Facultade de Física, Universidad de Santiago de Compostela, 15782 Santiago de Compostela, Spain

ABSTRACT

Thermal stability of five ionic liquids (ILs) was determined by thermogravimetric analysis (TGA). The ILs were selected with the common cation 1-butyl-1-methylpyrrolidinium and with the anions bis(trifluoromethylsulfonyl)imide, tetracyanoborate, trifluoromethanesulfonate, tris(pentafluoroethyl)trifluorophosphate and trifluorophosphate. Onset temperatures, t_{onset}, were determined from dynamic experiments under air atmosphere and scanning rate of 10 °C · min^{-1}. Additionally isothermal scans at lower temperatures than the t_{onset} values were performed for three of the selected ILs. The results showed that the ILs with the anions bis(trifluoromethylsulfonyl)imide and trifluoromethanesulfonate present the highest thermal stability. Although the influence of the cation on this property is lower than that of the anion, these pyrrolidinium based ILs showed less thermal stabilities than those of the corresponding imidazolium based ILs with the same anions published previously. Finally, the maximum operation temperature was estimated for three possible degradations levels.

© 2014 Elsevier Ltd. All rights reserved.

1. Introduction

Perfluoropolyethers are widely used as lubricants in commercial applications for extreme operating conditions due to their high temperature stability and extremely low vapour pressure. However, these oils are not appropriate for some nanotechnology applications because of their low electrical conductivity. Ionic liquids (ILs) are being explored as lubricants for several device applications [1] because of their high electrical conductivity and good thermal conductivity. Current high-temperature aircraft lubricants can operate only up to a temperature of 150 °C, whereas new aerospace technologies demand lubricants that can function between (−40 and 330) °C [2]. Zeng *et al.* [2] among others [3,4] have studied the performance for several ionic liquids as high temperature lubricants. Besides, lubricants must be constantly improved to reduce carbon emissions and to save energy [5]. As this regard, new studies on ILs aim to its future use in renewable energy, new transfer-fluids, and energy storage [6–8]. In these applications and in many others is important to determine the thermal behaviour of ILs and the temperatures which allow for a correct and safe application.

In most of the screening studies on the properties of ILs to select the best ones for any application, dynamic thermogravimetric analyses (TGA) are performed. In this type of evaluation the loss weight of the IL sample is measured during a temperature ramp with a heating rate usually of 10 °C · min^{-1}. This type of assays permits to determine the onset temperatures, t_{onset} of ILs, which can be used to roughly compare the relative thermal stability, but the maximum operation temperature for ILs must be calculated more carefully due to the influence of the experimental conditions [9–13]. Several studies show that the maximum operating temperatures are considerably lower than the t_{onset} value [14,15]. Thus, in our previous work we have found for 1-butyl-2,3-dimethylimidazolium bis(trifluoromethylsulfonyl)imide, a t_{onset} value of 424 °C but also a thermal degradation higher than 80% after keep it 100 min at 360 °C. Similar results were found for several research groups that have already applied this technique [16,17]. To overcome this problem and to obtain more profound information on the stability at temperatures below the t_{onset} values, it is necessary to perform 'long-term' isothermal TGA measurements for prolonged times (*e.g.* 0.5, 15 or 20 h) [9,10,12,14,18–20]. These thermal analyses provides to rates of decomposition at a given temperature instead of critical or onset temperatures.

Thermal stability of an IL mainly depends on the anion, although the effect of the cation on the stability is less important [12]. This property increases with the anion size and decreases with the IL hydrophilicity [21]. In a previous work [9] we have studied the thermal stability of five imidazolium ILs with different anions through dynamic and isothermal TG scans. In the present

* Corresponding author. Tel.: +34 881814005; fax: +34 881814085.
E-mail address: maria.villanueva@usc.es (M. Villanueva).

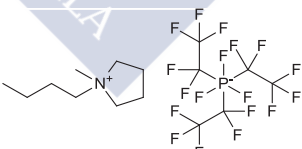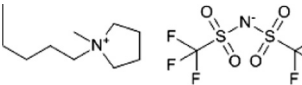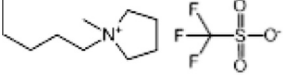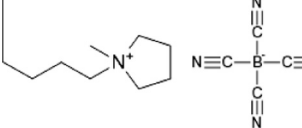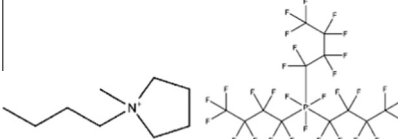work, the aim is to known both, anion and cation effects on the thermal stability of the ILs. Thus, to study in depth the anion effect, the ILs selected here present the same cation 1-butyl-1-methylpyrrolidinium ($[C_4C_1Pyrr]^+$) with five different anions, (trifluoromethyllsulfonyl)imide ($[NTf_2]^-$), tris(pentafluoroethyl) trifluorophosphate ($[FAP]^-$), trifluoromethanesulfonate ($[OTf]^-$), tetracyanoborate ($[B(CN)_4]^-$) and tris(nonafluorobutyl)trifluorophosphate ($[(C_4F_9)_3PF_3]$). Besides, three of these ILs have the same anions ($[NTf_2]^-$, $[FAP]^-$ and ($[OTf]^-$) than the imidazolium based ILs studied in the previous work. This selection permits to analyse also the effect of the cation on the thermal stability.

Most of the studies on ILs correspond to imidazolium-based ILs. The recent interest in pyrrolidinium-based ILs is mainly due to their wider electrochemical windows and higher electrochemical stability when compared to imidazolium-based ILs [22–26]. Gaciño *et al.* [27] have measured the densities and viscosities at atmospheric pressure in a broad density range of $[C_4C_1Pyrr][NTf_2]$, $[C_4C_1Pyrr][OTf]$ and $[C_4C_1Pyrr][FAP]$. In addition, for the first IL, Regueira *et al.* [28] and Gaciño *et al.* [29] reported the densities and the viscosities at high pressures. $[C_4C_1Pyrr][B(CN)_4]$ is an halogen-free IL, whose densities, viscosities, surface tensions at atmospheric pressure were measured by Meindersma *et al.* [30]. In addition, these authors have measured for this IL the onset temperature and the heat capacities at (25 and 50) °C. Besides, Minami *et al.* [31] have reported that its glass transition temperature is 22 °C. For $[C_4C_1Pyrr][(C_4F_9)_3PF_3]$ we have not found any published article.

2. Experimental

The samples of the five ILs were kindly provided by Merck KGaA with a specified fraction purity higher than 0.98. Chemical structure, molecular formula, water content and mass fraction purity are listed in table 1. It has been found by alkalimetry after ionic exchange that the purity of $[C_4C_1Pyrr][NTf_2]$ is 0.999 and that of $[C_4C_1Pyrr][B(CN)_4]$ obtained by electrophoresis is higher than 0.99. The ionic liquids were used without further purification.

Water contents were measured with a Karl Fischer Coulometer. As can be seen in table 1, these quantities could be considered important (except for $[C_4C_1Pyrr][(C_4F_9)_3PF_3]$), but ILs were employed in this work without purification because in many potential industrial applications as lubricants, contact with air cannot be avoided.

A thermogravimetric analyser (TGA7- Perkin Elmer) operating in dynamic and isothermal modes under dry air atmosphere was used to perform thermal stability analysis. Although the effect of the atmosphere becomes lower in studies of long-term thermal stability [10], air atmosphere was chosen because in dynamic studies it is more restrictive than N_2 [9], and it is more appropriate in order to estimate the maximum operation temperature in lubrication applications. Samples of (3 to 5) mg were placed in an open platinum pan. Dynamic experiments were performed at temperatures from (100 to 800) °C with a heating rate of 10 °C · min^{-1} and a purge gas flow of 20 cm^3 · min^{-1}. The onset and end set temperatures determination procedure is described in previous papers [9,10]. From these curves, the temperature at the 10% of mass loss ($t_{10\%}$), the mass loss at onset temperature (W_{onset}) as well as the temperature of the minimum of the DTG peaks (t_{1st} and t_{2nd}) were determined. Each analysis was repeated three times, the standard deviation average values being lower than 6 °C in all the cases.

On the other hand, isothermal TG analysis was used to determine the long-term thermal stability of ILs. This analysis provides rates of decomposition at a given temperature after a given isothermal-heating time. Seven temperatures in the interval (200 °C – t_{onset}) were selected for these scans. Taking into account that at 200 °C the mass loss was lower than 1% in 5 h for the studied ILs, experiments at temperatures lower than 200 °C were not performed.

3. Results and discussion

3.1. Dynamic study

For the five ILs both TG and DTG curves are plotted in figure 1. The $[C_4C_1Pyrr][FAP]$ and $[C_4C_1Pyrr][(C_4F_9)_3PF_3]$ show two resolved

TABLE 1
Ionic liquids used in this work. The five ILs were provided by Merck KGaA.

Name	Abbreviation CAS number	Chemical structure	Mass fraction purity	Water content 10^{-6}
1-butyl-1-methylpyrrolidinium tris(pentafluoroethyl) trifluorophosphate	$[C_4C_1Pyrr][FAP]$ 851856-47-8		⩾0.99	700
1-butyl-1-methylpyrrolidinium bis(trifluoromethylsulfonyl)imide	$[C_4C_1Pyrr][NTf_2]$ 223437-11-4		⩾0.999	1416
1-butyl-1-methylpyrrolidinium trifluoromethanesulfonate	$[C_4C_1Pyrr][OTf]$ 367522-96-1		⩾0.98	960
1-butyl-1-methylpyrrolidinium tetracyanoborate	$[C_4C_1Pyrr][B(CN)_4]$ 1266721-18-9		>0.99	1306
1-butyl-1-methylpyrrolidinium tris(nonafluorobutyl) trifluorophosphate	$[C_4C_1Pyrr][(C_4F_9)_3PF_3]$ Not available		⩾0.98	56

peaks, whereas the degradation of $[C_4C_1Pyrr][NTf_2]$, $[C_4C_1Pyrr]$ [OTf] and $[C_4C_1Pyrr][B(CN)_4]$ exhibits only one step. This observation agrees with results of a previous work [9], where we have also found that $[C_4C_1C_1Im]^+$ ILs with $[NTf_2]^-$, $[OTf]^-$ anions show one step degradation, whereas the $[FAP]^-$ IL presents two-steps. Figure 1 also shows that the residue after the main degradation step of $[C_4C_1Pyrr][B(CN)_4]$ is around the 20% of the initial weight. This residue is getting lost slowly and continuously, following a straight line with time; but whereas the rest of the ILs showed zero mass at 600 °C, approximately the 15% of the initial mass of this IL remains at this temperature. Shamsipur et al. [32], found a similar behaviour in the dynamic TG curves of $[C_2mim][BF_4]$ and $[C_4mim][OTf]$, attributing it to the mass loss of elementary carbon produced from the previous steps.

Table 2 presents the $t_{10\%}$, W_{onset}, t_{1st} and t_{2nd} values obtained from the dynamic thermogravimetric curves for the five 1-butyl-1-methylpyrrolidinium ILs. For these temperatures, t_{onset}, $t_{10\%}$ and t_{1st}, the anion trend observed is the following $[NTf_2]^- \geqslant [OTf]^- \approx [B(CN)_4]^- > [FAP]^- > [(C_4F_9)_3PF_3]^-$. Degradation temperature interval is similar for $[NTf_2]^-$, $[OTf]^-$ and $[B(CN)_4]^-$ ILs, about 40 °C, showing these ILs the lowest values of W_{onset}; whereas the difference between t_{endset} and t_{onset} in $[FAP]^-$ and $[(C_4F_9)_3PF_3]^-$ ILs is higher than 100 °C The highest values of W_{onset} observed for these ILs are due to the longest degradation intervals and consequently the slowest loss of weight.

As it is well known, the thermal stability of the ILs is highly anion dependent [11,19,33–37]. This sequence agrees with that of the previous works [19,36,37], which suggest that the $[NTf_2]^-$ anion confers the highest thermal stability to the ILs, but some $[OTf]^-$ and $[B(CN)_4]^-$ ILs have also excellent values of this property. These results are also in relative good concordance with the obtained in our previous article [9], where the thermal stability of ILs with the common cation $[C_4C_1C_1Im]^+$ and five different anions, sharing three of them with those of the present work, $[NTf_2]^-$, $[OTf]^-$ and $[FAP]^-$, was analysed. From the comparison, it can be seen that ILs with 1-butyl-1-methylpyrrolidinium cation are slightly less stable than the corresponding ILs with the $[C_4C_1C_1Im]^+$ cation. In particular, for both ILs with $[OTf]^-$ anion a difference in onset temperatures higher than 35 °C can be observed.

The number of references on thermal stability of these ILs is scarce. Up to our knowledge only in four published papers the thermal stability of two of the ILs presented in this work have been briefly analysed. Zhou et al. [38] obtained an onset value 6 °C higher than ours with the same heating rate but with N_2 gas. This is in complete agreement with our results because the thermal stability at dynamic conditions should be slightly worse with air. On the other hand, Chancelier et al. [8] reported for this IL an onset temperature with an uncertainty of 5 °C, measured by TGA using 5 °C · min^{-1} and argon flow, being this value only slightly higher (6 °C) than ours, which could be probably due to the different experimental conditions [10]. Nevertheless, Shamsipur et al. [32] studied the thermal stability of the $[C_4C_1Pyrr][NTf_2]$ by TG, in identical conditions to us, and also with DSC technique. These authors

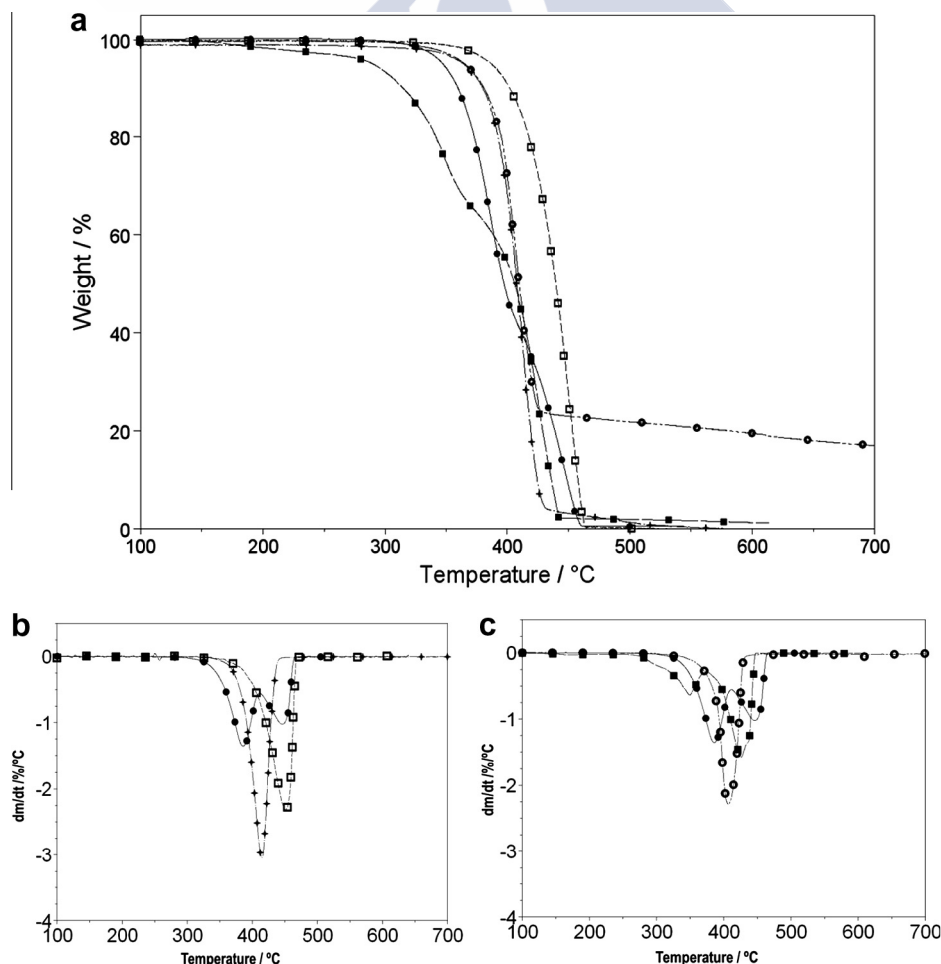**FIGURE 1.** TG (a) and DTG ((b) and (c)) curves of the five ILs: (●) $[C_4C_1Pyrr][FAP]$, (□) $[C_4C_1Pyrr][NTf_2]$, (+) $[C_4C_1Pyrr][OTf]$, (○) $[C_4C_1Pyrr][B(CN)_4]$, (■) $[C_4C_1Pyrr][(C_4F_9)_3PF_3]$.

TABLE 2
Thermal results from the dynamic scans in air atmosphere under pressure of (990.5 ± 0.5) hPa.

IL	t_{onset}/°C	t_{endset}/°C	$t_{10\%}$/°C	W_{onset}/%	t_{1st}/°C	t_{2nd}/°C
[C$_4$C$_1$Pyrr][FAP]	358	458	360	90	381	441
[C$_4$C$_1$Pyrr][(C$_4$F$_9$)$_3$PF$_3$]	315	440	316	90	350	426
[C$_4$C$_1$Pyrr][NTf$_2$]	417	461	402	81	452	
[C$_4$C$_1$Pyrr][B(CN)$_4$]	388	421	381	86	407	
[C$_4$C$_1$Pyrr][OTf]	399	436	382	88	414	

Expanded standard uncertainties are $U(t)$ = 6 °C and $U(W)$ = 2% (0.95 level of confidence).

obtained an exothermic degradation but it shifts 75 °C approximately towards minor temperatures, with respect to the results of this work, Zhou et al. [38] and Chancelier et al. [8]. We should point out that Chancelier et al. [8] also determined with a DSC the onset temperature of this IL under nitrogen with a heat rate of 5 °C · min^{-1} finding a value 105 °C higher than that of Shamsipur et al. [32], On the other hand, Meindersma et al. [30] obtained a similar TG and DTG pattern than us for the [C$_4$C$_1$Pyrr][B(CN)$_4$], although they reported the t_{onset} calculated from the temperature at which the $dW/dt \neq 0$ [39], which is approximately 100 °C lower than that obtained in this work. The first minimum obtained by these authors is quite close to that obtained in this work. Later on, the usefulness of taking one or another value as t_{onset} will be discussed.

3.2. Isothermal study

With a double aim, firstly the determination of the maximum operation temperature of the pyrrolidinium based ILs was done, and secondly, to compare with the results obtained for the imidazolium based ILs [9], [C$_4$C$_1$Pyrr][NTf$_2$], [C$_4$C$_1$Pyrr][OTf] and [C$_4$C$_1$Pyrr][FAP] were selected among the five ILs to perform several isothermal experiments at different temperatures. Corresponding TG scans are presented in figure 2.

As it was expected, the isothermal TG curves at the highest temperatures are characterised by a fast degradation. By the contrary, a thermal degradation is hardly appreciable in the TG scans during more than 5 h for [C$_4$C$_1$Pyrr][FAP] at 200 °C and for [C$_4$C$_1$Pyrr][NTf$_2$] and [C$_4$C$_1$Pyrr][OTf] at 260 °C.

After 50 min at the temperatures (260, 300 and 340) °C for [C$_4$C$_1$Pyrr][NTf$_2$] the mass losses were (0.5, 3 and 27)%; for [C$_4$C$_1$Pyrr][OTf] were (2, 6 and 48)% whereas for [C$_4$C$_1$Pyrr][FAP] values of (2, 47 and around 97)% were obtained. For the first IL we have found that the degradation in air is quicker than that in argon analysed by Chancelier et al. [8].

Figure 3 shows the isothermal TG curves at 340 °C of the three ILs analysed in this paper together with those for [C$_4$C$_1$C$_1$Im]$^+$ ILs with the same cations [9]. From this figure, it can be concluded that the imidazolium are slightly more stable than the pyrrolidinium ILs; thermal stability for the ILs with the anions [NTf$_2$]$^-$ and [OTf]$^-$ is similar, and the ILs with [FAP]$^-$ are the less stable with independence of the cation. Thus, degradation losses of 50% for [C$_4$C$_1$Pyrr][FAP] and [C$_4$C$_1$C$_1$Im][FAP] are reaching after (10 and 31) min, respectively, whereas for and [C$_4$C$_1$C$_1$Im][OTf] 142 min are needed. The differences between the [NTf$_2$]$^-$ and [OTf]$^-$ ILs are quite small, agreeing with the onset temperatures behaviour. Additionally, in a recent review, Maton et al. [14] collect the onset temperatures of 60 imidazolium base ILs with different anions, among those are [NTf$_2$]$^-$ and [OTf]$^-$. These results show that for ILs with the same cation, those with the [NTf$_2$]$^-$ anion present higher values of t_{onset} than the ILs with [OTf]$^-$ anion, except for the ILs with the cation [C$_2$C$_1$Im]$^+$. Additionally, Fredlake et al. [21] also studied the thermal stability of several imidazolium based ILs, reporting the onset and start temperatures, t_{onset} and t_{start} respectively, being the last one the temperature at which
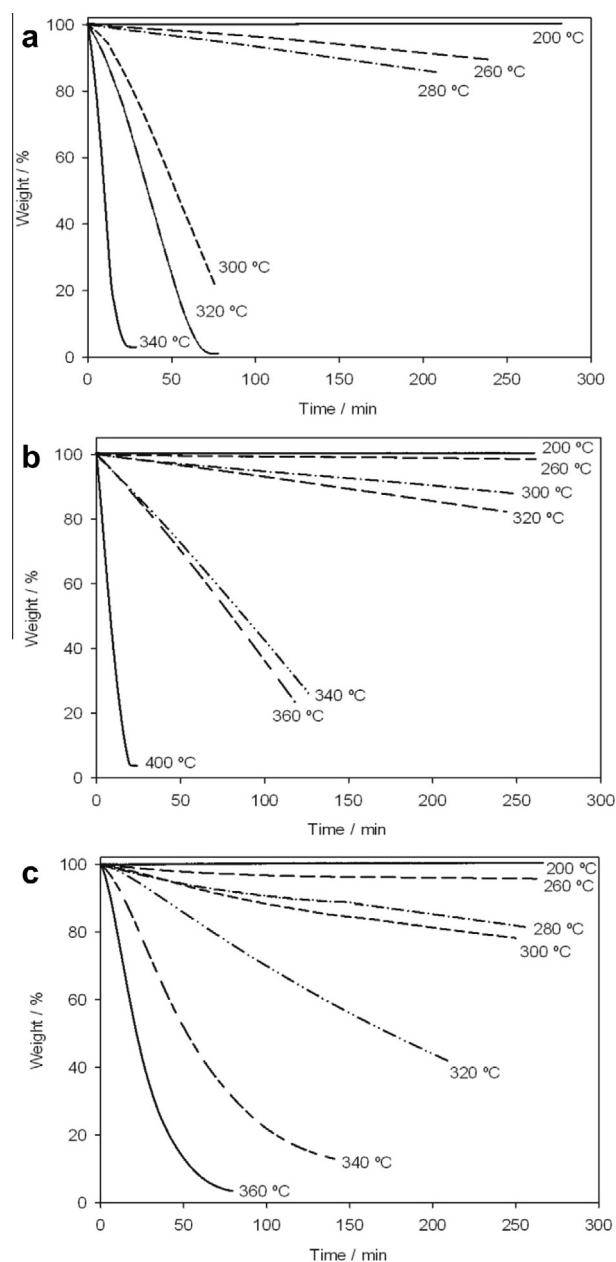
FIGURE 2. Isothermal scans of the three selected ILs: (a) [C$_4$C$_1$Pyrr][FAP], (b) [C$_4$C$_1$Pyrr][NTf$_2$] and (c) [C$_4$C$_1$Pyrr][OTf]. All experiments were performed at atmospheric pressure of (985 ± 10) hPa.

the decomposition begins. The values of t_{start} are determined as the temperature at which the baseline and the TG curve separate from each other. These last authors found that the t_{onset} of [C$_4$C$_1$Im][NTf$_2$] is higher than that of [C$_4$C$_1$Im][OTf], whereas the
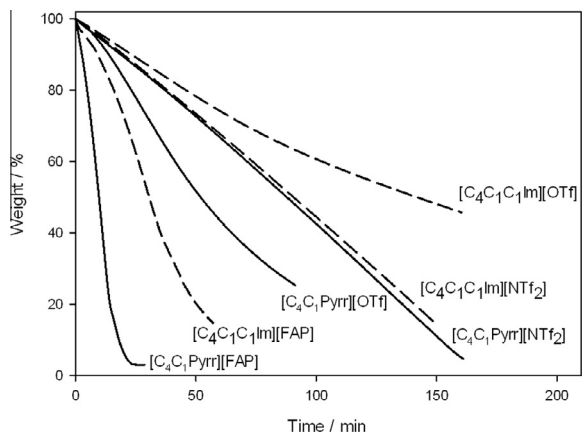
FIGURE 3. Comparison of the TG isothermal scans at 340 °C for [C$_4$C$_1$Pyrr][FAP], [C$_4$C$_1$Pyrr][NTf$_2$], [C$_4$C$_1$Pyrr][OTf] and for three ILs with the same anions from a previous work [9].

t_{start} displayed the opposite behaviour. All these facts reveals that both anions, [NTf$_2$]$^-$ and [OTf]$^-$, present similar results in thermal stability studies and then the cation effect is more appreciable than in other combinations.

3.3. Kinetics of isothermal decomposition

The kinetics of decomposition of 1-butyl-1-methylpyrrolidinium ionic liquids with the anions [NTf$_2$]$^-$, [OTf]$^-$ and [FAP]$^-$, was analysed from isothermal TGA results following the methodology reported in a previous paper [9].

The temperature dependence on the rate of loss mass, k, is represented by the Arrhenius equation:

$$k = A\exp\left(\frac{-E_a}{RT}\right), \tag{1}$$

where E_a is the activation energy and A is the pre-exponential coefficient. Figure 4 shows the relation between the values of ln k

FIGURE 4. Arrhenius plots for the three ILs: [C$_4$C$_1$Pyrr][OTf] (△), [C$_4$C$_1$Pyrr][FAP] (♦), [C$_4$C$_1$Pyrr][NTf$_2$] (□).

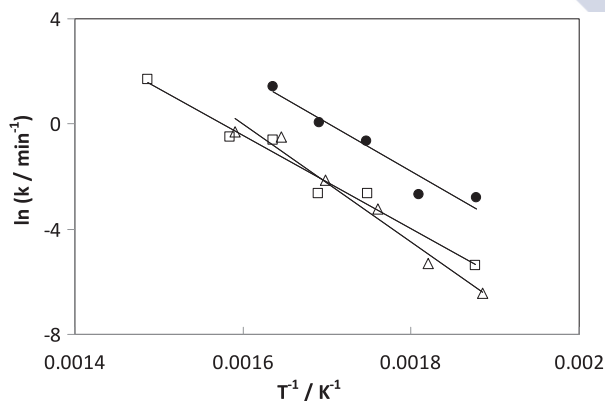**TABLE 3**
Pre-exponential coefficients, A, and activation energies, E_a, for the selected ILs obtained from the Arrhenius equation (1).

IL	$E_a/(kJ \cdot mol^{-1})$	A/min^{-1}
[C$_4$C$_1$Pyrr][NTf$_2$]	147	1.56 10^{12}
[C$_4$C$_1$Pyrr][OTf]	187	3.78 10^{7}
[C$_4$C$_1$Pyrr][FAP]	153	1.05 10^{16}

and T^{-1}. Thus, from the corresponding linear fitting, the activation energy of the degradation process has been obtained, as is shown in table 3, together the pre-exponential coefficients.

Up to know, no references with values of this parameter for these ILs have been found, although these values are in concordance with those reported in the literature for other ILs [9,17,20,40,41]. The activation energy of the imidazolium ILs [9] is lower than the pyrrolidinium ILs with the same anion. Besides, the sequence observed is the same: [NTf$_2$]$^-$ < [FAP]$^-$ < [OTf]$^-$ for both imidazolium and pyrrolidinium ILs.

3.4. Maximum operation temperature

Following the criterion established in a previous paper [9], three thermal degradation levels ((1, 5 and 10)% at different temperatures) were selected in order to obtain information about how much time an IL takes to degrade at different operation temperatures.

Firstly, from isothermal scans, the times that each ionic liquid takes to decompose (1, 5 and 10)% percentages of mass ($t'_{1\%}, t'_{5\%}$ and $t'_{10\%}$) were determined. Figure 5 shows $t'_{5\%}$ and $t'_{10\%}$ values against temperature for the three ILs. As it can be also seen from this figure, good correlations of the experimental data with a decreasing exponential function (equation (2)) were obtained:

$$t' = Be^{Ct}, \tag{2}$$

where t' is the time in minutes, t the temperature in °C, and, B and C correlation coefficients. Table 4 shows the values of the B and C parameters. From these fits the maximum time at which an IL could be used in reliable conditions can be estimated, taking into account
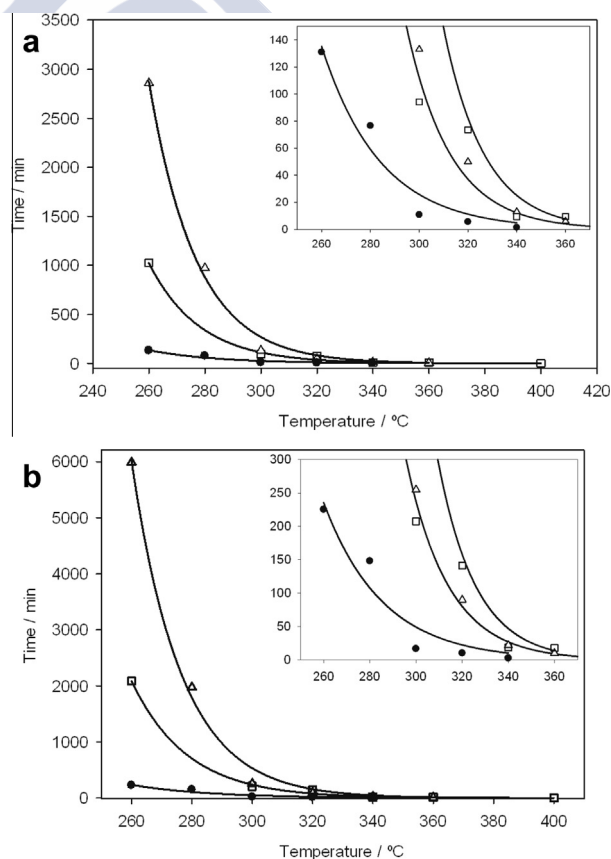
FIGURE 5. Correlation of experimental values of degradation times obtained in the isothermal scans for the three ILs against temperature for (a) 5% and (b) 10% of degradation. [C$_4$C$_1$Pyrr][OTf] (△), [C$_4$C$_1$Pyrr][FAP] (●), [C$_4$C$_1$Pyrr][NTf$_2$] (□).

TABLE 4

Parameters B and C for the equation (2) for the three selected ILs as well as for those selected in a previous work [9].

IL	B/min	C/°C^{-1}
1% weight loss		
$[C_4C_1Pyrr][NTf_2]$		
$[C_4C_1Pyrr][OTf]$	$1.449 \cdot 10^7$	-0.0389
$[C_4C_1Pyrr][FAP]$	$1.168 \cdot 10^8$	-0.0582
$[C_4C_1Im][NTf_2]$	$1.149 \cdot 10^8$	-0.0533
$[C_4C_1Im][OTf]$	$8.281 \cdot 10^6$	-0.0427
$[C_4C_1Im][FAP]$	$2.878 \cdot 10^{10}$	-0.0779
5% weight loss		
$[C_4C_1Pyrr][NTf_2]$	$3.194 \cdot 10^8$	-0.0489
$[C_4C_1Pyrr][OTf]$	$4.315 \cdot 10^{10}$	-0.0639
$[C_4C_1Pyrr][FAP]$	$6.099 \cdot 10^8$	-0.0576
$[C_4C_1Im][NTf_2]$	$4.744 \cdot 10^8$	-0.0529
$[C_4C_1Im][OTf]$	$1.615 \cdot 10^8$	-0.0464
$[C_4C_1Im][FAP]$	$6.354 \cdot 10^9$	-0.0658
10% weight loss		
$[C_4C_1Pyrr][NTf_2]$	$8.501 \cdot 10^8$	-0.0510
$[C_4C_1Pyrr][OTf]$	$1.737 \cdot 10^{11}$	-0.066
$[C_4C_1Pyrr][FAP]$	$8.787 \cdot 10^9$	-0.0583
$[C_4C_1Im][NTf_2]$	$6.394 \cdot 10^8$	-0.0546
$[C_4C_1Im][OTf]$	$4.784 \cdot 10^8$	-0.0475
$[C_4C_1Im][FAP]$	$8.685 \cdot 10^9$	-0.0639

TABLE 5

Estimated temperatures (in °C) corresponding to the loss of 1% during 10 h according to Wooster *et al.* [39], and to the loss of (1, 5, and 10)% obtained from isothermal scans.

IL	$t_{0.01/10\,h}$/°C	$t_{0.01/10\,h}$/°C	$t_{0.05/10\,h}$/°C	$t_{0.10/10\,h}$/°C
	Dynamic study	Isothermal study		
$[C_4C_1Pyrr][NTf_2]$	261		268	284
$[C_4C_1Pyrr][OTf]$	266	249	282	296
$[C_4C_1Pyrr][FAP]$	242	207	237	247
$[C_4C_1Im][NTf_2]$	252	231	257	266
$[C_4 C_1Im][OTf]$	274	225	276	284
$[C_4C_1Im][FAP]$	231	224	244	258

that, depending on intended application, different appropriate degrees of degradation and time periods should be chosen.

Wooster *et al.* [39] suggested that the temperature at which 1% degradation occurs in 10 h ($T_{0.01/10\,h}$) is as a good indicator of thermal stability and they established a method to estimate it from dynamic scans using the equation:

$$T_{0.01/10\,h} = 0.82\, T_{(dw/dT \neq 0)}, \tag{3}$$

being $T_{(dW/dT\neq0)}$ the lowest temperature (in Kelvin) at which the first derivative of the weight loss versus T curve is non-zero. The $T_{(dW/dT\neq0)}$ value provides an estimate of the lowest T at which volatile products are evolved, under the conditions of the experiment. Following this methodology, the estimation of maximum temperature operation as $T_{0.01/10\,h}$ was done for the ILs subjected to isothermal analysis in this work and in a previous article [9]. As it can be observed in table 5, the values obtained for $t_{0.01/10\,h}$ from the dynamic scans and equation (3) are significantly lower than the onset temperatures. With the aim to compare the results of this methodology with those obtained from isothermal scans, the temperature at which the (1, 5, and 10)% of the initial mass are lost after 10 h, $t_{0.01/10\,h}$, $t_{0.05/10\,h}$ and $t_{0.10/10\,h}$ respectively, were calculated from the above equation (2). These comparisons are summarized in table 5. The values obtained from both methods are in quite good concordance taking into account the influence of the experimental conditions [10] used to determine the coefficient 0.82 (Wooster *et al.* [39] used nitrogen instead air atmosphere and the sample

mass are five times higher than our samples) and the loss of accuracy of the extrapolations used in the isothermal studies for long periods of time. However, the $t_{0.01/10\,h}$ values obtained from Wooster *et al.* [39] method are higher than those obtained from isothermal scans, in all the cases. Thus, a better agreement was obtained between the predicted $t_{0.01/10h}$ values using Wooster *et al.* [39] relation and the $t_{0.05/10\,h}$ values obtained from isothermal scans and equation (2).

This fact indicates that in spite of Wooster *et al.* [39] presents a very good and rapid method to determine the long term stability from the dynamic scans, these results should be taken with caution if it will be used in an industrial application that need small loss of weight. In this situation a deeper study using isothermal experiments is needed.

4. Conclusions

Thermal stability of new ionic liquids with the common cation 1-butyl-1-methylpyrrolidinium was analysed using thermogravimetric analysis. The following conclusions were obtained:

– From dynamic experiments it was concluded that $[C_4C_1Pyrr][NTf_2]$ and $[C_4C_1Pyrr][(C_4F_9)_3PF_3]$ are the most and the less stable, respectively.
– Imidazolium based ILs showed a slightly higher thermal stability than the pyrrolidinium for the same anion. Isothermal analysis at temperatures 20 °C below the t_{onset} showed a fast degradation. TG scans at 200 °C revealed a hardly appreciable degradation after 5 h.
– Activation energies of the ILs with the anions $[NTf_2]^-$, $[OTf]^-$ and $[FAP]^-$ were obtained from the Arrhenius equation and their values are higher than the corresponding to the ILs with same anions and the cation $[C_4C_1Im]^+$. Besides, the trend with the anion is the same for both imidazolium and pyrrolidinium ILs.
– Maximum temperature operation was determined from the isothermal studies taking into account three possible degradation levels. The results were compared with the proposed methodology by Wooster *et al.* [39] to estimate the long term thermal stability from dynamic scans, obtaining a quite good concordance.

References

[1] M. Palacio, B. Bhushan, Tribol. Lett. 40 (2010) 247–268.
[2] Z. Zeng, B.S. Phillips, J.-C. Xiao, J.n.M. Shreeve, Chem. Mater. 20 (2008) 2719–2726.
[3] V. Pejaković, M. Kronberger, M. Kalin, Lubr. Sci. 26 (2014) 107–115.
[4] A. Jiménez, M.-D. Bermúdez, Tribol. Lett. 33 (2009) 111–126.
[5] M. Cai, R. Guo, F. Zhou, W. Liu, Sci. China Technol. Sci. 56 (2013) 2888–2913.
[6] J. Liu, F. Wang, L. Zhang, X. Fang, Z. Zhang, Renewable Energy 63 (2014) 519–523.
[7] H.-B. Han, K. Liu, S.-W. Feng, S.-S. Zhou, W.-F. Feng, J. Nie, H. Li, X.-J. Huang, H. Matsumoto, M. Armand, Z.-B. Zhou, Electrochim. Acta 55 (2010) 7134–7144.
[8] L. Chancelier, A.O. Diallo, C.C. Santini, G. Marlair, T. Gutel, S. Mailley, C. Len, Phys. Chem. Chem. Phys. 16 (2014) 1967–1976.
[9] J. Salgado, M. Villanueva, J.J. Parajó, J. Fernández, J. Chem. Thermodyn. 65 (2013) 184–190.
[10] M. Villanueva, A. Coronas, J. García, J. Salgado, Ind. Eng. Chem. Res. 52 (2013) 15718–15727.
[11] D.M. Fox, W.H. Awad, J.W. Gilman, P.H. Maupin, H.C. De Long, P.C. Trulove, Green Chem. 5 (2003) 724–727.
[12] M. Kosmulski, J. Gustafsson, J.B. Rosenholm, Thermochim. Acta 412 (2004) 47–53.

[13] H.L. Ngo, K. LeCompte, L. Hargens, A.B. McEwen, Thermochim. Acta 357–358 (2000) 97–102.
[14] C. Maton, N. De Vos, C.V. Stevens, Chem. Soc. Rev. 42 (2013) 5963–5977.
[15] R.E. Del Sesto, T.M. McCleskey, C. Macomber, K.C. Ott, A.T. Koppisch, G.A. Baker, A.K. Burrell, Thermochim. Acta 491 (2009) 118–120.
[16] A. Seeberger, A.-K. Andresen, A. Jess, Phys. Chem. Chem. Phys. 11 (2009) 9375–9381.
[17] M.E.V. Valkenburg, R.L. Vaughn, M. Williams, J.S. Wilkes, Thermochim. Acta 425 (2005) 181–188.
[18] P. Verdía, M. Hernaiz, E.J. González, E.A. Macedo, J. Salgado, E. Tojo, J. Chem. Thermodyn. 69 (2014) 19–26.
[19] R.G. Reddy, Z. Zhang, M.F. Arenas, D.M. Blake, High Temp. Mater. Processes 22 (2003) 87–94.
[20] V. Kamavaram, R.G. Reddy, Int. J. Therm. Sci. 47 (2008) 773–777.
[21] C.P. Fredlake, J.M. Crosthwaite, D.G. Hert, S.N.V.K. Aki, J.F. Brennecke, J. Chem. Eng. Data 49 (2004) 954–964.
[22] X. Paredes, J. Fernández, A.A.H. Pádua, P. Malfreyt, F. Malberg, B. Kirchner, A.S. Pensado, J. Phys. Chem. B 118 (2014) 731–742.
[23] V. Borgel, E. Markevich, D. Aurbach, G. Semrau, M. Schmidt, J. Power Sources 189 (2009) 331–336.
[24] A.M. O'Mahony, D.S. Silvester, L. Aldous, C. Hardacre, R.G. Compton, J. Chem. Eng. Data 53 (2008) 2884–2891.
[25] M. Hayyan, F.S. Mjalli, M.A. Hashim, I.M. AlNashef, T.X. Mei, J. Ind. Eng. Chem. 19 (2013) 106–112.
[26] S. Menne, R.S. Kühnel, A. Balducci, Electrochim. Acta 90 (2013) 641–648.
[27] F.M. Gaciño, T. Regueira, L. Lugo, M.J.P. Comuñas, J. Fernández, J. Chem. Eng. Data 56 (2011) 4984–4999.
[28] T. Regueira, L. Lugo, J. Fernández, J. Chem. Thermodyn. 48 (2012) 213–220.
[29] F.M. Gaciño, X. Paredes, M.J.P. Comuñas, J. Fernández, J. Chem. Thermodyn. 54 (2012) 302–309.
[30] G.W. Meindersma, B.T.J. Simons, A.B. de Haan, J. Chem. Thermodyn. 43 (2011) 1628–1640.
[31] I. Minami, T. Inada, Y. Okada, Proc. Inst. Mech. Eng. Part J J. Eng. Tribol. 226 (2012) 891–902.
[32] M. Shamsipur, A.A.M. Beigi, M. Teymouri, S.M. Pourmortazavi, M. Irandoust, J. Mol. Liq. 157 (2010) 43–50.
[33] E.M. Siedlecka, M. Czerwicka, S. Stolte, P. Stepnowski, Curr. Org. Chem. 15 (2011) 1974.
[34] A.S. Amarasekara, O.S. Owereh, J. Therm. Anal. Calorim. 103 (2011) 1027–1030.
[35] A. Fernández, J.S. Torrecilla, J. García, F. Rodríguez, J. Chem. Eng. Data 52 (2007) 1979–1983.
[36] J. Salminen, N. Papaiconomou, R.A. Kumar, J.-M. Lee, J. Kerr, J. Newman, J.M. Prausnitz, Fluid Phase Equilib. 261 (2007) 421–426.
[37] H. Shirota, T. Mandai, H. Fukazawa, T. Kato, J. Chem. Eng. Data 56 (2011) 2453–2459.
[38] Z.B. Zhou, H. Matsumoto, K. Tatsumi, Chem. Eur. J. 12 (2006) 2196–2212.
[39] T.J. Wooster, K.M. Johanson, K.J. Fraser, D.R. MacFarlane, J.L. Scott, Green Chem. 8 (2006) 691–696.
[40] Y. Jin, S. Fang, M. Chai, L. Yang, S.-I. Hirano, Ind. Eng. Chem. Res. 51 (2012) 11011–11020.
[41] Y. Hao, J. Peng, S. Hu, J. Li, M. Zhai, Thermochim. Acta 501 (2010) 78–83.

JCT 14-138

Liquid range temperature of ionic liquids as potential working fluids for absorption heat pumps

M. Villanueva [a], J.J. Parajó [a], Pablo B. Sánchez [b], J. García [b], J. Salgado [a],*

[a] *Thermophysical Properties of Fluids and Biomaterials Group, Applied Physics Department, University of Santiago de Compostela, E-15782 Santiago de Compostela, Spain*
[b] *Applied Physics Department, Experimental Science Building, University of Vigo, E-36310 Vigo, Spain*

A B S T R A C T

The liquid range temperature of six ionic liquids (ILs) was determined in this work with the aim to propose suitable absorbents for heat pump systems. The selected ILs have three different cations, imidazolium, pyridinium and choline and each was combined with four different anions $[NTf_2]^-$, $[OTf]^-$, $[MeSO_3]^-$ and $[BETI]^-$. The lower limit, given by solid − liquid transitions, was determined using differential scanning calorimetry (DSC). The upper limit is given by the degradation temperature. This temperature is determined using thermogravimetric technique (TGA). Dynamic and isothermal methods have been combined to estimate the maximum operation temperature. ILs ageing effect was also analysed in this work.

© 2015 Elsevier Ltd. All rights reserved.

1. Introduction

Ionic liquids (ILs) are usually defined as salts melting under 100 °C. This definition is broadly accepted even though there is no chemical or physical significance in this temperature which has been chosen for historical reasons [1]. From the enormous number of ILs, the most common chemical structure is based on an organic cation together with an inorganic polyatomic anion [2]. The unique properties of the ILs [3] have brought great interest over the last years from industry and academia due to a large number of potential applications [4]. Since climate change stands out as one of the main challenges for the next decades, technologies leading to efficient energy production will play a crucial role. In this framework, absorption heat pumps are a great opportunity to reduce energy consumption of heating and refrigeration systems, since this technology allows either recovering residual heat or using renewable energies (as solar, bio-hydrogen...) to produce profitable thermal energy. Subsequently, the use of additional electric power is almost negligible. Therefore it is a technology of high added value in regions where the electrical network is not developed in addition to its high ecological benefits. Nevertheless conventional working pairs present several drawbacks which have limited the potential of absorption heat pumps [5]. Some of these problems are corrosion and crystallisation in the case of $H_2O/LiBr$, high working pressures, low relative volatility and NH_3 toxicity for NH_3/H_2O. Thus, improvements of absorption heat pumps by developing new working pairs (refrigerant/absorbent) have drawn the attention of companies and researchers. Seeking new working pairs involving ILs as absorbents occupy a principal role in these investigations [6,7]. This work is framed into the analysis of different ILs as candidates for absorption processes together with natural refrigerants such as water [8], ammonia or carbon dioxide.

To meet the requirements of absorption heat pumps, a first screening was performed paying special attention to the liquid range temperature. As it has been pointed out, crystallisation at low temperatures is one of the drawbacks for commercial $LiBr/H_2O$ working pairs, therefore solid − liquid transitions should be analysed to prevent solid phase formations in the absorber [7], an important factor of any absorption refrigeration system [9]. On the other hand, since absorbents will remain within the system for long periods of time, thermal stability should be studied carefully not only as a function of temperature but also as a function of time.

* Corresponding author. Tel.: +34 881814110; fax: +34 881814085.
  E-mail address: j.salgado.carballo@usc.es (J. Salgado).

Differential scanning calorimetry (DSC) was used to determine melting point (T_m) as much as the glass transition (T_g). These values may constrain the lower temperature operation range [10,11]. However it should be taken into account that real working fluids will be solutions of refrigerant/IL, where these temperatures are expected to be lower than those of pure IL, thereby partially easing the constraint [12].

In addition, the absorbents should be highly stable over a wide range of operating temperature in absorption devices [9]. Although, no unique criterion has been defined to determine thermal stability for a particular fluid, two operation modes are broadly known when thermogravimetric analysis is used. The so-called dynamic methods consist of performing a ramp of temperature with time by measuring simultaneously how mass sample changes. Results obtained are usually expressed in terms of degradation temperature or onset temperature [13]. This value provides qualitative information, as it has been broadly pointed out in the literature [13–15], but never a maximum operation temperature since it is observed that degradation starts below the onset temperature. In other words, the onset temperature overestimates the maximum operation temperature. For a deeper knowledge of this parameter, this analysis must be refined with isothermal scans. Additionally isothermal scans allow kinetic analysis of the degradation process by using the Arrhenius equation and an estimation of the degradation time for a given temperature.

Besides dynamic and isothermal scans, temperature conditions of the absorption process have been reproduced. Since during absorption cycles, the ILs undergo temperature changes (from absorber to generator and backwards) for extended periods of time. ILs thermal stability after several heating and cooling cycles has been studied. To our knowledge, this is the first time this sort of test has been reported for ILs.

At this point, and due to potential capabilities of ILs as absorbents, knowledge of physical and chemical properties becomes critical in order to select suitable candidates among a huge number of available ILs. The influence of the cation and anion, the length of the alkyl chain or different functional groups over ILs properties will allow "absorbent tunning" based on process requirements. Apart from the temperature operation range, other thermophysical properties such as solubility with the refrigerant, density, heat capacity, viscosity, surface tension or thermal conductivity; and also, factors as toxicity and environmental impact must be taken into account.

With the aim to acquire a deeper knowledge of cation and anion influence over the temperature operation range, six ionic liquids have been chosen for evaluation as potential absorbents for natural refrigerants (ammonia, water and carbon dioxide). The selected ILs are based on four different anions together with imidazolium, pyridinium and choline cations.

Four of the six ILs involve [NTf$_2$]$^-$ and [OTf]$^-$ anions and they were chosen because of their high thermal stability [16]. Other anions, [BETI]$^-$ and [MeSO$_3$]$^-$ [17] are not so extensively studied and they were chosen due to their structural similarity with [NTf$_2$]$^-$ and [OTf]$^-$. The influence of the cation over this property is minor compared to the anion, however it cannot be considered as a negligible factor. Thus, imidazolium, pyridinium and choline cation families have been selected to explore the cation effect over the decomposition temperature of the ILs.

TABLE 1
Structure and identification of selected ILs (all of them supplied by IoLiTec).

Name	Abbreviation CAS number	Chemical structure	Mass fraction purity
1-Ethylpyridinium bis (trifluoromethylsulfonyl) imide	[C$_2$Py][NTf$_2$] 712354-97-7		>0.99
Choline bis (trifluoromethylsulfonyl) imide	[Chol][NTf$_2$] 827027-25-8		>0.99
1-Ethyl-3-methylimidazolium triflate	[C$_2$C$_1$Im][OTf] 145022-44-2		>0.99
1-Ethyl-3-methylimidazolium bis (perfluoroethylsulfonyl) imide	[C$_2$C$_1$Im][BETI] 216299-76-2		>0.98
1-Ethylpyridinium methanesulfonate	[C$_2$Py][MeSO$_3$] 681481-41-4		>0.95
1-Ethylpyridinium triflate	[C$_2$Py][OTf] 3878-80-6		>0.99

2. Materials and methods

2.1. Chemicals

Six ionic liquids, provided by IoLiTec, were considered for this work, three contain the common cation, *viz.* 1-ethylpyridinium $[C_2Py]^+$, and the anions bis (trifluoromethylsulfonyl) imide $[NTf_2]^-$, triflate $[OTf]^-$, and methanesulfonate $[MeSO_3]^-$ The other two ILs have the common cation 1-ethyl-3-methylimidazolium $[C_2C_1Im]^+$, with the anions triflate and bis (perfluoroethylsulfonyl) imide $[BETI]^-$, and the sixth IL is choline bis (trifluoromethylsulfonyl) Imide $[Chol]$ $[NTf_2]$. Identification names and numbers, purities and cations and anions chemical structures are presented in table 1.

2.2. Experimental

A differential scanning calorimeter DSC Q100 TA-Instruments with aluminium pans hermetically sealed was used to determine the different state transitions experienced by the IL during the heating and cooling cycles. Liquid nitrogen was used as the coolant fluid. Each sample (3 to 5 mg) was subjected to four ramps, two in cooling and two in the heating mode, with an isothermal step between them: (a) heating from (25 to 120) °C at 10 °C · min^{-1}, (b) isothermal step at 120 °C during 30 min to remove impurities [18] and to erase the thermal history of the sample, (c) cooling from (120 to −85) °C at 5 °C · min^{-1}, (d) isothermal step at −85 °C during 5 min and (d) heating from (−85 to 100) °C at 10 °C · min^{-1} and (e) cooling from 100 °C at −85 °C at 5 °C · min^{-1}. Temperatures transitions were determined from the DSC curves during the re-heating and re-cooling steps [19].

A thermogravimetric analyser (TGA 7-Perkin Elmer) operating in dynamic and isothermal modes under dry air atmosphere was used to perform thermogravimetric analysis [20]. Although the effect of the atmosphere becomes lower for long-term thermal stability studies [21], it was considered more appropriate to use air instead of an inert atmosphere in order to estimate the maximum operation temperature for different applications, where ILs can be in air contact.

Samples of (3 to 5) mg were placed in an open platinum pan. Dynamic experiments were performed at temperatures from (100 to 800) °C, with a heating rate of 10 °C · min^{-1} and a purge gas flow of 20 cm^3 · min^{-1}. Each analysis was repeated three times. Determination procedures of onset and ending temperatures were described in previous papers [20,21]. Furthermore, isothermal TG analysis at temperatures lower than t_{onset}, was used to determine the long-term thermal stability of ILs.

Besides the effects on the thermal stability owing to dynamic and isothermal regimes during absorption cycles, the ILs undergo temperature changes (from absorber to generator and backwards) for extended periods of time. For this reason, the thermal stability of the ILs after several heating and cooling cycles has been studied in order to reproduce roughly the effects of these temperature changes on this property. Each sample was subjected to two ramps, one in cooling and one in the heating mode, with an isothermal step between them: (a) heating from (50 to 175) °C at 5 °C · min^{-1}, (b) isothermal step at 175 °C during 15 min, (c) cooling from (175 to 50) °C at 5 °C · min^{-1}, (d) isothermal step at 50 °C during 15 min. The whole sequence was repeated eight times.

3. Results and discussion

3.1. DSC

Figure 1 shows the last ramp of heating and cooling of DSC analysis of the six ILs $[C_2Py][NTf_2]$, $[Chol][NTf_2]$, $[C_2Py][OTf]$, $[C_2C_1Im][OTf]$, $[C_2Py][MeSO_3]$ and $[C_2C_1Im][BETI]$.

All the ILs show melting and freezing peaks, presenting these ILs as very good crystal-formers, although the DSC curve profiles show important differences associated with different thermal behaviour. Table 2 summarises state transition temperatures, such as melting, freezing, cold crystallisation and glass temperatures determined from these curves. As far as we are aware, information on the thermal behaviour of these ILs in heating and/or cooling ramps is scarce in the literature. Those values of transition temperatures found in the literature for these ILs are also presented in table 2.

Important agreement between our results and those of and other authors is, thus for $[C_2C_1Im][BETI]$, Ngo *et al.* [22] obtained freezing temperature (−12 °C) similar to our result, but values for the melting point (−1 °C) differ considerably from ours, probably due to different experimental conditions and different thermal history. However on the contrary, our results are in good concord with those of Shirota *et al.* [23] for the melting point. The $[C_2C_1Im][BETI]$ shows a glass transition (−52 °C) with enthalpic recovery. To distinguish it from a solid − solid transition, we have zoomed in the DSC scan and checked that it corresponds to a "stair step" which is the common appearance for a glass transition [24]. Afterwards, $[C_2C_1Im][BETI]$ shows a sub-cooling phenomenon, characterised by an incomplete crystallisation on the cooling ramp. Then a part of this IL passes from a glassy to a subcooled state, suffering a cold crystallisation followed by the melting transition. This cold crystallisation phenomenon is usually observed in the thermal behaviour of many ionic liquids. Agreeing with these results, Calvar *et al.* [18] and Fredlake *et al.* [10] found that some imidazolium based ILs show similar behaviour. Nevertheless this cannot be observed in pyridinium based ILs.

The $[Chol][NTf_2]$ shows a very different profile on the heating ramp compared to the rest of the ILs. This profile is characterised by three endothermic peaks at (2, 27 and 33) °C. The first is attributed to a solid − solid transition and the last to the melting process. The origin of the peak at 27 °C, which is not completely resolved with the last peak, could be associated either to a solid − solid or to a melting transition. Taking into account that the temperatures of the second and third peaks (27 and 33) °C do not change when the heating rate increases at 10 °C · min^{-1} (results are not shown), we think that the melting process of this IL takes place in two different phases at (27 and 33) °C. Similar behaviour and temperatures were also found by Yoshizawa-Fujita *et al.* [25] for this IL, with the usual shape found in the DSC of polymers with high molar mass [26,27]. Additionally, Nockeman *et al.* [28], indicated that the melting temperature for $[Chol][NTf_2]$ is 30 °C although these authors do not show the DSC curves of this IL, this value is in relative good concordance with our results.

The $[C_2Py][OTf]$ shows two exothermic peaks in the cooling ramp and two endothermic peaks in the heating ramp. Other authors as Calvar *et al.* [18] have observed similar behaviour in some pyridinium and imidazolium based ILs with the same anion, $[OTf]^-$, which suggests a polymorphic-like behaviour that leads to the formation of crystals with different structures. Nevertheless, a deeper study is necessary to complement and confirm this result.

On the other hand, $[C_2Py][NTf_2]$ crystallises, at −21 °C, on cooling, but does not form a glass within the temperature range studied. A solid − solid transition at 21 °C and the melting point at 32 °C are detected during the heating ramp, agreeing in both cases with the results of Liu *et al.* [29]. This behaviour, not unusual in ILs, is also observed by Machanova *et al.* [30] and Stefan *et al.* [31] for ammonium and pyrrolidinium based IL, with the $[NTf_2]^-$ anion, observing in the last case, even two solid − solid transitions before the melting.

All melt at temperatures higher than 0 °C with the exception of $[C_2C_1Im][OTf]$ that melts at −14 °C. Wachter *et al.* [32] indicate that the solid − liquid transition of this IL is −10 °C, which is the maximum temperature of the melting peak, agreeing with the result of this work.
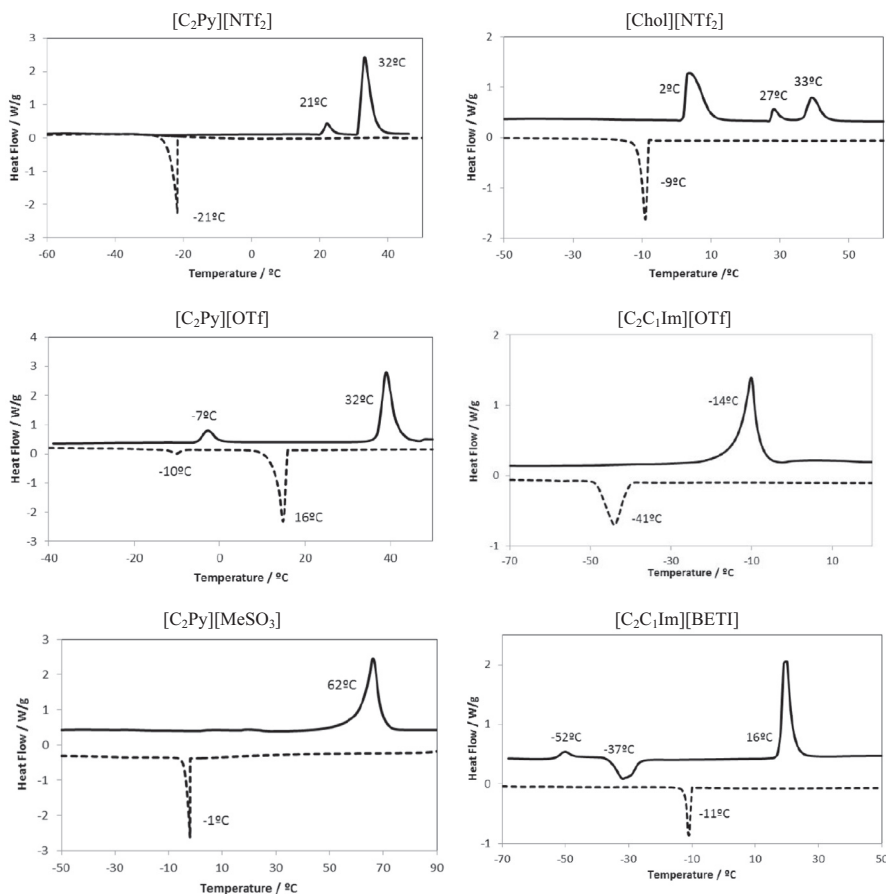
FIGURE 1. DSC curves (Exo down) on cooling (dashed line) and heating (solid line) scanning for the selected ILs.

TABLE 2
Freezing (t_f), melting (t_m), glass transition (t_g), cold crystallisation (t_{cc}) and solid – solid transition (t_{ss}) temperatures obtained from DSC curves under pressure of (990 ± 3) hPa and comparison with bibliographic results.

| IL	Cooling step	Heating step		
	$t_f/°C$	$t_m/°C$	$t_g/°C$	Other/°C
$[C_2Py][OTf]$	16/−10			
$[C_2Py][MeSO_3]$	−1	62		
$[Chol][NTf_2]$	−9	27/33		2 (t_{ss})
		27 [25]		−1 (t_{ss}) [25]
		30 [28]		
$[C_2C_1Im][BETI]$	−11	16	−52	−37 (t_{cc})
	−12 [22]	−1 [22]		
		15 [23]		
$[C_2Py][NTf_2]$	−21	32		21 (t_{ss})
		31 [29]	−38 [29]	20 (t_{ss}) [29]
$[C_2C_1Im][OTf]$	−41	−14		
		−10 [32]		

Expanded uncertainties are $U(t) = \pm 2$ °C (0.95 level of confidence).

The sequence obtained for lowest limit for the liquid range of selected ILs is:

$$[C_2Py][MeSO_3] > [C_2Py][OTf] \approx [C_2Py][NTf_2] \approx [Chol][NTf_2]$$
$$> [C_2C_1Im][BETI] > [C_2C_1Im][OTf].$$
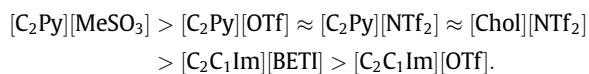
Imidazolium based ILs show the lowest melting temperatures, whereas the highest corresponds to ILs containing pyridinium cations. Nevertheless a trend with the anion cannot be established in the same way.

With regard to freezing temperatures the sequence is a little bit different:
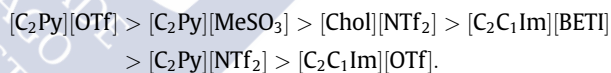
$$[C_2Py][OTf] > [C_2Py][MeSO_3] > [Chol][NTf_2] > [C_2C_1Im][BETI]$$
$$> [C_2Py][NTf_2] > [C_2C_1Im][OTf].$$

A trend with anion or cation cannot be established for freezing temperatures. Although it is important to remark that, in both sequences, the two first ILs remain the same.

Substantial super cooling is observed for all the ILs, with the freezing point significantly lower than the melting point, with differences $(T_m - T_f)$ occurring around (20 to 30) °C, except for $[C_2Py][NTf_2]$ and $[C_2Py][MeSO_3]$ which are higher than 50 °C, indicating a very slow crystallisation rate. This fact is very important and a positive observation for the application of ionic liquids as absorbents in absorption heat pumps to avoid the problem of crystallisation commonly observed in the current working pair, as previously pointed out.

3.2. Thermogravimetric analysis

3.2.1. Dynamic study
Figure 2 shows TG (a) and DTG (b) curves for the selected ILs. Reported curves have similar shapes for all ILs, characterised by a unique step with an intense loss weight, corresponding to a narrow DTG peak (50 °C approximately).

Table 3 shows onset and ending temperatures (t_{onset} and t_{endset}), weight at t_{onset} (W_{onset}), temperature corresponding to a 1% weight loss ($t_{1\%}$) and the temperature for DTG minimum (t_{peak}). These values were determined directly from TG and DTG curves using
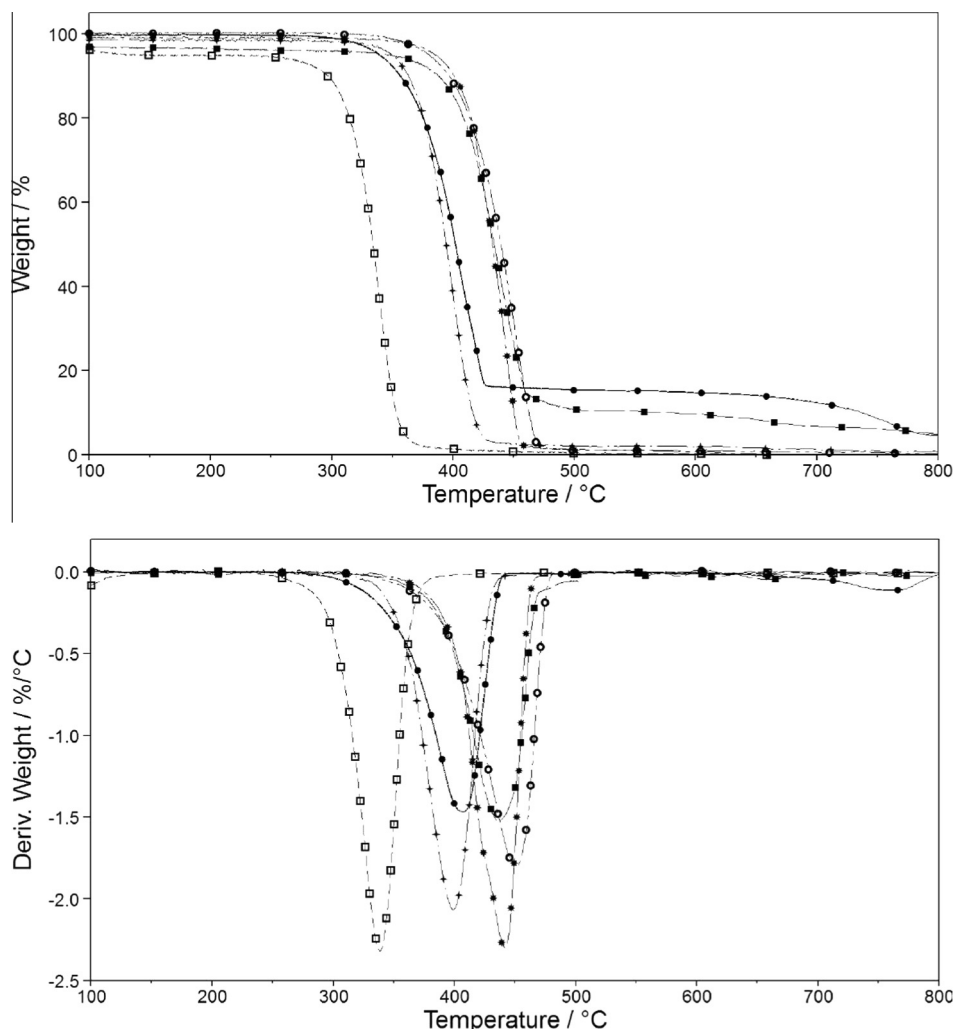
FIGURE 2. TG (a) and DTG (b) of ILs: (∗) [Chol][NTf$_2$], (■) [C$_2$C$_1$Im][OTf], (⬡) [C$_2$py][NTf$_2$], (○) [C$_2$py][OTf], (●) [C$_2$C$_1$Im][BETI], (□) [C$_2$py][MeSO$_3$].

TABLE 3
Thermal results from dynamic scans in air atmosphere under pressure of (990 ± 10) hPa. Onset and ending temperatures (t_{onset} and t_{endset}), weight at t_{onset} (W_{onset}), the temperature for DTG minimum (t_{peak}) and temperature corresponding to 1% loss weight ($t_{1\%}$).

IL	t_{onset}/°C	t_{endset}/°C	W_{onset}/%	t_{peak}/°C	$t_{1\%}$/°C
[Chol][NTf$_2$]	410	460	85	442	355
[C$_2$Py][NTf$_2$]	409	471	83	450	346
[C$_2$C$_1$Im][OTf]	404	458	87	436	338
[C$_2$Py][OTf]	371	416	86	399	328
[C$_2$C$_1$Im][BETI]	368	425	85	407	305
[C$_2$Py][MeSO$_3$]	315	353	85	339	265

Expanded uncertainties are $U(t) = \pm 4$ °C and $U(W) = 1\%$ (0.95 level of confidence).

methods widely described in previous papers published by our group [15,20,21]. Analysed ILs present a remarkable thermal stability, with onset temperatures higher than 350 °C, except for [C$_2$Py][MeSO$_3$] with t_{onset} of 315 °C. Although the onset temperature cannot be considered the upper limit of the liquid range as already noted, this parameter allows establishment of a sequence for the thermal stability of the ILs. Thus, the trend obtained is as follows:

[Chol][NTf$_2$] ≈ [C$_2$Py][NTf$_2$] > [C$_2$C$_1$Im][OTf] > [C$_2$Py][OTf]

> [C$_2$C$_1$Im][BETI] > [C$_2$Py][MeSO$_3$].
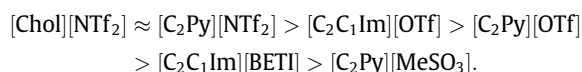
This sequence indicates that the anion has the strongest influence over the ILs thermal stability, with the [NTf$_2$]$^-$ conferring the highest resistance to thermal degradation, following closely by [OTf]$^-$. Thus, it is clear that the cation influence should also be taken into account with the imidazolium based ILs that provide the greatest thermal stability. These observations are in good agreement with previous works where ILs with similar cations or anions were studied [16,33–36].

Literature information regarding the degradation of these ILs is scarce and in most cases comparisons are difficult due to the influence of experimental conditions on results. Thus, Bittner *et al.* [36] use temperature of maximal decomposition rate (*i.e.* t_{peak} for us) and they found results similar to ours for [C$_2$Py][NTf$_2$].

Additionally, Heym *et al.* [17], with the scope of studying thermal stability, used temperature to reach a mass loss of 1% during TG experiments at different heating rates obtaining 348 °C for [C$_2$C$_1$Im][OTf]. This value is consistent with result obtained in this work (338 °C).

On the other hand, decomposition temperature (T_d) of [C$_2$C$_1$Im][BETI] was previously calculated by Ngo *et al.* [22], obtaining different values using either aluminium (423 °C) or alumina (462 °C) sample pan, both of them higher than the value obtained in this work. These authors used a nitrogen atmosphere and a heating rate of 20 °C · min^{-1}, whereas in this work
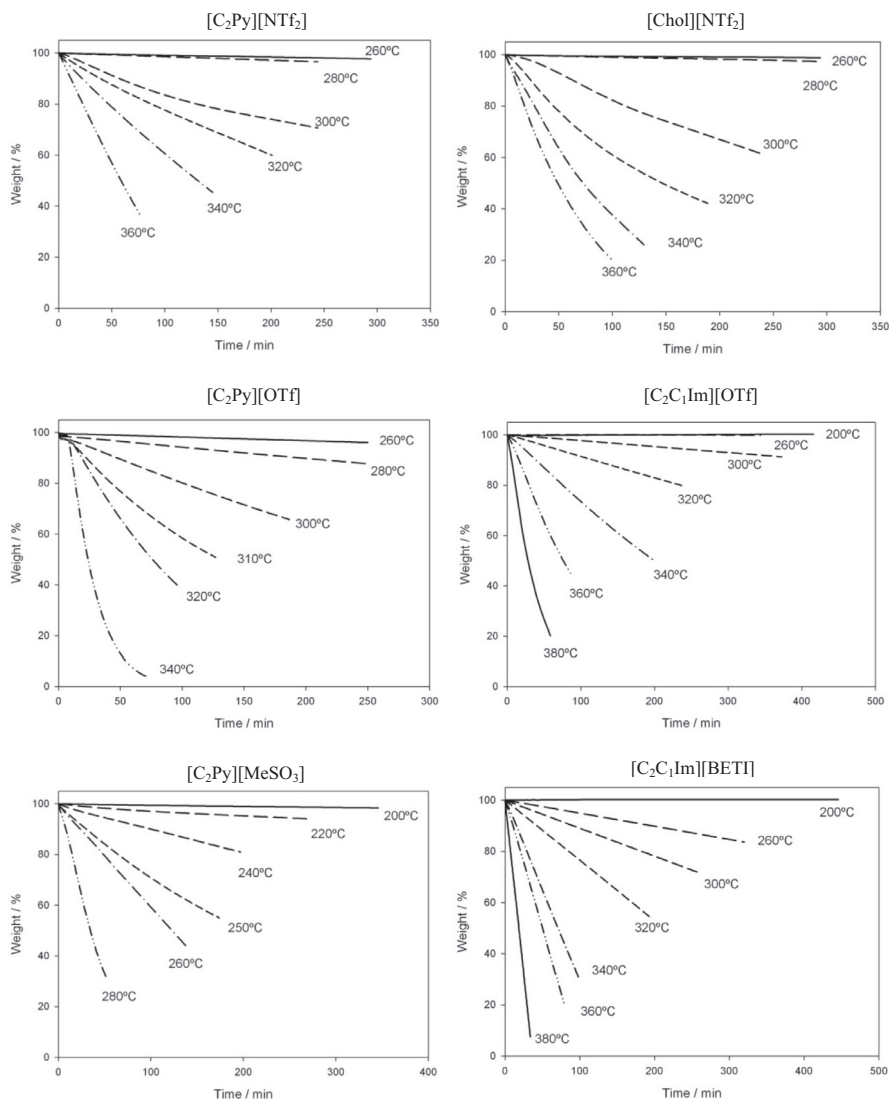
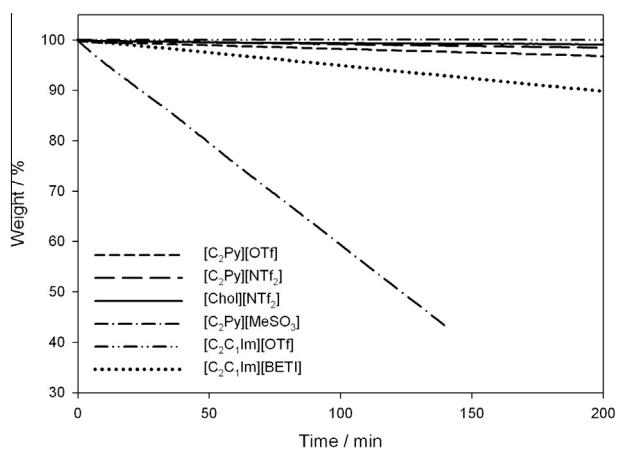**FIGURE 3.** Isothermal scans at different temperatures of selected ILs.

FIGURE 4. Comparison of isothermal scans of selected ILs at 260 °C.

TABLE 4
Activation energy, E_a, and pre-exponential factor of Arrhenius equation, A, of degradation process for the selected ILs.

IL	$E_a/(\text{kJ} \cdot \text{mol}^{-1})$	$A' = \ln A$
[C$_2$Py][OTf]	185 ± 10	37.57 ± 1.69
[Chol][NTf$_2$]	170 ± 20	33.12 ± 5.33
[C$_2$C$_1$Im][OTf]	160 ± 5	30.39 ± 0.98
[C$_2$Py][NTf$_2$]	140 ± 20	27.57 ± 4.39
[C$_2$Py][MeSO$_3$]	140 ± 10	31.52 ± 1.57
[C$_2$C$_1$Im][BETI]	110 ± 5	21.61 ± 1.17

effect takes place when the heating rate changes from (10 to 20) °C · min^{-1}.

Leaving aside the dynamic nature of the experiments, the loss of weight at t_{onset} is around 15% in all the ILs, too high to claim that this temperature is the upper limit of the operation range, as mentioned above. So, to establish this upper limit, isothermal studies are necessary [21].

3.2.2. Isothermal study

With the aim to determine the maximum operating temperature of these ILs, isothermal scans at different temperatures lower

air atmosphere and 10 °C · min^{-1} were chosen. As previous studies [21] have shown, the onset temperature can be up to 30 °C higher when the atmosphere changes from air to nitrogen. A similar
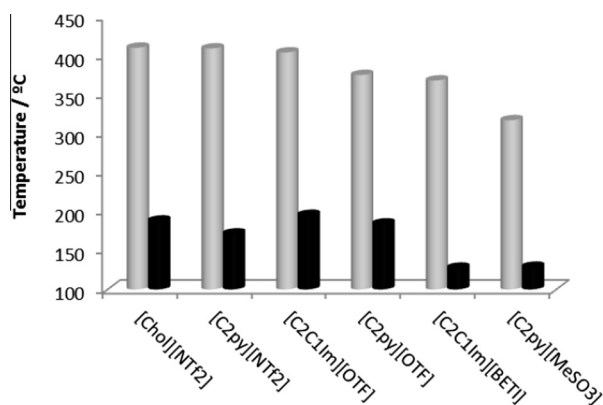
FIGURE 5. Comparison between t_{onset} (grey bar) and $t_{0.01/10h}$ (black bar).

TABLE 5

Maximum operating temperature (t, in °C) corresponding to three thermal degradation levels (1%, 5% and 10% in 10 h) calculated from Arrhenius parameter equation.

LI	t_{onset}/°C	$t_{0.01/10h}$/°C	$t_{0.05/10h}$/°C	$t_{0.1/10h}$/°C
[Chol][NTf$_2$]	410	190	205	215
[C$_2$Py][NTf$_2$]	409	170	190	200
[C$_2$C$_1$Im][OTf]	404	200	215	225
[C$_2$Py][OTf]	371	185	200	205
[C$_2$C$_1$Im][BETI]	368	130	150	160
[C$_2$Py][MeSO$_3$]	315	130	145	150

Uncertainties are $U(t_{onset})$ = ±4 °C (0.95 level of confidence) and $U(t_{0.01/10h})$ = $U(t_{0.05/10h})$ = $U(t_{0.1/10h})$ = ±10 °C (0.68 level of confidence).

than the corresponding t_{onset} were performed. Figure 3 shows these scans. As expected, weight loss corresponding to the highest selected temperature was very rapid, even for [C$_2$Py][NTf$_2$] at 360 °C (42 °C lower than the onset temperature), with one hour time enough to lose approximately the 60% of initial weight. Nevertheless scans at 260 °C for ILs with [OTf]$^-$ and [NTf$_2$]$^-$ anions and at 200 °C for other ILs during more than five hours do not imply detectable changes in mass samples.

Figure 4 shows a comparison between the isothermal scans at 260 °C. A similar trend than the one found with dynamic scans was obtained. The [OTf]$^-$ and [NTf$_2$]$^-$ based ILs are again the most stable, whereas [C$_2$Py][MeSO$_3$] weight loss at 260 °C is around 50% after 100 min.

The kinetics of decomposition was analysed from isothermal TGA results following the methodology reported in previous papers [18,19].

The temperature dependence on weight loss rate, k, is represented by the Arrhenius equation:

$$k = A \exp\left(\frac{-E_a}{RT}\right), \tag{1}$$

where E_a is the activation energy, R the gas constant and T the absolute temperature. The activation energy of the degradation process was obtained by fitting $\ln k$ and T^{-1}. The results are presented in table 4.

As far we are aware, activation energy values have not been published for these ILs, although these values are in agreement with those reported in the literature for other ILs with a similar cation and anion. From the results obtained and previous publications [14,18,19], it can be concluded that the activation energy follows the trend for a common anion ([NTf$_2$]$^-$ or [OTf]$^-$) choline > pyrrolidinium > pyridinium > imidazolium, whereas the anion sequence is:

$$[OTf]^- > [FAP]^- > [NTf_2]^- \approx [MeSO_3]^- > [BETI]^-.$$

3.3. Maximum operation temperature

As it was pointed out t_{onset} cannot be considered a maximum operating temperature. Thus, a long-term stability parameter, $t_{0.01/10h}$, that is the temperature necessary to reach a 1% weight loss after 10 h, is often used [16,27,29,37]. This parameter can be calculated from the Arrhenius equation, whose parameters are shown in table 4. A comparison between the values of t_{onset} and calculated $t_{0.01/10h}$ are presented in figure 5. Differences of 200 °C, approximately, between both temperatures are observed for all the selected ILs.

Depending on the application, the maximum operating temperature can vary, taking into account that the degradation level can be different. Thus, as expressed in previous papers [20], the criterion of $t_{0.01/10h}$ could be over strict, in which case the maximum operating temperature corresponding to three thermal degradation levels (1%, 5% and 10% in 10 h) is calculated using the above Arrhenius parameters that are shown in table 5.

In general, absorption systems will have operating temperatures lower than data shown in table 5. However, this issue must be analysed taking into account once the heat pump configuration is chosen. According to systems evaluated by Ayou et al. [38], these six ILs may accomplish the maximum operating temperature requirements with [C$_2$C$_1$Im][BETI] and [C$_2$Py][MeSO$_3$] which are close to this limit.

3.4. (Heating + cooling) cycles. ILs ageing

Regarding the application of absorption heat pumps, ILs behaviour after long periods of time remains as an open question, specifically the effects of ageing of the ILs after numerous absorption/desorption cycles. To the best of our knowledge, very few experiments have been done to study ageing effect on ILs [39].

His question is outlined using thermal techniques. (Heating + cooling) cycles were chosen to adapt the experimental procedure to absorption heat pump applications. The experimental procedure consists of 8 successive heating applications up to 175 °C and cooling up to 50 °C under air atmosphere.

Figure 6 shows the second (the first one was not considered because a low percentage of impurities, specially water, released to rise 100 °C) and the last heating TG curve for [C$_2$C$_1$Im][OTf] and [C$_2$Py][MeSO$_3$], which are the most and least thermally stable. No significant degradation related to successive (heating + cooling) cycles was found.

After the successive (heating + cooling) cycles, the same sample of these ILs was subjected to a heating from (50 to 800) °C at 10 °C · min^{-1} (figures not shown), i.e. the experimental conditions corresponded to dynamic studies, with the aim to determine the changes in characteristic temperatures after the cycles. Table 6 reports onset temperatures obtained from this dynamic study after the cycles (t'_{onset}). Results show there are no significant changes in dynamic curves as a consequence of the ageing.

Even though during this process ILs do not undergo other effects related with physical absorption, chemical interactions or mechanical factors, results seem to indicate that ageing does not affect to thermal stability.
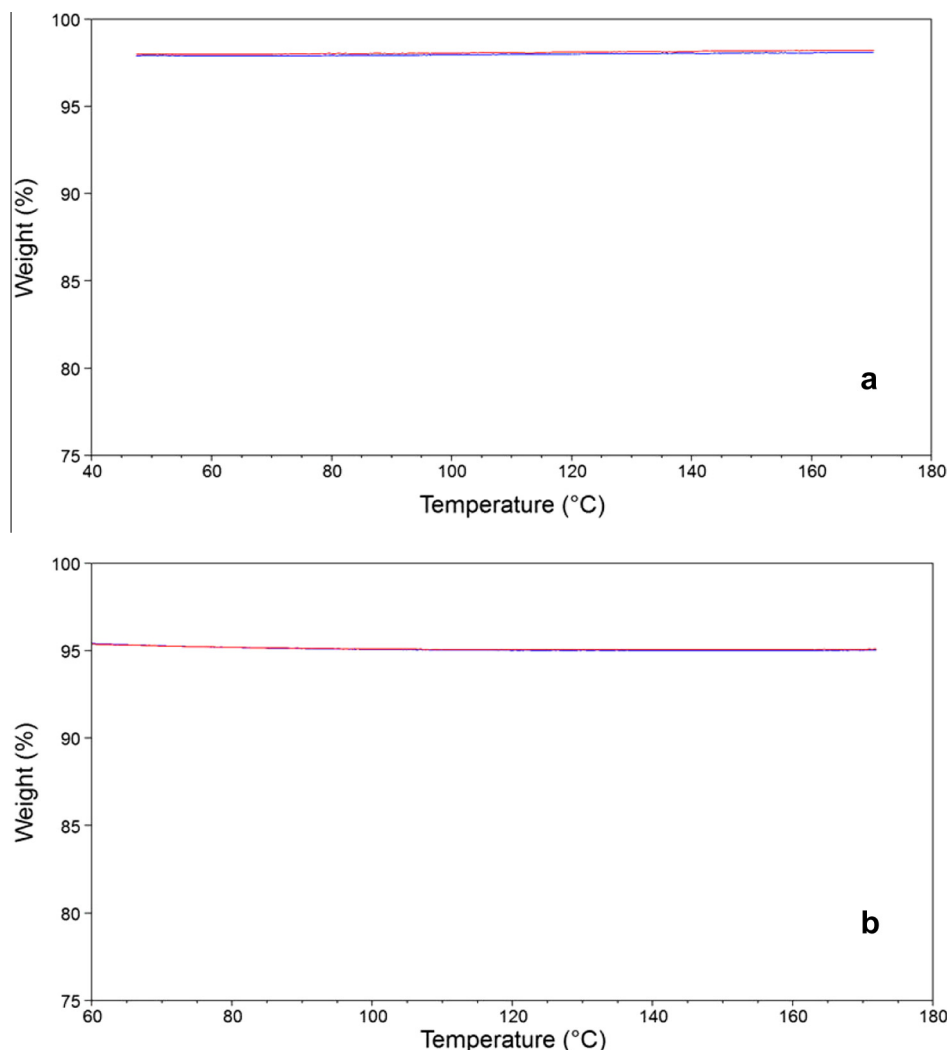
FIGURE 6. Comparison between the second and last curves of (heating + cooling) cycles of (a) [C₂C₁Im][OTf] and (b) [C₂Py][MeSO₃] ILs.

TABLE 6
Onset temperatures (t'_{onset}) of selected ILs obtained from dynamic studies after aging cycles.

IL	t'_{onset}/°C
[Chol][NTf₂]	410
[C₂py][NTf₂]	401
[C₂C₁Im][OTf]	405
[C₂py][OTf]	370
[C₂C₁Im][BETI]	362
[C₂py][MeSO₃]	321

Expanded uncertainties are $U(t)$ = ±4 °C (0.95 level of confidence).

4. Conclusions

The liquid range of six different ILs has been determined in this work, using thermal analysis techniques. The main results are the following:

– All ILs show DSC curves peaks attributed to melting and freezing processes in heating and cooling scanning, respectively. The [C₂Py][MeSO₃] and [C₂Py][OTf] show the highest melting and freezing temperatures and [C₂C₁Im][OTf] the lowest. Different ILs trends were obtained for melting and freezing processes.

– The six ILs studied show remarkable thermal stability with onset temperatures higher than 300 °C. The influence of the anion over this property is very strong with [NTf₂]⁻ and [OTf]⁻ anions the most resistant to thermal degradation. Nevertheless, temperatures provided by dynamic thermogravimetric studies cannot be considered to be the maximum operating temperature. Isothermal scans are necessary to determine this value.

– [MeSO₃]⁻ and [BETI]⁻ based ILs do not undergo significant thermal degradation up to 200 °C whereas for [NTf₂]⁻ and [OTf]⁻ based ILs significant degradation is not detected up to 250 °C under the same conditions.

– Activation energy of the degradation process has been determined using the Arrhenius equation and is compared with previous results for other ILs. Cation and anion influence on activation energy is defined by the following trends; for cation: choline > pyrrolidinium > pyridinium > imidazolium, and for anion: [OTf]⁻ > [FAP]⁻ > [NTf₂]⁻ ≈ [MeSO₃]⁻ > [BETI]⁻.

– The effect of successive heating to 175 °C and cooling to 50 °C cycles on the mass sample was analysed to estimate the effects on ageing of the ILs. Results indicate that this effect is negligible, since no detectable mass loss is associated with these cycles. Before and after the ageing, the TG curves show similar shapes and the same onset temperatures.

– According to the findings, the most adequate IL to operate in absorption devices is [C_2C_1Im][OTf] due to its lowest melting point and greatest thermal stability. Nevertheless, regarding their liquid range, none of the others should be discarded since they accomplish requirements for many heat pump configuration systems. To determine suitable ILs, other experimental and theoretical experimental studies will be made in the near future.

Acknowledgments

References

[1] N.V. Plechkova, K.R. Seddon, Chem. Soc. Rev. 37 (2008) 123.
[2] J.S. Wilkes, P. Wasserscheid, T. Welton, Ionic Liquids in Synthesis, Wiley-VCH Verlag GmbH & Co. KGaA, Weinheim, Germany, 2007.
[3] P. Wasserscheid, T. Welton, Ionic Liquids in Synthesis, Wiley-VCH Verlag GmbH & Co. KGaA, Weinheim, Germany, 2007.
[4] J.F. Wishart, Energy Environ. Sci. 2 (2009) 956.
[5] M. Seiler, A. Kühn, F. Ziegler, X. Wang, Ind. Eng. Chem. Res. 52 (2013) 16519.
[6] D. Zheng, L. Dong, W. Huang, X. Wu, N. Nie, Renew. Sustainable Energy Rev. 37 (2014) 47.
[7] P. Wasserscheid, M. Seiler, ChemSusChem 4 (2011) 459.
[8] M. Khamooshi, K. Parham, U. Atikol, Adv. Mech. Eng. 2013 (2013) 1.
[9] P. Srikhirin, S. Aphornratana, S. Chungpaibulpatana, Renew. Sustainable Energy Rev. 5 (2000) 343.
[10] C.P. Fredlake, J.M. Crosthwaite, D.G. Hert, S.N.V.K. Aki, J.F. Brennecke, J. Chem. Eng. Data 49 (2004) 954.
[11] J.M. Crosthwaite, M.J. Muldoon, J.K. Dixon, J.L. Anderson, J.F. Brennecke, J. Chem. Thermodyn. 37 (2005) 559.
[12] D. Rengstl, V. Fischer, W. Kunz, Phys. Chem. Chem. Phys. 16 (2014) 22815.
[13] C. Maton, N. De Vos, C.V. Stevens, Chem. Soc. Rev. 42 (2013) 5963.
[14] M. Kosmulski, J. Gustafsson, J.B. Rosenholm, Thermochim. Acta 412 (2004) 47.
[15] J. Salgado, J.J. Parajó, J. Fernández, M. Villanueva, J. Chem. Thermodyn. 74 (2014) 51.
[16] Y. Cao, T. Mu, Ind. Eng. Chem. Res. 53 (2014) 8651.
[17] F. Heym, B.J.M. Etzold, C. Kern, A. Jess, Green Chem. 13 (2011) 1453.
[18] N. Calvar, E. Gómez, E.A. Macedo, Á. Domínguez, Thermochim. Acta 565 (2013) 178.
[19] H. Tokuda, K. Hayamizu, K. Ishii, M.A.B.H. Susan, M. Watanabe, J. Phys. Chem. B 108 (2004) 16593.
[20] J. Salgado, M. Villanueva, J.J. Parajó, J. Fernández, J. Chem. Thermodyn. 65 (2013) 184.
[21] M. Villanueva, A. Coronas, J. García, J. Salgado, Ind. Eng. Chem. Res. 52 (2013) 15718.
[22] H.L. Ngo, K. LeCompte, L. Hargens, A.B. McEwen, Thermochim. Acta 357–358 (2000) 97.
[23] H. Shirota, T. Mandai, H. Fukazawa, T. Kato, J. Chem. Eng. Data 56 (2011) 2453.
[24] L.C. Thomas, Modulated DSC: Measurement of Glass Transitions and Enthalpic Recovery. TA-Instruments Series, Paper 5, 2005.
[25] M. Yoshizawa-Fujita, Y. Kousa, K. Kidena, A. Ohira, Y. Takeoka, M. Rikukawa, Phys. Chem. Chem. Phys. 13 (2011) 13427.
[26] J.N. Hay, in: E.L. Charsley, S.B. Warrington (Eds.), Thermal Analysis Techniques and Applications, The Royal Society of Chemistry, Cambridge, 1992, pp. 156–179.
[27] M. Anouti, L. Timperman, Phys. Chem. Chem. Phys. 15 (2013) 6539.
[28] P. Nockemann, K. Binnemans, B. Thijs, T.N. Parac-Vogt, K. Merz, A.-V. Mudring, P.C. Menon, R.N. Rajesh, G. Cordoyiannis, J. Thoen, J. Leys, C. Glorieux, J. Phys. Chem. B 113 (2009) 1429.
[29] Q.-S. Liu, M. Yang, P.-F. Yan, X.-M. Liu, Z.-C. Tan, U. Welz-Biermann, J. Chem. Eng. Data 55 (2010) 4928.
[30] K. Machanová, Z. Wagner, A. Andresová, J. Rotrekl, A. Boisset, J. Jacquemin, M. Bendová, J. Solution Chem. 44 (2015) 790.
[31] S.C. Stefan, D. Lemordant, P. Biensan, C. Siret, B. Claude-Montigny, J. Therm. Anal. Calorim. 102 (2010) 685.
[32] P. Wachter, H.G. Schweiger, F. Wudy, H.J. Gores, J. Chem. Thermodyn. 40 (2008) 1542.
[33] N.M. Yunus, M.I. Abdul Mutalib, Z. Man, M.A. Bustam, T. Murugesan, J. Chem. Thermodyn. 42 (2010) 491.
[34] P. Verdía, M. Hernaiz, E.J. González, E.A. Macedo, J. Salgado, E. Tojo, J. Chem. Thermodyn. 69 (2014) 19.
[35] R. Tao, G. Tamas, L. Xue, S.L. Simon, E.L. Quitevis, J. Chem. Eng. Data 59 (2014) 2717.
[36] B. Bittner, R.J. Wrobel, E. Milchert, J. Chem. Thermodyn. 55 (2012) 159.
[37] T.J. Wooster, K.M. Johanson, K.J. Fraser, D.R. MacFarlane, J.L. Scott, Green Chem. 8 (2006) 691.
[38] D.S. Ayou, M.R. Currás, D. Salavera, J. García, J.C. Bruno, A. Coronas, Energy Convers. Manage. 84 (2014) 512.
[39] E.B. Fox, L.T. Smith, T.K. Williamson, S.E. Kendrick, Energy Fuels 27 (2013) 6355.

JCT 15-250